Azotobacter vinelandii Nitrogenase: Effect of Amino-Acid Substitutions at the αGln-191 Residue of the MoFe Protein on Substrate Reduction and CO Inhibition

Kanit Vichitphan

Dissertation submitted to the Faculty of the Virginia Polytechnic Institute and State University in partial fulfillment of the requirement for the degree of

DOCTOR OF PHILOSOPHY
in
BIOCHEMISTRY

William E. Newton, Chair
Jiann-Shin Chen
Eugene M. Gregory
Timothy J. Larson
Robert H. White

December, 2001
Blacksburg, Virginia

Key word: Amino acid substitution, αGlutamine-191 residue, MoFe protein, Mo-nitrogenase, *Azotobacter vinelandii*

Azotobacter vinelandii Nitrogenase: Effect of Amino-Acid Substitutions at the αGln-191 Residue of the MoFe Protein on Substrate Reduction and CO Inhibition

By
Kanit Vichitphan

William E. Newton, Chairman
Biochemistry Department

(ABSTRACT)

The FeMo cofactor is one of two types of prosthetic group found in the larger of the two nitrogenase component proteins, called the MoFe protein, and it is strongly implicated as the substrate binding and reduction site. The glutamine-191 residue in the α-subunit of the MoFe protein of *A. vinelandii* nitrogenase was targeted for substitution because it is located between the P cluster (the second type of prosthetic group in the MoFe protein) and the FeMo cofactor. Moreover, its side chain is involved in a hydrogen-bond network from one of the terminal carboxylates of the homocitrate component of FeMo cofactor through to the backbone NH of αGly-61, which is adjacent to the P cluster-ligating residue, αCys-62. The effect of substitutions at the position α-191 on the properties of the FeMo cofactor could mediate electron and/or proton transfer from the P cluster through hydrogen bonding and the homocitrate-Mo linkage.

A variety of altered MoFe proteins produced by the *A. vinelandii* mutant strains, namely the αPro-191, αSer-191, αThr-191, αHis-191, αGlu-191, and αArg-191 altered MoFe proteins, have been purified to homogeneity and the catalytic properties of these altered MoFe proteins have been compared to those of wild type MoFe protein. The different properties of the side chains of the residues substituting for at αGln-191 residue on H^+-, C_2H_2-, N_2- and HCN-reduction suggest that the hydrogen-bonding link to homocitrate by αGln-191 residue is not absolutely required for reducing these substrates. A plausible movement of homocitrate is likely required for efficient nitrogenase catalysis.

The results from the pH and activity studies indicate that the substitutions on the MoFe protein have an effect on the contribution of the responsible acid-base group(s) involved in proton transfer for H^+- and C_2H_2-reduction. Furthermore, the inhibition by CO of hydrogen evolution by these altered MoFe proteins is likely from a lowering of the rate of both electron and proton transfer to the H^+- reduction site(s). The similar shift in pK_a of the acid-base group(s) from substitution at αGln-191 residue and from CO binding to wild type MoFe protein suggests that the CO-binding site is close to the αGln-191 residue.

These altered MoFe proteins also change the apparent affinities of the C_2H_2 and HCN binding sites. These sites could be located close to the αGln-191 residue. Further, the kinetic results from C_2H_2 reduction by these altered MoFe proteins support the presence of at least two C_2H_2-binding sites on the wild type MoFe protein as suggested by Shen *et al*. (1997), Christiansen *et al*. (2000a), and Fisher *et al*. (2000a).

Some altered MoFe proteins but not wild type MoFe protein can produce C_2H_6 from C_2H_2. This observation suggested a lower apparent binding affinity for C_2H_2 and a slower proton transfer to C_2H_2 reduction with these altered MoFe proteins, which allow the intermediate to stay at the site longer and be further reduced by two electrons and two protons to give C_2H_6. Furthermore, studies of the minor product, C_2H_6, from HCN reduction with the αSer-191 altered MoFe protein indicate that both HCN and CN^- could be substrates for this product.

These changes in the biochemical properties of these altered MoFe proteins indicate that the αGln-191 residue is intimately involved in substrate binding and reduction including proton delivery to substrate. This residue is probably an intermediary residue that provides the connection between the P cluster and the FeMo cofactor through the movement of homocitrate during nitrogenase catalysis.

ACKNOWLEDGEMENTS

I would especially like to express my sincere gratitude and apprectation to my advisor, Dr. William Newton. His insightful advice, encouragement, and mentoring have played a major part in my educational achievement. His concern for me as an individual meant a great deal to me. I like to thank the members of my Graduate Advisory Committee, Dr. Jiann-Shin Chen, Dr. Timothy Larson, Dr. Eugene Gregory, and Dr. Robert White, for their valuable and helpful suggestion through my research program. I also thanks to Dr. David Bevan for his support and encouragement during my preliminary examination. Thanks Dr. Dennis Dean for providing the mutant strains for my study.

I am grateful to a good number of both present and former graduate students and coworkers for being such a good friends; Karl Fisher, Hong Li, Christie Dapper, Steve, Ja-Hong, Murat, Karen Kloos, John Cantwell, Promjit, and Pramvadee. Special thanks to Dr Karl Fisher and Christie Dapper for their assistant and encouragement as coworkers and friends.

I am also grateful to the staff in the Biochemistry Department for their support especially Mary Jo, Ross, Karen, Sheila and Steve Lowe for their effort in helping me whenever I need. Thanks also go to mass spectrometry scientist Mr. Kim Harich for helping me obtain data.

Most importantly, I would like to thank my beloved wife, Sukanda, whose endless love assistance, understanding, and encouragement have made my Ph. D. education possible. I am also grateful for the unfailing support of my family in Thailand and all of my Thai friends in Blacksburg.

Finally, I would like to acknowledge the Royal Thai Government for providing financial support. This work was supported by grant from the National Institute of Health (DK-37255 to W.E.N.)

TABLE OF CONTENTS

LIST OF FIGURES

LIST OF TABLES

ABBREVIATIONS

ADP	adenosine diphosphate
ADP:AlF_4^-	adenosine diphosphate aluminium tetrafluoride
ATP	adenosine triphosphate
B-media	Burk media without nitrogen source
Bis-Tris	Bis[2-Hydroxyethyl] imino-Tris[hydroxymethyl] methane
BN-media	Burk media with nitrogen source (urea)
CD	circular dichroism
CHES	2-[N-Cyclohexylamino] ethanesulfonic acid
DNA	deoxyribonucleic acid
CPK	creatine phosphokinase
ENDOR	electron nuclear double resonance
EDTA	ethylene diamine tetraacetic acid
EPR	electron paramagnetic resonance spectroscopy
ESEEM	electron spin echo envelope modulation
GC-MS	gas chromatography-mass spectrometry
HEPES	N-[2-Hydroxyethyl] piperazine-N'-[2-ethanesulfonic acid]
HEPPS	N-[2-Hydroxyethyl] piperazine-N'-[3-propanesulfonic acid]
ICP-AES	inductively coupled plasma atomic emission spectrometry
K_m	Michaelis constant
M_r	relative molecular mass
MWCO	molecular weight cut-off
NMF	*N*-methylformamide
NMR	nuclear magnetic resonance spectroscopy
P^N	P cluster in dithionite-reduced state
P^{OX}	P claster in two-electron-oxidized state
PCR	polymerase chain reaction
SA	specific activity
SD	standard deviation

SDS-PAGE	sodium dodecyl sulfate-polyacrylamide gel electrophoresis
SF-FTIR	stopped-flow Fourier transform infrared spectroscopy
St 1	dinitrogenase
St 2	superoxide oxidoreductase
St 3	carbon monoxide dehydrogenase
Tris-HCl	Tris[hydroxymethyl] aminomethane hydrochloric acid
V_{max}	maximum velocity

CHAPTER 1

Literature Review

1.1 Introduction

Nitrogen is a major essential constituent of all living cells and is present in proteins, nucleic acids (DNA and RNA), and many other biomolecules. Although 79% of the atmosphere is gaseous nitrogen, animals and plants cannot use it in that form. Instead, the nitrogen must be "fixed" (combined) with other elements, such as oxygen or hydrogen, to give a usable form, such as ammonia or nitrate. The total amount of nitrogen fixed on a global basis is estimated to be about 2.4×10^8 tons annually (Eady, 1992). The three ways that nitrogen fixation occurs in the biosphere are: 1) lightning and natural combustion processes; 2) the industrial Haber-Bosch process; and 3) biological nitrogen fixation. Fixed nitrogen most frequently limits plant productivity. Although industrially produced nitrogenous fertilizers can supply about 25% of the total annual use, this process has a number of disadvantages, such as the need for expensive and sophisticated industrial installation, the high cost in energy of both production and transportation to the field, and the potential hazard of nitrate run-off to the natural ecosystem. Of these three, biological nitrogen fixation is the most significant contributor accounting for about 65% of the total annual fixation to sustain life on earth (Newton, 1996).

Biological nitrogen fixation is performed by organisms known as diazotrophs and the enzyme that catalyzes this process is called nitrogenase. Diazotrophy is a term that means an ability to grow on N_2 gas as the sole nitrogen source. It is widely distributed among, but restricted to, the Archaea and Eubacteria kingdoms. Examples of diazotrophs include: *Azotobacter vinelandii* (an obligate aerobe), *Clostridium pasteurianum* (an obligate anaerobe), *Klebsiella pneumoniae* (a facultative anaerobe), *Rhodospirillum rubrum* (a photosynthetic eubacterium), *Anabaena sp* 7120 (a heterocyst forming cyanobacterium), and *Bradyrhizobium japonicum* (a symbiotic bacterium). Although they display a wide spectrum of habitats, which range from free-living forms to those

associated symbiotically with various plants, diazotrophs all utilize the same basic biochemical machinery for nitrogen fixation.

The biochemical and biophysical properties of molybdenum (Mo)-containing nitrogenase from a variety of diazotrophic organisms have been extensively studied especially those from *Azotobacter vinelandii* and *Klebsiella pneumonia*. There is, however, another class of nitrogenases that do not contain Mo and these have been designated as alternative nitrogenases (Bishop and Premakumar, 1992). Two types of alternative nitrogenase have been identified thus far, the vanadium (V) dependent and the iron (Fe) dependent nitrogenase systems. Also, a recent report has identified the existence of a novel Mo-dependent nitrogenase from *Streptomyces thermoautotrophicus* that is unlike any other known Mo-dependent system studied so far (Ribbe *et al*., 1997).

A major challenge in the enzymology of nitrogenase is to establish a detailed mechanism for reduction of the nitrogen molecule and other substrates in terms of the structures and properties of the nitrogenase proteins. With structures now available for both the Fe protein and MoFe protein, it is possible to begin to formulate a structural foundation for these mechanistic questions. Of particular interest is the energy transduction pathway required to couple ATP hydrolysis to electron transfer for substrate reduction at the active center. A better understanding of the molecular mechanism of nitrogenase should generate targets and methodologies for what (and how) beneficial modifications might be made to nitrogenase for Man's benefit in the future.

1.2 Nitrogenase

1.2.1 Molybdenum nitrogenase

With the exception of *Streptomyces thermoautotrophicus* nitrogenase (section 1.2.3), the common feature of all nitrogenases is that they are composed of two separable component proteins. The individual nitrogenase component proteins of the most commonly occurring molybdenum-containing nitrogenase (Mo-nitrogenase) have been designated as the Fe protein (or component 2 or dinitrogenase reductase) and the MoFe protein (or component 1 or dinitrogenase). These names reflect the content of their respective metal-containing prosthetic groups. The Fe protein is a γ_2 homodimer (M_r ~ 64,000), encoded by *nifH*, that contains two MgATP-binding sites and a single [4Fe-4S]

cluster located at the interface between the similar subunits (Georgiadis *et al*., 1992). The MoFe protein is an $\alpha_2\beta_2$ heterotetramer ($M_r \sim 230{,}000$), encoded by *nifDK*, that contains two pairs of novel metalloclusters. The P clusters (each composed of a [8Fe-7S] cluster) are located at the interface between the α- and β-subunits; the other cluster is the FeMo cofactor (a [Mo-7Fe-9S-homocitrate] cluster) located exclusively in the α subunit (Kim and Rees, 1992a; Bolin *et al*., 1993). The Fe protein serves as a specific reductant for the MoFe protein, which contains the site(s) of substrate binding and reduction.

During *in vitro* nitrogenase turnover using sodium dithionite as the reductant, one electron is delivered from the Fe protein to the MoFe protein per cycle, which involves association and dissociation of the two component proteins and hydrolysis of at least two MgATPs for each electron transferred (Figure 1.1). Under optimal conditions, the overall stoichiometry of N_2 reduction by nitrogenase has been established (Simpson and Burris, 1984) as

$$N_2 + 8H^+ + 8e^- + 16\text{MgATP} \rightarrow 2NH_3 + H_2 + 16\text{MgADP} + 16\text{Pi}$$

Thus, nitrogenase catalyzes not only the reduction of dinitrogen to ammonia but also the reduction of protons to hydrogen gas, which is an obligatory part of ammonia formation. Alternative substrates are often studied as probes for the nature of substrate-enzyme interactions. Besides N_2, the reduction of protons (H^+), acetylene (C_2H_2), cyanide (HCN), and azide (HN_3) are the alternative substrates that are commonly studied. Carbon monoxide (CO) is an inhibitor of all nitrogenase-catalyzed reactions with the exception of H^+ reduction (Hwang *et al*., 1973).

1.2.2 Alternative nitrogenases (Mo-independent nitrogenases)

In the alternative nitrogenase systems, the molybdenum is replaced by either vanadium or iron (Bishop *et al*, 1980; Robson *et al*, 1986; Chisnell *et al*, 1988). The first alternative nitrogenase, the vanadium-containing nitrogenase (V-nitrogenase), has a cofactor with a V atom substituting for the Mo atom in the larger of its two component proteins. This replacement results in a VFe protein containing a FeV-cofactor. The second alternative nitrogenase, the iron-containing nitrogenase (Fe-nitrogenase), contains

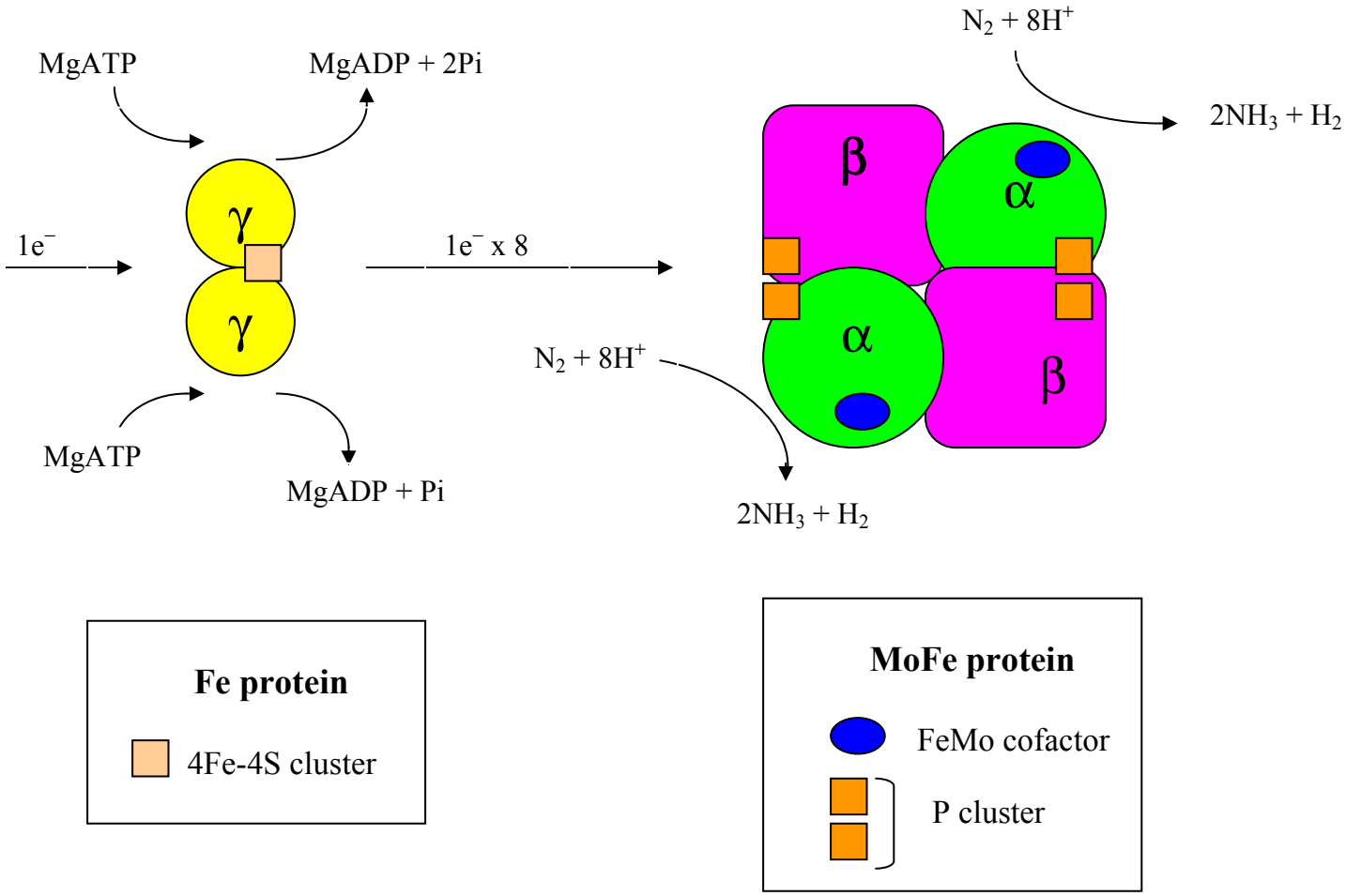

Figure 1.1 Schematic diagram of the nitrogenase complex and generalized nitrogen fixation reaction

a cofactor where the Mo atom is substituted by Fe to produce a FeFe protein containing a FeFe-cofactor. A major structural difference between these alternative nitrogenases and Mo-nitrogenase is that the VFe and FeFe proteins are hexameric rather than tetrameric, consisting of $\alpha_2\beta_2\delta_2$ subunit constituents ($M_r \sim 250{,}000$). These alternative nitrogenases have attracted considerable attention because of their differences in structure and reactivity. In general, they are less active than the Mo-nitrogenase, and they differ somewhat in substrate specificity. For example, V-nitrogenase has the ability to reduce C_2H_2 to both ethylene (C_2H_4) and ethane (C_2H_6) whereas wild type Mo-nitrogenase cannot produce C_2H_6 (Eady *et al.*, 1987).

These alternative nitrogenases are encoded by separate sets of structural genes. DNA sequencing established that the structural genes of the alternative nitrogenases (*vnfHDK*, V-nitrogenase; *anfHDK*, Fe-nitrogenase) share extensive sequence homology with those (*nifHDK*) of Mo-nitrogenase (Dean and Jacobson, 1992). A major difference is that both the alternative V- and Fe-nitrogenases carry a third subunit, called δ, that is encoded by *vnfG* and *anfG*, respectively. All three nitrogenase types are found in *A. vinelandii*. The expression of each nitrogenase is under hierarchical control through the availability of either Mo or V in the growth medium (Luque and Pau, 1991). Whenever Mo is available, expression of the Mo-nitrogenase is stimulated and the expression of the others is repressed. Similarly, when V is available and Mo is absent, expression of V-nitrogenase only occurs. If both metals are absent, then only the Fe-nitrogenase is expressed. Such control by metal availability is physiologically reasonable because Mo-nitrogenase is the most efficient nitrogen reducer.

1.2.3 Superoxide-dependent nitrogenase

Streptomyces thermoautotrophicus is a thermophilic, aerobic and obligate chemolithoautotrophic bacterium. It is able to fix N_2 with CO or H_2 plus CO_2 as growth substrates. An unusual N_2-fixing enzyme system in *S. thermoautotrophicus* named superoxide-dependent nitrogenase (sdn) has been characterized by Ribbe *et al*. (1997) (Figure 1.2). This enzyme system is composed of three enzymes: 1) a heterotrimeric molybdenum-containing nitrogenase (St1); 2) a homodimeric manganese-containing superoxide oxidoreductase (St2); and 3) a heterotrimeric molybdenum-containing carbon

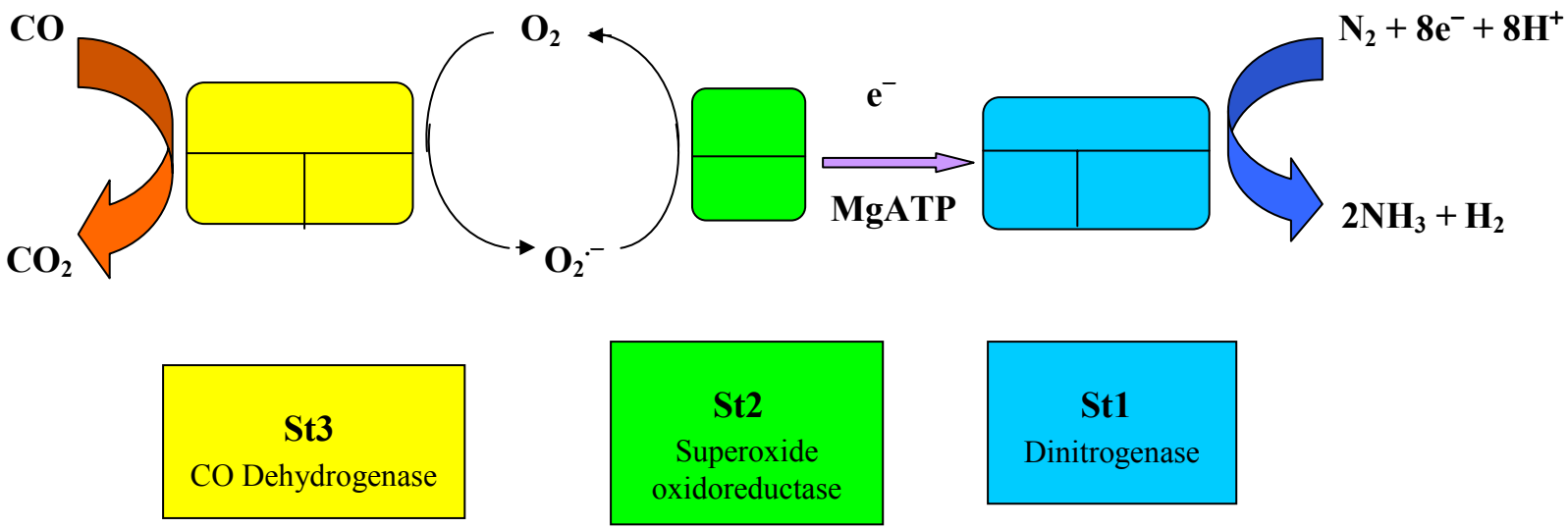

Figure 1.2 Schematic representation of N_2 fixation in *S. Thermoautotrotrophicus* (Ribbe *et al*., 1997). Superoxide is produced by CO dehydrogenase through the oxidation of CO and the subsequent transfer of the electron to O_2. The superoxide ($O_2^{\cdot -}$) is reoxidized by superoxide oxidoreductase that delivers the electrons to a dinitrogenase. The dinitrogenase is capable of reducing N_2 and H^+, but not C_2H_2. The scheme has not been designed to give the correct stoichiometries.

monoxide dehydrogenase (CODH or St3). In contrast to the *in vivo* electron donor to the Fe protein, which is either ferredoxin or flavodoxin in the Mo-nitrogenase system, the St3 operates by coupling the oxidation of CO to CO_2 and then reduces O_2 to produce superoxide. The Fe-protein component of the classical nitrogenase is replaced by St2, which reoxidizes superoxide to O_2, and then transfers the electrons to St1 at which N_2 is reduced by eight electrons to two molecules of ammonia and one molecule of H_2. This reaction appears to require the hydrolysis of less MgATP per N_2 reduced than does the classical Mo-nitrogenase. Other unique features of this nitrogenase include the insensitivity of its nitrogen fixation reaction toward O_2, CO, and H_2, all of which are potent inhibitors of nitrogen fixation in the classical system. Finally, this nitrogenase does not catalyze the reduction of C_2H_2 to C_2H_4.

1.3 Molybdenum nitrogenase

1.3.1 The Fe protein

Although Fe protein can be separated from MoFe protein, it is essential for the nitrogenase enzymatic process. The Fe protein acts as an obligate electron donor to the MoFe protein in an MgATP-activated reaction. No other reductant has been shown to substitute for the Fe protein in this reaction, and it seems probable that the role of the Fe protein and its interaction with the MoFe protein is more complex than simply that of electron donation.

The X-ray crystal structure of the Fe protein from *A. vinelandii* (Georgiadis *et al.*, 1992) reveals that each subunit of the homodimer consists of a single large domain with an eight-stranded β sheet flanked by nine α helices (Figure 1.3). The [4Fe-4S] cluster is bridged between the identical subunits and is symmetrically coordinated by the thiolate groups of Cys-97 and Cys-132 from each subunit. (Note: *A. vinelandii* primary amino acid sequence numbering will be used unless otherwise noted.) It appears to be highly solvent exposed. In addition to the cluster, there are numerous van der Waals and polar interactions in the interface beneath the cluster that help stabilize the dimer structure.

A good indication of where and how MgATP binds to the Fe protein was first indicated by the comparison of Fe protein primary sequences to the primary sequences of

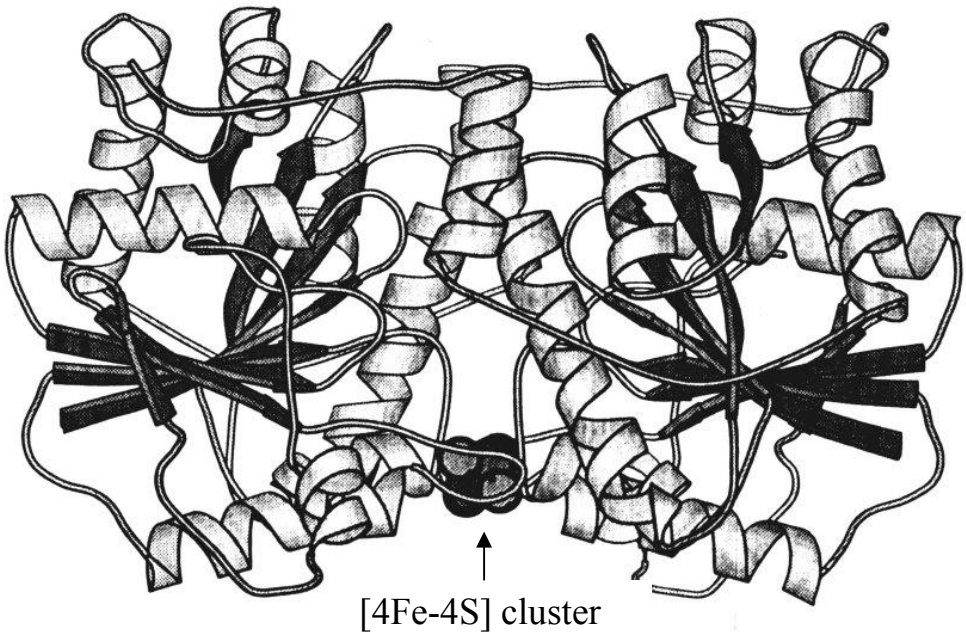

Figure 1.3 Ribbon diagram of polypeptide fold of the Fe protein dimmer from *A. vinelandii*, with space filling model for the [4Fe-4S] cluster (Adapted from Shen, 1994).

various other nucleotide binding proteins (Robson, 1984; Seefeldt *et al.*, 1992). These comparisons revealed that the Fe protein is a member of a large family of nucleotide binding proteins (e.g., RasP21 and RecA) that contain two sets of consensus amino acid sequences. There are Walker A-type (GX_4GKS/T; Walker *et al*., 1982; Robson, 1984) and Walker B-type (DXXGD; Walker *et al*., 1982) motifs that are identified in the crystal structure of the Fe protein from *A. vinelandii* as residues Gly-9 through Ser-16 and as residues Asp-125 through Asp-129, respectively. In the absence of MgATP, the Asp-125 residue is hypothesized to form an intra-subunit salt bridge to the Lys-15 residue.

A much clearer view of the MgATP binding site emerged by comparing the structural features of the Fe protein to the three-dimensional structural motifs of other nucleotide binding proteins (Howard and Rees, 1994; Schindelin *et al*., 1997; Jang *et al*., 2000). In the Fe protein, each MgATP binding site (one per subunit) is situated on the interfacial cleft between the subunits. The nucleotide binding sites are about 15-20 Å away from the edge of the [4Fe-4S] cluster, implying that MgATP hydrolysis and electron transfer are not directly coupled, but are mediated by allosteric effects. Nucleotide binding (and/or hydrolysis) causing a switch between alternative conformational states of a protein is a general transducing mechanism for coupling a variety of biochemical processes (Kim and Rees, 1994; Howard and Rees, 1994).

MgATP appears to serve at least three important functions in the proposed reaction mechanism. First, MgATP binding induces conformational changes in the Fe protein necessary for docking to the MoFe protein. Second, MgATP hydrolysis is coupled to intercomponent electron transfer. Finally, MgATP hydrolysis is coupled to the dissociation of the Fe protein from MoFe protein (Lanzilotta *et al*., 1996).

MgATP binding to the Fe protein is also known to result in a change in the properties of the [4Fe-4S] cluster, suggesting long-range communication through protein conformational changes. Nucleotide-induced changes in the properties of the Fe protein [4Fe-4S] cluster include e.g., its electron paramagnetic resonance (EPR) (Zumft *et al*., 1972), circular dichroism (CD) (Ryle et al., 1996), and ^{1}H NMR (Lanzilotta *et al*., 1995a) spectra, and a -120 mV shift in the redox potential of the $[4Fe\text{-}4S]^{2+/1+}$ couple (Watt *et al*., 1986). How does the nucleotide binding become communicated to the [4Fe-4S] cluster? At least one potential communication pathway that connects the MgATP site to

the cluster is a short protein chain extending from the MgATP binding site (Asp-125) to the [4Fe-4S] cluster ligand Cys-132 designed as switch II (Figure 1.4) (Ryle and Seefeldt, 1996). It appears that MgATP binding induces changes in the position of this switch, resulting in changes in the protein environment around the [4Fe-4S] cluster.

MgATP binding was proposed to trigger movement of switch II by breaking a salt bridge between Asp-125 and Lys-15. In this way, switch II could communicate events at the MgATP binding site to the [4Fe-4S] cluster *via* conformational changes. Evidence supporting this model was provided by characterization of altered Fe proteins substituted at either the Lys-15 (Seefeldt *et al*., 1992; Ryle *et al*., 1995) or the Asp-125 (Wolle *et al*., 1992) position. Substitution of Lys-15 by Gln results in an Fe protein that remains able to bind MgATP, but this binding event is not communicated to the [4Fe-4S] cluster (Seefeldt *et al*., 1992). This result suggests that the breaking of the salt bridge between Lys-15 and Asp-125 and the ionic interaction formed between Lys-125 and the γ-phosphate of MgATP may be a trigger that initiates the conformational change. Conversely, substitution of Asp-125 by Glu results in an Fe protein that mimics certain properties of the MgATP-bound form when it has MgADP, rather than MgATP, bound (Wolle *et al*., 1992). This latter result makes sense when it is considered that the extra methylene group in Glu compared to Asp should permit it to reach the α- and β-phosphates of bound MgADP in a way that might approximate the normal Asp interaction with β- and γ-phosphates of MgATP. By far the most interesting altered Fe protein is provided by shortening the Asp-125-to-Cys-132 switch II segment by deleting the intervening Leu-127 (ΔLeu-127) (Ryle and Seefeldt, 1996). This altered Fe protein becomes locked into a conformation that shows a striking resemblance to the MgATP-bound state even in the absence of any nucleotide. The picture that emerges from these studies is that the binding of the γ-phosphate of MgATP initiates a conformational change *via* the Asp-125 to Cys-132 signal transduction pathway that allows its communication with the [4Fe-4S] cluster.

Switch II also participates in defining the affinity for association with the MoFe protein. The conformational change associated with MgATP binding is a prerequisite for the correct docking of the Fe protein to the MoFe protein. Substitution of Lys-15 by Gln, which cannot form salt bridge to Asp-125 in switch II, produces an altered Fe protein that

cannot compete with the normal Fe protein for interaction with the MoFe protein. The Gln-15 altered Fe protein binds MgATP but does not undergo the nucleotide-induced conformation change and so is unable to correctly bind to the MoFe protein (Seefeldt *et al*., 1992). This feature contrasts with other altered Fe proteins that are inactive but are still able to undergo the MgATP-induced protein conformational change. For example, when Asp-129 is substituted by Glu (Glu-129) (Lanzilotta *et al*., 1995b), the altered Fe protein is able to compete with the normal Fe protein for interaction with MoFe protein. Glu-129, however, could not hydrolyze MgATP, transfer electrons to the MoFe protein, or reduce substrate. Asp-129 is part of switch II and has been suggested to be a possible general base that could activate water for hydrolysis of MgATP.

A second possible communication pathway within the Fe protein, which is structurally similar to another switch in other nucleotide switch proteins, is called switch I (Howard and Rees, 1994). In the Fe protein, the switch I domain extends from Asp-39, which is located near the terminal phosphate of bound nucleotide through a loop that is located on the surface of the Fe protein at the proposed docking interface, to Val-67 (Figure 1.4). This loop region approximately comprises residues 59 to 67 and has been suggested to participate in interaction with MoFe protein (Peters *et al*., 1994). Thus, it can be imagined that the surface loop connected to switch I serves as a toggle through which the nucleotide-bound state can communicate its readiness for docking with the MoFe protein.

An early investigation by EPR spectroscopy demonstrated that, as the Fe protein is reduced, it goes from an EPR "silent", diamagnetic state to an S = 1/2 paramagnetic spin state to give a broadened "rhombic" EPR signal in the $g = 2$ region of the spectrum (Orme-Johnson *et al*., 1972). Addition of MgATP to the reduced Fe protein sharpens this signal into an "axial" spectrum. The [4Fe-4S] cluster in reduced Fe protein is in the 1+ redox state with three Fe^{2+} and one Fe^{3+} ions. On careful examination, this EPR spectrum of $[4Fe\text{-}4S]^{1+}$ in Fe protein in frozen buffer solution exists partially in a S = 3/2 spin state (Lindahl *et al.*, 1985; Watt and McDonald, 1985). This observation, which may have implications for nitrogenase turnover (reviewed by Burgess and Lowe, 1996; Smith, 1999), indicates that the Fe protein can exist in at least two conformations of similar energy.

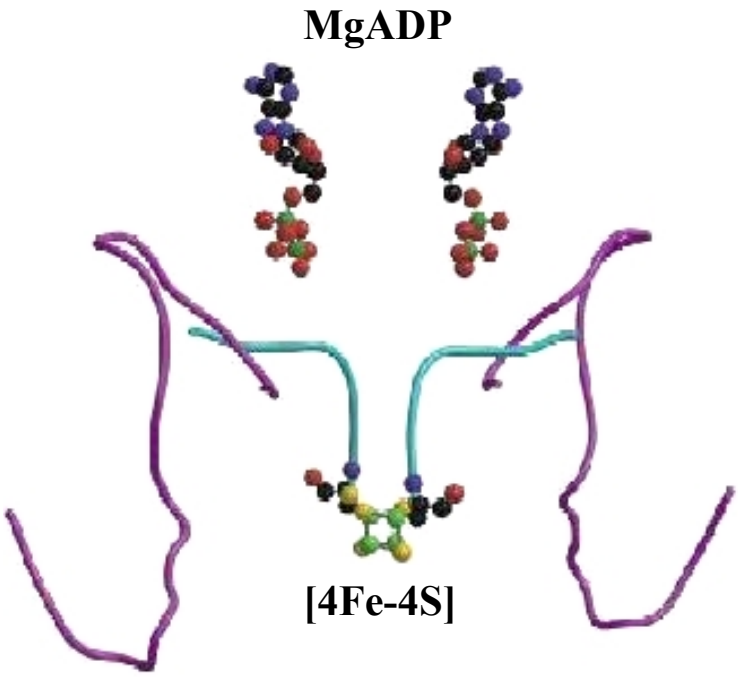

Figure 1.4 Switch I (magenta), switch II (cyan), the [4Fe-4S] cluster, and the two bound MgATP molecules (Christiansen and Dean, 2001). Atoms colors are carbon in black, iron in green, sulfur in yellow, nitrogen in blue, oxygen in red, and phosphorous in dark green.

Until the mid-1990s, the Fe protein was regarded as a one-electron donor to the MoFe protein and cycled between the $[4Fe\text{-}4S]^{1+}$ and $[4Fe\text{-}4S]^{2+}$ redox states during turnover. However, it is now known that, in the presence of either flavodoxin (in its hydroquinone state) or the artificial electron donors (methyl viologen or titanium(III) citrate) instead of sodium dithionite, the Fe protein can be reduced further to the $[4Fe\text{-}4S]^{0}$, all Fe^{2+}, redox state (Watt and Reddy, 1994). These data indicate that, *in vivo*, the Fe protein may act as a two-electron donor to the MoFe protein.

Finally, in addition to its electron transfer function, the Fe protein has at least two and possibly three other functions. First, it is required for the biosynthesis of the FeMo cofactor. Second, it is required for the insertion of preformed FeMo cofactor into the separately biosynthesized FeMo cofactor-deficient MoFe protein. Third, it has been implicated as being involved the regulation of the alternative nitrogenase systems.

1.3.2 The MoFe protein

Although there is minimal amino acid sequence homology between the α- and β-subunits, the X-ray crystallographic structure of the *A. vinelandii* MoFe protein (Kim and Rees, 1992a,b) shows that the α- and β-subunits exhibit similar polypeptide folds, which consist of three domains of the parallel β-sheet/α-helix type (Figure 1.5). At the interface between the three domains in the α-subunit is a wide shallow cleft with the FeMo cofactor located at the bottom of this cleft. The P cluster, in contrast, is buried about 10 Å below the protein surface at the interface between each pair of α- and β-subunits, and is bound by cysteine residues from both subunits. A pseudo-two fold rotation axis passes between the two halves of the P cluster and relates the α- and β-subunits. Each αβ pair of subunits contains one FeMo cofactor and one P cluster and each pair is often envisaged as a functional unit, although they have never been isolated in this form. Between the two αβ dimers is an open channel of about 8 Å diameter with the tetrameric two-fold axis passing through it. The tetrameric interface is dominated by interactions between helices from the two β subunits and exhibits a cation-binding site (probably occupied by either calcium or magnesium) that is coordinated by residues from both β-subunits.

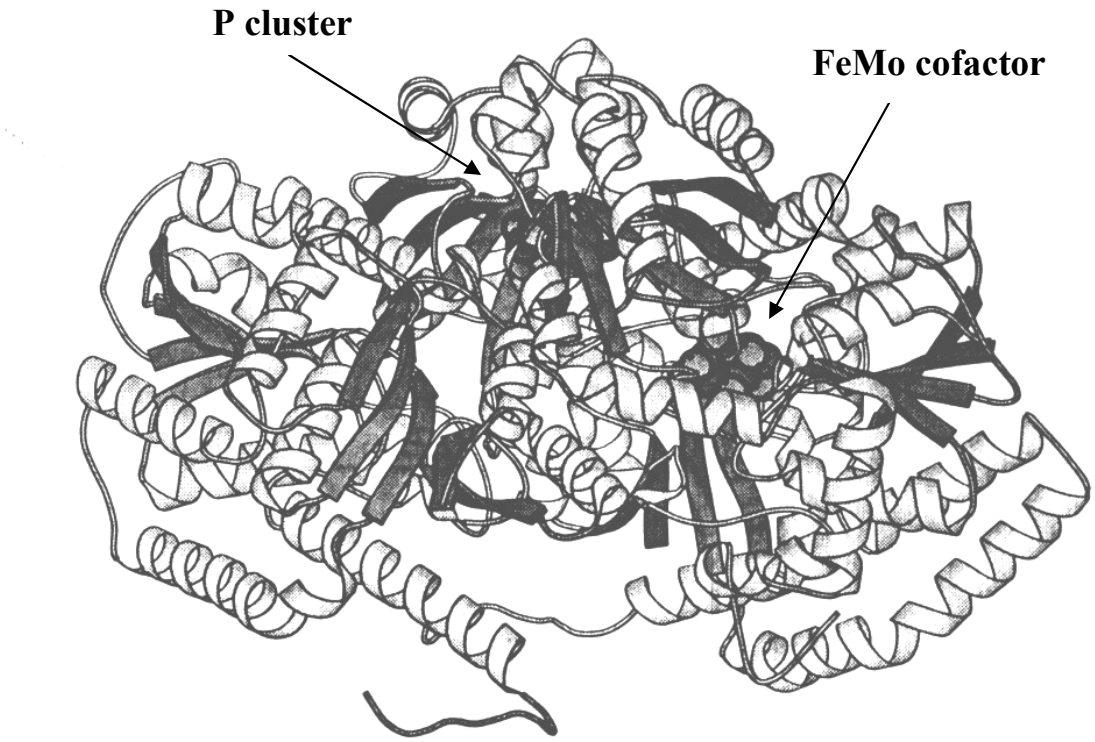

Figure 1.5 Ribbon diagram of the polypeptide fold of MoFe protein αβ subunit dimmer from *A. vinelandii*, with space-filling models for the P cluster and the FeMo cofactor (Adapted from Shen, 1994).

1.3.2.1 The P cluster

As noted previously, the P clusters are bonded at the interface of the α- and β-subunits by cysteine ligands (Kim and Rees, 1992b; Chan *et al*., 1993). Each P cluster contains eight Fe atoms and seven sulfides that are arranged as two linked, cuboidal [4Fe-4S] subcluster fragments (Figure 1.6). Four cysteines, two from the α-subunit (αCys-62 and αCys-154) and two from the β-subunit (βCys-70 and βCys-153), coordinate individual Fe atoms of the P cluster as typical terminal cysteinyl thiolate ligands. Two cysteines (αCys-88 and βCys-95) link the subclusters by each bridging two Fe atoms, one from each subcluster.

The precise structure of the P cluster has proved controversial, but has now been rationalized. Initially, it was suggested that the P cluster consisted of two [4Fe-4S] clusters linked only through the bridging cysteine residues (Kim and Rees, 1992b). This proposal was then modified so that the two [4Fe-4S] clusters were also joined through a disulfide bond at one corner of each subcluster (Chan *et al*., 1993, Figure 1.6A). This interpretation of the data was challenged by Bolin *et al*., (1993) who proposed a third structure, where the two [4Fe-4S] clusters, as well as being bridged by two cysteine ligands, are joined through a common sulfur atom to give an overall stoichiometry of [8Fe-7S] (Figure 1.7A). The data have now been fully rationalized using MoFe protein from two bacterial sources, *A. vinelandii* (Peters *et al*., 1997) and *K. pneumoniae* (Mayer *et al*., 1999), by showing that the original structure was most likely a mixture of two P cluster redox states, P^N and P^{OX} (Figure 1.7). During the relatively long time required to produce crystals of the MoFe protein, some of the P clusters become oxidized from P^N (the normal redox state) to P^{OX} (the oxidized state). During oxidation, two of the iron-sulfur bonds break to generate a more open structure in one half of the P cluster. These broken bonds are replaced by βSer-188 becoming bound to the same Fe atom as βCys-153 and by the backbone amide-N of αCys-88 also binding to Fe. Thus, the first described model of the P cluster as an [8Fe-8S] likely reflects the inappropriate modeling of a single structure to a mixture of two P cluster redox states.

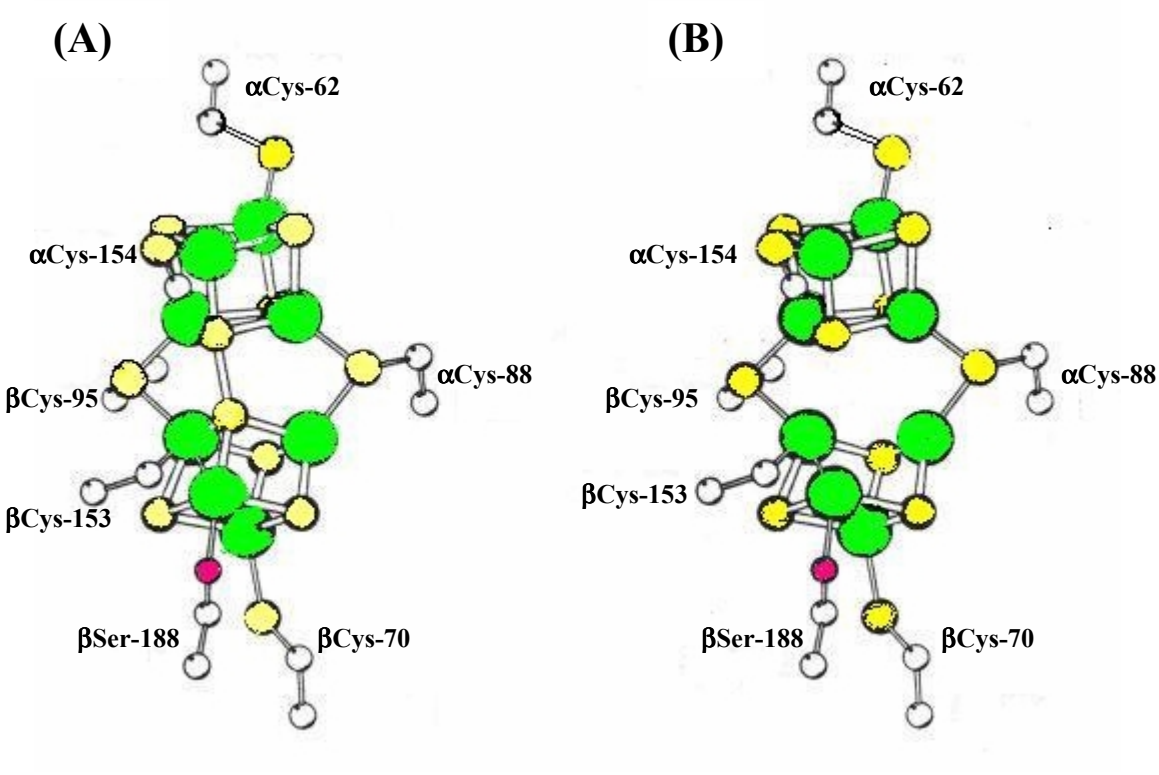

Figure 1.6 P cluster: A) 8Fe-8S model of the P cluster and surrounding environment of MoFe from *A.vinelandii*. B) 8Fe-7S model of the P cluster as seen in structure analyses of the MoFe protein from *A. vinelandii*). Atom colors are carbon in white, iron in green, sulfur in yellow, and oxygen in red (Adapted from Howard and Rees, 1996).

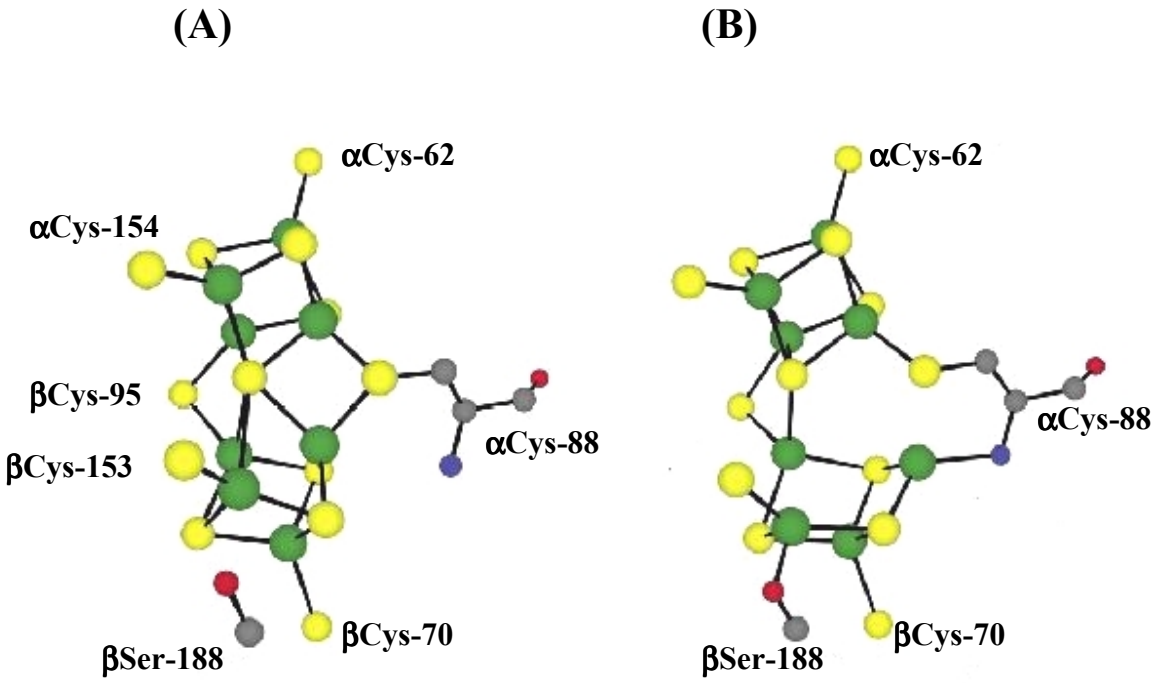

Figure 1.7 The two difference structures of the P cluster in A) the reduced state (P^N state) and B) the oxidized state (P^{OX} state). Atom colors are carbon in black, iron in green, sulfur in yellow, nitrogen in blue, and oxygen in red (Adapted from Peters *et al.*, 1997).

1.3.2.2 The FeMo cofactor

Unlike with the P cluster, the X-ray diffraction data from the MoFe protein of *A. vinelandii* (Kim and Rees, 1992a,b), *C. pasteurianum* (Kim *et al*., 1993) and *K. pneumoniae* (Mayer *et al*., 1999), all agree on the composition, structure, and location of the FeMo cofactor (Figure 1.8). The FeMo cofactor is buried 10 Å below the protein surface of the α subunit. The [Mo-7Fe-9S-homocitrate] metallocluster is composed of two subclusters, [Mo-3Fe-3S] and [4Fe-3S], which are bridged by three sulfides to link the opposing Fe atom from each subcluster in a trigonal arrangement. The organic constituent, homocitrate, is coordinated to the Mo atom through its 2-hydroxyl and 2-carboxyl groups. The FeMo factor is covalently attached to the protein only through a thiolate ligand provided by αCys-275 to an Fe atom at one end of the cofactor and by the side-chain ε-nitrogen atom of αHis-442 to the Mo atom at the opposite end.

Although the FeMo cofactor is buried at the interface between three domains of the α subunit, the protein environment around the FeMo cofactor contains many polar and charged groups and includes some hydrophobic groups. Hydrogen bonds to sulfur atoms in the cluster are provided by the polar side chain of residues αArg-96, αHis-195, αArg-359 and the NH groups of αGly-356 and αGly-357. Along with the side chains of αVal-70 and αPhe-381, these residues pack against the central 'waist' of the FeMo cofactor containing the trigonal irons and bridging sulfurs. The protein environment surrounding the homocitrate is also relatively polar. Each of the terminal carboxylate groups of homocitrate forms a hydrogen bond to the side chain of either αGln-440 or αGln-191. Furthermore, the homocitrate is surrounded by a "pool" of about 10 water molecules that participate in hydrogen-bonding interactions.

The distance from edge-to-edge between the homocitrate site of FeMo cofactor and the closest P cluster is about 14 Å. Fours helices (α63-α74, α88-α92, α191-α209, and β93-β106) link the two metal-containing centers as does the hydrogen-bonding network involving the NH of αGly-61 (adjacent to the P cluster ligand, αCys-62), αGln-191 and homocitrate. All could play roles as electron- and/or proton-transfer pathways.

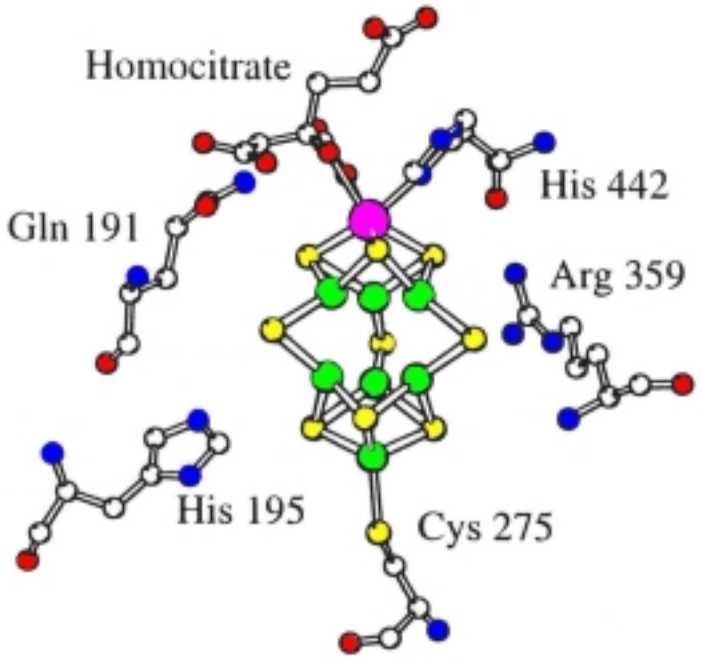

Figure 1.8 Ball and Stick model of *A vinelandii* FeMo cofactor and polypeptide environment. Atom colors are carbon in white, iron in green, sulfur in yellow, molybdenum in purple, nitrogen in blue, and oxygen in red (Adapted from Peters *et al*., 1995b).

1.3.2.3 Redox states and spectroscopic properties of the MoFe protein.

The MoFe protein exhibits complex redox properties. Each tetrameric $\alpha_2\beta_2$ molecule of the MoFe protein contains two P clusters and two FeMo cofactors. As normally isolated in the presence of sodium dithionite, the FeMo cofactors are in an S = 3/2 spin state and so exhibit an EPR spectrum with *g* values near 4.3 and 3.7 and 2.01 (Figure 1.9). The P clusters are EPR silent.

EPR and Mössbauer spectroscopies have been used to characterize distinct oxidation states of the P cluster mainly from the *A. vinelandii* MoFe protein (Surerus *et al*., 1992; Pierik *et al*., 1993; Tittsworth and Hales, 1993). Mössbauer studies on the dithionite-reduced state or native state (P^N) of the P cluster indicate that all the iron atoms in the cluster are in the ferrous state (Surerus *et al*., 1992). More reduced forms of the P cluster (if they exist) have not yet been detected. However, the combined analyses provide a sequence of redox state levels of the P cluster with each level correlating to a unique EPR spin state, and some cases with a mid point potential value (Pierik *et al*., 1993).

The MoFe protein is often considered as two functionally equivalent $\alpha\beta$ units each with its own P cluster. The sequence of one-electron oxidation advances from the fully reduced state, P^N (or P) state, to the $P^{SEMI\text{-}OX}$ (or P^+) state, followed by the P^{OX1} (or P^{2+}) state, and then the P^{OX2} (or P^{3+}) state (Table 1.1). There is also an additional one-electron oxidation from P^{OX2} to $P^{SUPEROX}$ that results in irreversible damage to the P cluster. An interesting model of P cluster oxidation assumes that the paramagnetism is not delocalized over the entire 8Fe structure but instead occurs on each [4Fe-4S] half of double cubane structure. As half is oxidized, a unique spin state is established and, if both halves become oxidized, spin coupling between them could generate an integer-spin signal. This model of P cluster oxidation might also explain the equal probability of P to P^+ and P^+ to P^{2+} transitions that is found on oxidation of the P clusters using limiting thionine (Tittsworth and Hales, 1993).

The crystal structure of the MoFe protein from *A. vinelandii* has been refined to 2.0-Å resolution in two different oxidation states, P^N and P^{OX} (P^{2+}), that were confirmed by EPR spectroscopy (Peters *et al*., 1997). The reduced state, P^N, has six Fe atoms

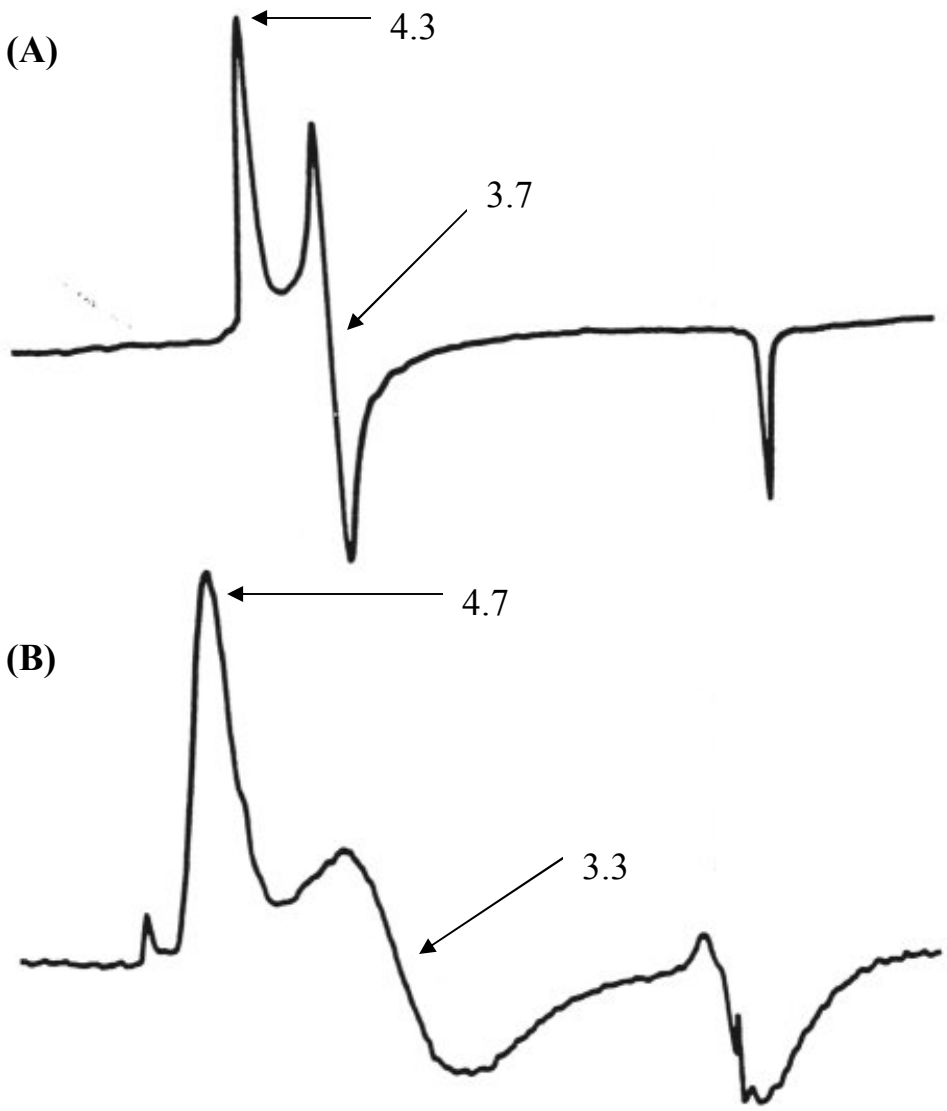

Figure 1.9 Comparison of S = 3/2 signals of FeMo cofactor: A) protein-bound FeMo cofactor (g = 4.3, 3.7) and B) of isolated FeMo cofactor (g = 4.7, 3.3). Adapted from Newton and Dean, 1993.

Table 1.1 Multiple redox levels and EPR spin state of the P cluster

Name[a]	Alternative name[b]	Redox potential vs. NHE[c]	EPR spin state	Comments
P^N	P	- 307 mV	0	As isolated, dithionite-reduced state
$P^{SEMI-OX}$	P^+	- 307 mV	1/2 and 5/2	Transient state in oxidative titrations
P^{OX1}	P^{2+}	+ 90 mV	3 and 4	Excited state, parallel mode EPR at $g = 12$
P^{OX2}	P^{3+}	+ 345 mV	1/2 and 7/2	Mixed spin state of unknown origin
$P^{SUPEROX}$	-	-	> 2	Irreversible damage

[a] Adapted from Pierik *et al*., 1993. [b] Adapted from Tittsworth and Hales, 1993. [c] Midpoint potential for transition to next oxidation level, $P^N \rightarrow P^{N+1}$.

bonding to a central hexacoordinate sulfur with distorted octahedral geometry and both the Oγ of βSer-188 and the backbone amide N of αCys-88 are not coordinated to the Fe atoms of the P cluster (Figure 1.7A). In the two-electron-oxidized form, P^{OX}, two of these iron-sulfur bonds are broken and replaced by bonds to βSer-188 and αCys-88, which become coordinated to the Fe atoms (Figure 1.7B). Because these two residues are likely to be deprotonated when they bind to the Fe atoms and protonated when they are not bound, this redox-driven structure rearrangement may be a mechanism by which proton transfer is coupled to electron transfer.

Smith (1999) has suggested that breaking one or other of these two iron-sulfur bonds could be responsible for the two spin states observed on dye oxidation. Breaking one bond could result in the S = 1/2 state and breaking the other would result in generation of the S = 5/2 state. The different spin states arise because of the slightly different environments of the two halves of the cluster in the one-electron oxidized forms. If this is the case, then it seems likely that the bonds are broken randomly to give a mixture of the two structures, one which exhibits the S = 1/2 state and the other exhibits the S = 5/2 state of P^+ state.

1.3.3 The nitrogenase complex

Complex formation between the Fe protein and MoFe protein has been known for years to be a critical step in the overall mechanism of nitrogenase catalysis. A docking model based on the crystal structures of the separate components that takes into account chemical cross-linking studies and amino acid-substitution studies has been proposed (Howard, 1993; Howard and Rees, 1994; Kim and Rees, 1992a). This model pairs the two-fold symmetric surface of the Fe protein homodimer with the exposed surface of a MoFe protein pseudosymmetric αβ-subunit interface. In this arrangement, the [4Fe-4S] cluster of Fe protein is positioned as close as possible to the P cluster of MoFe protein, which accommodates the view that the primary electron-transfer event involves transient delivery of an electron from the [4Fe-4S] cluster of the Fe protein to a MoFe protein P cluster. Also, the arrangement of several charged groups on the respective surfaces of the Fe and MoFe proteins could permit reciprocal ionic interactions between the component proteins.

This model has been confirmed by the X-ray crystal structure of the ADP:AlF_4^--stabilized nitrogenase complex from *A. vinelandii* at 3-Å resolution (Schindelin *et al*., 1997). A non-hydrolyzable nucleotide triphosphate analogue, ADP:AlF_4^-, which is believed to mimic the transition state for hydrolysis of MgATP to MgADP, is bound to the Fe protein which then docks with the MoFe protein (Figure 1.10). Because the nucleotide analogue cannot hydrolyze, the docked complex has an extended lifetime when compared to the transient existence of the complex when MgATP is used. However, there are some structural features that can only be described and quantified in detail by the crystal structure. Two Fe proteins bind to the MoFe protein tetramer along a pseudo-2-fold axis of symmetry.

The structure shows that, upon binding a nucleotide triphosphate analogue and complexation, large structural changes occur in the Fe protein, but not in the MoFe protein. In the Fe protein, the interface between the two γ-subunits becomes closer due to a 13º-rotation of the two subunits towards the interface region, rendering the structure more compact. These structural changes in Fe protein also result in complete burial of the [4Fe-4S] cluster in the interface between the Fe protein and the MoFe protein. The conformational changes in the Fe protein result in a smaller inter-cluster distance between the [4Fe-4S] and P cluster than was anticipated from modeling studies (14 Å as opposed to 18 Å) which is important when considering electron transfer between these centers. It should be noted that two ADP:AlF_4^- molecules in the complex were bound to each Fe protein molecule, with one nucleotide associated largely with each subunit and bound roughly parallel to the dimer interface. This nucleotide conformation differs from that observed in isolated Fe protein with partial occupancy by ADP where the ADP bound across the subunit interface (Georgiadis *et al*., 1992).

This complex structure supports the idea of nucleotide-induced conformational shifts as the catalytic driving force in the early steps of the nitrogenase mechanism. The net contraction of the subunit interface of the Fe protein may represent the conformation necessary for effective protein docking, ATP hydrolysis and electron transfer. After hydrolysis and phosphate release, many of the inter-subunit contacts in the Fe protein might cause a relaxation into the more open conformation that could drive both the dissociation of the complex and the exchange of MgATP for MgADP. The need for

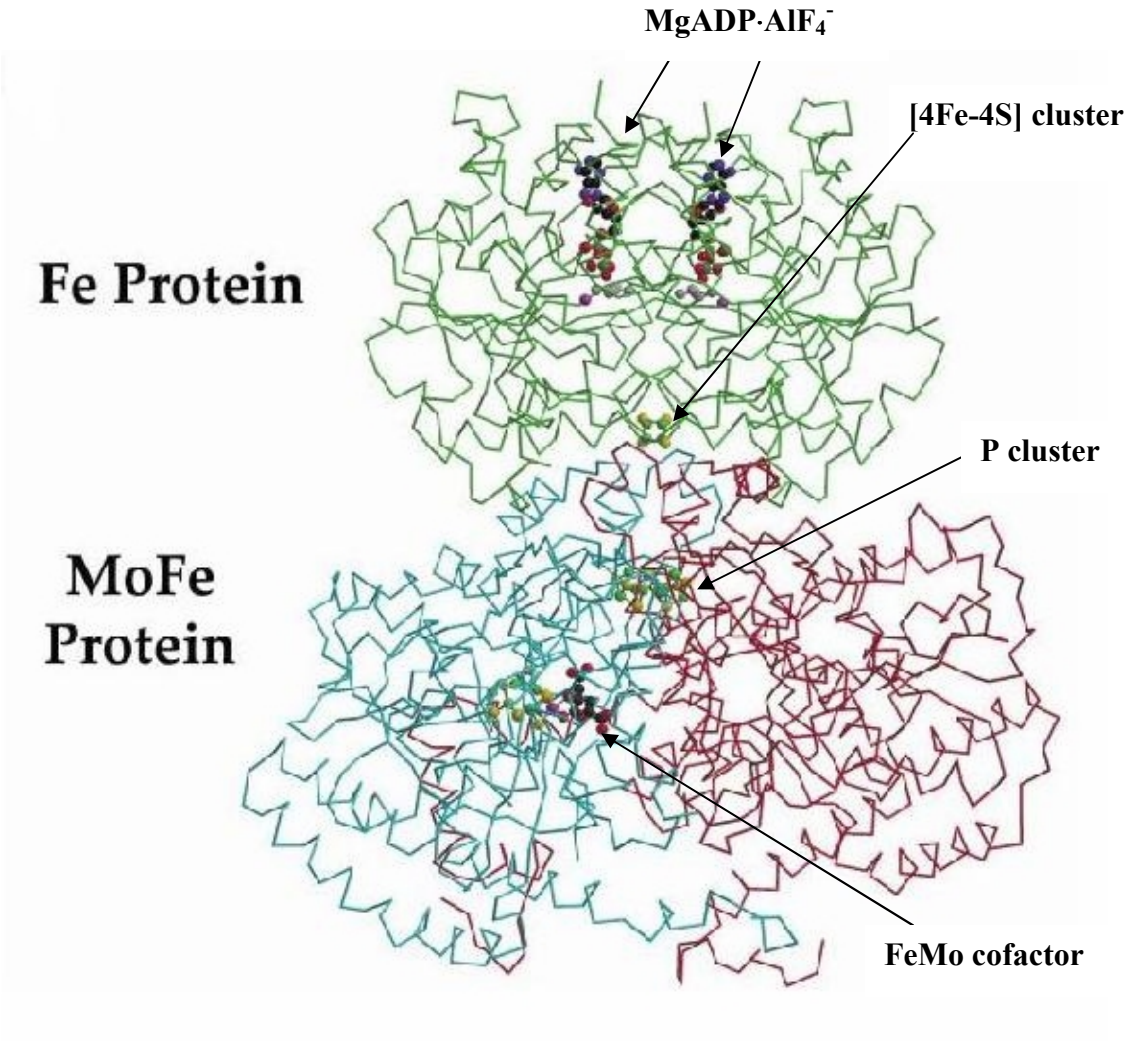

Figure 1.10 The putative "transition-state" complex from between the Fe protein:MgADP·AlF_4^- and MoFe protein (Adapted from Christiansen and Dean, 2001). For simplicity only one αβ pair of subunits of the MoFe protein is shown. The figure indicates the relative positions of the two bound MgADP·AlF_4^- molecules, the Fe protein [4Fe-4S] cluster, the MoFe protein P cluster and FeMo cofactor.

dissociation of the complex is likely communicated to a loop on the surface of the Fe protein through the switch I region after MgATP hydrolysis occurs (see section 1.3.1).

A tight Fe protein-MoFe protein complex is formed when an Fe protein whose switch II region has been shortened by one amino acid by deletion of Leu-127 (ΔLeu-127) is mixed with MoFe protein (Lanzilotta *et al*., 1996). The ΔLeu-127 mutation results in an Fe protein that adopts a MgATP-like bound form even in the absence of nucleotide (Ryle and Seefeldt, 1996). Redox studies on the resulting complex show that the midpoint potential of the [4Fe-4S] cluster of the Fe protein is lowered by about - 200 mV from - 430 to - 620 mV in the complex and that of the P cluster is lowered by about - 80 mV from - 310 to - 390 mV but there was no significant change at the FeMo cofactor (Ryle and Seefeldt, 1996; Lanzillotta and Seefeldt, 1997). The net outcome of these redox potential changes is that the free energy change for electron transfer is increased by about 300 - 600 mV making it much more thermodynamically favorable. Both the arrangement of the clusters and the changes in redox potential of the clusters in the complex strongly suggest that the electron transfer pathway is from Fe protein *via* the P cluster to the FeMo cofactor, where substrate reduction occurs.

1.3.4 Biosynthesis of molybdenum nitrogenase

Nitrogenase is a complicated enzyme and its biosynthesis is tightly regulated in microorganisms. If there is sufficient fixed nitrogen available for growth, then nitrogenase is not required and its biosynthesis is repressed. All nitrogenase enzymes are damaged by exposure to O_2 and so, if the level of O_2 within the cell is too high, then nitrogenase synthesis is again suppressed. The intracellular pathway, which senses the levels of fixed nitrogen and oxygen, have been elucidated to some extent, but major questions still remain.

1.3.4.1 The *nif* genes

Because of its amenability to using the classical bacterial genetic manipulations developed for *E. coli*, the facultative anaerobe *K. pneumoniae* was used in early work involved in identifying the genes involved in nitrogen fixation. This organism has contiguous 20 *nif* genes organized into seven transcriptional units. A diagram of the physical organization of *nif* and *nif*-associated genes from *K. pneumoniae* and *A.*

vinelandii is shown in Figure 1.11. In *A. vinelandii*, *nifJ* has not been found and it, therefore, contains only 19 *nif* genes. There are, however, about a dozen more open reading frames (designated as *orf1* and so on) scattered within the *A. vinelandii nif* clusters whose functions are not clear.

Two of the twenty *nif*-specific genes are the regulatory genes, *nifA* and *nifL* (Arnold *et al*., 1988). The products of these two genes control the last step in the regulation of the expression of the other *nif* genes in response to fixed nitrogen and O_2 levels (Dixon, 1998). NifA is the activator for expression of the seven transcriptional units of *nif* genes and NifL is a repressor of NifA activity. NifL is a flavoprotein that is inactive when reduced but, when oxidized, binds to NifA and inactivates it, thus preventing activation of the other transcriptional units. In addition, NifL is sensitive to energy charge (e.g., the ratio of ADP to ATP) and possibly directly sensitive to the presence of ammonia.

The *nifJ* and *nifF* genes encode the electron transport proteins, pyruvate:flavodoxin oxidoreductase and a flavodoxin, respectively. The gene *nifJ* is required for nitrogen fixation in *K. pneumoniae*. Because it is absent in *A. vinelandii*, there must be another gene product that serves as part of the *in vivo* electron donor system to the nitrogenase system. Similarly, the *nifF* gene product is not absolutely required for nitrogenase activities in *A. vinelandii* (Martin *et al*., 1989) and so alternatives to this electron transfer agent must also exist.

1.3.4.2 Biosynthesis of the Fe protein and MoFe protein

The primary translation products of the nitrogenase structural genes, *nifH* and *nifDK* are not active. Many other *nif*-specific genes are required to activate these immature structural components. The function of the products of many of these *nif*-specific maturation genes is to catalyze the formation and then insertion of the individual metalloclusters into the apo-form of the Fe protein and MoFe protein.

The Fe protein polypeptide is encoded by the *nifH* structural gene. Only the *nifM* gene product is specifically required for its biosynthesis. The *nifM* gene product has not yet been isolated in active from, but it appears to be a member of a family of

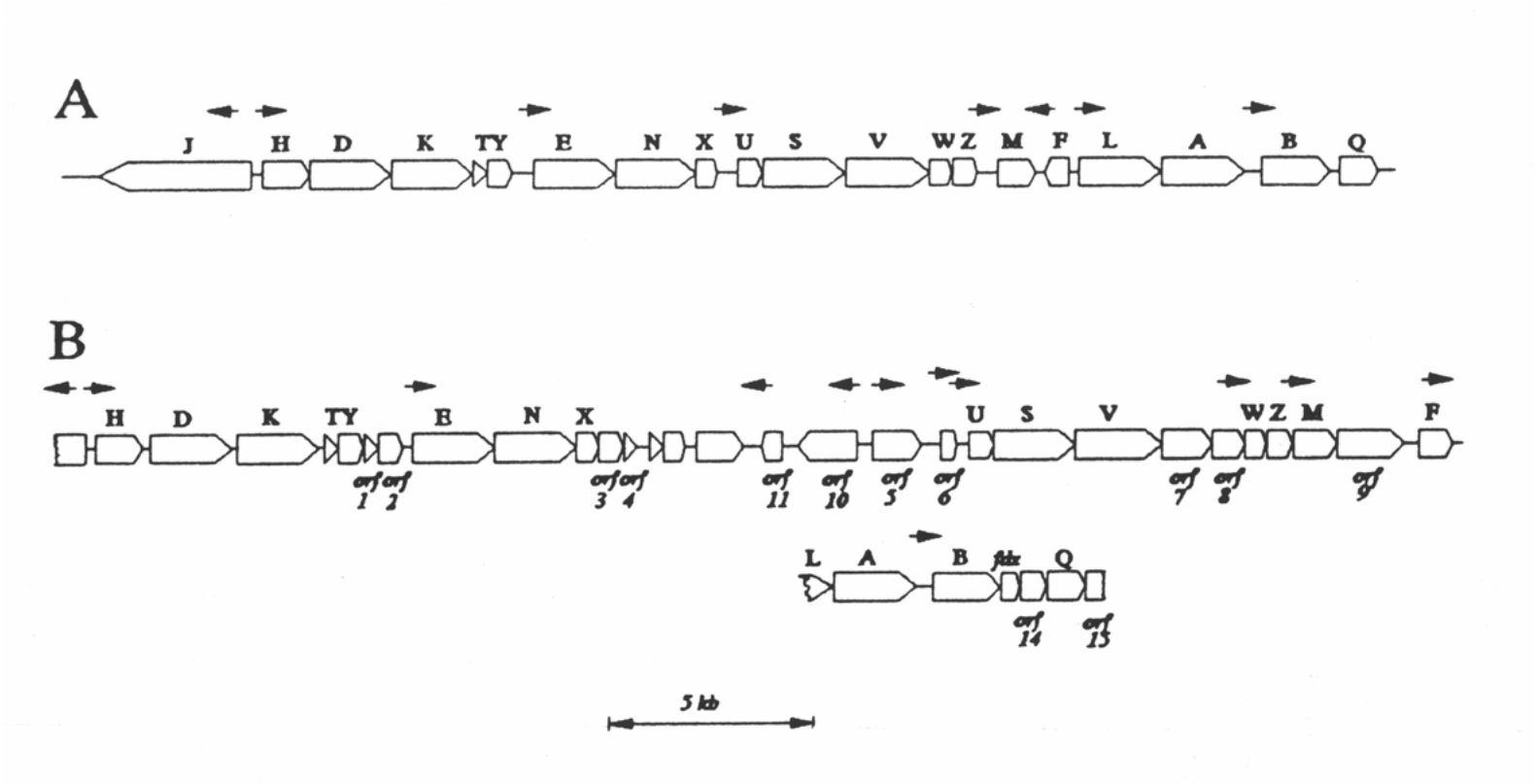

Figure 1.11 Comparison of the physical organizations of *nif* genes from: (A) *K. pneumoniae* and (B) *A. vinelandii* (Adapted from Dean and Jacobson, 1992)

peptidyl-prolyl isomerases (Rudd *et al*, 1995), which assist protein folding by catalyzing the cis/trans isomerization of certain peptidyl-prolyl bonds. It is not obvious why such a requirement exists for the maturation of the Fe protein, but it might involve the formation of a transient state of the immature Fe protein necessary for insertion of the [4Fe-4S] cluster.

The biosynthesis of the MoFe protein is extremely complex. The products of at least six genes, *nifQ*, *nifB*, *nifV*, *nifN*, *nifE*, and *nifH*, are involved in the biosynthesis of the FeMo cofactor alone. The nitrogenase Fe protein, whose subunits are the product of *nifH*, is required for both formation and insertion of the FeMo cofactor (Filler *et al*., 1986; Robinson *et al*., 1987). The Fe protein's specific function in this processe is unknown but neither its MgATP-binding and -hydrolysis properties nor its electron-transfer capability are involved (Gavini and Burgess, 1992). Biochemical complementation experiments show that the FeMo cofactor is initially synthesized elsewhere and then inserted into a FeMo cofactor-deficient MoFe protein that contains intact P clusters (Ugalde *et al*., 1984).

The *nifQ* gene product has a role in providing the Mo atom for the FeMo cofactor, especially under Mo-deficient conditions, but its exact role is unknown. The *nifV* gene encodes a homocitrate synthase that catalyzes the condensation of acetyl-CoA and α-ketogutarate to form homocitrate, the organic constituent of FeMo cofactor (Hoover *et al*., 1987; Zheng *et al*., 1997). The product of the *nifB* gene catalyzes the formation of a FeMo cofactor precursor called NifB cofactor (Shah *et al*., 1994). NifB cofactor appears to provide the basic Fe-S framework necessary for FeMo cofactor construction and becomes accommodated within the NifEN complex (Roll *et al*., 1995). A portion of the biosynthetic process occurs within a complex of the products of *nifEN*. The *nifEN* gene products bear primary sequence similarity to the products of the *nifDK* structural genes (Brigle *et al*., 1987) and a heterotetrameric complex of NifEN likely serves as a molecular scaffold for FeMo cofactor assembly (Brigle *et al*., 1987; Paustian *et al*., 1989).

The *nifS* and *nifU* gene products catalyze reactions that are involved in the general mobilization of S and, possible, Fe for metallocluster assembly (Zheng *et al*., 1994; Zheng and Dean, 1994; Fu *et al*., 1994). The *nifS* gene product is a pyridoxal phosphate-

activated cysteine desulfurase that activates S for Fe-S cluster formation (Zheng *et al*., 1993; Zheng *et al*., 1994). The *nifU* gene product might have a role in providing Fe (Fu *et al*., 1994; Yuvaniyama *et al*., 2000). Homologues to *nifU* and *nifS* whose expression is not under *nif*-specific control, are present in many organisms and these may function in general Fe-S cluster formation and repair (Flint, 1996).

The products of the *nifX*, *nifW* and *nifZ* genes might also have some role in FeMo cofactor biosynthesis (Jacobson *et al*., 1989; Shah *et al*., 1998). NifW may be involved in either homocitrate transport or in the incorporation of this compound into the FeMo cofactor of nitrogenase (Masepohl *et al*., 1993). With *K. pneumoniae*, a small molecular-weight protein, encoded by *nifY*, appears to be associated with the apo-MoFe protein produced in strains lacking either *nifB* or *nifEN* activity. The NifY may stabilize an apo-MoFe protein conformation that is amenable to FeMo cofactor insertion (White *et al*., 1992; Homer *et al*., 1993). A different small molecular-weight protein, which is called gamma and is not encoded by *nifY*, appears to serve the same function in *A. vinelandii* (Homer *et al*., 1995).

1.4 The reaction mechanism of molybdenum nitrogenase

Nitrogenase is one of the slowest enzymes present in bacteria and it has a turnover time of approximately 1.5 sec at 23 ºC for the reduction of N_2 to ammonia and the concomitant evolution of one equivalent of H_2. Its slowness is compensated by its relative abundance of up to 10% of the total soluble protein of free-living diazotrophs. It is widely accepted that the direction of electron flow is from reductant to Fe protein to MoFe protein and finally to bound substrate. The exact details of the mechanism of nitrogenase are still not clear. The long turnover time has made it possible to study partial reactions kinetically and the pre-steady state phase of the functioning enzyme by employing techniques, such as stopped-flow spectrophotometry, rapid freeze EPR and rapid chemical quench (Thorneley and Lowe, 1983).

1.4.1 The Lowe/Thorneley kinetic model of nitrogenase action

The Lowe/Thorneley model was derived from a pre-steady-state kinetic study of *K. pneumoniae* nitrogenase activity at 23 ºC, pH 7.4 with sodium dithionite as the reductant for the Fe protein (Lowe and Thorneley, 1984a,b; Thorneley and Lowe,

1984a,b). This model was developed in terms of two main processes, the Fe protein oxidation-reduction cycle and the MoFe protein cycle.

1.4.1.1 The Fe protein oxidation-reduction cycle

The Fe protein (FeP) with bound two MgATP functions as a single electron donor to the MoFe protein (MoFeP) in the Fe protein cycle (Thorneley and Lowe, 1983) (Figure 1.12). The Fe protein cycle is broken down into four discrete steps, each of which may be a composite of several reactions. 1) The initial step is the reduced FeP protein$(MgATP)_2$ complex associating with the MoFe protein. 2) An electron is transferred from the Fe protein to the MoFe protein coupled with MgATP hydrolysis to MgADP and P_i. 3) The oxidized Fe protein$(MgADP)_2$ complex dissociates from the reduced MoFe protein. 4) Fe protein is re-reduced by sodium dithionite and the MgADP is replaced by MgATP. In this cycle, step 3, the dissociation of the two proteins, is rate determining for the overall enzyme turnover when all components are at saturating concentration.

Following the first round of electron transfer, we are left with the free reduced MoFe protein. This protein can proceed to form a complex with reduced Fe protein$(MgATP)_2$ and the cycle can be repeated over and over again. This sequence leads to the concept, which will be discussed next, that several reduced states of the MoFe protein exist during turnover. These states will be referred to as E_0, E_1, E_2, etc. with the numbers indicating the level of reduction (number of electrons accepted) of the MoFe protein (E) relative to the dithionite reduced state (E_0).

1.4.1.2 MoFe protein cycle

The kinetics of nitrogenase action is best understood in terms of the MoFe protein cycle. This cycle (Figure 1.13) comprises the eight Fe protein cycles that are required to transfer eight electrons and eight protons to one $\alpha\beta$-half of the MoFe protein in order to reduce N_2 to two ammonia and to evolve one H_2 (Thorneley and Lowe, 1984a). To obtain successive redox states of the MoFe protein, it is necessary to undergo successive cycles of complex formation, MgATP hydrolysis coupled with electron transfer, and complex dissociation. The kinetic constants of the Fe protein cycle are assumed to be the

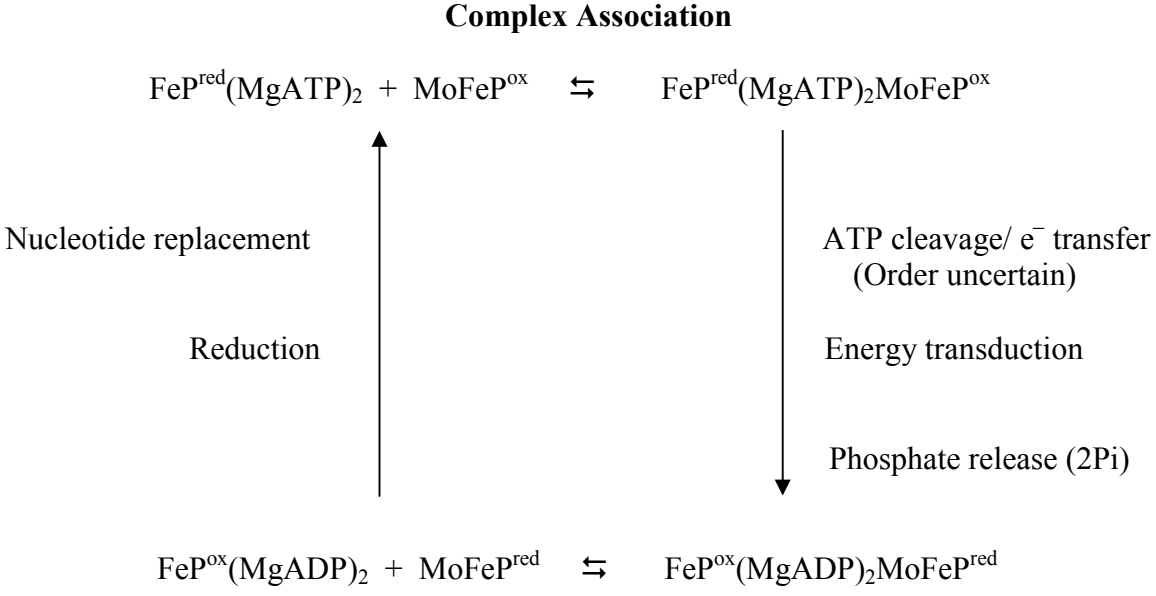

Figure 1.12 The Fe protein oxidation-reduction cycle of Mo-nitrogenase (Adapted from Thorneley and Lowe, 1985). MoFeP represents one αβ-subunit dimer of the two functionally equivalent halves of the MoFe protein, while FeP represents the Fe protein. The redox states are indicated by the superscripts ox (oxidized) and red (one-electron-reduced).

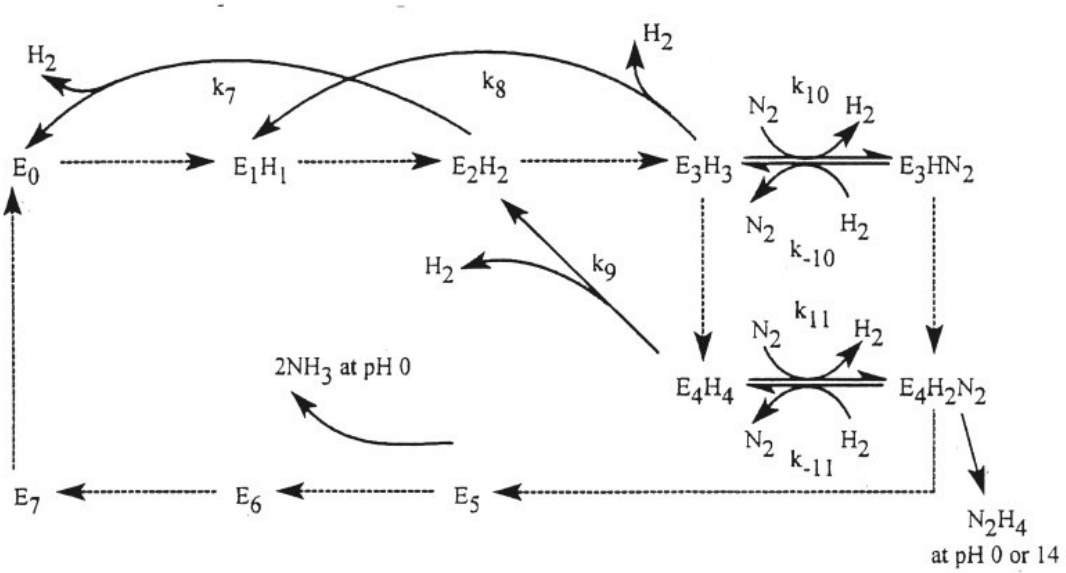

Figure 1.13 MoFe protein cycle. En represents *Av1* (αβ dimmer of the MoFe protein), and n refers to the number of times *Av1* completes the Fe protein cycle (Thorneley and Lowe, 1985).

same no matter what the redox state of the MoFe protein and this assumption has been shown to hold true for the first two steps of the MoFe protein cycle (Fisher *et al*., 1991).

The Lowe/Thorneley model was developed to explain the lag and burst phases of product release during substrate reduction. By monitoring the time course of product appearance and determining the rate constants of the individual partial reactions, the following conclusions were reached. 1) The rate-limiting step is the Fe protein dissociating from its complex with the MoFe protein. 2) Only free MoFe protein can bind substrates and release products. 3) The first redox state that is capable of evolving product is E_2, which releases H_2 and thus reverts to E_0. 4) N_2 binds only to a more reduced form of MoFe protein (probably E_3). 5) A N_2 reduction intermediate, the hydrazido(2−) group (=N−NH_2), is probably bound to oxidation state E_4, which releases hydrazine on quenching with acid or alkali. 6) Ammonia may be released at redox state E_5. 7) If the electron flux is low, then the redox state, E_2H_2, will prefer to evolve H_2 and revert to state E_0, rather than to proceed to more reduced states.

An extension of the Lowe/Thorneley model of the N_2 reduction mechanism was applied to the mechanism of C_2H_2 reduction. The product of the two-electron reduction of C_2H_2 is C_2H_4. The C_2H_2 binds to the E_1 and E_2 states and C_2H_4 is released from the E_3 state in the MoFe protein cycle (Fisher *et al*., 1990; Ashby *et al*., 1987). In contrast, using both stopped-flow spectrophotometric and EPR methods, H_2 was found to be evolved from the E_2, E_3, or E_4 states and was independent of any N_2 binding (Lowe *et al*., 1993). This conclusion was based on the appearance of the spectrum associated with the E_4 state, which was only observed under either an Ar or N_2 atmosphere, and not under a C_2H_2 atmosphere.

1.4.2 The role of MgATP hydrolysis and electron transfer

One of the key functions of the Fe protein is the coordination of MgATP binding and hydrolysis with the electron transfer between its [4Fe-4S] cluster and the MoFe protein. Upon binding MgATP to the Fe protein and forming a complex with the MoFe protein, the Fe protein undergoes a conformational change and dramatic shifts occur in the reduction potentials of the redox centers (see section 1.3.3). Such changes probably reflect a repositioning of the [4Fe-4S] cluster for the electron-transfer event that is

coupled to MgATP hydrolysis, which in turn is triggered by Fe protein-MoFe protein complex formation.

There has been some confusion as to the exact order of events following the formation of the Fe protein-MgATP-MoFe protein complex. The original stopped-flow spectroscopic studies support a model where MgATP hydrolysis preceded electron transfer (Thorneley *et al*., 1989). More recent stopped-flow studies indicate that electron transfer precedes MgATP hydrolysis (Lowe *et al*., 1995; Duyvis *et al*., 1996). This latter possibility was supported by using the ΔLeu-127 altered form of the Fe protein, which has a conformation in the absence of MgATP similar to that induced by binding MgATP the wild type Fe protein (Ryle and Seefeldt, 1996). Upon complex formation, this altered Fe protein transfers a single electron to the P cluster of the MoFe protein even though nucleotide is absent (Lanzilotta and Seefeldt, 1996). This result shows that the energy released by MgATP hydrolysis is not absolutely required for inter-component electron transfer and implies that MgATP hydrolysis occurs later than electron transfer during nitrogenase turnover.

Moreover, the altered Fe protein, Asn-39, which has Asp-39 substituted by Asn in its nucleotide-binding site, was found to complex with the wild type MoFe protein and transfer an electron in an MgATP-dependent reaction. It could not then dissociate. These results suggest that inter-molecular electron transfer induces conformation changes, which increase the affinity of the proteins for one another, and indicate a role for γAsp-39 in a signal transduction pathway leading to complex dissociation (Lanzilotta *et al*., 1997).

What, then, is the purpose of MgATP hydrolysis? Two possibilities have been suggested. One is that MgATP hydrolysis is necessary to induce another conformational change by the conversion of the Fe protein from the MgATP-bound state to the MgADP-bound state and that this change will allow the complex to dissociate so allowing the Fe protein to be reduced again (Lowe and Thorneley, 1984a,b). This possibility seems unlikely because it would be biologically inefficient to utilize so much energy simply to allow dissociation of electron transfer partners. The second suggestion is that the conformational change induced by MgATP hydrolysis is transmitted to the MoFe protein and in some way "gates" the electron transfer so that electrons cannot return to the Fe

protein. Gating would then ensure that multiple electrons can be accumulated and so drive intramolecular electron transfer within the MoFe protein prior to their donation to the substrate reduction site. In support of this concept, primary amino-acid sequence and structural comparisons show that the Fe protein is a member of a large class of signal-transduction proteins that undergo conformational change upon MgATP binding and hydrolysis.

1.4.3 P cluster and electron transfer within the MoFe protein

Even the simplest substrate requires a minimum of two electrons for reduction. Where and how these electrons are stored prior to the binding and reduction of substrate remains a mystery. However, the X-ray crystallographic structure of the putative transition state complex clearly places the P cluster on the electron transfer pathway between the [4Fe-4S] cluster of the Fe protein and the FeMo cofactor of MoFe protein (Schindelin *et al*., 1997 and also see section 1.3.3 and Figure 1.10).

There is no direct evidence of a function for the P cluster. However, there is currently one spectroscopic and kinetic observation that supports a role in electron transfer (Lowe *et al*., 1993). Optical changes occurring during the first 600 ms of turnover have been correlated with the appearance of EPR spectra with *g* values near 5.4 and 5.7. These spectroscopic changes were only observed under either an Ar or N_2 atmosphere and not under either C_2H_2 or CO. These EPR signals are similar to the signals seen in thionine-oxidized MoFe protein that are hypothesized to arise from a S = 7/2 spin state of oxidized P cluster. Thus, under either Ar or N_2, the P cluster may become transiently oxidized during turnover. This observation was rationalized in terms of the P clusters transferring electrons to FeMo cofactor when bound N_2 is irreversibly committed to being reduced and is protonated of the E_4 state.

Further support for the P cluster's role as an electron transfer mediator comes from studies of electron transfer in the tight complex of the ΔLeu-127 Fe protein with the wild type MoFe protein (Lanzilotta and Seefeldt, 1996). The two major conclusions from that work are: 1) the P cluster is an immediate electron acceptor; and 2) only the MgATP-bound conformation of the Fe protein, and not MgATP hydrolysis, is required for primary electron transfer to the P cluster.

Additional evidence that there is an intermediate step in the transfer of an electron from the Fe protein to the FeMo cofactor was obtained by perturbing the reaction through increasing the salt concentration level (Duyvis *et al*., 1997). In the presence of high salt, a lag period was observed after the Fe protein was oxidized but before the FeMo cofactor was reduced. It was proposed that electrons were transferred to the FeMo cofactor in two steps. First, an electron was transferred from the Fe protein to an unidentified site on MoFe protein and then it was transferred from that site to the FeMo cofactor. The unidentified site is probably the P cluster.

The possible involvement of the P cluster in intra-molecular electron transfer has been investigated by substituting either residues in the P cluster environment (Peters *et al*., 1995a) or residues that actually ligate to the P cluster (May *et al*., 1991). One study used substitution of βTyr-98, which is on a helix that spans the distance between the P cluster and FeMo cofactor, because its substitution might affect both intramolecular electron transfer and overall reduction activities. Substituting this residue by His (Peters *et al*., 1995a) resulted in a significant decrease in the rate of diazotropic growth by the mutant and a significantly lowered maximal specific activity for N_2 fixation, H_2 evolution and C_2H_2 reduction by the purified altered-enzyme. When monitoring H_2 evolution, component protein ratio titrations involving the βHis-98 altered MoFe protein revealed that its specific activity maximized at a lower Fe protein:MoFe protein ratio (5:1) than that of the analogous titration involving the wild type MoFe protein (10:1). This effect was even more apparent in the analogous titration performed during C_2H_2 reduction. Because the rates of intermolecular electron transfer were found to be similar for the βHis-98 MoFe protein and the wild type MoFe protein, the reduction in steady state maximum activity observed for the βHis-98 MoFe protein must be a consequence of an alteration in electron transfer after this event. These data are consistent with electrons being transferred through the protein between the P cluster and FeMo cofactor.

The other study used substitution of βCys-153, known as a P cluster ligand, by Ser (May *et al*., 1991) and resulted in an altered MoFe protein that supports only 50% of the maximum activity compared with the wild type protein under conditions of high electron flux. Under low-flux conditions, both proteins have approximately the same specific activity. This result suggests that, under conditions of high electron flux, the

maximum specific activity of the βCys-153 MoFe protein must be limited by the intramolecular delivery of electrons to the substrate-reduction site. Therefore, P clusters function in intramolecular delivery of electrons to the FeMo cofactor.

The redox potential values for the P cluster +2/+1 redox couple is pH-dependent, corresponding to the uptake of one proton per cluster upon reduction, whereas the redox potential value for the +1/0 couple is pH-independent (Lanzilotta *et al*., 1998). The observation correlates with the recent structure analysis of the MoFe protein from *A. vinelandii* in two redox states at 2.0-Å resolution (Peters *et al*., 1997). EPR spectroscopy on the crystals indicates that the structures correspond to the spectroscopically distinct oxidized and the native (or dithionite-reduced) forms of the enzyme. Upon oxidation, the P cluster structurally rearranges through movement of two of its eight Fe atoms, both of which also undergo a change in their ligand environment (see section 1.3.2.1). This observation raises the possibility that a two-electron oxidation of P cluster also releases two protons. Thus, at physiological pH, the coupled proton electron transfer for the +2/+1 redox change, plus the redox-dependent structural change of P cluster, make it likely that electron transfer to the FeMo cofactor and substrate might also involve the concerted delivery of protons.

1.5 Substrate reduction

The spectroscopic and catalytic properties of the wild type MoFe protein and some aspects of the reactivity of altered MoFe proteins produced by certain mutant strains (reviewed by Newton and Dean, 1993) indicate that the FeMo cofactor is intimately involved in substrate binding and reduction.

First, mutant strains (*nifE*, *nifN*, or *nifB* mutants), which produce cofactorless MoFe protein (apo MoFe protein), exhibit neither the characteristic S = 3/2 signal nor catalytic activity. When the FeMo cofactor extracted from the native MoFe protein is inserted into the apo MoFe protein from each mutant strain, both EPR signal and catalytic activity are restored (Shah and Brill, 1977; Brigle *et al*., 1987; Paustein *et al*., 1990). The association of the FeMo cofactor with both the spectroscopic and catalytic features of the MoFe protein indicates that the FeMo cofactor is the substrate reduction site.

Second, compelling evidence has come from the study of *nifV* mutants of *K. pneumoniae* (McLean and Dixon, 1981; Hawkes *et al*., 1984; Liang *et al*., 1990). The $NifV^-$ altered MoFe protein has homocitrate replaced by citrate. This altered MoFe protein reduces N_2 at a lower rate and exhibits CO sensitive H_2 evolution. FeMo cofactor extracted from either wild type or the $NifV^-$ altered protein was incubated individually with the apo MoFe protein from the *nifB* mutant in the presence of Fe protein. The reconstituted MoFe protein exhibited catalytic properties characteristic of the MoFe protein from which the FeMo cofactor was extracted.

Finally, parallel changes in both EPR spectrum and catalytic properties of the nitrogenase in mutant strains with amino acid substitutions in the FeMo cofactor-binding environment also support FeMo cofactor as the substrate reduction site (Scott *et al*., 1990).

Nitrogenases reduce N_2 to ammonia with the concomitant production of H_2, in the presence of MgATP, an electron source and under anaerobic conditions. Because the MgADP resulting from MgATP hydrolysis inhibits nitrogenase catalysis, an ATP-generating system was developed to avoid ADP accumulation (Bulen and LeComte, 1966). The assay system is described in section 2.7.3. In the absence of an added reducible substrate, nitrogenase catalyzes an MgATP-dependent H_2-evolution reaction (Bulen *et al*., 1965) because nitrogenase reactions are run in aqueous solution and the proton is always available to the enzyme.

The electrons needed for nitrogenase substrate reduction reactions are usually supplied by sodium dithionite *in vitro* and by either ferredoxin or flavodoxin *in vivo*. During nitrogenase turnover, the rate of MgATP hydrolysis is often related to the rate of substrate reduction and expressed as an ATP/$2e^-$ ratio, which represents the number of ATP molecules hydrolyzed per electron pair used by nitrogenase to reduce substrate. Although for many nitrogenase reactions this ratio is constant at ca. 4 (Kennedy *et al*., 1968), this number does not hold true for all reactions and so the rate of MgATP hydrolysis is not necessarily a measure of the rate of electron flow through nitrogenase to substrate.

It is still not clear how the protons are delivered to the substrate reduction site. One possibility for proton transfer is from water molecules around the FeMo cofactor.

Another is through the hydrogen-bonding network around the FeMo cofactor by coupling their translocation (with electrons) through the amino acids that are located between the P cluster and FeMo cofactor. A start in understanding this process has involved the pH dependence of nitrogenase activity. The resulting bell-shape pH profile has been interpreted such that a functional group with a $pK_a \sim 6.3$ must be deprotonated for activity and another group with a $pK_a \sim 9.0$ must be protonated for activity (Pham and Burgess, 1993). The pK_a of the latter group was moved about - 0.5 pH units (in the acid direction) in the presence of either C_2H_2 or CO. The groups with these pK_a values are suggested to be associated with amino acid residues close to the active site. The behavior of the group with the pK_a of 9.0 is fully consistent with an earlier observation (Smith *et al*., 1973) on the effect of added C_2H_2 on the pH dependence of the EPR signal from the isolated MoFe protein. However, care must be taken when sodium dithionite is used in the assay at a pH lower or higher than 7.4. The actual pH value after adding sodium dithionite solution has to be measured. Further, it should be noted that more than one group may be responsible for the donation of protons enzyme catalysis and may, therefore, contribute to the measured pK_a values.

1.5.1 Nitrogenase substrates, products and proposed intermediates

The physiological substrate for nitrogenase is N_2. However, nitrogenase is a relatively promiscuous enzyme and a wide range of neutral and anionic substrates containing NN, NO, NC or CC triple or double bonds have been identified and more recently (Seefeldt *et al*., 1995; Rasche and Seefeldt, 1997) CS_2, CO_2 and COS as new substrates (Table 1.2). Hydrazine is the only substrate known in which a single bond is attacked. All products require the enzyme to supply multiples of two electrons with two protons. Reactions requiring between 2 and 8 electrons have been described.

Some substrates give multiple products and, at high electron flux (which can be generated by increasing the ratio of Fe protein to MoFe protein), products requiring a larger number of electrons are favored. This variation in the product distribution with electron flux implies that any introduced effect that changes the rate of inter- and intra-molecular electron transfer is likely to change the product distribution and specificity.

Table 1.2 Multiple substrates of nitrogenase[a]

	Reactants		Products
1.	$N_2 + 6H^+ + 6e^-$	$\rightarrow$	$2NH_3$
2.	$N_2H_4 + 2H^+ + 2e^-$	$\rightarrow$	$2NH_3$
3.	$2H^+ + 2e^-$	$\rightarrow$	H_2
4.	$C_2H_2 + 2H^+ + 2e^-$	$\rightarrow$	C_2H_4
5.	$C_2H_4 + 2H^+ + 2e^-$	$\rightarrow$	C_2H_6
6.	$HCN + 6H^+ + 6e^-$	$\rightarrow$	$CH_4 + NH_3$
7.	$HCN + 4H^+ + 4e^-$	$\rightarrow$	CH_3NH_2
8.	$CH_3NC + 6H^+ + 6e^-$	$\rightarrow$	$CH_4 + CH_3NH_2$
9.	$CH_3NC + 4H^+ + 4e^-$	$\rightarrow$	CH_3NHCH_3
10.	$HN_3 + 6H^+ + 6e^-$	$\rightarrow$	$N_2H_4 + NH_3$
11.	$N_3^- + 3H^+ + 2e^-$	$\rightarrow$	$N_2 + NH_3$
12.	$N_2O + 2H^+ + 2e^-$	$\rightarrow$	$N_2 + H_2O$
13.	$NO_2^- + 7H^+ + 6e^-$	$\rightarrow$	$NH_3 + 2H_2O$
14.	$NCNH_2 + 6H^+ + 6e^-$	$\rightarrow$	$CH_3NH_2 + NH_3$
15.	$NCNH_2 + 8H^+ + 8e^-$	$\rightarrow$	$CH_4 + 2NH_3$
16.	$CO_2 + 2H^+ + 2e^-$	$\rightarrow$	$CO + H_2O$
17.	$COS + 2H^+ + 2e^-$	$\rightarrow$	$CO + H_2S$

[a] Data are adapted from Yates, 1992 and Seefeldt *et al*., 1995.

Thus, such results should not be interpreted as necessarily directly affecting the enzyme's active site.

1.5.1.1 H_2 evolution

Among all the substrates for wild type Mo-nitrogenase, H^+ reduction to H_2 is the only process that is not inhibited by added carbon monoxide (CO). This property of the nitrogenase H_2 evolution reaction distinguishes it from H_2 evolution from conventional hydrogenase. In the absence of other substrates, H^+ is reduced by nitrogenase to evolve H_2 in aqueous solution. Studies of the ratios of H_2:HD:D_2 evolved from mixed H_2O-D_2O solutions of nitrogenase turnover (Jackson *et al*., 1968) demonstrated that hydronium ions (H_3O^+) are the ultimate source of nitrogenase-catalyzed H_2 evolution as shown in the following equation.

$$2H_3O^+ + 2e^- \rightarrow H_2 + 2H_2O$$

At present, both the chemical mechanism and site of H_2 evolution by nitrogenase are unknown, although, like all other substrates, the H^+ is almost certainly reduced at FeMo cofactor. One possibility is either a metal hydride or dihydride, which can produce H_2 evolution either by reaction with a H^+ or by reductive elimination, respectively. However, it is currently unknown which metal atoms on the FeMo cofactor are responsible.

$$E + H^+ + 2e^- \rightarrow E\text{-}H + H^+ \rightarrow E + H_2$$
$$E^{2-} + 2H^+ + 2e^- \rightarrow H\text{-}E\text{-}H \rightarrow E^{2-} + H_2$$

H_2 is first evolved at the E_2 state in the Lowe/Thorneley MoFe-protein cycle, so conditions of low flux favor H_2 evolution. Further, this scheme suggests that N_2 binding occurs *via* H_2 displacement. The reduction of N_2 is, thus, always accompanied by H_2 evolution. The minimum stoichiometry of the reaction is one H_2 evolved per N_2 reduced and this holds true even at extremely high (6-50 atm) N_2 partial pressures (Simpson & Burris, 1984).

1.5.1.2 N_2 reduction

N_2 is reduced by nitrogenase to ammonia. Under physiological condition, the substrate N_2 is present at saturating levels (Hardy, 1979). Although no free reduction intermediates have ever been observed during N_2 reduction, indirect evidence strongly suggests the formation of enzyme-bound intermediates during the 6-electron reduction of N_2 to NH_3. Because all known substrates of nitrogenase are reduced by an even number of electrons (and, almost always, require an equivalent number of protons), some reduction schemes have focused on the successive addition of pairs of electrons to N_2, leading to the formal reduction sequence of N_2, diazene, hydrazine, and ammonia. The first unequivocal evidence of such intermediates was reported when hydrazine (N_2H_4) was produced after acid or base treatment of turning-over nitrogenase under N_2 (Thorneley *et al*., 1978). Although N_2H_4 is not a free product of N_2 reduction, it is a nitrogenase substrate (Bulen, 1976). However, the bound intermediates in the N_2 reduction pathway remain controversial.

H_2 has several unique relationships with N_2 fixation. It is not only a product but also a competitive inhibitor of N_2 reduction to NH_3 (Hadfield and Bulen, 1969). N_2 is the only substrate whose reduction is inhibited by H_2 (Burgess *et al*., 1981). A special feature of H_2-N_2 interactions is the nitrogenase-catalyzed formation of HD in the presence of N_2 and D_2 (Burgess *et al*., 1981). HD formation is dependent on MgATP, reductant, and N_2 and is not a simple D_2-H_2O exchange process. Electrons appearing as HD under N_2/D_2 (one electron is required for each HD formed) are diverted exclusively from NH_3 formation, and therefore, concomitant H_2 evolution is unaffected.

Because of the N_2 dependence of HD formation, both HD production and the inhibition of the N_2-to-NH_3 reaction by H_2 have been considered to be different manifestations of the same nitrogenase chemistry, and a variety of models have been proposed to incorporate both phenomena. However, there are some discrepancies between these models and each model either conflicts with some experimental observations or places restriction on its chemistry. For example, the Thorneley/Lowe model for nitrogenase action explains HD formation (Thorneley and Lowe, 1985; reviewed by Burgess and Lowe, 1996; Figure 1.14) by requiring the production of a form of the enzyme reduced by three electrons, two involved in a dihydride and one elsewhere,

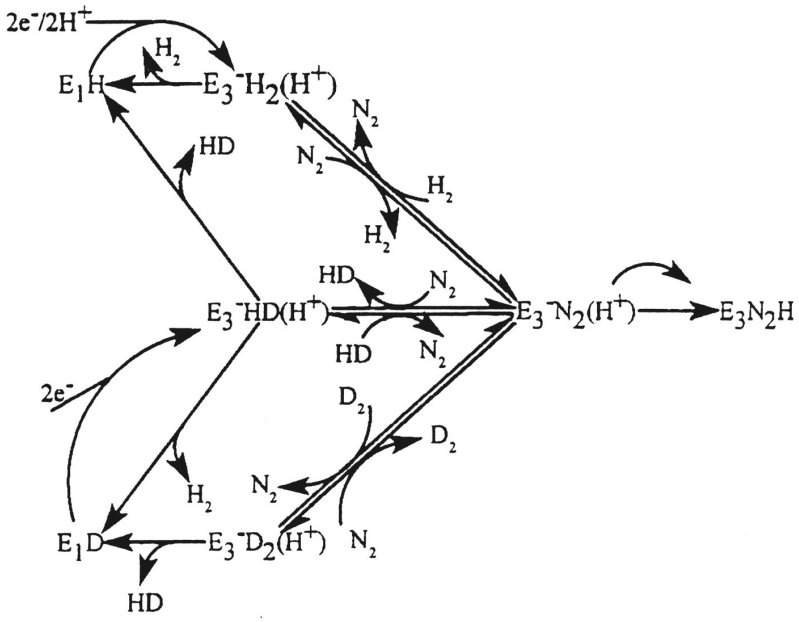

Figure 1.14 Scheme for the formation of HD by nitrogenase. This is a subset of the Thorneley/Lowe scheme with the single additional assumption that proton in parentheses cannot exchange with the hydrogen derived from the gas phase (Thorneley and Lowe, 1985).

but with a separately bound H^+, $E_3H_2(H^+)$. N_2 binds to this intermediate by displacing H_2, but N_2 can, in its turn, be displaced by D_2 to produced $E_3D_2(H^+)$. Internal electron transfer then results in HD and E_1D which, after addition of two further solvent protons and two electrons, gives a further HD and E_1H. An important restriction of this model is that the proton in parentheses cannot exchange with the hydrogen derived from the gas phase. The continued study of HD formation will guide the understanding of the mechanism for nitrogenase catalysis.

1.5.1.3 C_2H_2 reduction

The first demonstrated reduction of C_2H_2 to C_2H_4 by nitrogenase was performed with crude extracts of nitrogenase-derepressed *C. pasteurianum* cells (Dilworth, 1966). The reaction is described by

$$C_2H_2 + 2H^+ + 2e^- \rightarrow C_2H_4$$

C_2H_2 reduction is routinely used for estimating the nitrogenase activity both *in vivo* and *in vitro* because C_2H_4 is relatively easy to quantify by a very sensitive gas chromatographic method, especially when compared with ammonia determinations (Hardy *et al*., 1973). C_2H_2 is a good substrate, when compared to other alternative substrates, with measured K_m values ranging from about 0.003 to 0.02 atm (Hardy, 1979). The reduction of C_2H_2 by Mo-nitrogenase in D_2O has definitively established that *cis*-$C_2H_2D_2$ is in the major product (Dilworth, 1966; Kelly, 1969). The stereospecificity of this reaction and the retention of the both acetylene protons, when C_2D_2 and H_2O are used (Fisher *et al*., 2000a), supports a model for side-on binding followed by a rotation to the end-on position and protonation to *cis*-$C_2H_2D_2$ if the initial protonation occurs at the metal atom in nitrogenase (Stiefel, 1973; Henderson, 1996). It has been proposed that C_2H_2 binds to at least two sites or two oxidation states (Davis *et al*., 1979; Ashby *et al*., 1987; Shen *et al*., 1997; Fisher *et al*., 2000a; Christiansen *et al*., 2000a) and that C_2H_4 is released at the E_3 state of the MoFe-protein cycle (Fisher *et al*., 1990).

Although wild type Mo-nitrogenase reduces C_2H_2 by two electrons to give the product C_2H_4 as the only product, some altered Mo-nitrogenases and the alternative

nitrogenases can reduce C_2H_2 by both two and four electrons to give C_2H_4 and C_2H_6, respectively (Dilworth *et al*., 1987; Dilworth *et al*., 1988: Scott *et al*., 1990: Scott *et al*., 1992; Fisher *et al*., 2000a). It is not clear how C_2H_6 is formed. One hypothesis is that with wild type Mo-nitrogenase as soon as C_2H_4 is formed, it is displaced from the active site by C_2H_2 and so no C_2H_6 is formed (Ashby *et al*., 1987; Scott *et al*., 1992). In contrast with some altered MoFe proteins, the substrate may languish for an extended period of time on the enzyme, indicating a lower affinity for C_2H_2 and/or a higher affinity for C_2H_4 (Fisher *et al*., 2000a), thus leading to further reduction and so C_2H_6 formation. However, the amount of ethane formed must result from a delicate balance between having an affinity for C_2H_2 that is high enough to have reasonable binding but not so high that it rapidly and effectively displaces the bound intermediate (C_2H_4).

1.5.1.4 HCN reduction

Cyanide reduction by nitrogenase was first demonstrated in 1967 (Hardy & Knight). Sodium cyanide in solution contains both HCN and CN^-, the relative amounts varying with pH. HCN is a weak acid with a pK_a of 9.11. So, in the normal assay (pH ~ 7.4), the relative amount of HCN dominates (more than 95%). The concentration of CN^- is dramatically changed by change pH. With wild type Mo-nitrogenase, HCN is the substrate that can be reduced by six electrons to give two easily quantifiable products, namely ammonia and methane (CH_4). In contrast, CN^- anion acts as a potent inhibitor of electron flux without affecting the rate of MgATP hydrolysis (Li *et al*., 1982) resulting in significant increase in the ATP/$2e^-$ ratio.

The proposed mechanism for HCN reduction can be considered as a series of two-electron/two proton steps in the reduction pathway as shown below, where [ ] indicates an enzyme bound species.

$$\begin{array}{ccccccc} & +2e^-/2H^+ & & +2e^-/2H^+ & & +2e^-/2H^+ & \\ [HCN] & \rightarrow & [CH_2{=}NH] & \rightarrow & [CH_3{-}NH_2] & \rightarrow & CH_4 + NH_3 \\ & & \downarrow & & \downarrow & & \\ & & CH_2{=}NH & & CH_3{-}NH_2 & & \\ & & \downarrow + H_2O & & & & \\ & & H_2C{=}O + NH_3 & & & & \end{array}$$

The methyleneimine (CH_2=NH) intermediate has not been confirmed but is suggested because the rate of NH_3 production is always higher than the rate of CH_4 production. Thus, if a portion is released it would be hydrolyzed to formaldehyde (H_2C=O), which has never been detected, and the excess NH_3. Additional two-electron/two-proton steps would yield methylamine (CH_3–NH_2), some of which also escapes and is detected, and finally to give CH_4 and NH_3. Very small amounts of C_2H_4 and C_2H_6 are also detected (0.08% of CH_4 production) during HCN reduction catalyzed by nitrogenase (Kelly *et al*., 1967). The formation of C_2 products from a single C species is proposed to arise from interaction of adjacent C_1 particles on adjacent binding sites.

HCN reduction, which proceeds *via* two-electron reduced intermediates, is therefore analogous to one of the proposed mechanisms for N_2 reduction. It could be considered as a good model for N_2 reduction. There are, however, three differences concerning the reactivity of N_2 and HCN (Li *et al*., 1982). First, unlike N_2, HCN reduction is not inhibited by H_2. Second, comparing the two proposed 4-electron-reduced intermediates, N_2H_4 is a substrate but not a product of N_2 reduction, whereas CH_3NH_2 is a product of HCN reduction but not a substrate for the enzyme. Finally, as the ratio of the Fe protein to MoFe protein increases, the reduction of N_2 is favored over H_2 evolution, whereas the reduction of HCN becomes less favored relative to H_2 evolution. Also unlike N_2, HCN reduction can completely suppress H_2 evolution and is optimally reduced at a relatively low Fe protein to MoFe protein ratio. These observations have been interpreted as indicating that HCN is reduced when the MoFe protein is at a redox level more oxidized even than the one from which H_2 is evolved, which is E_2, in the MoFe protein cycle (Li *et al*., 1982).

Pre-steady-state kinetics of HCN reaction shows that, after a short lag (100 ms), there is a phase (lasting about 3 sec) where the evolution of H_2 is linear and only after this phase was CH_4 released. This long lag prior to HCN reduction would correspond to 18-to-20 electron transfers from the Fe protein. More realistically, this delay probably involves a cyanide-induced modification of the binding site, which is necessary before either inhibition or product release can occur (Lowe *et al*., 1989).

An early conclusion (Li *et al*., 1982) that CN^- and HCN bind at independent sites on the MoFe protein has been questioned. The more recent interpretation suggests that

both inhibitor and substrate bind at the same site and that CN^- only acts as an electron flux inhibitor until it is protonated to give the substrate HCN (Lowe *et al*., 1989; reviewed by Burgess and Lowe, 1996). Results from kinetic experiments with altered MoFe proteins are consistant with the "single HCN/CN^- binding site" hypothesis (Fisher *et al*., 2000b).

It is not possible to define whether the CN^- binds through its carbon or nitrogen atom. In model systems cyanide is always bound through its carbon atom. This result is consistent with the extensive chemical studies on the protonation of simple RNC complexes, where carbon coordination is enforced. Moreover, it has now been shown that the Mo-nitrogenase is not capable of reducing simple organic cyanides, such as MeCN or PhCN, as was originally proposed presumably because the RCN molecule would be forced to bind to the enzyme through a nitrogen atom (Fisher *et al*., 1990). Thus, CN^- almost certainly binds to nitrogenase through its C atom.

1.5.2 Inhibitors of substrate reduction

1.5.2.1 Competition among substrates

The inhibition of nitrogenase-catalyzed substrate reduction has been studied extensively. Substrates can inhibit each other because they all compete for electron flux from the same source within reduced nitrogenase. The patterns of mutual inhibition observed from kinetic experiments cannot often be explained by conventional enzymatic models because different substrates likely bind to different oxidation states of the enzyme (Liang and Burris, 1988c; Thorneley and Lowe, 1985). The inhibition patterns observed between N_2 and C_2H_2 are good examples. C_2H_2 is a non-competitive inhibitor for N_2 reduction, whereas N_2 is a competitive inhibitor of C_2H_2 reduction (River-Ortiz and Burris, 1975). This lack of reciprocating patterns of inhibition may reflect binding to different oxidation states of the enzyme rather than to different sites on the enzyme. Thus, if N_2 binds at the active site of the enzyme only when it is reduced by at least three electrons and C_2H_2 binds when the enzyme has accepted one or two electrons, then C_2H_2 can completely overcome N_2 inhibition by ensuring that the three-electron state is never achieved.

1.5.2.2 H_2 as an inhibitor

H_2 involvement with nitrogenase catalysis is particularly complex. Not only is H_2 a product of nitrogenase turnover, but it is also a specific competitive inhibitor of N_2 reduction but it does not affect the reduction of any other substrates. The specific competitive inhibition of N_2 reduction by H_2 has been interpreted as arising from them binding to a common site on the enzyme (Kim *et al*., 1995). Similarly, electrons appearing as HD under a N_2/D_2 atmosphere are diverted exclusively from NH_3 formation without affecting concomitant H_2 evolution. Moreover, both the rate of MgATP hydrolysis and the rate of electron flux to give products do not change during HD formation resulting in an unchanged ATP/$2e^-$ ratio.

1.5.2.3 CO as an inhibitor

CO is a potent non-competitive inhibitor of N_2 reduction and of the reduction of all other alternative substrates, except H^+ reduction (Hwang *et al*., 1973; Hardy, 1979). When CO is present, electron flux is diverted to H_2 evolution so that neither the rate of electron flux through the enzyme nor the rate of MgATP hydrolysis is affected, resulting in an unchanged ATP/$2e^-$ ratio.

However, an altered MoFe protein produced in the *nifV*$^-$ mutant strain of *K. pneumoniae*, where citrate replaces homocitrate as the organic constituent of the FeMo cofactor, exhibits H^+ reduction that is inhibited by CO (McLean *et al*., 1983). This change must disrupt the hydrogen-bonding network around the homocitrate, but exactly how this effect is produced is not clear. Support for this idea comes from the study of an altered MoFe protein that was constructed to interrupt the hydrogen bonding between αGln-191 and homocitrate at the FeMo cofactor. When Gln is substituted by Lys to give the αLys-191 altered MoFe protein, the phenotype includes CO-inhibition of proton reduction (Scott *et al*., 1992). Here, CO inhibits electron flux to substrate but not MgATP hydrolysis, resulting in an increased ATP/$2e^-$ ratio.

Spectroscopy has been widely employed to gain information about CO binding sites on the MoFe protein. EPR, electron nuclear double resonance (ENDOR) and stopped-flow Fourier transform infrared spectroscopy (SF-FTIR) techniques have all been used in determination of the CO binding to the FeMo cofactor of the nitrogenase.

Under turnover conditions, two distinct EPR signals can be observed from the enzyme under CO. At low partial pressures of CO, a rhombic signal with *g* values of 2.09, 1.97, and 1.93 is seen and is replaced, under higher CO partial pressure, by an axial signal with *g* values of 2.17, 2.06, and 2.06 (Yates and Lowe, 1976; Lowe *et al*., 1978; David *et al*., 1979). Using ^{13}C ENDOR spectroscopy, it has been shown that the "low-CO" signal arises from a single CO bound to the metal cluster whereas the "high-CO" signal arises from two CO's bound to the same metal cluster (Pollock *et al*., 1995). ^{57}Fe ENDOR spectroscopy confirmed that these EPR signals arose from the FeMo cofactor (Christie *et al*., 1996). Recently, orientation-selective ^{13}C and ^{57}Fe ENDOR spectroscopy has revealed that the single CO in the "low-CO" form is likely bound in a bridging mode, whereas both CO's in the "high-CO" form are terminally bound (Lee *et al*., 1997).

CO binding to nitrogenase has also been investigated by SF-FTIR. A single CO-based infrared absorption was detected under low CO concentrations and 3-4 absorption peaks under high CO concentrations (George *et al*., 1997). The authors speculate that all bands must arise from different species because they appear and disappear with different time courses. It should be noted that ENDOR and SF-FTIR are potential techniques to observe the binding and reduction of a wide range of nitrogenase substrates and inhibitors. The ENDOR technique, however, will only detect CO molecules bound to paramagnetic species, whereas SF-FTIR technique should detect all species. Although, the data analysis and interpretation from SF-FTIR may be technically difficult, it should be well worth the effort.

1.5.2.4 C_2H_4 as an inhibitor

Although C_2H_4 is a poor substrate, it is an inhibitor of Mo-nitrogenase (Ashby *et al*., 1987). As a substrate, it is only slowly reduced to C_2H_6 and accounts for no more than 1% of total electron flux under conditions of high electron flux. However, C_2H_4 inhibits both electron flux and MgATP hydrolysis equally and, therefore, retains a coupled ATP/$2e^-$ ratio. The extent of the inhibition by C_2H_4 with the *K. pneumoniae* nitrogenase depends on the electron flux, which is determined by the ratio of Fe protein to MoFe protein. At an Fe protein:MoFe protein molar ratio of less than 1:10 (low electron flux) and greater than 20:1 (high electron flux), H_2 evolution rates under C_2H_4

are effectively inhibited. However, at an Fe protein:MoFe protein molar ratio equal to 1:1, inhibition is minimal. Furthermore, C_2H_4 is a more potent inhibitor of H_2 evolution at low electron flux ($K_i < 1$ atm) than at high electron flux ($K_i \sim 4$ atm). The higher affinity for the less-reduced states of MoFe protein is perhaps not surprising, because C_2H_4 is the product of C_2H_2 reduction and presumably dissociates from a relatively oxidized state(s) of the MoFe protein in the catalytic cycle. The weak binding of C_2H_4 to MoFe protein under condition of both high and low electron flux is consistent with C_2H_4 not being a product inhibitor of C_2H_2 reduction under normal assay conditions where C_2H_4 formation is linear with time.

CO does not relieve the inhibition of H_2 evolution induced by C_2H_4 under either high or low electron-flux conditions, even though CO (at ~ 0.09 atm) completely inhibits C_2H_6 formation from C_2H_4. The differential response to CO suggests that CO and C_2H_4 in its inhibitory mode can both be bound at the same time. Further, because CO completely relieves the electron flux inhibition caused by CN^-, C_2H_4 and CN^- cannot share a common binding site (Li *et al*., 1982). Substituting αHis-195 by Gln leads to an altered MoFe protein that apparently does not bind CN^- as an inhibitor but does bind CO (Dilworth *et al*., 1998; Fisher *et al*., 2000b). Together, these data indicate that C_2H_4 inhibits electron flux by binding to a site separate from site that binds CN^- and that these two sites are distinct from the site that binds CO.

1.5.2.5 NO as an inhibitor

Nitric oxide (NO) was first described as a potent, but fully reversible, competitive inhibitor of N_2 fixation (Lockshin and Burris, 1965). However, the effect of NO inhibition on C_2H_2 reduction was later described as non-competitive (Trinchant and Rigaud, 1982). Crude nitrogenase preparations from *C. pasteurianum* showed that NO was indeed a non-competitive inhibitor of both C_2H_2 and N_2 reduction (Liang and Burris, 1988b). NO also inhibits H_2 evolution by nitrogenase although inhibition required higher levels of NO than those needed to inhibit N_2 reduction. Inhibition studies with NO also produced equivocal results because it reacts with O_2 and its inhibitory effects are seen at very low partial pressure. Other studies using a variety of approaches have demonstrated

that the Fe protein is very susceptible to irreversible inactivation by NO (Meyer, 1981; Liang and Burris, 1988b) whereas the MoFe protein is more insensitive.

The effect of NO on the individual components of *A. vinelandii* nitrogenase has been examined by kinetic and spectroscopic methods (Hyman *et al*., 1992). NO reacts with the [Fe-S] cluster of the Fe protein where less than a 2-fold molar excess of NO over protein leads to complete inactivation. At these low concentrations, NO oxidizes the cluster and abolishes the ability of the Fe protein to bind nucleotides. Inactivation of MoFe protein requires considerably higher concentrations of NO than those required for inactivating the Fe protein. The kinetic evidence suggests that a MoFe protein-catalyzed, NO-dependent consumption of dithionite occurs before the MoFe protein is inactivated. Finally, the description of NO as a non-competitive inhibitor of nitrogenase activity might be explained by the fact that catalytically active Fe protein is "removed" from the reaction mixture. The inactivation of nitrogenase by nitrite (NO_2^-) is controversial but is probably caused by NO generated nonenzymatically from the reduction of NO_2^- by dithionite (Meyer, 1981).

1.5.3 Substrate interactions and potential binding sites

It is generally accepted that substrates bind to and are reduced at the FeMo cofactor center of MoFe protein. However, it is clear that the polypeptide environment around the FeMo cofactor is important for its activity. Where and how do substrates bind on FeMo cofactor?

1.5.3.1 Evidence from sited-directed mutants

The evidence from kinetic studies of altered MoFe proteins, produced by individually substituting a number of amino acids in the environment of FeMo cofactor has shown substantial effects on substrate reduction activity and also changes of the substrate-binding affinity. For example, αArg-277 is close to αCys-275, which is a ligand to FeMo cofactor. Substitution by His yields an altered MoFe protein that does not reduce N_2 but does reduce C_2H_2, HCN, azide, and H^+ (Shen *et al*., 1997). Under nonsaturating CO concentrations, C_2H_2 reduction activity of this αHis-277 MoFe protein showed inhibitor-induced cooperativity, which was interpreted in terms of there being

two C_2H_2 reduction sites. HCN and azide kinetics did not respond in a similar sigmoidal fashion in the presence of partial inhibiting levels of CO. These results imply that there are multiple binding and reduction sites on the FeMo cofactor. Furthermore, the K_m values for reduction of these substrates by the αHis-277 MoFe protein are different to those for substrate reduction by wild type and show the effect of amino acid near the FeMo cofactor on the substrate binding sites (see section 1.7.3).

The most interesting altered MoFe proteins discovered thus far are those substituted at αHis-195 (Kim *et al*., 1995; Dilworth *et al*., 1998; Fisher *et al*., 2000a,b,c). The αGln-195 altered MoFe protein has a phenotype where N_2 is only very slowly reduced but effectively inhibits both C_2H_2 and proton reduction. Altered MoFe proteins with other substitutions at this position cannot reduce N_2 and, furthermore, N_2 does not inhibit C_2H_2 and proton reduction. This observation must mean that N_2 can bind to, but is not significantly reduced by, the αGln-195 MoFe protein. The imidazole ε-N of this His residue forms a hydrogen bond to one of the central S atoms of FeMo cofactor in wild type MoFe protein. Recently, the structure of αGln-195 altered MoFe was crystallographically determined and found that the amide N of the substituting Gln residue retains the hydrogen bond to a central bridging sulfur as identical to that of the wild type MoFe protein (Sørlie *et al*., 2001). Then this hydrogen bond is probably important for N_2 binding and probably for the positioning of FeMo cofactor to make it particularly accessible to N_2 (see also section1.7.2.3).

1.5.3.2 Theoretical predictions

The proposed models for N_2 binding generally fall into two categories: either binding to the Mo atom or binding to one or more of the Fe sites. Theoretical calculations have been used to predict the mode of N_2 binding and the mechanism of its reduction since the structure of FeMo cofactor was determined. These calculations have focused solely on the central Fe sites in the FeMo cofactor. There are at least three reasons to support N_2 binding on central Fe sites in the FeMo cofactor. First, the common factor between all three nitrogenase cofactors is that each contains Fe atoms. Second, the Mo atom in FeMo cofactor is apparently coordinatively saturated (six coordinate). Third, the central Fe atoms within the FeMo cofactor are apparently

coordinatively unsaturated (three coordinate). One of the more intriguing proposals is that N_2 could bind inside the FeMo cofactor, roughly along the Mo atom to end-Fe atom axis, with bonds to all six central Fe atoms (Orme-Johnson, 1992). Although the cavity size in the FeMo cofactor structure is too small by about 0.5 Å for N_2 to fit in this manner, the more reduced forms of the cofactor that are believed to actually bind N_2 may have a larger cavity. However, it must be remembered that different substrates, reaction intermediates and inhibitors may utilize alternative binding modes and sites.

There is now a substantial amount of literature on the feasibility of binding N_2 and reducing it at the Mo site. It is well known that the Mo atom can become seven or eight coordinated. So, the apparent coordinate saturation of the Mo atom in the FeMo cofactor need not rule out the Mo atom as the site of N_2 binding (Pickett, 1996; Evans *et al*., 1999). Moreover, both of these models (binding at Fe and binding at Mo) might be partially correct. For the multi-electron reduction of N_2, intermediates may relocate during enzyme turnover from one site to another (Mo to Fe or *vice versa*) or change from "end on" to "side on" at different points in the catalytic cycle.

Theoretical studies on the apparently unsaturated Fe atoms at the center of the cofactor have used a range of theoretical methods. Nine geometrical models have been proposed from the extended Hückel calculations of Deng and Hoffman (1993). One of these models favors N_2 binding in an end-on fashion with one N atom bound to four Fe atoms on one of the central faces of the FeMo cofactor (Figure 1.15). *Ab initio* density functional calculations (Dance, 1994; Dance, 1997) support side-on binding of N_2 to four Fe atoms on the face of the trigonal cavity. This model uses flexing of the cofactor cluster to assist in twisting and breaking the N–N bond.

A chemical model study has revealed that reduction and protonation of Mo sites with bound carboxyl ligands can lead to dissociation of the carboxyl groups to yield a site where N_2 can bind, followed by H_2 evolution (Hughes *et al*., 1994). This sequence would accord precisely with the stoichiometry observed for N_2 reduction and H_2 evolution by nitrogenase and would rationalize the need for the puzzling homocitrate ligand on the Mo atom. In this model, the carboxyl group of the homocitrate would dissociate from the Mo atom, leaving it still bonded by its hydroxyl group (Figure 1.16). N_2 reduction chemistry

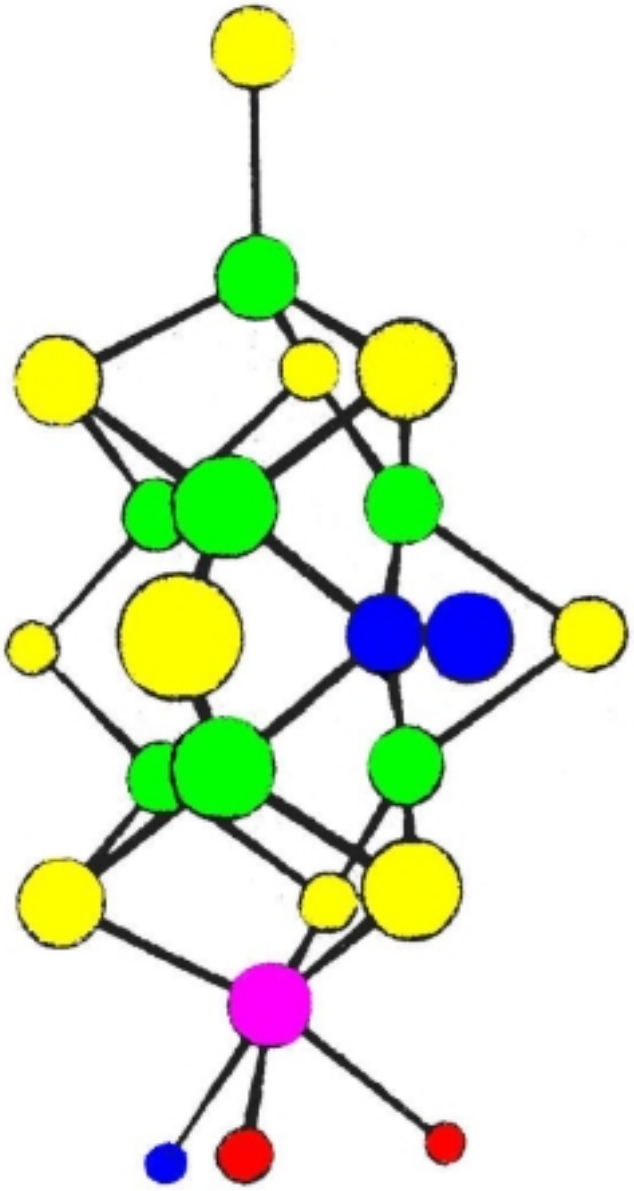

Figure 1.15 Geometrical models for N_2 bound to the 4Fe face of FeMo cluster (Adapted from Dance, 1996). Atom colors are iron in green, sulfur in yellow, molybdenum in purple, nitrogen in blue, and oxygen in red.

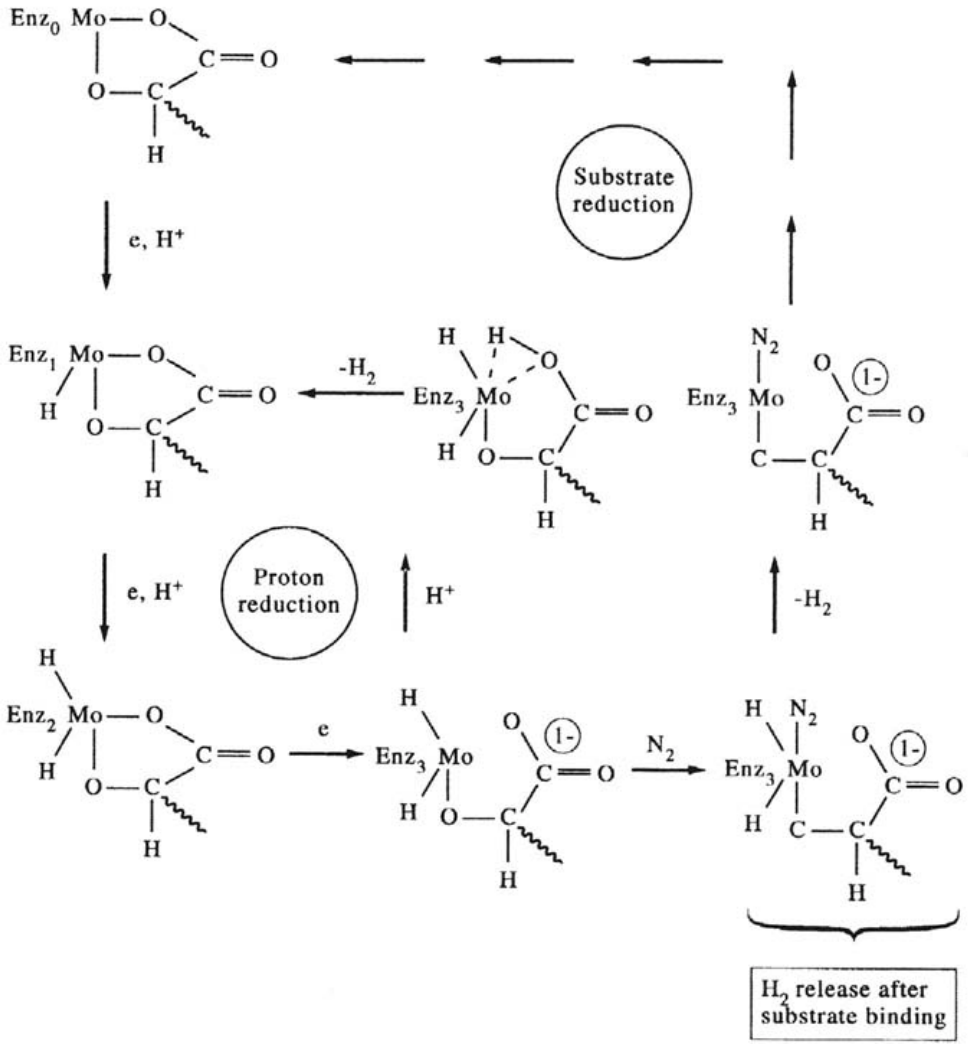

Figure 1.16 Proposed scheme for H_2 evolution, H_2 binding and reduction at a Mo site. This scheme is consistent with the Thorneley/Lowe mechanism, is based on know chemical reaction, and suggests a role for homocitrate as the provider of a carboxylate leaving group (Hughes *et. al*., 1994). Enz_n Mo corresponds to En in the Thorneley/Lowe scheme (Figure 1. 13).

could then take place at the Mo site in a manner similar to that established with model complexes.

1.5.3.3 Reactions of isolated FeMo cofactor and molecular modeling approach

Reactions of isolated FeMo cofactor have been used in attempts to identify substrate-binding sites. The FeMo cofactor, after being extracted from the MoFe protein into *N*-methylformamide (NMF) (Shah *et al*., 1977), also exhibits the S = 3/2 EPR signal, although broadened relative to the signal from the MoFe protein (Rawlings *et al*., 1978). The FeMo cofactor can be oxidized and also reduced electrochemically by one electron (Schultz *et al*., 1985) but substrate reduction by this one-electron reduced state has not been established.

There are numerous investigations into the binding of ligands to FeMo cofactor. As isolated, the FeMo cofactor lacks the amino acid ligands that were present in the protein. Therefore, there are vacant coordination sites on the "end" Fe and Mo atoms that can be taken up by other ligands. FTIR spectroscopy indicates that the NMF anion is bonded to extracted-FeMo cofactor through the N atom (Walters *et al*., 1986). ^{19}F NMR (Conradson *et al*., 1988) and x-ray absorption experiments (Conradson *et al*., 1989) and EPR data (Richards *et al*., 1994) have demonstrated that CN^-, thiolate, and methyl isocyanide (CH_3NC) bind to isolated FeMo cofactor. The EPR data indicated that there is probably more than one site for CN^- binding and that one of these may be the terminal tetrahedral Fe atom that binds cysteine in the protein.

More recently, following ligand substitution studies on synthetic Fe-S-based clusters, a kinetic approach has been used to identify substrate-binding sites on isolated FeMo cofactor (Grönberg *et al*., 1997). In these experiments, perturbation of the rate of binding of thiophenolate (PhS^-) to the FeMo cofactor by a range of added nitrogenase substrates was studied. The data indicate that CN^- binds to the terminal tetrahedral Fe atom but, in the presence of an excess of CN^-, a second CN^- binds at or close to Mo. No evidence for binding of CO or C_2H_2 was obtained. Imidazole and azide bind exclusively at or close to the Mo atom whereas H^+ probably binds at a bridging-sulfur close to the terminal tetrahedral Fe atom.

In an extension of this work, the reactivity of wild type FeMo cofactor and the FeMo cofactor extracted from the NifV$^-$ MoFe protein were compared (Grönberg *et al*., 1997). NifV$^-$ FeMo cofactor from *K. pneumoniae* nitrogenase has citrate rather than homocitrate bound to the Mo atom (Liang *et al*., 1990). No differences were observed between the reactivity of wild type and NifV$^-$ FeMo cofactor with PhS^- in the presence of CN^-, N_3^-, and H^+. However, when imidazole was bound, the kinetics of the reaction of PhS^- with the two cofactors was very different. These data were interpreted in terms of (R)-homocitrate, but not citrate, being able to hydrogen bond to the imidazole ligand on Mo atom because homocitrate has a chain that is one C atom longer than citrate. This interaction perturbs the electron distribution within the FeMo cofactor cluster and changes its reactivity with PhS^-. In effect, the hydrogen bonding of homocitrate to imidazole gives it imidazolate character. The X-ray crystal structure of the MoFe protein clearly shows that homocitrate cannot directly hydrogen bond to the αHis-442, which is a ligand of the Mo atom. However, studies on model complexes (Hughes *et al*., 1994) have suggested that homocitrate may become monodentate during nitrogenase turnover, with the Mo-carboxylate bond breaking to open up a vacant site at Mo suitable for binding N_2.

A molecular modeling approach shows that monodentate homocitrate may rotate to form a hydrogen bond between the carboxylate group of its longer $CH_2CH_2COO^-$ and the δ-NH group of the imidazole αHis-442 without the imidazole group changing its orientation (Grönberg *et al*., 1998). In the crystal structure, the $CH_2CH_2COO^-$ arm of homocitrate hydrogen bonds to the backbone NH of αIle-425 (Figure 1.17A). This bond would be broken by the rotation of homocitrate necessary to hydrogen bond to αHis-442. However, a new hydrogen bond would then be formed to a side-chain nitrogen of the next residue, αLys-426, which is conserved in all known nitrogenases (Figure 1.17B). The proposed rotation in homocitrate does not substantially perturb the other hydrogen bond between the shorter CH_2COO^- arm of homocitrate and the side-chain amide nitrogen of αGln-191. The αGln-191 residue has been proposed as essential for nitrogen fixation (Scott *et al*., 1992) because the altered MoFe protein in which αGln-191 residue

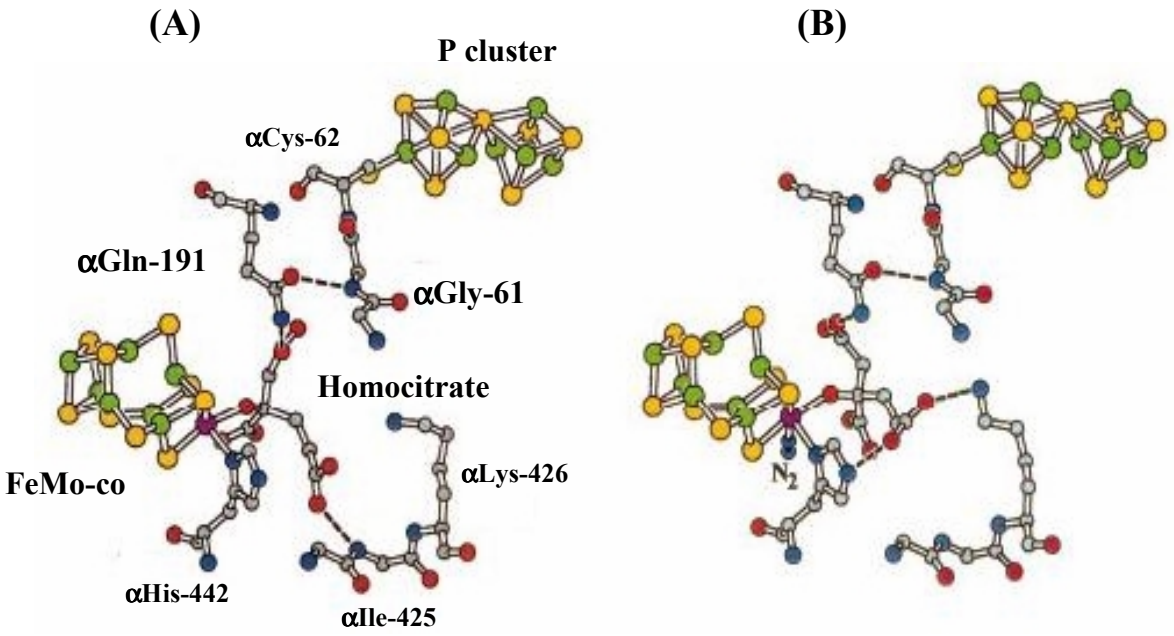

Figure 1.17 Hydrogen-bonding network in the vicinity of the homocitrate ligand. A) as established by crystallography and B) proposed hydrogen-bonding network in the same region after the carboxylate group of homocitrate has dissociated from Mo and N_2 has bound. This structure is that optimized by molecular mechanics calculations (Grönberg *et al*., 1998). Atom colors are iron in green, sulfur in yellow, molybdenum in purple, nitrogen in blue, and oxygen in red.

has been replaced by either Lys or Glu cannot fix nitrogen when complemented with wild type Fe protein.

If a hydrogen bond is formed between homocitrate and αHis-442, it could effectively release electron density into the cluster. In this context, studies on structurally defined dinitrogen complexes (Evans *et al*., 1993) have shown that both the binding of N_2 to a metal site and the ability of that N_2 ligand to be protonated are favored by electron-rich sites. Thus, the electron-richness of the FeMo cofactor could be modulated by using the hydrogen bonding of homocitrate as a switch to enhance N_2 binding and reduction.

It should be noted that the O atom of the amide side chain of the αGln-191 residue is hydrogen-bonded to the backbone NH of αGly-61, which is adjacent to the P cluster-ligating residue, αCys-62. The switching of homocitrate to a monodentate coordination mode could trigger (or be triggered by) a change at the P cluster *via* the homocitrate/αGln-191/αGly-61/αCys-62 hydrogen bonding network during nitrogenase turnover. These residues, therefore, form a potential electron-transfer pathway from the P cluster through homocitrate to the FeMo cofactor and bound substrate. Furthermore, such an arrangement could provide tight correlation between both the reduction and the protonation of bound substrate through the intermediacy of homocitrate.

1.6 Homocitrate substitution by other organic acids

An early study had established that the *nifV* gene was required for production of fully functional MoFe protein and had identified the FeMo cofactor as the defective component of the MoFe protein isolated from a *nifV*$^-$ strain (McLean *et al*., 1983; Hawkes *et al*., 1984). The NifV$^-$ nitrogenase shows nearly wild type levels of H^+ reduction and C_2H_2 reduction but very poor rates of N_2 reduction. Further, in contrast to the wild type enzyme, the NifV$^-$ MoFe protein exhibits H_2 evolution that is sensitive to CO inhibition. Later, homocitrate was identified as the organic acid component of FeMo cofactor in the MoFe protein (Hoover *et al*., 1989) whereas the organic acid extracted from purified MoFe protein isolated from a *nifV*$^-$ mutant of *K. pneumoniae* has been identified as citrate (Liang *et al*., 1990). Therefore, inactivation of the *nifV* gene results in formation of an altered FeMo cofactor that contains citrate rather than homocitrate. The *nifV* gene product from *A. vinelandii* has been identified and confirmed as

homocitrate synthase which catalyzes the condensation of acetyl coenzyme A and α-ketoglutarate to produce homocitrate (Zheng *et al*., 1997). Further, the *A. vinelandii* Nif V^- MoFe protein has been shown to also contain citrate (Newton *et al*., 2001).

An *in vitro* synthesis system for substituting the organic component of the FeMo cofactor and the subsequent incorporation of the product into MoFe protein has been developed (Hoover *et al*., 1988; Imperial *et al*., 1989; Madden *et al*., 1990; Madden *et al*., 1992). When citrate was substituted for homocitrate in the *in vitro* FeMo cofactor synthesis system, the resulting MoFe protein had the substrate reduction properties of the $NifV^-$ MoFe protein (Hoover *et al*., 1988). Table 1.3 presents additional accumulated information regarding substitution of organic acids for homocitrate in the *in vitro* FeMo cofactor synthesis assay. The structures of homocitrate and some representative organic acids are shown in Figure 1.18 (Ludden *et al*., 1993). A model for the minimum organic moiety required for both the *in vitro* synthesis of the FeMo cofactor and substrate reduction is shown in Figure 1.19 (Imperial *et al*., 1989). These organic entities appear to need: 1) stereochemistry at the chiral C-2 carbon like that of the *R* isomer of homocitrate; 2) a hydroxyl group on the chiral carbon atom; 3) a carboxyl group on the chiral carbon atom; 4) a carboxyl group α to the chiral center; and 5) a four-to-six carbon chain with two terminal carboxylates. This information is consistent with the FeMo cofactor model based on crystallographic analysis, which shows that the Mo atom receives two ligands from homocitrate (Kim and Rees, 1992a).

Comparisons of substrate reduction activities, using organic entities substituted at C_1, C_2, C_3 and C_4, indicate that the requirements for H_2 evolution at the FeMo cofactor are not very stringent. C_2H_2 reduction is more sensitive, with some organic substitutions (e.g., isocitrate and homoisocitrate) giving H_2 evolution activity almost as high as homocitrate but showing only 10-20% of the C_2H_2 reduction activity. By far the most stringent requirements are for N_2 reduction, which occurs at only 1-3% of the homocitrate-incorporated rate. Significant levels of NH_3 were only observed for homocitrate, *erythro*-fluorohomocitrate and *R*-citroylformate (Table 1.3).

The *R* and *S* isomers of several organic acids were available and have been incorporated into FeMo cofactor during synthesis (Madden *et al*., 1991). For each pair of isomers, both *R* and *S* forms allow enzyme function, but with marked differences. In the

Table 1.3 Summary of reduction activities of MoFe protein-containing FeMo cofactor with various organic acids[a].

Organic acid	Concen-tration (mM)	N_2 reduction activity	C_2H_2 reduction activity	H^+ reduction activity	
				(-) CO	(+) CO
None	0	1.2	3.3	7	7.1
R-homocitrate	0.08	100	100	100	100
Citrate	8	7.3	47.3	49.5	18
Isocitrate	1.6	3	15.9	71.3	78.2
Homoisicitrate	0.3	1.6	5.9	77.7	83.3
erythro-fluorohomocitrate	0.16	27.9	59.3	75	75
threo-fluorohomocitrate	0.16	2.9	51.9	60.7	24.9
R-citroylformate	0.16	45.6	62.9	71.4	71.4
S-citroylformate	0.16	4.4	10	21.4	9.9

[a] Adapted from Ludden *et al*., 1993. The FeMo cofactor synthesis and substrate reduction activity assay were performed as described by Imperial *et al*., 1989 and Madden *et al*., 1990. Reduction activities are expressed in percentage of reduction activity of *R*-homocitrate under particular substrate and CO

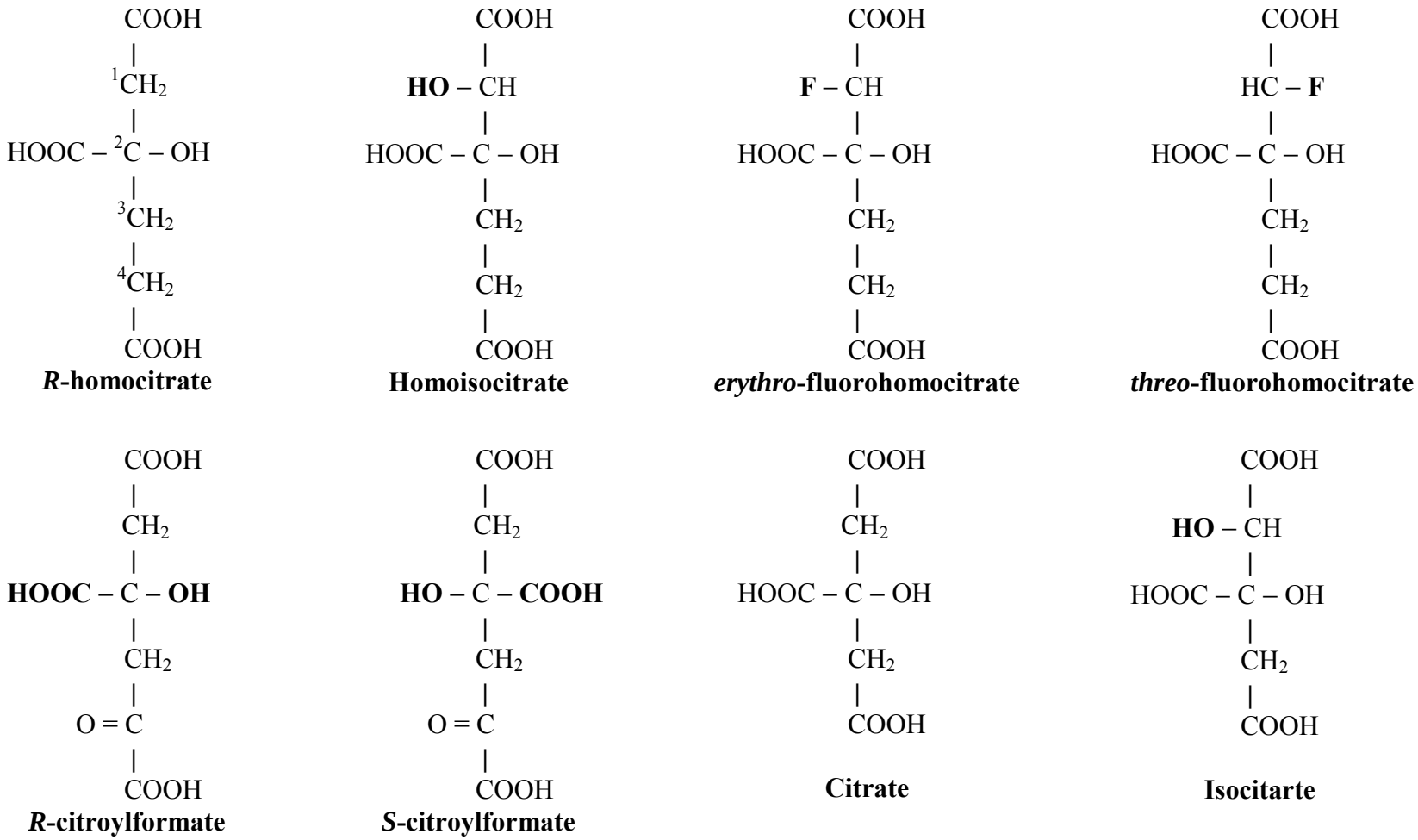

Figure 1.18 Structures of homocitrate and its analogs (Adapted from Ludden *et al*., 1993).

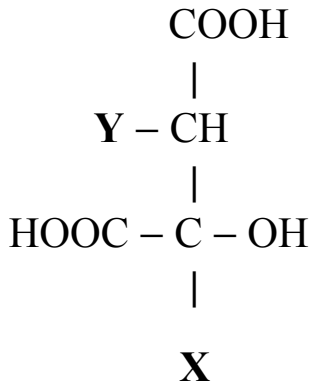

X = CH_2COOH (citrate)
= CH_2CH_2COOH (homocitrate)

Y = H (citrate or homocitrate)
= OH (isoacids)

Figure 1.19 Model for structural requirements for organic acid component of FeMo cofactor (Adapted from Ludden *et al*., 1993)

case of citroylformate, the *R* analog yields the MoFe protein with a rate of H^+ reduction nearly equal to that of the homocitrate enzyme and H^+ reduction is not inhibited by CO. *S*-Citroylformate yields an enzyme with much lower proton-reduction activity and that activity is significantly inhibited by CO. The FeMo cofactor synthesis assay has a strong preference for the *R*-isomers of the organic acids.

The differential effectiveness of organic acids extends to compounds with two chiral centers. Both the *erythro* and *threo* forms of 1-fluoro-homocitrate can be incorporated into FeMo cofactor, but the resulting enzymes show marked difference in activities (Madden *et al*., 1991). Of all analogs tested, the *erythro* form of 1-fluoro-homocitrate is second only to homocitrate and *R*-citroylformate in reconstituting an enzyme capable of N_2 reduction, whereas the *threo* form is essentially inert to N_2. The two forms differ in the sensitivity of proton reduction to CO, with the *erythro* form being insensitive whereas the *threo* form is strongly inhibited.

As the above examples show, substitution of homocitrate by other organic acids has produced MoFe proteins with altered reactivity toward CO. Some homocitrate analogues with either substitution at the C_1 carbon (e.g., *threo*-1-fluoro-homocitrate) or a particular *S* isomer (e.g., *S*-citroylformate) or a missing C_4 (e.g., citrate) produce MoFe proteins where CO is an inhibitor of H_2 evolution. However, similar effects on substrate reactivity can be induced in homocitrate-containing MoFe proteins. Thus, the altered MoFe protein in which αGln-191 is substituted with Lys (described in section 1.7.2.2) also exhibits CO inhibition of H_2 evolution (Scott *et al*., 1992). Of course, the αGln-191 group hydrogen bonds to homocitrate and the effect of this substitution may be mediated through changes in the homocitrate interaction with the Mo atom.

These data show that the substrate specificity and inhibitor susceptibility of the MoFe protein is dramatically affected by the chain length, stereochemistry, and the position of the hydroxyl group of the organic acid present in the FeMo cofactor as well as by amino acid substitution in polypeptide environment near homocitrate. At present, it is not known if homocitrate participates directly in substrate reduction, for example, by serving as a proton donor or a component of the electron transfer pathway or if it is simply important as a ligand for Mo. In this last capacity, it may be needed to guarantee

the required geometry at the Mo site, the proper fit of the cluster into the protein, or the proper juxtaposition of other catalytic groups.

The ability of so many organic acids to be incorporated into the FeMo cofactor raises the question of how the *in vivo* system ensures that homocitrate is specifically incorporated. The answer may be that the substrate specificity of the proteins involved in FeMo cofactor biosynthesis may reflect the concentration of each organic acid required for optimal activity of the FeMo cofactor synthesis assay. *In vitro*, homocitrate is saturating at 80 μM whereas most other acids must be present at 10-100 fold higher concentrations for optimal FeMo cofactor synthesis (Table 1.3). The 0.2 mM homocitrate that was observed to accumulate in the medium of *nif*-derepressed cells (Hoover *et al*., 1986) is sufficient to prevent other organic acids from being incorporated.

1.7 Site-directed mutagenesis of amino-acid residues around the FeMo cofactor

Investigations into the effect of the FeMo cofactor's polypeptide environment on its activity have given significant insights into substrate reduction. Two groups, the *A. vinelandii* model system in Blacksburg (USA) and the *K. pneumoniae* model system in Sussex (UK), initiated site-directed amino-acid substitution studies at about the same time and well before the crystal structures were available (Brigle *et al*., 1987; Scott *et al*., 1990; Scott *et al*., 1992; Kent *et al*., 1989; Kent *et al*., 1990). The rationale for this approach involved making specific substitutions of amino acid residues targeted either as direct ligands to or as being located near the FeMo cofactor. Investigations focused on the catalytic and spectroscopic consequences of the substitutions in order that they should provide information concerning the specific functions of individual amino acids located within the FeMo cofactor environment. For example, such functions could include: 1) provision of proton- or electron-delivery systems; 2) contributions to the electronic features of the substrate-reduction sites; and 3) proper orientation of FeMo cofactor within the polypeptide matrix through coordination to particular amino acid residues.

Prior to the availability of structural information, one study was used to target potential metallocluster polypeptide environments and to assign their arrangements within the MoFe protein. The results from these experiments turned out to be correct, although not all residues were identified, when the nitrogenase three-dimensional

structures become available (reviewed by Newton and Dean, 1993). Some features of the altered MoFe proteins, which have amino acid substitutions at the FeMo cofactor, have been characterized in order to understand the role of the FeMo cofactor polypeptide environment in catalysis.

1.7.1 αCys-275 and αHis-442 ligate to FeMo cofactor

Extrusion of the FeMo cofactor into NMF and electron spin echo envelope modulation (ESEEM) experiments on the *A. vinelandii* MoFe protein indicated His as a possible N-donor ligand to the FeMo cofactor (Thomann *et al*., 1987). The reaction of isolated FeMo cofactor with a thiol in a 1:1 stoichiometry indicated that one cysteinyl residue could also provide a ligand to the FeMo cofactor (Burgess *et al*., 1980). Nuclear magnetic resonance (NMR) (Masharak *et al*., 1982) and X-ray absorption spectroscopies (Newton *et al*., 1985) on isolated FeMo cofactor clearly showed that an added thiol binds to an Fe atom and not at the unique Mo atom. Deduced amino acid sequences of the MoFe protein α- and β-subunit from different microoganism were used to show that one of eight strictly conserved cysteinyl residues was probably responsible for binding the FeMo cofactor. The most likely candidate was determined to be αCys-275 (Brigle *et al*., 1985; Brigle *et al*., 1987) and α-subunit Cys residues 62, 88 and 154 and β-subunit Cys residues 70, 95 and 153 appeared more likely to form a symmetrical set of the P cluster ligands. Moreover, αCys-275 is surrounded by a concentration of conserved residues with amide functions, unmatched elsewhere in the primary sequence, which might be simulated by NMF.

The prediction of αCys-275 binding to an Fe atom of the FeMo cofactor was supported by site-directed mutagenesis results at this position. The initial substitutions of αCys-275 by either Ser (Brigle *et al*., 1987) or Ala (Kent *et al*., 1989) and other substitutions, such as Asp, Glu, Gly, Thr, and Val (reviewed by Newton and Dean, 1993), resulted in inactive phenotypes in the usual nitrogenase activity assays. Evidence that these substitutions disrupt the FeMo cofactor-binding domain comes from the studies of a crude extract of the αAla-275 mutant, using EPR spectroscopy, "apo-MoFe protein" reconstitution, and non-denaturing gel assays (Kent *et al*., 1989; Kent *et al*., 1990). The S = 3/2 EPR spectrum of the αAla-275 extract exhibited the characteristics of isolated,

rather than bound, FeMo cofactor. The free FeMo cofactor in this extract could be used to reconstitute the C_2H_2 reduction activity of wild type "apo-MoFe protein" from a *nifB*$^-$ strain. Further the migration of the MoFe protein in this extract on non-denaturing gels is slower than that of the native MoFe protein (from a wild type extract) but similar to the "apo-MoFe protein" in the *nifB*$^-$ strain. The interpretation of these data is that the FeMo cofactor is loosely attached to the MoFe protein matrix in the αAla-275 mutant.

A significant mutagenesis-based study of the involvement of αCys-275 in FeMo cofactor binding was under taken by substituting residues that immediately flank αCys-275 in *A. vinelandii* and *C. pasteurianum*. Primary sequences around the αCys-275 residue were compared. The *A. vinelandii* sequence within this region, His-Cys-Tyr, was replaced by the sequence, Gln-Cys-His, of *C. pasteurianum* (Dean *et al*., 1990). Substitution of this portion of the *C. pasteurianum* sequence for the corresponding *A. vinelandii* sequence resulted in a significant change in the EPR spectrum of MoFe protein from the resulting mutant strain, however, the catalytic function was not seriously impaired. This spectral change might arise from different constraints placed on the FeMo cofactor and suggests that the αCys-275 residue is a thiolate ligand. The result from the X-ray structure of MoFe protein (Kim and Rees, 1992a) has proved all these interpretations to be correct by showing that αCys-275 provides the direct thiolate ligand to FeMo cofactor through its unique terminal Fe atom.

The structural information has also revealed that αHis-442 provides direct N-coordination to the Mo atom on the other end of FeMo cofactor. The amino acid substitution of αHis-442 by Asn results in the complete inactivation of the MoFe protein and also eliminates the S = 3/2 EPR signal characteristic of the protein bound FeMo cofactor. Thus, αHis-442 appears to play a major role in anchoring FeMo cofactor to the polypeptide matrix. The functional role of αHis-442 residue for catalytic activity of FeMo cofactor in MoFe protein is being investigated in our lab (H. Li, K. Kloos and W.E. Newton, unpublished data). Six mutant strains that have αHis-442 substituted by Ala, Cys, Asn, Gln, Arg and Tyr were studied in crude extracts. Some of those altered MoFe proteins can reduce H^+ and C_2H_2 although their activities are very low. This result supports the requirement of αHis-442 for nitrogenase catalysis. One of the six altered

MoFe proteins, αCys-442, which exhibits the highest activity, is being purified and characterized.

1.7.2 Effect of amino acid substitution at either αHis-195 or αGln-191

The rationale for targeting the domain that is included αHis-195 and αGln-191 is primarily based on the fact that the FeMo cofactor is assembled upon the NifEN scaffold. It must escape from the biosynthetic complex during maturation of the MoFe protein. Therefore, an FeMo cofactor-binding domain located within the NifEN complex would probably be structurally similar but functionally different when compared with the corresponding domain contained within the MoFe protein (Brigle *et al*, 1987; Scott *et al*, 1990). If so, then certain residues in the α-subunit with functionalities that might serve to interact with FeMo cofactor may not be replicated in the corresponding domain of the NifE biosynthetic protein. Among those not replicated are the highly conserved His-195 and Gln-191 residues of the α-subunit, which are replaced by Asn and Lys, respectively, in NifE. Substitution of either αHis-195 by Asn or αGln-191 by Lys should, therefore, alter the functional properties associated with the FeMo cofactor while introducing only minor perturbations in the structural integrity of the resulting altered MoFe protein.

1.7.2.1 Substitution at αHis-195

The MoFe protein αHis-195 residue was originally targeted for amino acid substitution studies because primary amino acid sequence comparisons indicated that this residue might be located within an FeMo cofactor-binding domain (Scott *et al*., 1990). ESEEM spectroscopy suggested that His might be covalently coordinated to one of the FeMo cofactor's metal atoms (Thoman *et al*., 1987). Many mutant strains, each with a strictly conserved His residue individually substituted by a variety of residues (e.g., αHis-83, αHis-196, αHis-274, or αHis-195), have been used to test this possibility. The N-ligation of protein-bound FeMo cofactor was shown to require the αHis-195 because, when αHis-195 is replaced by Asn, the characteristic ESEEM signal disappeared (Thomann *et al*., 1991) together with a concomitant loss of N_2 reduction.

Although the most logical interpretation of these data was that αHis-195 is directly coordinated to one of FeMo cofactor's metal atom, the structural model revealed

that αHis-442, rather than αHis-195, is covalently attached to the Mo atom of FeMo cofactor. However, αHis-195 is hydrogen bonded to one of the central bridging sulfides (Kim and Rees, 1992a) and therefore, likely manifests its effects *via* this route. It was later shown that substitution of αHis-195 by Gln, rather than Asn, had no detectable change on the ESEEM signal. These results indicate that the observed nitrogen modulation is not directly associated with the hydrogen bond provided by αHis-195, but rather with the nitrogen moiety of a different residue whose proximity to the FeMo cofactor is sensitive to certain substitutions at the αHis-195 position. A correlation of the ESEEM properties and catalytic activities of the altered MoFe proteins suggested that the side chain of the αArg-359 is a source of this ESEEM signal (Lee *et al*., 1998). Thus, the NH-S hydrogen bond normally provided by αHis-195 might be important in positioning the FeMo cofactor within the polypeptide pocket.

Comparisons of the catalytic features of the MoFe protein resulting from replacement of αHis-195 by a number of other amino acids (Gln, Tyr, Leu, Thr or Gly) show that the altered MoFe proteins have a variety of phenotypes (Kim *et al*., 1995). None of these altered MoFe proteins were originally reported to be able to reduce N_2 but all retain a range of activity for proton reduction to H_2 and C_2H_2 reduction either to C_2H_4 alone or to a mixture of C_2H_4 and C_2H_6. The MoFe protein in which the αHis-195 has been replaced with Gln is one of the most interesting. The nitrogenase containing this altered MoFe protein still interacts with N_2, as evidenced by the fact that N_2 inhibits H_2 evolution and C_2H_2 reduction. This inhibition by N_2 of H_2 evolution is not accompanied by an inhibition of ATP hydrolysis. Thus, a significant increase occurs in the ATP/$2e^-$ ratio, which is measure of how many molecules of MgATP are hydrolyzed for each pair of electrons transferred to substrate. A simple explanation is that the unidirectional flow of electrons from the Fe protein to the MoFe protein that occurs during nitrogenase turnover is controlled by the substrate serving as an effective electron sink. The αGln-195 MoFe protein is also somewhat more sensitive to CO inhibition of both N_2 binding and C_2H_2 reduction. It was reasoned that the Gln substitution might make an Fe atom in the cofactor structure more accessible to attack by CO.

The crystal structure is in accordance with the suggestion that the substituting Gln might be able to simulate the ε-nitrogen of the imidazole ring of αHis-195, which is close enough to a bridging sulfide to form a NH-S hydrogen bond. Thus, the αHis-195 residue has, at least, a structural role, which serves to keep the FeMo cofactor attached to the MoFe protein and to correctly position FeMo cofactor within the polypeptide matrix, so that N_2 binding can occur.

The extensive study by Dilworth *et al*. (1998) sought to characterize the ability of the αGln-195 altered MoFe protein both to catalyze the reduction of alternative substrates (azide and HCN), and to bind inhibitors (CN^- and CO and, in this case, N_2). Through developing a method to determine the small amount of ammonia produced from azide reduction (Dilworth and Fisher, 1998), it was found that this protein can reduce N_2 to ammonia but at a low rate of < 2% of that of the wild type. N_2 binding to the αGln-195 MoFe protein retained two properties of the wild type by suffering H_2 inhibition of N_2 binding by producing HD under a mixed N_2/D_2 atmosphere. The rate of HD production and the fraction of total electron flow allocated to HD are similar to those for wild type nitrogenase under the same conditions. The reduction of HCN is not impaired with the αGln-195 nitrogenase but the inhibition by CN^- of total electron flux to substrate, which is observed with the wild type MoFe protein, is completely absent. Surprisingly, azide is a very poor substrate for this αGln-195 MoFe protein with a reduction rate only about 5-7% of that for wild type. Azide also inhibited H_2 evolution and increased the ATP/$2e^-$ ratio as occurs with N_2. These data have been interpreted as indicating that N_2, CN^- and azide bind to the FeMo cofactor in the region encompassing αHis-195, whereas H^+, C_2H_2, HCN, and CO do not.

1.7.2.2 Substitution at αGln-191

To investigate the role of αGln-191, mutants containing amino acid substitutions at this position have been constructed. The ability of mutant cells to grow without an added fixed nitrogen source (diazotrophic growth) has been found to range from cannot grow (Nif^-) as for αLys-191, through grows slowly (Nif^{slow}) as for αSer-191 to grow at similar rates as wild type rate (Nif^+) as for αAla-191 and αPro-191 (reviewed by Newton and Dean, 1993). The ability to grow on fixed nitrogen-free media as shown by the

αSer-191, αAla-191 and αPro-191 substitutions, implie that Gln is not rigorously required for reducing N_2.

Because αLys-191 cannot grow in nitrogen-free media and because its crude extract can reduce C_2H_2 to C_2H_6 (unlike wild type), this altered MoFe protein was selected for purification and for the study of its catalytic properties to compare to wild type MoFe protein (Scott *et al*., 1992). This substitution results in an altered MoFe protein that cannot reduce N_2 but can still reduce H^+ and C_2H_2, although at a low level. This altered MoFe protein also differs from wild type MoFe protein in that it exhibits proton reduction that is ~ 60% sensitive to CO. This feature is characteristic of both the MoFe protein produced by *nifV*$^-$ mutant strain (Hawkes *et al*., 1984) and when some organic acids are substituted homocitrate (Imperial *et al*., 1989) (see section 1.6). This similarity of phenotype in responses to CO can be understood in the light of the structural model where αGln-191 is normally hydrogen bonded to a terminal carboxylate group of homocitrate (Kim and Rees, 1992a). The fact that either an alteration in the organic acid attached to the Mo or the substitution of the amino acid that coordinates the organic acid leads to CO-sensitive proton reduction indicates that, at least, homocitrate likely plays an integral role in the mechanism of hydrogen evolution.

The CO sensitivity of proton reduction catalyzed by the αLys-191 altered MoFe protein is also a characteristic of *K. pneumoniae nifV*$^-$ mutant which contains a compromised FeMo cofactor. Thus, the possibility arises that either the molecular structure or the composition of the FeMo cofactor may be altered as a consequence of its insertion into the αLys-191 polypeptide environment. This possibility was tested by using FeMo cofactor isolated from the αLys-191 MoFe protein to reconstitute an apo-MoFe protein wild type (Scott *et al*., 1992). Apo-MoFe protein reconstituted in this way exhibits H^+ reduction that is not sensitive to CO inhibition, that is, the wild type phenotype. The reverse experiment showed that, when FeMo cofactor isolated from the wild type MoFe protein is used to reconstitute an apo-form of the αLys-191 MoFe protein, the reconstituted protein does exhibit CO-sensitive H^+ reduction. Thus, the CO-sensitive phenotype of the αLys-191 MoFe protein is a consequence of alteration in the

polypeptide environment of the FeMo cofactor rather than a structural alteration in the FeMo cofactor itself.

Another interesting feature of the αLys-191 MoFe protein is its poor ability to catalyze the reduction of C_2H_2. However, it can reduce C_2H_2 by both two electrons and four electrons to give either C_2H_4 or C_2H_6, respectively, whereas wild type MoFe protein is only able to catalyze the two-electron reduction of C_2H_2 to give C_2H_4. Reduction of C_2H_2 to both C_2H_4 and C_2H_6 is also a property of the V-nitrogenase (Dilworth *et al*., 1987) and the Fe-nitrogenase (Pau *et al*., 1989). However, the possibility that either of these alternative nitrogenases was present in the extracts under study was eliminated (Scott *et al*., 1990). Further, C_2H_6 production by the αLys-191 MoFe protein was not shown to occur by a mechanism similar to that of C_2H_6 catalyzed by the V-nitrogenase. Unlike V-nitrogenase, the αLys-191 MoFe protein: 1) does not exhibit a lag before C_2H_6 production, thus, no similar intermediate accumulates; 2) exhibits an increased sensitivity to inhibition by CO; 3) does not show a different temperature dependence for C_2H_4 and C_2H_6 formation; and 4) catalyzes C_2H_4 and C_2H_6 formation in a ratio that does not change with variations in electron flux (Scott *et al*., 1992).

Since these observations of C_2H_6 produced from C_2H_2 were reported, this same phenotype has also been observed from the MoFe protein isolated from a *nifV*$^-$ strain of *A. vinelandii* which contains citrate as its organic acid component of FeMo cofactor (Newton *et al*., 2001). Also, this NifV$^-$ MoFe protein exhibits CO-sensitive H_2 evolution. The observations that substitution of V for Mo or of citrate for homocitrate or substitution of a residue coordinated to homocitrate all lead to profound changes in catalytic properties of the MoFe protein again point to an important role for homocitrate in the catalytic mechanism. Whether or not this role is a structural one that serves to properly orient FeMo cofactor within the polypeptide pocket or a functional one that involves the direct participation of homocitrate in substrate binding, reduction or protonation is not yet known. The recent model proposed by Grönberg *et al* (1998) states that homocitrate facilitates the binding of substrate by allowing access to Mo through dissociation of the Mo-carboxyl bond (see section 1.5.3.3). The whole process is mediated by hydrogen bonding of amino acid side chains to the carboxylate groups of

homocitrate. If true, then the extensive hydrogen-bonding network in the region of homocitrate and homocitrate itself play important roles in substrate reduction.

1.7.2.3 Interaction of substrates and inhibitors with αGln-195, αAsn-195 and αLys-191 altered MoFe proteins.

Some aspects of the reactivity towards substrates and inhibitors of αGln-195 and αLys-191 altered MoFe proteins were described above (see section 1.7.2.1 and 1.7.2.2). In an attempt to gain more insight into the interaction of C_2H_2, C_2H_4, CO, and H_2 with Mo-nitrogenase, the αGln-195, αAsn-195, and αLys-191 altered MoFe proteins have been studied to compare with wild type MoFe protein (Fisher *et al*., 2000a,b). The results from K_m determinations and the use of C_2D_2 to measure the proportion of both *cis*- and *trans*-$C_2D_2H_2$ isomers produced by these four MoFe proteins were used to probe their interactions (Fisher *et al*., 2000a).

An early report indicated that proton addition across the acetylenic triple bond of C_2D_2 was completely of *cis*-stereochemistry with wild type *C. pasteurianum* nitrogenase (Dilworth, 1966), however, 5-17% *trans*-isomer has been reported for nitrogenase-derepressed cultures of wild type and *nifV⁻ K. pneumoniae* cells (Lin-Vein *et al*., 1989). The early experiments were designed to determine if a correlation existed between the stereospecificity of proton addition to C_2H_2 and the production of C_2H_6. Would those altered MoFe proteins that produced C_2H_6 from C_2H_2 also lose the stereospecificity of proton addition? Because the affinity of wild type nitrogenase for C_2H_2 is much greater than its affinity for C_2H_4 (Ashby *et al*., 1987), it was theorized that, as soon as C_2H_4 is formed, it must be displaced so quickly from the active site by C_2H_2 that no C_2H_6 is formed (Scott *et al*., 1992). Therefore, the amount of C_2H_6 formed must result from a delicate balance between having an affinity for C_2H_2 that is high enough to have reasonable binding but not so high that it rapidly and effectively displaces the bound intermediate. In the case of C_2H_6 formers, any enzyme-bound intermediate would have a longer lifetime on the site and so might have time to rearrange and lose the stereochemical specific reduction and protonation.

The results (Fisher *et al*., 2000a) showed that both the wild type and αGln-195 altered MoFe protein have a low K_m, both are 0.005 atm, and high specific activity for

C_2H_4 formation from C_2H_2 and neither produces C_2H_6. In contrast, both the αAsn-195 and αLys-191 altered MoFe proteins have a higher K_m, 0.01 atm and 0.35 atm, respectively, and both produce C_2H_6. Moreover, the αLys-191 MoFe protein has a high K_m and low specific activity for C_2H_4 formation and produces very little C_2H_6. These observations are consistent with the suggestion that too high a C_2H_2 affinity results in a loss of C_2H_6-production potential whereas too low an affinity would result in very little product. These data further indicate that the C_2H_2 affinity of the αLys-191 MoFe protein is only just sufficient to allow effective C_2H_2 binding (91% of the electron flux produces H_2). The αAsn-195 MoFe protein has the appropriate C_2H_2 affinity, which is required to balance effective binding against efficient displacement of intermediates, and directs 23% of the total electron flux to C_2H_6 formation.

All four MoFe proteins produced some *trans*-$C_2D_2H_2$ but the most extensive loss of stereospecificity occurred with the αAsn-195 MoFe protein, 37% of the total $C_2D_2H_2$ product was *trans*-$C_2D_2H_2$. The next highest producer was αLys-191 with 21% of the total $C_2D_2H_2$ product as *trans*-$C_2D_2H_2$. Thus, high C_2H_6 production by those two altered MoFe proteins correlates with *trans*-$C_2D_2H_2$ production. These data are consistent with a common intermediate at the ethylenic state on the enzyme being responsible for both C_2H_6 production and loss of proton-addition stereochemistry.

A further experiment to test this conclusion uses their abilities to reduce C_2H_4 to C_2H_6. The altered nitrogenase, which produces the most C_2H_6 product from substrate C_2H_2, would be predicted to produce the most C_2H_6 from C_2H_4 substrate. This prediction was fulfilled because the αAsn-195 MoFe protein had a specific activity for C_2H_6 formation from C_2H_4 that was 10-fold higher than the others. This result also indicates that the C_2H_4-reduction site is affected by substitution at residue α-195.

However, C_2H_4 was found to inhibit both total electron flux and MgATP hydrolysis to the same extent for all four *A. vinelandii* nitrogenases under study, indicating two C_2H_4-binding sites, one of which is a C_2H_4-reduction site and the other a C_2H_4 flux-inhibition site. When CO was added, C_2H_4 reduction was eliminated but CO did not fully relieve the electron-flux inhibition with any of the four MoFe proteins implying that electron-flux inhibition by C_2H_4 is not directly connected to C_2H_4 reduction.

HCN reduction and CN^- inhibition of electron flux was also studied through their interactions with these four MoFe proteins (Fisher *et al.*, 2000b). With wild type nitrogenase, the NH_3-production rate from HCN reduction is always higher than the CH_4-production rate. This observation has been ascribed to the production, partial release and subsequent hydrolysis of a two-electron-reduced intermediate, CH_2=NH, to produce the "excess NH_3" (Li *et al.*, 1982 and see section 1.5.1.4). When C_2H_2 is added, the rate of CH_4 production from HCN reduction is enhanced with wild type nitrogenase (Rivera-Ortiz and Burris, 1975). One goal of this study was to gain insight into how added C_2H_2 enhanced HCN reduction to CH_4.

The first experiments confirmed the response of wild type nitrogenase, without C_2H_2 added, and the tendency of the NH_3 production rate to be higher than the CH_4 production rate. However, the rate of CH_4 was found to increase with the HCN concentration until it became equal to NH_3 production at 5 mM NaCN suggesting that the higher HCN concentrations somehow discourage the escape of CH_2=CN. In addition, the wild type MoFe protein suffered the greatest inhibition of total electron flux with increasing NaCN concentration of all four MoFe proteins, suggesting that it has the highest affinity for CN^-. Thus, the drastically decreased electron flux at higher NaCN concentration may well lower the apparent affinity of the wild type MoFe protein for HCN, resulting in poorer HCN binding and, consequently, less displacement of any intermediate from the site.

These data also confirmed the earlier results from added C_2H_2, where the rate of CH_4 production from HCN reduction was enhanced to equal the rate of NH_3 production, which was unchanged. It may well be that either the additional electron flux inhibition by the added C_2H_2 or its competition with HCN for reducing equivalents (or both) decreases the overall electron flux to HCN reduction in much the same way as when the NaCN concentration is increased. The consequence would be a lowering of the affinity of the wild type enzyme for HCN, retention of the CH_2=NH intermediate at the site, a decrease in excess NH_3 formation, and increased CH_4 production, exactly as observed.

In the absence of C_2H_2, with the αAsn-195 MoFe protein, total electron flux decreased with increasing NaCN concentration like wild type. However, the rates CH_4 and NH_3 production, although unequal, were maximal at 1 mM NaCN. With the αGln-

195 MoFe protein, the rates of production of both CH_4 and NH_3 were equal at all NaCN concentrations, and total electron flux was hardly affected by changing the NaCN concentration. With the αLys-191 MoFe protein, the rates of both CH_4 and NH_3 production were very low, but the rate of NH_3 production was higher, and both rates slowly increased with increasing NaCN concentration.

A hypothesis, which is based on the varying apparent affinities of the three altered MoFe proteins for HCN and CN^-, was advanced to explain the higher rate of NH_3 production versus the rate of CH_4 production and the effect of increasing NaCN concentration on electron flux to products. For example, the αAsn-195 protein behaved similarly to wild type except for when its "higher than wild type" apparent affinity for HCN and its "lower than wild type" affinity for CN^- come into play. The rates of both CH_4 and NH_3 production remained unequal, even at 5 mM NaCN, implying that excess NH_3 production from CH_2=NH release and hydrolysis occurs more readily than with wild type MoFe protein. The lower apparent affinity for CN^- would cause a smaller decrease in total electron flux and, consequently, a smaller decrease in HCN binding affinity than occurs with wild type. The outcome of its higher apparent HCN affinity compared to that of wild type, would allow HCN to be a more effective competitor for the site on the αAsn-195 MoFe protein and would always displace some of the intermediate to produce excess NH_3.

This study shows that the amino acid residues residing at position α-195 and α-191 clearly influence the course of HCN reduction. They modulate the affinity of nitrogenase for HCN, the release of intermediates formed during its reduction, and the electron flux flowing to substrate and resulting in product. The αLys-191 is poorest catalyst of all these MoFe proteins in HCN reduction and CN^- inhibition and suggests a significant role of this αGln-191 in HCN reduction and CN^- binding.

Added CO significantly inhibited both CH_4 and NH_3 production from HCN with all MoFe proteins except for the αLys-191 MoFe protein, which still manifested its very low rate of NH_3 production but without CH_4 production. This result implies that, with the αLys-191 MoFe protein, excess NH_3 formation and consequently the two-electron reduction of HCN to CH_2=NH is insensitive to CO. This result is the second example of

a change in the effect of CO binding on substrate reduction by the αLys-191 MoFe protein because H_2 evolution from this altered MoFe protein is sensitive to CO. The generally low activity of the α-191-substituted MoFe proteins, for example towards HCN, attests to the importance of the αGln-191 residue in nitrogenase catalysis. Moreover, it suggests that the binding of both CO and some reducible substrates occurs on (or near) the [$MoFe_3S_3$-homocitrate] subcluster of the FeMo cofactor.

The αGln-195, αAsn-195, and αLys-191 altered MoFe proteins have also been used to gain insight into the interaction of nitrogenase with N_2 (Kim *et al*., 1995; Dilworth *et al*., 1998; Fisher *et al*., 2000c). N_2 is the only nitrogenase substrate whose reduction is competitively inhibited by H_2 (Burgess *et al*., 1981). With wild type MoFe protein, the Lowe-Thorneley scheme indicates that N_2 binds reversibly to E_3 (or to E_4) and displaces H_2 when doing so to produce E_3N_2 (or E_4N_2) (Lowe and Thorneley, 1984a,b and see section 1.4.1.2 and 1.5.1.2). This interaction provides a basis for explaining the ability of H_2 to inhibit competitively N_2 reduction to NH_3 because H_2 can, in its turn, displace N_2. The resulting bound hydrides may be protonated to produce H_2. Another feature of the H_2/N_2 interaction with wild type MoFe protein is the nitrogenase-catalyzed formation of HD in the presence of N_2 and D_2 (Burgess *et al*., 1981).

The interaction of the αGln-195, αAsn-195, and αLys-191 altered MoFe proteins with N_2 are different from each other. The αGln-195 MoFe protein can bind and reduce N_2 and also produce HD as found for wild type (Kim *et al*., 1995; Dilworth *et al*., 1998). Both the αAsn-195 and αLys-191 MoFe proteins (Fisher *et al*., 2000c) are incapable of catalyzing the reduction of N_2 but their rates of H_2 evolution respond differently when assayed under a N_2 atmosphere rather than the normal Ar atmosphere. The rate of H_2-evolution under N_2 with the αLys-191 MoFe protein was unchanged compared with Ar, whereas the αAsn-195 MoFe protein's rate of H_2 evolution was decreased relative to the rate under Ar. Therefore, N_2 interacts with the αAsn-195 MoFe protein but, unlike both of the αGln-195 and wild type MoFe protein (Dilworth *et al*., 1998), N_2 is not a substrate for the αAsn-195 MoFe protein. N_2 appears to behave only as a reversible inhibitor of electron flux through the αAsn-195 MoFe protein (Fisher *et al*., 2000c). Moreover, N_2 appears to do so through binding at its normal reduction site because added H_2 relieved

the N_2 inhibition of electron flux to substrate reduction and H_2 is a well-known, specific inhibitor of N_2 binding and reduction with wild type Mo-nitrogenase.

All evidence presented so far indicates that H_2 inhibition of N_2 binding (and reduction, where it occurs) and HD formation under a D_2/N_2 atmosphere are manifestations of the same molecular process. Because H_2 relieved the N_2 inhibition of electron flux to substrate, HD formation would be expected, as found with the αGln-195 MoFe protein (Kim *et al.*, 1995; Dilworth *et al.*, 1998), when the αAsn-195 MoFe protein was turned over under a 1:1 D_2/N_2 atmosphere. However, quite surprisingly, no HD was formed under these conditions with the αAsn-195 MoFe protein. The only observable effect of the added D_2 was relief of the N_2-induced inhibition of electron flux. This result is the first observation to indicate that H_2 (and, of course, D_2) inhibition of N_2 binding is not the result of exactly the same reaction that leads to HD formation under a D_2/N_2 atmosphere.

An explanation (Fisher *et al.*, 2000c) for this distinction between these two processes is based on the inability of the αAsn-195 MoFe protein both to reduce N_2 to NH_3 and to produce HD, whereas both the αGln-195 and wild type MoFe proteins catalyze N_2 reduction to NH_3 and produce HD. This difference may be the source of discrimination between the H_2-inhibition and HD-formation reactions. In the Lowe-Thorneley scheme, N_2 binds at the E_3 redox level and suffers competition from H_2 at this level, but reduction of N_2 may occur only after the E_4 redox level is attained. Thus, the ability to bind N_2 may simply not be sufficient for HD formation, which may require a reduced from of N_2 as described below where ( ) indicates D_2 used as H_2 and possible intermediates.

$$E_3H_2(D_2)H \underset{+N_2/-H_2}{\overset{+H_2(D_2)/-N_2}{\rightleftarrows}} E_3N_2H \xrightarrow{e^-} E_4N_2H_2 \underset{+H_2(D_2)/-N_2}{\overset{+N_2/-H_2(D_2)}{\rightleftarrows}} E_4H_4(D_2H_2) \rightarrow E_2H(D) + H_2(HD)$$

Therefore, the αAsn-195 MoFe protein may be incapable of reaching the E_4 redox level ($E_4N_2H_2$) and so is incapable of catalyzing both N_2-reduction and HD-formation

reactions. This explanation can be extended to αLys-191 MoFe protein, which cannot bind N_2 because it is incapable of achieving even the E_3 redox level (E_3H_2H).

An attractive thought is that the αHis-195 residue is involved in proton transfer during N_2 reduction (Dilworth *et al*., 1988). If so, the very different pK_a of an imidazole N–H compared to that of an amide N–H could contribute to the different reactivity toward N_2. Further, the presence or absence of an NH→S hydrogen bond, which could affect the pK_a of the involved group, could explain the difference in reactivity of the αGln-195 MoFe protein compared with the αAsn-195 MoFe protein. The αHis-195 may be required as a proton donor for N_2 but it is clearly not necessary for proton delivery to HCN/CN^- (Fisher *et al*., 2000b), which likely utilizes the αGln-191 residue-homocitrate combination as a proton channel into the FeMo cofactor. The availability of alternative proton donors would help explain the comparable rates of substrate reduction exhibited by the αGln-195, αAsn-195 and αLys-191 altered MoFe proteins.

1.7.3 Substitutions at αArg-277

The αArg-277 residue was targeted for substitution because of its proximity to the FeMo cofactor ligand, αCys-275. Moreover, it is a member of one of three stretches of residues, involving αArg-277, αSer-192, and αGly-356, that form a flap over the FeMo cofactor, which could open and close, making FeMo cofactor accessible, during catalysis (Kim and Rees, 1992a). It, therefore, has a potential role in the pathway for the entry/exit of substrates/products and also for the insertion of FeMo cofactor during biosynthesis. The characterization of amino acid substitutions at this position reveals a variety of substrate-reduction and inhibitor interactions that are different from wild type (Shen *et al*., 1997). Several of eight mutant strains constructed have the capability to grow on fixed nitrogen-free medium. Their MoFe proteins contain the FeMo cofactor as indicated by its biologically unique S = 3/2 EPR signal. These observations indicate that the positively charged αArg-277 residue is not required for acceptance of the negatively charged FeMo cofactor during biosynthesis.

When αArg-277 is substituted by His, the resulting altered MoFe protein exhibits an interesting phenotype that differs from wild type. First, the αHis-277 MoFe protein cannot either bind or reduce N_2, however, this altered MoFe protein can reduce C_2H_2,

HCN, H^+, and azide. These observations were interpreted to mean that the αHis-277 MoFe protein could not attain the more reduced redox states necessary to bind and reduce N_2.

Second, the αHis-277 MoFe protein has an unusual the pattern of CO inhibition of C_2H_2 reduction. Instead of the typical hyperbolic response of increasing specific activity with increasing concentrations of C_2H_2, in the presence of CO, the altered MoFe protein responded in a sigmoidal pattern that indicates cooperativity. Thus, CO induces cooperativity between at least two C_2H_4 evolving sites on the FeMo cofactor of αHis-277 MoFe protein. The non-competitive pattern of CO inhibition observed for all substrate reductions could be due to either CO binding to a different site than do the substrates or CO binding to the same site but at a different redox level. The CO-induced cooperativity observed for C_2H_2 reduction by αHis-277 MoFe protein clearly demonstrates that CO binds simultaneously with C_2H_2. Thus, CO binds to a different site on the MoFe protein but the same redox level.

Third, CN^- did not induce cooperativity in C_2H_2 reduction and, therefore, CO and CN^- are unlikely to share a common binding site. Finally, these results indicate that the nitrogenase MoFe protein should be viewed as a very versatile enzyme component, which is capable of presenting multiple substrate- and inhibitor-binding sites and assuming multiple redox levels.

1.7.4 Substitutions at αGly-69

The kinetic and spectroscopic evidence obtained using the wild type MoFe protein (Lowe *et al*., 1978; Davis *et al*., 1979) as well as an altered MoFe protein (Shen *et al*., 1997) indicates that there are at least two C_2H_2-binding sites located within the MoFe protein. In addition, the presence of both a high-affinity and low-affinity C_2H_2-binding site on the *C. pasteurianum* nitrogenase has been reported (Davis *et al*., 1979).

More resently, the substitution of αGly-69 by Ser gave the αSer-69 altered MoFe protein (Christiansen *et al*., 2000a,b), which is severely altered in its ability to reduce C_2H_2 but is only modestly affected in its ability to reduce N_2. This αSer-69 MoFe protein exhibits a K_m of 0.14 atm, an approximately 20-fold increase from the K_m for C_2H_2 binding of the wild type MoFe protein, but has kinetic parameters for N_2 reduction almost

identical to what is observed for wild type MoFe protein. These results were suggested that, of the two C_2H_2-binding sites, the high affinity C_2H_2-binding site appears to have been eliminated or severely altered without significantly altering the capacity of the altered enzyme to reduce N_2. Retention of the low-affinity C_2H_2-binding site was proposed because the K_m value found is similar to the value of low affinity of C_2H_2-binding site previously reported, $K_m \sim 0.23$ atm (Davis *et al*., 1979). The pattern of C_2H_2 inhibition of N_2 reduction catalyzed by αSer-69 MoFe protein was also changed from non-competitive (as found with wild type) to competitive, the same pattern found for N_2 inhibition of C_2H_2 reduction. This result is further interpreted as indicating that the low affinity C_2H_2-binding site and the N_2-binding site are the same.

The αSer-69 altered MoFe protein was extensively examined for its interaction with the alternative substrates, N_2O and azide, and CO as an inhibitor (Christiansen *et al*., 2000b). The K_m values determined for N_2O and azide for both the wild type and αSer-69 are similar and implied no change in binding affinity for both substrates. C_2H_2 was found to be a competitive inhibitor of N_2O and azide substrates with the αSer-69 altered MoFe protein, which is a change from the non-competitive inhibition observed with wild type MoFe protein (Liang and Burris, 1988c). Based on the previous conclusion of two C_2H_2-binding sites for wild type MoFe protein and elimination of the high affinity for C_2H_2-binding site by the αSer-69 substitution (Christiansen *et al*., 2000a), these results suggested that N_2O and azide likely bind to the low affinity for C_2H_2-binding site.

CO is a non-competitive inhibitor of all nitrogenase substrate-reduction activities except for proton reduction (Hwang *et al*., 1973). In the case of the αSer-69 altered MoFe protein, CO is converted from a non-competitive inhibitor (as found for wild type MoFe protein) to a competitive inhibitor with N_2, C_2H_2, N_2O and azide substrates (Christiansen *et al*., 2000b). Comparison of the K_{is} values with respect to CO obtained for both wild type MoFe protein and αSer-69 MoFe protein shows that they are all quite similar. This result indicates that this aspect of the interaction of CO with both MoFe proteins is unchanged.

These results are interpreted in terms of the two-site model. CO most likely binds to both the low affinity and high affinity C_2H_2-binding sites on wild type. Site 1 is the high affinity C_2H_2-binding site to which CO also binds, but N_2, N_2O, and azide do not

bind. This site is the one primarily accessed during typical C_2H_2 assays. Site 2 is a low affinity for C_2H_2-binding site to which CO, N_2, N_2O, and azide also bind.

In terms of the FeMo cofactor structure and its polypeptide environment, the αGly-69 residue is located immediately adjacent to the αVal-70 residue that caps one of the 4Fe-4S faces at the center of FeMo cofactor. These two residues are located near the end of a short helix that is positioned between the P cluster and FeMo cofactor. The high affinity C_2H_2-binding site is proposed to be provided by the 4Fe-4S face capped by αVal-70 and the αSer-69 substitution likely produces movement of αVal-70 so that the high affinity C_2H_2-binding site is no longer accessible. In the light of these observations, it was also suggested that both the high affinity and low affinity C_2H_2 binding sites are functionally distinct but located within the same 4Fe-4S face of the FeMo cofactor that is approached by the αVal-70 residue.

1.8 Summary and comments

In the early 1960s, only crude cell-free preparations were available for investigating the nitrogen-fixation phenomenon, whereas now highly purified, crystalline preparations of the nitrogenase component proteins are available for study. The crystal structures of the Fe protein, the MoFe protein, and the docked complex of these two proteins represent major advances in our understanding of nitrogenase. With the detailed structural information now in hand, a combined biochemical-biophysical-genetic approach has been used to probe functional aspects of the nitrogenase. One of these aspects is where and how substrates bind and get reduced on the MoFe protein.

The crystal structure of the Fe protein-MoFe protein complex stabilized by MgADP:AlF_4^- strongly suggests that the electron-transfer pathway is from Fe protein *via* the P cluster to the FeMo cofactor, where substrate reduction occurs. Several lines of evidences support the proposal that the P cluster is the immediate acceptor in the intermolecular electron-transfer event. What happens to the P cluster and FeMo cofactor in the polypeptide pocket during nitrogenase catalysis? How are amino acids around the two metalloclusters involved in electron-transfer, proton-transfer, and substrates binding/reduction? One approach to answer these questions is to specifically alter the polypeptide environments of the individual metalloclusters and subsequently determine

the spectroscopic, redox, and catalytic consequences that results from such alterations. The functional impact of the polypeptide around both the P cluster and FeMo cofactor is being probed in our laboratory and the results are starting to accumulate. In this dissertation, the spectroscopic and kinetic studies of the purified altered MoFe proteins, which have amino acid substitutions at αGln-191 residue, have revealed information that helps us understand where and how substrates bind and get reduced at FeMo cofactor.

CHAPTER 2

Materials and Methods

2.1 Materials

2.1.1 Chemicals and gases

The general chemicals used were purchased from Fisher Scientific Company (Pittsburgh, PA) unless otherwise specified.

The chemicals used for buffer solutions (e.g., Tris-HCl, HEPES, Bis-Tris, HEPPS, and CHES) were purchased from Sigma Chemical Co. (St. Louis, MO).

Sodium dithionite ($Na_2S_2O_4$) was purchased from Mallinckrodt Chemical Company (Berkeley, CA).

The resins used in purification (e.g., Q-Sepharose, Sephacryl S-200 and S-300, and Phenyl Sepharose) were purchased from Phamacia LKB (Uppsala, Sweden). Dowex AG1-X2 resin and Dowex AG50-X8 were purchased from Bio-Rad (Hercules, CA).

Cylinder gases used (e.g., nitrogen, argon, hydrogen, helium and air) were purchased from Holox (Narcross, GA). Carbon monoxide was purchased from Matheson Products Inc. (East Rutherford, NJ). Acetylene gas was produced in the laboratory by the reaction of calcium carbide with water. The standard gases used for gas chromatography quantification (e.g., hydrogen, acetylene, ethylene, ethane, and methane) were purchased from Scotty Specialty Gases (Plumsteadville, PA).

2.1.2 Instruments

The different types of instruments used and their manufacturers are shown in Table 2.1.

2.1.3 Mutant strains

Ten mutant strains each having a site-specific substitution for residue αGln-191 in the MoFe protein of *Azotobacter vinelandii* were produced using site-directed

Table 2.1 Instruments utilized in experiments

Type	Company	Location
1. G-25 Incubator Shaker	New Brunswick Scientific Co. Inc	Edison, NJ
2. Model G76 Gyrotory Water Bath Shaker	New Brunswick Scientific Co. Inc	Edison, NJ
3. MF-128S Microferm Fermentor	New Brunswick Scientific Co. Inc	Edison, NJ
4. Model 601S Peristatic Pump	Watson-Marlow	Falmouth, Cornwall, UK
5. Rabbit Plus Peristaltic Pump	Rainin Instruments Co. Inc	Woburn, MA
6. Durapore Pellican Cassette	Millipore Corp.	Bedford, MA
7. Amicon Stirred-Cell Membrane Concentrator	Amicon Inc.	Beverly, MA
8. Model XL 2015 Sonicator	Heat Systems Inc.	Farmingdale, NY
9. Beckman L5-50B Ultracentrifuge	Beckman Instruments, Inc.	Palo Alto, CA
10. Sorvall RC-5B Refrigerated Superspeed Centrifuge	DuPont Instruments	Wilmington, DE
11. Klett-Summerson Colorimeter	Klett Mfg. Co. Inc.	NY
12. UA-5 Absorbance/Fluoresence Detector	ISCO	Lincoln, NE
13. Model 8452 Diode Array Spectrophotometer	Hewlett-Packard	Palo Alto, CA

Table 2.1 Continue

Type	Company	Location
14. Model SE 250 Mini-Gel Apparatus	Hoefer Scientific Instruments	San Francisco, CA
15. Plasma 400 Emission Spectrometer	Perkin-Elmer	Norwalk, CT
16. Model GC-8A Gas Chromatograph	Shimadzu	Kyoto, Japan
17. Model GC-14A Gas Chromatograph	Shimadzu	Kyoto, Japan
18. Electrophoresis system PB-PDC-34 Polaroid Camera	Polaroid Corp.	Cambridge, MA
19. Model AR 15 pH meter	Fisher Scientific	Pittsburgh, PA
20. Accu-pHast Combination Electrode	Fisher Scientific	Pittsburgh, PA
21. Series A-2 Gas-tight Syringes	Alltech Associates, Inc.	Deerfield, IL
22. Varian E-Line EPR spectrometer	Varian associates	Palo Alto, CA
23. Model VG-7070E-HF Mass spectrometer	Research Scientific Services, Inc.	Gaithersburg, MD

mutagenesis and gene replacement techniques. The original mutant strains were generated and sequenced by Dr. John Peters in collaboration with Dr. Dennis Dean. The DJ64, αGlu-191, sequence was reconfirmed by using PCR and automated DNA sequencing at the Virginia Tech facility.

2.2 Schlenk line and anaerobic techniques

Because nitrogenase is extremely oxygen sensitive, all of the procedures were performed in anaerobic buffer under an argon atmosphere. A Schlenk line is a two line manifold system, one line is connected to a vacuum pump and the other line connected to an argon gas supply. During the degassing procedure, moisture is collected at a dry ice trap and a mercury manometer monitors the negative atmospheric pressure in the vacuum line. The argon supplied from the argon cylinder is continuously passed through a heated column filled with BASF-copper-based catalyst to remove trace amounts of oxygen and the gas flow is monitored a gas bubbler.

The Schlenk line is used in the laboratory regularly for the purpose of preparing *A. vinelandii* crude extracts, purifying nitrogenase component proteins, and assaying nitrogenase activity. Alternating cycles of filling with argon and pulling a vacuum are required to produce an anaerobic atmosphere in a container. In order to replace air with argon in the buffer-containing flask, it was first degassed by applying vacuum over the closed system for 30 min to 60 min depending on the volume of buffer contained in flask, until rapid bubbling ceased (normally 60 min is sufficient to degas 2.0 L of buffer). Argon was then introduced in place of the vacuum and solid sodium dithionite was added to a final concentration of 2 mM to maintain a reducing environment. Finally, the flask was evacuated and flushed with argon for three cycles before being kept under a positive pressure of argon. In the case of an empty container, air was to be replaced with argon by evacuation and flushing at least three cycles, before being kept under a positive pressure of argon.

2.3 *Azotobacter vinelandii* cell growth and nitrogenase derepression

2.3.1 Media composition and preparation

The *A. vinelandii* wild type and mutant strain cells were grown on modified Burk medium (Strandberg and Wilson, 1968). This medium is comprised of 2% sucrose, 0.2 g/L $MgSO_4.7H_2O$, 0.073 g/L $CaCl_2.2H_2O$, 20 μM $FeCl_3.6H_2O$, and 10 μM $Na_2MoO_4.2H_2O$ in 2.0 mM phosphate buffer, pH 7.4 (0.2 g/L KH_2PO_4 and 0.8 g/L K_2HPO_4). Urea (20 mM) is added to the medium when a fixed nitrogen source is needed for cell growth. Agar (2%) is added when a solid medium is needed as in agar plates.

The agar, sucrose, and Mg^{2+} and Ca^{2+} salts were added to distilled/deionized water and autoclaved. The MoO_4^{2+}, Fe^{3+}, and urea solutions were filter-sterilized as concentrated stock solutions and were added separately to the autoclaved mixture after it had cooled down below 60°C. The phosphate buffer was separately autoclaved and cooled before it was added to the above mixture to minimize the formation of insoluble precipitates, e.g., $Ca_3(PO_4)_2$.

2.3.2 Nitrogenase Nif phenotype

Initial screening of mutant *A. vinelandii* strains was accomplished by the qualitative method of growth on agar plates incubated at the optimal growth temperature of 30°C. Agar plates consisted of 2% agar in Burk modified medium plus or minus a fixed nitrogen source of urea. Mutant strains of *A. vinelandii* were grown on solid medium with urea for about 2 days and then transferred to urea-free medium plates to probe growth ability. The wild type strain was always used as a control. Cells exhibiting a Nif^+ phenotype grew to thick colonies in 2-3 days, Nif^{slow} typically took 4-7 days, and Nif^- strains showed no growth on urea-free plates in 7 days.

2.3.3 Doubling time determination

Doubling times were determined for mutant strains exhibiting a Nif^{slow} phenotype by monitoring cell growth during the logarithmic stage on liquid Burk medium. The recipe for Burk medium was the same as in section 2.3.1 except that agar and urea were excluded.

A Klett flask is an Erlenmeyer flask with a glass Klett tube annealed at an oblique angle to the top half of the flask. It is designed in order to measure the cell turbidity as a closed system and minimizes risk of contamination during cell growth.

Cells were grown on agar plates containing a fixed nitrogen source and then used to inoculate a 250-mL Klett flask filled with 50 mL of Burk medium plus urea (denoted BN-medium). The cells in the Klett flask were grown in a G-25 Incubator Shaker operating at 30^{o}C and aerated by shaking at 250 rpm. Cell growth was monitored by turbidity measurements on a Klett-Summerson colorimeter fitted with a green No. 54 filter. When the Klett reading was 150-200, which corresponds to the mid- to late-logarithmic phase, the entire contents of the flask were centrifuged using a Sorvall RC-5B Refrigerated Superspreed centrifuge with a GSA-type rotor at 8,000xg for 10 min at 4^{o}C. The cell pellet was resuspended with 10 mL of Burk nitrogen-free medium (denoted as B-medium), and centrifuged as stated above. The pellet was once again resuspended in 10 mL of urea-free medium and used to inoculate two Klett flasks so that they had a starting Klett reading of about 30. The flasks were returned to the shaker and the turbidity was measured every hour. The doubling time (generation time, g) was calculated from the equation

$$g = 0.693\ (t - t_o)/(\ln N - \ln N_o)$$

where N and N_o are the measured Klett number at time t and t_o, respectively, in the logarithmic phase of growth curve. Wild type *A. vinelandii*, whose doubling time is well established at 2.5-3.0 hrs, was used as a control in the experiments.

2.3.4 Large scale cell growth in the fermentor

Cell cultures for crude extract activity assays and for preparative-scale purification were grown in a 24-L MF-128S Microferm fermentor. Inocula of different sizes were taken from a 2-day-old culture plate and used to inoculate three Klett flasks containing 50 mL BN-medium. Cells were grown in an incubator-shaker at 30^{o}C with shaking at 250 rpm overnight. A suitable aliquot of a cell culture with a Klett of approximately 150-200 was used to inoculate a Fernbach flask containing 500 mL BN-

medium. The inoculated cell culture in the Fernbach flask was grown under the same conditions as the Klett flasks until a cell density of 150-200 Klett was achieved. This culture was then used as an inoculum for the fermentor. Depending on the cell density, 150-500 mL of inoculum were added to 24-L of pre-sterilized BN-medium. Fermentation conditions are overnight (12-18 hrs) growth at 30^{o}C, an agitation rate of 300 rpm, and a 40-45 L/min aeration rate. When the cell density reached about 200 Klett units, the nitrogenase enzymes were expressed by changing the medium from BN to B. The BN-medium was removed with a peristaltic pump over a 0.45 μm Pellicon cassette system until the cell culture was concentrated to approximately 2 liters. Cells were then washed twice with 2 L of 2.0 mM phosphate buffer (pH 7.4) in order to remove any residual urea. The concentrated cells were then restored to 24 L with B-medium and the culture was allowed to derepress for 3-4 hrs. After derepression, the cells were concentrated to 2 L and washed with 5L of 2.0 mM phosphate buffer, pH 7.4. The cell suspension was then transferred to 500-mL centrifuge bottles and centrifuged in the Sorvall RC-5B in a GS-3 rotor at 6,000xg for 20 min. The cell pellets were scraped into a plastic bag and stored in the - 80^{o}C freezer until further use.

2.4 Crude extract preparation

There are two types of crude extract preparation protocol. A small-scale preparation is used to screen for *A. vinelandii* wild type and mutant strain phenotypes at the crude-extract level. A large-scale preparation is performed in order to obtain a large amount of protein, normally from 100-200 gm wet weight of the cells, for purification.

A sonicator (Heat systems model XL 2015) and a rosette cell with a cooling system mounted in a sound-dampening polyacrylic box is utilized during the cell breakage procedure for both large and small crude-extract preparations. Cells were thawed and diluted anaerobically at 4^{o}C with degassed 50mM Tris-HCl (pH 8.0), 2mM sodium dithionite, at the approximate ratio of 1.0 gm of cells to 2.0 mL of buffer. The rosette cell was immersed in an ice water bath in order to minimize heat generated by the activated probe.

Small-scale crude-extract preparation was performed in a 10-mL rosette cell by using the micro-probe, a 75% power output and 6 cycles of 30 sec on followed by 30 sec

off to minimize heating effects. Extracts were transferred anaerobically into centrifuge tubes and centrifuged for 90 min using a Beckman L5-50B Ultracentrifuge at 98,000g at 4^{o}C. The dark brown supernatant was removed from the centrifuge tube under argon flushing using a Hamilton syringe and pelleted into liquid nitrogen and stored until used.

Large-scale preparation was performed in the 200-mL rosette cell, using a large probe and 6 sonication cycles of 1 min with 1 min intervals for cooling after every cycle. A heat treatment at 50-55^{o}C for 5 min was included as a standard step during crude extract preparation of heat-stable mutants and wild type. After the heat step, the extract is cooled down to 15^{o}C or less using an ice-water bath before centrifuging at 98,000xg for 90 min. The supernatant was transferred under argon flushing either to another degassed Schlenk flask if it was to be processed further or to a separatory funnel for freezing as pellets and later use.

2.5 Protein purification

2.5.1 Separation of nitrogenase component proteins by anion exchange chromatography

The volume of crude extract typically used was in the range of 250-350 mL and had a protein concentration of about 25-40 mg/mL. The Q-Sepharose anion exchange column, typically 5 x 10 cm, was pre-equilibrated overnight with 3-4L of 25 mM NaCl in 25 mM Tris-HCl (pH 7.4), 2 mM sodium dithionite. Filter paper, pre-soaked with methylviologen and dried, was used to check that the effluent from the column was reducing before the extract was loaded onto the column with a Rabbit Plus peristaltic pump at a flow rate of about 300 mL/hr. After the extract was loaded, a linear salt gradient was initiated using an additional peristaltic pump that added 25 mM Tris-HCl buffer (pH 7.4), 1M NaCl, 2 mM sodium dithionite, into the salt-free 25 mM Tris-HCL (pH 7.4), 2 mM sodium dithionite, at half the rate of the pump loading onto the column. A linear gradient from 0.0-1.0 M NaCl was applied in order to separate the MoFe protein from the Fe protein. An in-line UA-5 Absorbance/Fluoresence detector with a 405 nm filter was used to detect the yellow-to-brown colored proteins. The MoFe protein was eluted from the column at 0.3-0.35 M NaCl, whereas the Fe protein was eluted at 0.5-0.6 M NaCl. The two component proteins were collected in separate anaerobic Schlenk

flasks before being concentrated in an Amicon stirred-pressure concentrator immersed in an ice water bath and fitted with a suitable molecular weight cut-off (MWCO) membrane. The MoFe protein was concentrated with a 100K MWCO membrane (Millipore Corp., Bedford, MA), whereas the Fe protein was concentrated with a 30K MWCO membrane. The concentrated protein fractions were frozen and stored in droplet form in liquid nitrogen.

2.5.2 MoFe protein purification

After the two component proteins were separated by Q-Sepharose anion exchange chromatography, the MoFe protein was further purified by gel filtration chromatography. A large S-200 Sephacryl column (7.5 x 50 cm) was typically used at this stage due to the relatively large amount of protein (1.0-2.0 gm). The gel filtration column was equilibrated overnight and run with 25 mM Tris-HCl (pH 7.4), 200 mM NaCl, 2 mM sodium dithionite. Three or four fractions were collected separately from the large single peak eluting from the column. The fractions with the highest specific activity were selected for further purification.

The final step of MoFe protein purification was hydrophobic interaction chromatography. Fractions from gel filtration chromatography exhibiting similar specific activities were pooled and then concentrated with a 100K MWCO membrane concentrator. Concentrated MoFe protein was diluted with equal volume of 0.8 M $(NH_4)_2SO_4$, 25 mM Tris-HCl (pH 7.4), 2 mM sodium dithionite, to a final concentration of 0.4 M $(NH_4)_2SO_4$ before being loaded on to a Phenyl Sepharose column (2.5 x 20 cm). The Phenyl Sepharose resin was pre-equilibrated with at least 2 L of 25 mM Tris-HCl (pH 7.4), 0.4 M $(NH_4)_2SO_4$, 2 mM sodium dithionite. The high concentration of $(NH_4)_2SO_4$ forces an interaction of the protein with the hydrophobic Phenyl Sepharose on the resin matrix. A decreasing $(NH_4)_2SO_4$-concentration gradient from 0.4 M $(NH_4)_2SO_4$ to 0 was applied in order to develop the column. The MoFe protein eluted at approximately 0.1 M $(NH_4)_2SO_4$. About 4-6 fractions were collected for the MoFe protein. Each fraction was concentrated with a 100K MWCO membrane concentrator. The high activity fractions were pooled together and exchanged into 25 mM HEPES buffer (pH 7.4), 200 mM NaCl, 2 mM sodium dithionite, on a small (2.5 x 35 cm) S-300

gel filtration column under anaerobic conditions. Purity was assessed by a combination of SDS-PAGE, specific activity, and metal analysis (see section 2.5.4). The MoFe protein in this highly purified state was used for all kinetic experiments and spectroscopic characterization.

2.5.3 Fe protein purification

Typically, the Fe protein from the first anion exchange column contained MoFe protein and other contaminating proteins due to the incomplete resolution of the component proteins on the column. High specific activity Fe protein was obtained by application of a second Q-Sepharose anion exchange column. The Fe protein from the first Q-Sepharose column was diluted 3-fold with degassed 25 mM Tris-HCl (pH 7.4), 2 mM sodium dithionite, in order to reduce the salt concentration to below 150 mM prior to loading to the column. Using the same procedure as described in section 2.5.1, an increasing NaCl gradient from 0.0-1.0 M was utilized to elute the Fe protein from the column. A small peak of contaminating MoFe protein was first eluted before the large peak of Fe protein. The Fe protein peak was collected in 3-4 separate fractions and the fractions with the highest activity were typically from the downslope side of the eluted peak. These fractions were buffer exchanged into 25 mM HEPES, 200 mM NaCl, 2 mM sodium dithionite.

2.5.4 Determination of nitrogenase protein purity

During the various stages of protein purification, it was necessary to establish the level of purity of the different fractions collected from each chromatographic column. The typical procedures used in our laboratory are SDS-PAGE, determination of specific activity, and metal analysis

Sodium dodecyl sulfate-polyacrylamide gel electrophoresis (SDS-PAGE) was a qualitative but fast and easy method for estimating and comparing the purity of fractions. Sample and gel were prepared according to Laemmli (1970). The running gel used was 12% polyacrylamide (0.32% cross-linker) and the stacking gel was 4% polyacrylamide (0.1% cross-linker). All gels were made from a 30% acrylamide (0.8% cross-linker) stock solution of Proto Gel (National Diagnosis, Atlanta, Georgia). Samples were denatured by boiling in SDS- and β-mercaptoethanol-containing sample buffer for 5 min

and then 5-20 μg total protein was loaded into each well. Electrophoresis was performed at 25 mA/gel constant current for 1.5 hrs in a Hoefer model SE 250 mini-gel apparatus. The gels were stained with 0.1% Coomassie Blue (R_{250}), destained in a mixture of 40% (v/v) methanol and 10% acetic acid, and then stored in 5% methanol, 7% acetic acid. A 667 instant film Polaroid photograph was taken as a permanent record of each gel.

Specific activity measurements were obtained from steady-state H_2 evolution or acetylene reduction assays (see section 2.7.3).

Protein was estimated using the Lowry method (Lowry *et al*., 1951). Bovine serum albumin, BSA, (20-100 μg/ml) was used as a standard. Absorbance was determined at 750 nm with a Diode Array Spectrophotometer. Protein concentration was estimated from the standard curve.

Metal analysis is not only useful for estimating the purity of the nitrogenase proteins but also for determining the active site concentration and the Mo:Fe ratio for the MoFe protein. The Mo and Fe content of nitrogenase proteins was measured by Mrs. C. Dapper by inductively coupled plasma atomic emission spectrometry (ICP-AES). Samples were generally diluted to the final concentration of 0.2 mg/mL in 25 mM HEPES buffer (pH 7.4), 200 mM NaCl, 2 mM sodium dithionite. A minimum of three determinations for both Mo and Fe content could be obtained from a 5mL solution. The results were recorded as parts per million (ppm) of either Mo or Fe and were converted into gram atoms of either Mo or Fe per mole of protein, respectively.

2.6 Determination of homocitrate content by gas chromatography-mass spectrometry (GC-MS)

The homocitrate content of the FeMo cofactor in the MoFe protein was determined because the side chain of glutamine at the 191-position in the alpha subunit forms a hydrogen bond to one of the caboxylate groups of homocitrate and substitution of glutamine-191 by the other residues might result in the loss of homocitrate from the FeMo cofactor.

Purified nitrogenase MoFe protein (1 mg) was diluted to 0.5 mL with water and heated at 100^{o}C for 10 min in a sand filled heat block. The supernatant from the denatured protein, after centrifugation at 14,000 rpm for 10 min in an Eppendorf tube,

was passed through a Dowex AG50-X8 cation exchange (H^+) resin packed in a Pasteur pipette column (0.6 x 1.5 cm) and washed twice with 0.5 mL of water. The eluant containing homocitrate (total 1.5 mL) was dried by warming in a heat block and flushing with dry nitrogen gas and then resuspended in 0.5 mL of 1.0 M HCl in methanol overnight. After evaporation of the HCl and methanol from solution with dry nitrogen gas, the sample was dissolved in 1 mL of methylene chloride. This sample was then washed with a saturated solution of $NaHCO_3$, dried with Na_2SO_4 powder and evaporated with dry nitrogen gas. The sample was dissolved in 20 μL of methylene chloride and analyzed by GC-MS.

The samples (1-3 μL) were injected into a GC fitted with an Omegawax 320 capillary column (0.32 mm x 30 m), that was operated with 10 psi of helium as a carrier gas over the temperature range of 95 to 275°C, 16°C/min. The appropriate m/z fragment was detected with a VG-70-70E-HF mass spectrometer at 70 eV. The homocitrate methyl ester was quantified by the abundance of most intense fragment ion at m/z 129.

2.7 Nitrogenase steady-state assay

2.7.1 Reaction mixture

The reaction mixture is an ATP-regenerating system, which was prepared as a 3.3x stock solution for the nitrogenase activity assay, whose function is to eliminate the inhibiting effect of ADP produced during nitrogenase catalysis. This solution is comprised of 2.5 mM ATP, 5.0 mM $MgCl_2$, 30 mM creatine phosphate, and 25 units of creatine phosphokinase (CPK) in 25 mM HEPES buffer (pH 7.4).

The reaction mixture used in a three-buffer-system experiment contained the same concentration as above, except a mixture of 75 mM Bis-Tris, 38 mM HEPPS, and 38 mM CHES buffer (pH 7.4) was used instead of 25 mM HEPES buffer (pH 7.4). Again, a 3.3x stock reaction mixture solution was prepared and stored as 10-mL aliquots in the - 20°C freezer until used.

2.7.2 Substrate preparation

Gaseous nitrogenase substrates were used in kinetic studies either as a 100% pure gas or as a mixture. The 100% Ar and 100% N_2 gas phases were filled directly from an

automated vacuum/gas machine (Corbin, 1978). The C_2H_2 gas was prepared from the reaction of CaC_2 with water, collected over water in a 500-mL separating funnel, and then capped with a serum stopper before removing the funnel from the water. A positive hydrostatic pressure was maintained by a connection to a water reservoir.

The following formula was used to calculate the required volume of an added gas for a gas mixture in a vial with an average gas volume of 8.25 mL.

Required volume = 8.25 x (desired concentration) / [100% - (desired concentration)]

For example, a 10% C_2H_2 / 90% Ar atmosphere was achieved by dilution of one atmosphere pressure of 100% Ar with 0.92 mL of 100% C_2H_2.

The anaerobic 100 mM NaCN stock solution used to provide the HCN substrate of nitrogenase was prepared as follows. After flushing 0.049 gm of solid NaCN in a sealed serum vial with argon, 10 mL of degassed 25 mM HEPES buffer (pH7.4), 2 mM sodium dithionite, were added, followed by a predetermined amount of degassed 6 M HCl to obtain the desired pH. An appropriate volume of the stock solution was added to an assay mixture by syringe at the start of the preincubation period for temperature equilibration.

2.7.3 Determination of the specific activity of MoFe protein and Fe protein

Assays were performed in 9.25-mL sealed serum vials. An aqueous assay volume in a reaction vial consists of 0.3 mL of 3.3x stock reaction mixture, 0.1 mL of 200 mM sodium dithionite in 25 mM of HEPES buffer (pH 7.4), the desired volume of nitrogenase component proteins, and water to bring the total assay mixture to 1.0 mL. The procedure is outlined below. For all reactions, at least duplicate assays were performed.

1) The stock reaction mixture (0.3 mL) and water were added to the vials.
2) After the vials were capped with butyl rubber stoppers and aluminum seals, they were subjected to degassing with four cycles of 100 sec of evacuation and 10 sec of gassing using a custom-made vacuum/gas manifold (Corbin, 1978) with either argon or nitrogen.

3) The excess gas pressure of each vial was released by venting with a 3-mL syringe fitted with a 16-gauge needle filled with 1 mL water, before either assay or dilution of certain stock gases.
4) The stock gases (e.g., acetylene and/or carbon monoxide) were injected into the vials by using a gas-tight Hamilton syringe (Reno, Nevada) to achieve the calculated concentration (see section 2.7.2) before 100 μL of degassed 200 mM sodium dithionite in 25 mM HEPES buffer (pH 7.4) were added.
5) The vials were then placed in a water bath shaker at 30^{o}C for 5 min and each vial then was vented to atmospheric pressure again.
6) The stock substrate solution (when used) was added, followed by the nitrogenase component proteins (MoFe protein and Fe protein).
7) After a preset time interval, reactions were stopped by addition of 0.3 mL of 0.5 M sodium EDTA (pH 8.0).
8) The gas products of each assay vial were analyzed by gas chromatography (see section 2.8.1) and the products in the aqueous assay solution were estimated by colorimetric analysis (see section 2.8.2 and 2.8.3).

For crude extract activity assays, 50-100 μL of crude extract were used in each assay. Assays were performed on each extract alone and then separately with an excess of one or the other of the purified complementary proteins to determine either maximum MoFe protein or maximum Fe-protein activity.

In the purified MoFe protein nitrogenase activity assay, a total of 0.5 mg of nitrogenase protein is normally used to avoid complications introduced by both high and low protein concentration. In most cases, 0.423 mg of purified Fe protein and 0.077 mg of purified MoFe protein were used resulting in an Fe protein to MoFe protein molar ratio of 20 to 1.

Because a high concentration of MoFe protein inhibits nitrogenase turnover, during titration of the Fe protein with the MoFe protein, the molar ratio of Fe protein:MoFe protein was varied from 0.5:1 to 2:1 at a total protein of 0.5 mg. The maximum specific activity of Fe protein was determined from the highest activity of the titration curve plotted as nmoles of H_2 evolved (min.mg Fe protein)$^{-1}$ vs. Fe protein:MoFe protein molar ratio.

2.7.4 Kinetic experiments

2.7.4.1 Electron flux titration

The ability to reduce substrates depends on the electron flux through the nitrogenase enzyme because nitrogenase substrates are reduced by different numbers of electrons. Electron flux was controlled by varying the molar ratio of Fe protein to MoFe protein in activity assays containing a fixed amount of total-protein. The total protein was fixed at either 0.5 or 1.0 mg per 1 mL of assay solution depending on the individual nitrogenase activity. The procedure was performed as described in section 2.7.3 by using amounts of Fe protein or MoFe protein, which are varied in compensatory fashion, to give the desired molar ratio, while maintaining a constant total protein concentration. Electron flux ranged from 1:1 to 40:1 molar ratio of Fe protein:MoFe protein were used.

2.7.4.2 Substrate concentration dependence and K_m determination

There are two aspects to consider in a study of the substrate-concentration dependence. An increase in substrate concentration may cause substrate inhibition of electron flux during enzyme turnover in addition to being an indirect indicator of the binding affinity of the substrate for the enzyme (via the Michaelis constant, K_m). The K_m is the substrate concentration at which the specific activity of the enzyme of interest is half the value of the maximum specific activity (V_{max}). Determination of K_m was performed as described in section 2.7.3 by using 0.5 mg of total protein with the Fe protein:MoFe protein molar ratio of 20:1 unless otherwise stated. The various substrate concentrations were added to ensure that the concentration range covers 5-10 fold both higher and lower than the K_m. The K_m and V_{max} were determined from a double reciprocal plot of substrate concentration versus specific activity of proteins (Lineweaver-Burk plot).

It should be noted that the C_2H_2-concentration dependence experiments used C_2H_2 concentrations as high as 100%. The procedure for these assays involved replacing the argon in the vial with acetylene, which was then diluted with argon. This technique was used when the desired acetylene concentration was higher than 70%.

2.7.4.3 pH-activity profile study

The profile of activity versus pH was determined in order to study the effects of pH on nitrogenase catalysis and to gain insight into proton transfer during nitrogenase catalysis. The three-buffer system for developing a pH profile of nitrogenase activity was modified from Pham and Burgess (1993). This procedure allows a pH titration to be performed on this complex enzyme system over a pH range of 5.0-9.0. For each pH value, the reaction mixture in the three- buffer system was adjusted individually by adding either 6 M HCl or 6 M NaOH. Four vials were used for each pH assay. Because the sodium dithionite added to each assay causes a pH change, one of four vials was spared for measuring the actual pH during the assay. One of the other vials at each pH point was assayed for proton reduction under 100% Ar as a control to compare with the results from different sets of experiments.

2.8 Determination of nitrogenase reduction products

2.8.1 Quantification of the gaseous products

Gas products were quantified by gas chromatography. A pressure-lock gas tight syringe from Precision Sampling Corp. (Baton Rouge, LA) was used to inject the 100-200 μL of sample into a GC.

H_2 produced during the nitrogenase reaction was analyzed with a Shimadzu Model 8A GC fitted with a thermal conductivity detector (TCD). H_2 was separated from O_2 and N_2 on a 1 m x 2 mm I.D. molecular sieve 5 A, 60/80 mesh column, from Supelco Inc. (Bellefont, PA), operated at an oven temperature of 40^{o}C. Argon was the carrier gas at a flow rate of 60 mL/min. Peak area was integrated by a Shimadzu CR501 Chromatopac integrator, (Kyoto, Japan) and calibrated with reference to a standard with 1% H_2 in N_2 gas.

CH_4, C_2H_2, C_2H_4, and C_2H_6 were analyzed on a Shimadzu model GC-14A GC fitted with a flame ionization detector (FID). The hydrocarbon gases were separated with a 3 m x 2 mm Porapak N column, from Supelco Inc. (Bellefonte, PA) operated at a column oven temperature of 80^{o}C, with a detector temperature of 200^{o}C. Helium was the carrier gas at a flow rate of 90 mL/min. Whenever C_2H_6 was produced from C_2H_2 reduction with an altered MoFe protein, the flow rate was decreased to 45 mL/min for

effective separation between C_2H_4 and C_2H_6. The gases eluted from the column were identified by having the same retention time as the 1,000 ppm CH_4, C_2H_2, C_2H_4, or C_2H_6 in helium gas standards, which were also used for quantification.

2.8.2 Ammonia assay

Ammonia produced from both N_2 and HCN reduction was assayed by the phenol/hypochlorite colorimetric determination using ammonium sulfate as a standard (Dilworth *et al*., 1992). In these assays, a HEPES-based reaction mixture was used because it interferes less with the color development. As an improvement to our application of the indophenol method, the reactions were terminated with 0.3 mL of 0.5 M sodium EDTA (pH 8.0). After all gas products were quantified, an aliquot (0.5-1.0 mL) was removed from each reaction vial and applied to individually prepacked Dowex AG 1-X2 anion exchange columns (0.6 x 2.0 cm) to remove most of the inhibitors (the major one is creatine) of the color development reaction. The liquid flow-through and two 0.5-mL water washes were combined.

Due to the presence of remaining trace amounts of color-inhibiting substances in the assay, a spiked-blank was created and used as a color-inhibition correction factor. A spiked-blank consisted of a nitrogenase activity assay that was inactivated with EDTA prior to the start of the enzyme reaction. After passage over the column as for the sample, an appropriate known concentration of the ammonia standard was added. The percentage decrease in absorbance of the spiked standard was the inverse of the correction factor. As an alternative, a cation exchange column (after the anion exchange column above) was used to remove completely all of interfering creatine. A Dowex AG 50-X8 column (0.6 x 1.2 cm) was used to separate creatine and ammonia (Dilworth and Fisher, 1998). After the sample was passed through this column, creatine was washed from the column by two 0.5-mL portions of of water. The ammonia was eluted from the column by two 1-mL washes of 2.0 M NaCl, which were combined together.

An aliquot of 0.5 to 1.0 mL of each sample was diluted to 1.5 mL with water for the ammonia assay. A 0.3 mL aliquot of a 5% phenol in 2.5% NaOH (sodium phenate) solution was added, mixed, and followed by the simultaneous addition of 0.45 mL of 10% sodium hyperchlorite and 0.45 mL of 0.02% sodium nitroprusside. After a 40 min

incubation at room temperature, the absorbance of each solution was measured at 630 nm using $(NH_4)_2SO_4$ in the range of 0-200 nmoles as a standard.

2.8.3 ATP hydrolysis as determined by creatine formation

The ATP hydrolysis rates in nitrogenase activity assays were obtained from measurement of the creatine released from creatine phosphate upon the rephosphorylation of the ADP produced in the reaction as catalyzed by creatine phosphokinase. The interfering compounds from the nitrogenase reaction were removed by small anion-exchange columns as described for the ammonia assay. The combined eluent from the column (50-200 μL) was diluted to 0.5 mL with water and mixed with 2 mL of a solution containing 1% α-naphthol in 6% NaOH and 16% Na_2CO_3. **The reaction was started by adding 0.5 mL of 0.05% diacetyl solution.** After a 20-min incubation, 2.5 mL of water was added. The absorbance was then measured at 530 nm using creatine in the range of 0-250 nmoles as a standard.

2.9 Electron paramagnetic resonance (EPR) spectroscopy

EPR spectroscopy gives information about an unpaired electron and its immediate surroundings (because the *g*-values and line shapes are affected by the environment surrounding the unpaired electron). EPR is particularly useful as a method of studying the Fe-S clusters in proteins. The S = 3/2 EPR signal from the nitrogenase MoFe protein is a spectroscopic fingerprint for monitoring the presence of the FeMo cofactor. The purified MoFe protein was frozen in EPR tubes and the S=3/2 spectrum recorded at a microwave frequency of 9.2 GHz and a microwave power of 10-20 mW at liquid helium temperature. For the most part, EPR samples were run in the laboratory of Dr. Richard Dunham at the University of Michigan (Ann Arbor, MI) on a Varian E-line spectrometer built by Varian Associates (Palo Alto, CA).

The quartz EPR tubes used were 3x 200 mm obtained from Wilmad Glass Co. Inc. (Buena, NJ). Capped EPR tubes were flushed with argon gas. The purified MoFe protein (250 μL and at a concentration of at least 20 mg/mL) was injected into EPR tubes. The protein solution was frozen in liquid nitrogen from the bottom up to prevent

cracking (by gradually lowering the tube into liquid nitrogen). The tube was then uncapped and stored submersed in liquid nitrogen until examined.

CHAPTER 3

Catalytic Consequences of Substitutions at the Nitrogenase MoFe Protein αGln-191 Residue: a Study with Crude Extract and Purified MoFe Protein.

Summary

Amino-acid substitutions at the αGln-191 residue introduce a modification in catalytic activity compared with wild type MoFe protein. All altered MoFe proteins exhibit a rate of H_2 evolution under Ar that is lower than wild type in either crude extracts or as purified proteins. Six altered MoFe proteins, which have amino acid substitutions with side chains of different properties (Pro, Ser, Thr, His, Glu, and Arg) were purified and characterized.

The EPR spectra of six altered MoFe proteins, when compared with the wild type spectrum, show no significant change in terms of either the line shape or the *g*-value of the characteristic FeMo cofactor EPR signal. This result suggests that the substitutions most likely produce only a minor perturbation within the local cofactor environment.

The results of substrate reduction with these altered MoFe proteins suggest that N_2 reduction is more sensitive to these substitutions than C_2H_2 reduction and C_2H_2 reduction is more sensitive than H^+ reduction. The αPro-191, αSer-191, or αThr-191 altered MoFe proteins, which either eliminate or weaken the putative hydrogen bonding to homocitrate, have less effect on both C_2H_2 and N_2 reduction. Thus, the hydrogen bonding to homocitrate by glutamine (when present) is not absolutely required for reducing C_2H_2 and N_2. In contrast, the αHis-191, αGlu-191, or αArg-191 altered MoFe proteins, which have side chains that might block any movement of homocitrate, have a more damaging effect on both C_2H_2 and N_2 reduction. These results imply that movement of homocitrate is likely required for reducing C_2H_2 and N_2.

Unlike wild type, the six altered MoFe proteins exhibited H_2 evolution that was partially inhibited by added CO. Moreover, those MoFe proteins with lower specific activity for the C_2H_4 production, namely the αHis-191, αGlu-191, and αArg-191 altered MoFe proteins, can produce C_2H_6 from C_2H_2.

3.1 Introduction

Our laboratory has sought insight into the catalytic mechanism of nitrogen fixation by disrupting selected localized areas of FeMo cofactor's environment through directed amino acid substitution. The investigations have focused on: 1) the spatial relationships among the binding sites of various nitrogenase substrates and inhibitors (Scott *et al*., 1992; Kim *et al*., 1995; Shen *et al*., 1997; Lee *et al*., 1998; Dilworth *et al*., 1998; Fisher *et al*., 2000a,b,c); 2) the residues mediating the electron transfer between P cluster and FeMo cofactor (May *et al*., 1991; Peters *et al*., 1995a); and 3) the involvement of nearby amino acids in proton transfer during substrate reduction (Dilworth *et al*., 1998; Fisher *et al*., 2000a,b,c). Major targets are the closeby α-subunit residues, for example, αGln-191 and αHis-195, which are not covalently bonded to the FeMo cofactor.

αGln-191 is a good target because its amide NH forms a putative hydrogen bond with a terminal carboxylate of homocitrate and homocitrate is ligated by its 2-carboxyl and 2-hydroxyl to the Mo atom of the FeMo cofactor. The crystal structure of the Fe protein-MoFe protein complex stabilized by a nucleotide triphosphate analogue, MgADP:AlF_4^-, shows the location of the P cluster between the 4Fe-4S cluster of the Fe protein and the FeMo cofactor of MoFe protein (Schindelin *et al*., 1997). This arrangement strongly suggests that the electron-transfer pathway is from Fe protein via the P cluster to the FeMo cofactor. Because the distance from edge-to-edge between the homocitrate site of FeMo cofactor and the closest P cluster is about 14 Å, it is, therefore, unlikely that the two metal centers come into contact during catalysis. Electron transfer between the two centers must involve the polypeptide matrix that separates them. The hydrogen-bonding network from αCys-62, the P cluster-ligating residue, through the NH of αGly-61, αGln-191 to homocitrate, as well as water molecules, provides a link between these two metal centers (Figure 3.1). These residues, therefore, form a potential electron-transfer pathway and could provide tight correlation between both reduction and the protonation of bound substrate through the intermediary of homocitrate.

The extensive hydrogen-bonding network in the region of homocitrate is likely to be important for substrate reduction. An altered FeMo cofactor is produced in the *nifV*$^-$ mutant strain of *K. pneumoniae*, where citrate replaces homocitrate as the organic

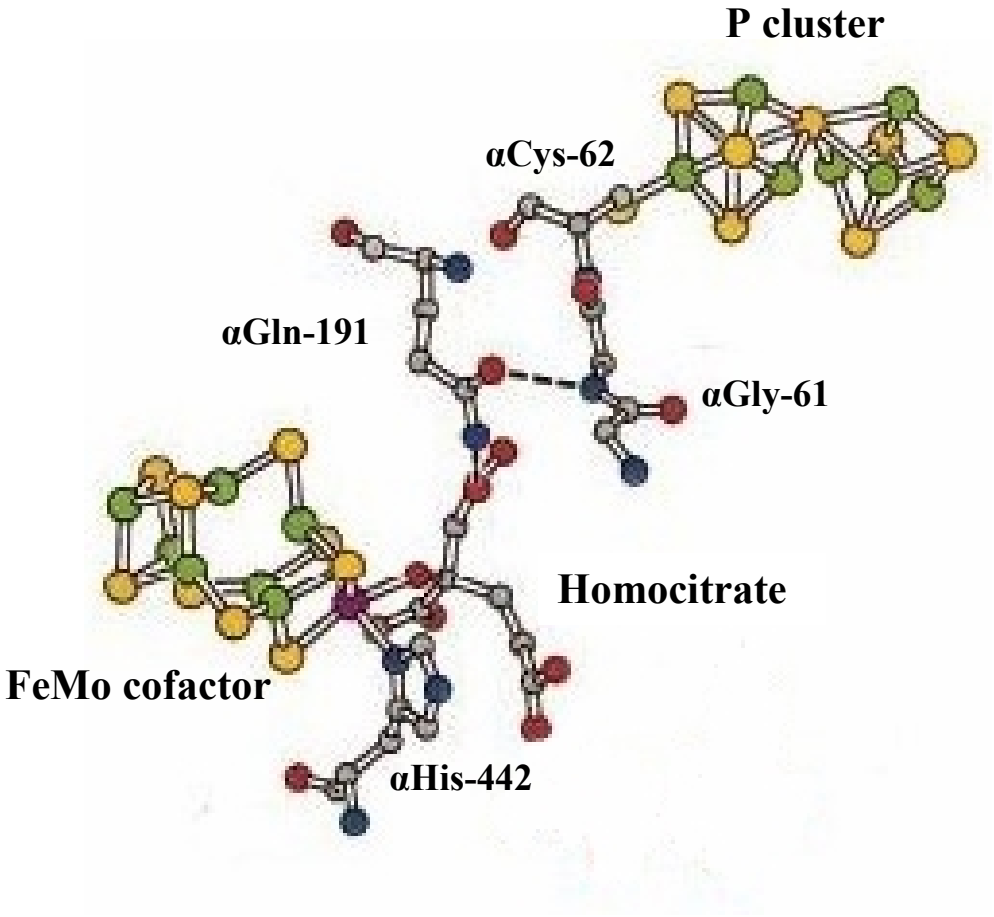

Figure 3.1 The protein environment between the P cluster and FeMo cofactor of MoFe protein (Adapted from Grönberg *et al*., 1998). Atom colors are iron in green, sulfur in yellow, nitrogen in blue, and oxygen in red.

constituent (Liang *et al*., 1990). This replacement results in a phenotype of both decreased nitrogen-fixation capacity and CO-sensitive proton reduction (McLean *et al*., 1983). Thus, the organic entity plays an important role in directing the MoFe protein's substrate reduction and inhibitor susceptibility. Moreover, *in vitro* reconstitution of the FeMo-cofactor, using a wide variety of carboxylic acids, implies that only homocitrate itself is capable of supporting significant reduction of N_2, with C_2H_2- and H^+-reduction being successively less stringent (Imperial *et al*., 1989). These changes must disrupt the hydrogen-bonding network around homocitrate, but exactly how they produce their effects is not yet clear.

This substitution of Lys for Gln at position 191 results in an altered MoFe protein (the αLys-191 MoFe protein) that cannot reduce N_2 but can still reduce H^+ and C_2H_2. This altered MoFe protein also differs from wild-type MoFe protein in that it exhibits H^+-reduction that is about 50% sensitive to CO (Scott *et al*., 1992). This last feature is characteristic of the MoFe protein produced by the *nifV*$^-$ mutant strain where FeMo-cofactor contains citrate rather than homocitrate. Another interesting feature of αLys-191 altered MoFe protein is its poor ability to catalyze the reduction of C_2H_2. Even so, it can reduce C_2H_2 by both two and four electrons to give C_2H_4 and ethane (C_2H_6), whereas wild type produces only C_2H_4. Reduction of C_2H_2 to both C_2H_4 and C_2H_6 is also a property of the V-nitrogenase (Dilworth *et al*., 1988) although there are differences in the catalytic mechanism (Scott *et al*., 1992). The observation of phenotypes that combine the phenotypes of substituting of V for Mo and an alteration in the organic acid attached to the Mo atom points to an important role in the catalytic mechanism for Gln in this position and its relationship to homocitrate.

In this chapter, altered MoFe proteins with known amino-acid substitutions for the αGln-191 residue are analyzed to detect catalytic modification at both the crude-extract level and the purified protein level with selected substrates and inhibitors. A change in the size, charge, or functional group of the amino-acid side chain could impact the strength of hydrogen bonding, the proposed subsequent movement of the terminal carboxylate group of homocitrate and, therefore, the catalytic efficiency of the resulting nitrogenase. We have two major goals of this study. First, the reaction of these altered MoFe proteins should give insight into whether or not the hydrogen bond to the

carboxylate group of homocitrate is required and undergoes motion, that involves making and breaking of this hydrogen bonding, for substrate reduction during nitrogenase catalysis. Second, we extend the study to understand whether or not the two unusual properties of CO-sensitive H^+-reduction and C_2H_2 reduction to both C_2H_4 and C_2H_6 could be exhibited by altered MoFe proteins other than the αLys-191 altered MoFe protein.

We compare the characteristics in crude extracts of ten *A. vinelandii* mutants, each having a single amino-acid substitution at αGln-191 of the MoFe protein, with those of wild type. We also analyze the N_2-, H^+-, C_2H_2- reduction properties and CO inhibition properties of purified MoFe proteins isolated from six of these mutant strains to compare with those of wild type purified MoFe protein.

3.2 Experimental procedures

The experimental procedures in this chapter have been provided in more detail in Chapter 2 and are only briefly described below.

3.2.1 PCR and DNA sequencing

The DNA fragment in a region of the MoFe protein α-subunit containing the α-subunit residues of interest was amplified using oligonucleotides Fp1 (CGTAACAAGCACCTGGCC, sense) and Rp1 (GAGCATGACGCGCTTGCC, antisense) as the primers by PCR (Fisher *et al*., 2000c). Automated DNA sequencing was performed in Virginia Tech's DNA sequencing facility using standard methods on an ABI 377 Automated DNA Sequencer and using PE Biosystems Big Dye Terminator chemistry.

3.2.2 Growth condition and media

Wild type and mutant strains were grown at 30°C in a modified Burk medium (Strandberg and Wilson, 1968). This medium contained 10 μM Na_2MoO_4 to ensure that only Mo-dependent nitrogenase was under study. When required, a fixed-nitrogen source of filtered-sterilized urea was added to a final concentration of 20 mM. Diazotropic growth characteristics of the strains were determined by inoculating 50 mL of nitrogen-free Burk medium in a 250-mL side-arm flask to a 20-30 Klett-Summerson colorimeter fitted with a no. 54 filter. Cultures were grown under air with shaking at 250 rpm.

Large-scale *A. vinelandii* cultures were grown in a 24-L MF-128S Microferm fermentor (New Brunswick Scientific Company, New Brunswick, NJ) on modified Burk medium, plus Na_2MoO_4 and urea as described above, with an air-flow rate of 40-45 L/min and vigorous stirring of 300 rpm. When the cell density reached about 200 Klett units, the cultures were then derepressed for nitrogenase synthesis (Jacobson *et al*., 1989). *A. vinelandii cells* were harvested and stored at - 80^{o}C until further use.

3.2.3 Crude extract preparation

Cells were anaerobically thawed and diluted at 4^{o}C in degassed 50 mM Tris-HCl, pH 8.0, containing 2 mM sodium dithionite, at the ratio of 1.0 gm of cells to 2.0 mL of buffer. The cell suspension was broken using a Sonicator model XL2015 either in a 25-mL Rosette cooling cell (Heat Systems-Ultrasonics, Inc.) with 6 cycles of 30 min on/off intervals for small-scale preparation or in a 200-mL Rosette cooling cell with 6 cycles of 1 min on/off intervals for large-scale preparation. The Rosette cell was immersed in an ice-water bath to offset increasing temperature. In either case, the resulting extract was heat-treated for 5 min at 52-55^{o}C (if the protein is heat stable) and cooled, before being anaerobically transferred into centrifuge tubes and centrifuged at 4^{o}C for 90 min at 98000g. The supernatant was frozen and stored in liquid nitrogen until used.

3.2.4 Protein purification

The MoFe proteins produced by wild type and mutant strains were purified in parallel from crude extracts by using the following procedure. The purification of the nitrogenase MoFe protein component involved (Kim *et al*., 1995; Fisher *et al*., 2000a): 1) Q-Sepharose anion-exchange chromatography using a linear NaCl-concentration gradient; 2) gel filtration on Sephacryl S-200, and 3) phenyl-Sepharose hydrophobic interaction chromatography. The Fe protein was applied to a second Q-Sepharose anion-exchange column and purified to homogeneity. Unless otherwise stated, all buffers were saturated with argon (Ar) and contained 25 mM Tris-HCl (pH7.4), 2 mM sodium dithionite. The purified component proteins were concentrated, using an Amicon microfiltration cell in an ice-water bath and exchanged into 25 mM HEPES (pH 7.4), 200 mM NaCl, 2 mM sodium dithionite, by a small S-300 gel filtration column under anaerobic conditions. The Lowry method was used for protein estimation with bovine

serum albumin as a standard (Lowry *et al*., 1951). The SDS-PAGE was used to confirm that all proteins were homogeneous (Laemmli, 1970). The Mo and Fe content of the proteins, in gram atom of Mo or Fe per mole of protein, were measured by inductively coupled plasma atomic emission spectroscopy (ICP-AES) on a Perkin-Elmer Plasma 400 spectrometer (Norwalk, CT).

3.2.5 Nitrogenase activity assay

MoFe protein and Fe protein specific activities in both crude extracts and purified proteins in the presence of an optimal amount of the purified complementary component protein were determined as described previously (Kim *et al*., 1995). Substrate reduction assays were performed at 30^{o}C in 9.25-mL reaction vials fitted with butyl rubber septa held by aluminum caps. Each assay contained 30 μmol of creatine phosphate, 25 μmol of HEPES buffer (pH 7.4), 20 μmol of sodium dithionite, 5 μmol of $MgCl_2$, 2.5 μmol of ATP, and 25 units of creatine phosphokinase in a final volume of 1.0 mL. Gaseous substrates and/or inhibitors were added by gas-tight syringe to a 100% Ar atmosphere and then vent to atmospheric pressure. Reaction was initiated by nitrogenase protein after a 5-min incubation period at 30^{o}C. Reaction was terminated, usually after 10 min, by injection of 0.3 ml of 0.5 M EDTA-Na_2, pH 8.0. For crude extract activity assays, 50-100 μL of crude extract were used in each assay. The MoFe protein and Fe protein activities of each crude extract were assayed for H^+- or C_2H_2-reduction in the presence of an optimal concentration of its purified complementary protein. In the purified MoFe protein nitrogenase activity assay, a total of 0.5-1.0 mg of nitrogenase protein was used at a constant Fe protein:MoFe protein molar ratio of 20:1.

Gaseous nitrogenase substrates were normally used as either 100% pure or as a mixture. Catalyzed H^+-, N_2- and C_2H_2- reduction assays were performed under a 100% Ar, 100% N_2 and 10% C_2H_2/ 90% Ar gas phase, respectively.

3.2.6 Analytical methods

H_2 evolution was measured by gas chromatography on a molecular sieve 5A column with TC detector. C_2H_4 and C_2H_6 were quantified with a Porapak N column with

FID detector. Calibration gases used were 1000 ppm C_2H_4 in helium, 1000 ppm C_2H_6 in helium, and 1% H_2 in N_2 (Scott Specialty Gases, Plumsteadville, PA).

For NH_3 produced from N_2 reduction, each reaction was individually applied to a Dowex 1x2 anion-exchange column (Dilworth *et al*., 1992) before NH_3 was determined by phenol/hypochlorite colorimetry. Due to the presence of remaining trace amounts of color-inhibiting substances in the assay, a spiked-blank with known amount of NH_3 was created and used as a color-inhibition correction factor. Creatine, as a measure of MgATP hydrolysis, was also measured from the liquid sample collected from the Dowex column by method of Ennor (1967).

3.2.7 Electron paramagnetic resonance spectroscopy

Purified MoFe proteins were prepared and were run for EPR spectroscopy as previously described in section 2.9.

3.3 Results

3.3.1 Diazotropic growth and crude extracts analysis

All mutant strains used in this study were constructed by Dr John Peters in an earlier collaborative project with Dr. Dennis Dean (Virginia Tech). Ten different *A. vinelandii* mutant strains, each of which produces an altered MoFe protein having an individual amino acid substitution located at the αGln-191 position, were studied. These mutant strains (coded by DJ) contain the following amino acid substitutions: Val (DJ 779), Pro (DJ776), Ala (DJ796), Ser (DJ780), Thr (DJ782), His (DJ792), Gly (DJ803), Arg (DJ794), Phe (DJ790), or Glu (DJ64). A region of the *nifD* gene of one mutant strain, DJ64, was resequenced to ensure that we did indeed have the correct mutant strain carrying the desired altered MoFe protein. DNA sequencing of both strands confirmed that the original mutation was still in place.

Characterization with these strains compared with wild type is shown in Table 3.1. The growth characteristics on the no-fixed-nitrogen Burk medium on plates in air exhibit a complete range of phenotypes. Three of these strains (αVal-191, αPro-191, and αAla-191) can grow comparably to the wild type (Nif^+). The αSer-191 and αThr-191

grow more slowly (Nif ^{slow}), whereas αHis-191, αGly-191, αPhe-191, and αGlu-191 cannot grow (Nif $^{-}$) under this n0-fixed-nitrogen condition.

The doubling time of the two Nif ^{slow} phenotype mutants, αSer-191 and αThr-191 was determined and found to be higher than wild type during the logarithmic growth on no-fixed-nitrogen Burk liquid media. The four Nif $^{-}$ phenotype mutants, αHis-191, αGly-191, αPhe-191, and αGlu-191, cannot grow in no-fixed-nitrogen liquid medium. These results are in agreement with diazotrophic-growth behavior on plates.

Crude extracts prepared from both nitrogenase-derepressed wild type and mutant strains were assayed for nitrogenase component-protein activities and the results of these assays are compared in Table 3.1. It should be noted that, because crude extracts were prepared from nitrogenase-derepressed cells, it is difficult to accurately compare activities of MoFe protein in different preparations without an estimate of the relative levels of nitrogenase derepression. In this experiment, an estimation of the relative levels of nitrogenase accumulation in crude extracts from different strains was accomplished by measuring the corresponding levels of Fe protein activity. The Fe protein specific activities in crude extracts are roughly similar (Table 3.1). This result means that the level of nitrogenase derepression is comparable. Then, the quantitative differences in MoFe protein specific activities present in crude extracts of different mutant-strain can be attributed to the specific alteration in their respective MoFe proteins.

The MoFe proteins of various mutant strains exhibit varying H^+-reduction activities ranging from 3 to 69% of wild type MoFe protein. One strain, αGlu-191, in which the uptake hydrogenase structural genes (*hoxKG* genes) are not deleted, retains its hydrogen uptake activity (Hup). Then, it cannot be accurately compared with the H^+-reduction of the other MoFe proteins. The percentage of the electron flux allocated to reduce C_2H_2 ranges from 3% to 80% for the mutant strains compared to 84% for wild type. Most of the altered MoFe proteins exhibit CO-sensitive H_2 evolution (Table 3.1).

3.3.2 Purification of the MoFe proteins and their substrates reduction

Six mutant strains (αPro-191, αSer-191, αThr-191, αHis-191, α-Glu-191, and αArg-191) promised interesting phenotypes and were selected for a comparative study of

Table 3.1 Nif phenotypes, crude extract MoFe protein specific activities, and Fe protein specific activities of α-191 mutant strains.

Strain	Substitution at αGln-191	Nif phenotype	100% Ar[a]	10%CO + 90% Ar[a]	10% C_2H_2 + 90% Ar[a]		Fe protein[d]
			H_2	H_2	H_2	C_2H_4	H_2
DJ527	None	+	118	133(+13)[b]	19(16)[c]	103(84)[c]	72
DJ779	Val	+	81	62(-24)	14(20)	58(80)	93
DJ776	Pro	+	80	67(-16)	21(26)	59(74)	84
DJ796	Ala	+	78	64(-18)	20(29)	48(71)	88
DJ780	Ser	slow	81	60(-26)	45(55)	37(45)	74
DJ782	Thr	slow	68	58(-15)	16(26)	46(74)	71
DJ792	His	–	73	56(-23)	51(72)	20(28)	81
DJ803	Gly	–	48	54(+12)	32(69)	14(31)	82
DJ794	Arg	–	32	19(-41)	24(75)	8(25)	66
DJ790	Phe	–	3.4	5.3(+56)	3.3(97)	0.1(3)	57
DJ64[e]	Glu	–	ND	ND	ND	ND	ND

[a] The MoFe protein specific activities are in nmole of products per minute per milligram of MoFe protein under different gaseous atmospheres. [b] The number in parenthesis is the percentage change in the presence of CO. [c] The numbers in the parenthesis are the percentage of electron distribution between H_2 and C_2H_4 produced under 10%C_2H_2/90%Ar. [d] The specific activities of Fe protein are in nmole of H_2 evolved per minute per milligram of Fe protein under 100%Ar. [e] Strain is not deleted for the uptake hydrogenase structural genes and so the proton-reduction activities could not be reliably measured in crude extracts. ND represents no determination.

substrate reduction along with wild type. Four types of amino-acid substitutions are represented: 1) the hydrophobic side chain (αPro-191); 2) small and polar side chain (αSer-191 and αThr-191); 3) large, but putatively hydrogen-bonding side chain (αHis-191); and 4) charged species (αGlu-191 with a negative charge and αArg-191 with a positive charge). The MoFe proteins produced by wild type and mutant strains were purified in parallel from their crude extracts to minimize any variation potentially introduced by different purification protocols. By careful selection of fractions eluting from both the Q-Sepharose and Sephacryl S-200 columns before application of phenyl-Sepharose chromatography, all seven MoFe proteins used in this study were purified to high specific activities. Table 3.2 is the purification table for wild type and the six altered MoFe proteins. Similar levels of purification were achieved for both wild type and altered MoFe proteins as shown by their MoFe protein specific activities and fold of purification. The purified MoFe-protein fraction from this procedure is judged by the migration pattern and the intensity of the protein bands on SDS-PAGE to be more than 90% pure and reveals two bands which correspond to the α- and β-subunits of the MoFe protein (Figure 3.2).

The results for H^+-, C_2H_2-, and N_2-reduction and CO-inhibition are shown in Table 3.3. The variation in the amount of Mo in the MoFe protein indicates the amount of intact FeMo cofactor in the MoFe protein (e.g., less Mo means less FeMo-cofactor) after the MoFe protein is purified. The specific activities of all proteins under Ar, when calculated on a per Mo atom basis, indicate that they all exhibit a rate of H_2 evolution lower than wild type. The percentage of H_2 evolution inhibited by added CO and the electron distribution to products under 10% C_2H_2/ 90% Ar are all in agreement with the results from crude extracts. These observations indicate that the purification protocol did not introduce any of the changes in the respective catalytic activities of these MoFe proteins. The N_2- reduction results are in accord with the growth phenotype in that αPro-191, αSer-191, and αThr-191 direct 44%, 26%, and 10% of the electron flux to produce ammonia, respectively. On the other hand, αHis-191, αGlu-191, and αArg-191 cannot reduce N_2. Interestingly, three of these altered MoFe proteins reduce C_2H_2 poorly and produce C_2H_6 under 10% C_2H_2/ 90% Ar. The percentage of electron flux going to the

Table 3.2 Purification table for wild type and altered MoFe proteins

MoFe protein		Crude extract[a]	Q-sepharose	Sephacryl S-200	Phenyl Sepharose[b]
αGln-191* (Wild type)	SA	260	920	1900	2700
	Fold	1	3.5	7.3	10.4
αPro-191*	SA	130	400	560	1700
	Fold	1	3.1	4.3	13.0
αSer-191*	SA	150	370	800	1500
	Fold	1	2.5	5.3	10.0
αThr-191	SA	64	160	380	940
	Fold	1	2.5	5.9	14.7
αHis-191*	SA	120	300	750	1650
	Fold	1	2.5	6.2	13.8
αGlu-191	SA	70	100	180	990
	Fold	1	1.4	2.6	14.1
αArg-191	SA	30	80	190	490
	Fold	1	2.7	6.3	16.3

[a]Crude extract after the cells were broken and centrifuged at 98,000g for 90 min. *A heat treatment was done at 52°C, 5 min before the cell extract was centrifuged. [b]The MoFe protein was exchanged into 25 mM HEPES buffer (pH 7.4), 200 mM NaCl, 2 mM sodium dithionite, before assay but after chromatography. SA represents the specific activity of MoFe protein that is expressed as nmole of H_2 evolution per minute per milligram of MoFe protein. Fold of the purification is determined by the specific activity of protein from each purification step divided by the specific activity of protein from crude extract.

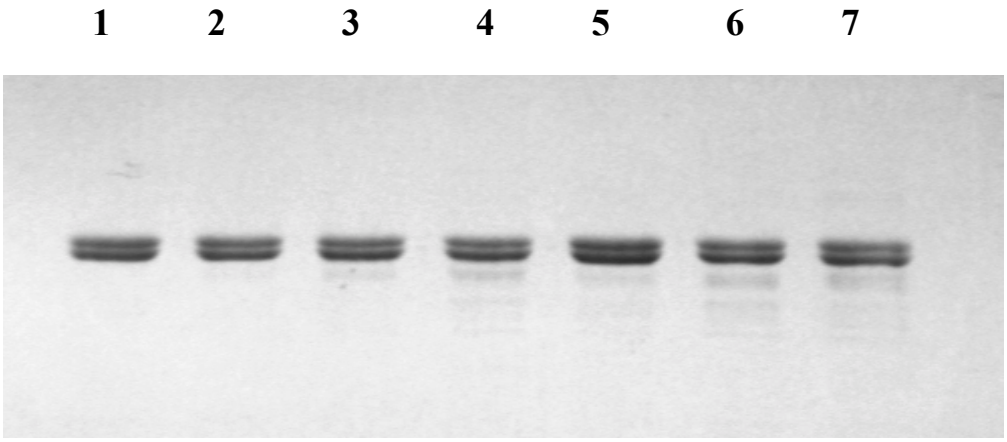

Figure 3.2 SDS-PAGE of purified wild type and six altered MoFe proteins. Lane 1: αGln-191 (wild type) MoFe protein; Lane 2: αPro-191 MoFe protein; Lane 3: αSer-191 MoFe protein; Lane 4: αThr-191 MoFe protein; Lane 5: αHis-191 MoFe protein; Lane 6: αGlu-191 MoFe protein; Lane 7: αArg-191 MoFe protein.

Table 3.3 Molybdenum content, specific activities under various atmospheric gaseous phases, and ATP/$2e^-$ ratios with purified wild type and six purified altered MoFe proteins

MoFe protein	Mo con-tent[a]	Atmospheric gaseous phase	Products formed[b]				Total flux[c]	ATP/ $2e^{-}$[d]
			H_2	C_2H_4	C_2H_6	NH_3		
Wild type	2.0	100%Ar	2700	-	-	-	2700	4.5
		10%C_2H_2 + 90%Ar	290	2400	0	-	2690	4.2
		100%N_2	890	-	-	1900	2790	5.1
		10%CO + 90%Ar	2800	-	-	-	2800	4.6
αPro-191	1.7	100%Ar	1700	-	-	-	1700	4.6
		10%C_2H_2 + 90%Ar	300	1190	0	-	1490	5.0
		100%N_2	950	-	-	740	1690	4.7
		10%CO + 90%Ar	1380	-	-	-	1380	5.6
αSer-191	1.4	100%Ar	1500	-	-	-	1500	5.4
		10%C_2H_2 + 90%Ar	650	560	0	-	1210	6.2
		100%N_2	1130	-	-	130	1260	5.9
		10%CO + 90%Ar	970	-	-	-	970	8.2
αThr-191	1.2	100%Ar	940	-	-	-	940	5.6
		10%C_2H_2 + 90%Ar	190	660	0	-	850	6.8
		100%N_2	520	-	-	180	700	8.3
		10%CO + 90%Ar	720	-	-	-	720	7.7
αHis-191	1.6	100%Ar	1650	-	-	-	1650	5.1
		10%C_2H_2 + 90%Ar	1270	330	1	-	1601	5.2
		100%N_2	1630	-	-	0	1630	5.6
		10%CO + 90%Ar	1240	-	-	-	1240	7.5

Table 3.3 Continue.

αGlu-191	1.1	100%Ar	990	-	-	-	990	5.9
		10%C_2H_2 + 90%Ar	590	240	20	-	850	6.7
		100%N_2	980	-	-	0	980	5.9
		10%CO + 90%Ar	800	-	-	-	800	7.5
αArg-191	0.8	100%Ar	490	-	-	-	490	7.8
		10%C_2H_2 + 90%Ar	360	140	2	-	502	8.1
		100%N_2	420	-	-	0	420	9.1
		10%CO + 90%Ar	270	-	-	-	270	14.1

[a] Expressed as the number of molybdenum atoms in one molecule of MoFe protein. The ideal value is two molybdenum atoms per molecule of MoFe protein. [b] Specific activity is expressed as nmole of electron pairs per minute per milligram of MoFe protein appearing in each product in the presence of a 20-fold molar excess of wild type Fe protein. For C_2H_6 and NH_3 products, these rates must be divided by 2 and 1.5, respectively, to give specific activity in terms of nmol of products. [c] Total electron flux is expressed as nmole of electron pairs per minute per milligram MoFe protein appearing in all measured products per assay. [d] Expressed as the number of MgATP molecules hydrolyzed for each electron pair found in measured products.

combined production of C_2H_4 and C_2H_6 under the same conditions decreases from 89% (C_2H_4 only) for wild type to 21%, 31%, and 28% for the αHis-191, αGlu-191, and αArg-191, respectively. C_2H_6 is not produced by wild type. C_2H_6 production accounted for 0.3%, 7.7%, and 1.4% of the electron flux allocated to C_2H_2 reduction with αHis-191, αGlu-191, and αArg-191, respectively.

The number of ATP molecules hydrolyzed per electron pair (ATP/$2e^-$ ratio) appearing as products is a measurement of the efficiency of the Fe protein-MoFe protein interaction. Most of the altered MoFe proteins, when assayed under 100% Ar, showed an increase in the ATP/$2e^-$ rate indicating uncoupling of electron transfer from ATP hydrolysis compared to wild type (4.5). When 10% CO is introduced, the ATP/$2e^-$ ratio increases further (from 5.6 - 14.1) and the degree of uncoupling correlates well with the extent to which CO inhibits H^+-reduction. The different distribution of electron flux to products, the unusual product (C_2H_6 from C_2H_2 reduction), atypical inhibitor effects (CO-inhibiting H_2 evolution) and abnormal ATP uncoupling from electron transfer under CO have all been clearly observed with the MoFe protein substituted at the α 191 position.

3.3.3 EPR spectra of dithionite-reduced wild type and altered MoFe proteins

The EPR spectra of purified wild type and altered MoFe proteins were recorded both in our laboratory and in Dr. Richard Dunham's laboratory on a Varian E-line spectrometer. The results show that there are no significant differences in the spectra of the wild type MoFe protein and the six altered MoFe proteins in term of either line shape or *g*-values of the characteristic FeMo cofactor EPR signal. Figure 3.3 shows the S = 3/2 EPR signal for wild type, αSer-191, and αGlu-191 MoFe proteins. The S = 3/2 EPR signal of these three MoFe proteins exhibit the same *g*-values, which are 4.3 and 3.6. However, the peak intensity of the g = 3.6 line of both the αSer-191 and αGlu-191 altered MoFe proteins, when they were calculated as a function of Mo content in each MoFe protein, were about 62% and 28%, respectively, of the intensity of wild type MoFe protein. The weak EPR signal intensities may indicate that there is either some "EPR inactive" FeMo cofactor, which does not contribute to the EPR signal of both the αSer-191 and αGlu-191 altered MoFe proteins in the resting state under the dithionite-reduced

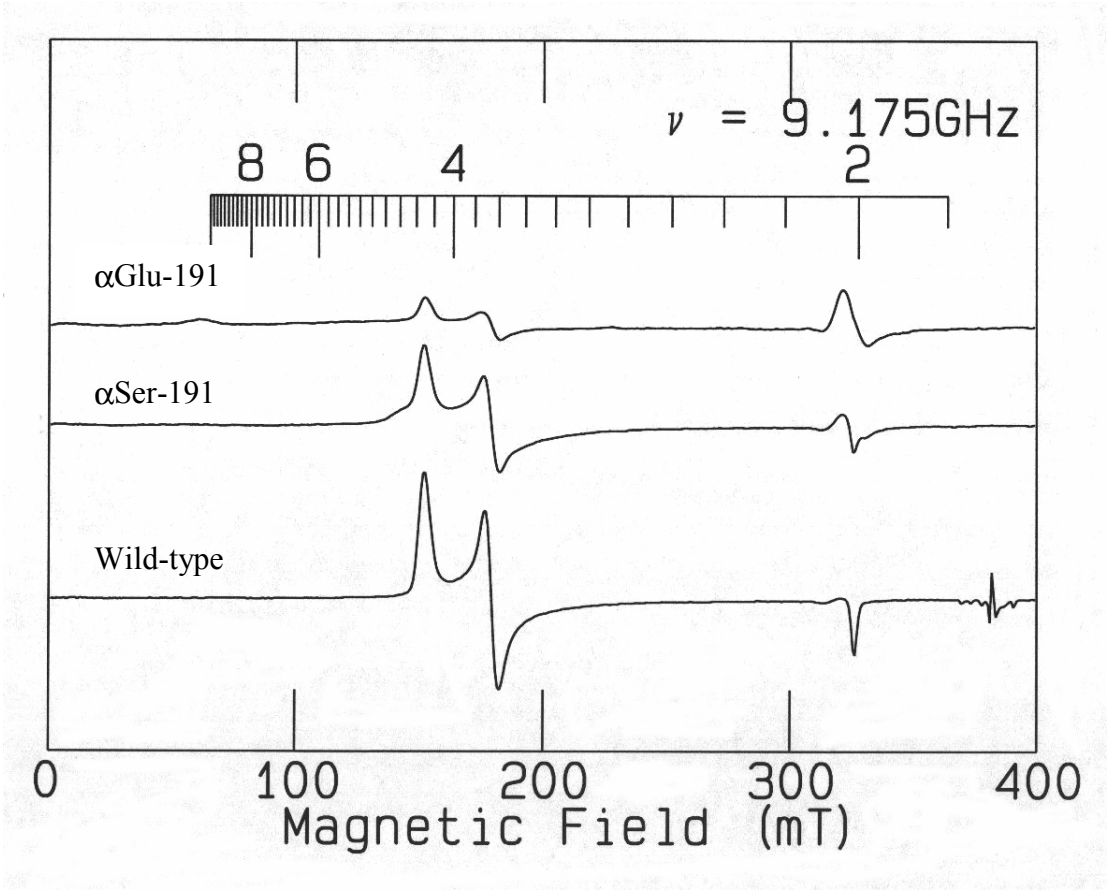

Figure 3.3 Comparison of the EPR spectra for wild type, αSer-191, and αGlu-191 MoFe proteins.

condition, or more likely that each sample contains a FeMo cofactor of lower activity and that the change in properties of these altered MoFe protein results from a relatively minor perturbation within the local FeMo cofactor environment rather than from any gross structure change.

3.4 Discussion

Based on the *in vitro* synthesis of FeMo cofator, it has been shown that the organic constituent (homocitrate in wild type) of FeMo cofactor plays an important role in directing the MoFe protein's substrate-reduction and inhibitor-susceptibility properties (Hoover *et al*., 1988; Imperial *et al*., 1989; Madden *et al*., 1990). The MoFe protein produced in $NifV^-$ strains of *K. pneumoniae* contains an altered FeMo cofactor, with citrate replacing homocitrate (Liang *et al*., 1990) and exhibits both a lower rate of N_2 fixation and also H^+-reduction that is partially inhibited by CO (McLean and Dixon, 1981). Moreover, the heterometal to which homocitrate is ligated also affects substrate reduction. V-nitrogenase, which is synthesized by cells starved of Mo but supplemented with V (Robson *et al*., 1986; Hales *et al*., 1986; Bishop and Premakumar, 1992) exhibits different substrate specificities from those of Mo-nitrogenase (Eady *et al*., 1987). For example, C_2H_6, in addition to C_2H_4, is a product of the V-nitrogenase-catalyzed reduction of C_2H_2 (Dilworth *et al*., 1988).

In the previous studies (Scott *et al*., 1990; Scott *et al*., 1992), it was shown that the polypeptide environment of FeMo cofactor also plays an important role in directing its substrate-reduction properties. Certain amino acid substitutions placed within targeted region of the α-subunit of the *A. vinelandii* MoFe protein, which encompasses the αGln-191 and αHis-195 residues, resulted in changes in the catalytic activity of altered MoFe protein. Substitution of αGln191 by Lys results in an altered MoFe protein that cannot reduce N_2 but still reduces H^+ and C_2H_2, although at lower levels (Scott *et al*., 1992). The αLys-191 MoFe protein also differs from the wild type MoFe protein in that its proton reduction is sensitive to CO and it reduces C_2H_2 by four electrons to C_2H_6. These last two properties are characteristic of $NifV^-$ MoFe protein and V-nitrogenase, respectively. The similar biochemical consequences of these changes can now be understood in light of the MoFe protein structure because αGln-191 is hydrogen bonded to a terminal

carboxylate of homocitrate and homocitrate forms covalent bonds by its both hydroxyl and carboxylate to Mo of FeMo cofactor. Then, homocitrate likely has an important role in the mechanism of nitrogenase catalysis.

Both the ability to grow on no-fixed-nitrogen medium and the rate of C_2H_2-reduction (70% - 80% of wild type) of the αVal-191, αPro-191, and αAla-191 MoFe proteins are comparable to wild type. Because their side chains might not form a hydrogen bond to homocitrate, these results imply that the hydrogen-bonding link between carboxylate group of homocitrate and side chain of the 191-Gln residue is not rigorously required for reducing these substrates. Those substituting amino acids, which have a charged (positive or negative) and large side chain, exhibit an inability to fix N_2 and poor ability to reduce C_2H_2. An interpretation of these results is that substitution with a large bulky group or a charged group may block the proposed movement of the carboxylate group of homocitrate and so decrease the catalytic reduction activity. This interpretation is consistent with some recent work on FeMo cofactor isolated from both wild type and $NifV^-$ strains of *K. pneumoniae*, where movement of homocitrate during nitrogenase turnover was proposed (Grönberg *et al*., 1998).

When an estimate of the Mo content of each of these purified altered MoFe proteins was made based on their H_2-evolution specific activity, the estimated Mo content was always lower than that directly determined from ICP-AES. For example, the αArg-191 has an activity-based estimate of 0.4 Mo atom per molecule instead of the determined 0.8 Mo atom per molecule. The higher Mo content of the purified altered MoFe proteins could be due to: 1) some inactive FeMo cofactor in the MoFe protein; 2) electron transfer becoming rate limiting during catalysis; and/or 3) an impairment of the substrate-reduction site.

These possibilities were studied by controlling the electron flux through nitrogenase by manipulating the Fe protein:MoFe protein molar ratio in enzyme assays (Hageman and Burris, 1980; Wherland *et al*., 1981). At high Fe protein:MoFe protein molar ratios, the flux through nitrogenase is greatest, specific activity is maximized and is limited by the rate of complex dissociation (Thorneley and Lowe, 1983). In contrast, a low Fe protein:MoFe protein molar ratio results in a condition of low flux and the specific activity is relatively lower because catalysis becomes limited by the availability

of Fe protein that can participate in the delivery of electrons to the MoFe protein. Flux titrations, by varying the Fe protein:MoFe protein molar ratio, were used to investigate the electron transfer between the P cluster and the substrate reduction site.

Previously, MoFe proteins with substituted amino acid residues either coordinated to P cluster, βCys-153 (May *et al*., 1991) or located between P cluster and FeMo cofactor, βTyr-98 (Peters *et al*., 1995a), have been examined by this technique. Substitution of βCys-153 by Ser gave an altered MoFe protein that was found to exhibit approximately the same specific activity as wild type under conditions of low flux but only about 50% of normal activity when assayed under high flux (May *et al*., 1991). The interpretation offered was that, under conditions of high flux, the reaction catalyzed by the βCys-153 protein is limited by intramolecular electron transfer between P cluster and the substrate reduction site owing to a rearrangement in the P cluster polypeptide environment. Similar titrations have shown that the specific activity of an altered MoFe protein with the βTyr-98 residue substituted by His maximized at a lower Fe protein:MoFe protein molar ratio (5:1) than that of the analogous titration involving the wild type MoFe protein (10:1). This result was also interpreted in terms of changed intramolecular electron transfer (Peters *et al*., 1995a).

The flux titration for H^+ reduction under 100% Ar has been determined with the αSer-191, αThr-191, and αArg-191 altered MoFe proteins and compared with wild type MoFe protein (data not shown). Under conditions of both low flux and high flux, these altered MoFe proteins exhibited a maximum specific activity lower than wild type and maximized their activities at a similar Fe protein:MoFe protein molar ratio as wild type (10:1). These results imply that intramolecular electron transfer is not limited by the amino acid substitution at αGln-191 residue. The decrease in catalytic activities of these altered MoFe proteins is most likely due to a detrimental effect on their catalytic reduction mechanism.

These results confirm that a more damaging effect on both C_2H_2 and N_2 reduction occurs with charged substitutions. These substitutions may either enhance (by introducing positive charge, αArg-191) or disrupt (by introducing negative charge; αGlu-191) the hydrogen bonding to homocitrate. Also, increased bulk (or charge; αHis-191)

may block the proposed movement of homocitrate. Substitutions either eliminating or weakening the putative hydrogen bonding (αPro-191, αThr-191, and Ser-191) have less effect. Again, these results are consistent with movement of homocitrate during catalysis and indicate a critical role during N_2 and C_2H_2 reduction by Mo-nitrogenase.

The results of diminished EPR intensities of both αSer-191 and αGlu-191 altered MoFe proteins support their lower specific activity compared with wild type under Ar alone when calculated on per Mo atom basis (79% and 45%, respectively, of wild type MoFe protein). Moreover, the correlation of signal intensity with the ability of these altered MoFe proteins to reduce both C_2H_2 and N_2 reduction when compared to wild type MoFe protein was apparent. These results suggest that substitutions at αGln-191 might both lower EPR signal intensity in the resting state and lower the ability to reduce H^+, C_2H_2 and N_2 substrates in the turnover state compared with wild type MoFe protein.

In wild type Mo-nitrogenase, where no C_2H_6 is produced from the catalyzed reduction of C_2H_2, the affinity for C_2H_2 is very high relative to the affinity for C_2H_4 (Ashby *et al*., 1987). This difference in affinity would favor C_2H_4 loss from, and C_2H_2 binding to, the active site. In contrast, with the altered MoFe proteins, the affinities for C_2H_2 and C_2H_4 are such that any putative bound-intermediate is sufficiently long lived at the site that it can become further reduced with two electrons and two protons to produce C_2H_6 when finally released (Scott *et al*., 1992). The lower specific activity for C_2H_2 reduction with αGlu-191, αHis-191 and αArg-191, which correlates with C_2H_6 production, supports this hypothesis. However, the amount of C_2H_6 formed must result from a delicate balance between having an affinity for C_2H_2 that is high enough to give reasonable binding but not so high that it rapidly and effectively displaces the bound intermediates (Fisher *et al*., 2000a). The affinities of C_2H_2 in these altered MoFe proteins compared to that of wild type will be examined in Chapter 4 to gain insight into this balance.

H_2 evolution has been established as an intimate part of the chemical mechanism of N_2 reduction (Hadfield and Bulen, 1969) with a minimum stoichiometry of one H_2 evolved per N_2 reduced with Mo-nitrogenase (Newton *et al*., 1976). This observation has been used to suggest that N_2 can only bind to nitrogenase by displacement of H_2 to give H_2 evolution (Guth and Burris, 1983; Thorneley and Lowe, 1985). However, V-

nitrogenase can reduce N_2 and it evolves at least three H_2 per N_2 reduced (reviewed by Eady, 1996). The large amount of H_2 evolved with V-nitrogenase could be because of either a nonobligatory waste of reducing equivalents by a less efficient nitrogenase or a fundamental mechanistic difference from Mo-nitrogenase (Dilworth *et al*., 1993). The αPro-191, αThr-191, and αSer-191 MoFe proteins exhibit a phenotype that also evolves more than one H_2 per N_2 reduced. However, the rate of overall electron flow did not change compared with H_2 evolution under Ar. The decrease in the ability to reduce N_2 with these three altered MoFe proteins in the same way as occurs with V-nitrogenase suggests that the strength of the bonds of both the hydroxyl and carboxylate groups of homocitrate to Mo is important for N_2 reduction with nitrogenase. This thought is consistent with an attempt to integrate chemical and biochemical models for the enzymic reduction of N_2. If the proposed movement of homocitrate occurs during enzyme turnover (Hughes *et al*., 1994; Pickett, 1996), it likely involves dissociation of the carboxylate group from Mo, thereby freeing up a site for N_2 to bind to Mo on the FeMo cofactor.

The αGlu-191, αHis-191, and αArg-191 are incapable of catalyzing the reduction of N_2, their rates of H_2 evolution are unchanged when assayed under a 100% N_2 or 100% Ar. Because there is no change in the rate of electron flux under N_2 or Ar atmosphere, these altered MoFe proteins also do not bind N_2. Blocking the movement of homocitrate by either added charge or large side-chains may be responsible for the inability of these altered MoFe proteins to bind N_2.

Measurement of the rate of MgATP hydrolysis is a very important aspect of the steady-state assays that can give insight into the basis for lowered activity. The MgATP hydrolyzed per electron pair appearing as product(s) (compared with wild type) can determine whether the rate of MgATP hydrolysis always follows the rate of H^+ (or C_2H_2 or N_2) reduction or if it is uncoupled from electron transfer. An increased ATP/$2e^-$ ratio (Table 3.3), when CO is introduced with these altered MoFe proteins, indicates that electron transfer is uncoupled from ATP hydrolysis. There is no effect of CO on the Fe protein-MoFe protein interaction because the ATP-hydrolysis rate does not change. However, an unfavorable conformation could be evoked by these substitutions and so inhibit electron flux to products.

It might also be the case that CO affects proton transfer to products. A pH-activity profile study with wild type MoFe protein showed, when CO was introduced, that a pK_a of a basic group(s) was shifted in the acid direction about 0.5 pH units (Pham and Burgess, 1993). Thus, CO can inhibit H_2 evolution by wild type, but only when an assay is done at high pH. The group(s) responsible for the pK_a shift might be involved in proton transfer to substrate. So, CO inhibits H_2 evolution with wild type MoFe protein at high pH, the $NifV^-$ MoFe protein (McLean *et al*., 1983), and with certain altered MoFe proteins with amino acid substitutions near the homocitrate (Scott *et al*., 1992). Because all six purified altered MoFe proteins exhibit specific activities lower than wild type and all exhibit CO inhibition of H_2 evolution, it may be that the pK_a of an essential group(s) becomes shifted in the acid direction in an additive fashion. To examine whether either the Gln residue or other residues nearby have responsibility in proton transfer, a pH-activity profile study of these MoFe proteins was undertaken to gain information about the involvement of acid-base groups in nitrogenase turnover and is described in Chapter 4.

CHAPTER 4

Azotobacter vinelandii Mo-Nitrogenase with Substitutions at the αGln-191 of the MoFe Protein: Effect on the Reduction of Protons and Acetylene and the Interaction with CO

Summary

The effect of substitutions at the αGln-191 residue in producing two unusual properties for MoFe proteins was investigated. There are (i) the sensativity of H_2 evolution to the presence of CO; and (ii) the production of C_2H_6 from C_2H_2 reduction.

The first effect was investigated using pH-activity correlations. Under Ar, the various substitutions shifted for the pK_a of acid-base groups, particularly those required to be protonated for nitrogenase catalysis, in the acid direction. Added CO also affects the pK_a of the protonated group(s) with both wild type and altered MoFe proteins. A similar shift in the acid direction of the pK_a from ca. 8.3 to at ca. 8.0 with either amino acid substitutions or added CO suggests that a CO-binding site is close to the αGln-191 residue. When CO is added to the altered MoFe protein, this pK_a shifts further in the acid direction to ca. 7.5. It appears that CO may "mask" the contribution of two acid-base groups (with pK_a values at ca. 8.3 and at ca. 8.0) and leave just one acid-base group (with pK_a of ca. 7.5) which is still sufficient for nitrogenase catalysis. This result suggests that there are at least three acid-base groups that must be protonated for efficient catalysis. Furthermore, because substitutions at position α-191 impact both the pK_a at ca. 8.3 and at ca. 8.0, these acid-base groups are likely to be closely associated with the αGln-191-homocitrate system. This study also indicates that CO inhibits H_2 evolution in the normal pH assay (~ 7.4) by either a CO-induced shift in the acid direction of the pK_a of the protonated group(s) or a lower rate of electron transfer to the H^+-reduction site or both.

The second effect, C_2H_6 production by those altered MoFe proteins (αHis-191, αGlu-191, and αArg-191) altered MoFe proteins with low C_2H_2-reduction activities, might be explained by their high K_m values and their low rates of electron transfer for C_2H_2 reduction. The low apparent affinity for C_2H_2 of these altered MoFe protein and low rates of electron transfer for C_2H_2 reduction likely allow an intermediate to stay

longer at the active site and acquire more electrons and protons to form C_2H_6. However, the pH-activity profile for C_2H_6 production, which is shifted in the basic direction compared to C_2H_4 production, suggests that C_2H_2 reduction may use different acid-base group(s) for C_2H_6 production than for C_2H_4 production.

4.1 Introduction

In addition to N_2 reduction, nitrogenase can reduce several other alternative substrates, which resemble N_2 on the basis of the triple-bond in their structures. These include acetylene (C_2H_2) and cyanide (HCN). C_2H_2 has proven to be a particularly useful substrate in nitrogenase research in both *in vivo* as well as *in vitro* studies because the reduction product, ethylene (C_2H_4), is easily quantified by GC (Dilworth, 1966). CO is not a nitrogenase substrate but is a non-competitive inhibitor of all nitrogenase catalyzed substrate reductions with the exception of H^+ reduction (Burns and Bulen, 1965). In the presence of CO, electron flux is diverted to H_2 evolution whether or not any other substrate is available.

Recent studies with altered proteins containing substitutions at the αHis-195 and αGln-191 residues of MoFe protein have focused on substrate interactions with the MoFe protein. When the αHis-195 residue was replaced with glutamine (αGln-195), the resulting altered MoFe protein resembled wild type in its interactions with H^+, C_2H_2, and CO, but only poorly catalyzed the reduction of both N_2 and azide (Kim *et al*., 1995; Dilworth *et al*., 1998). It is tempting to speculate that the interaction of N_2 and azide with nitrogenase is affected by the αGln-195 residue but H^+, C_2H_2, HCN, and CO do not bind in the vicinity of the αHis-195 residue (Dilworth *et al*., 1998). Substitution of the αGln-191 residue by lysine (αLys-191) results in a protein that is relatively ineffective in C_2H_2 reduction and whose H_2-evolution activity is inhibited by CO (Scott *et al*., 1992; Fisher *et al*., 2000a).

As described in the Literature Review (Chapter 1), the three-dimensional crystal structure shows that the αGln-191 residue is located between the P cluster and the FeMo cofactor (Kim and Rees, 1992a). The hydrogen bonded network between the two metal centers is from the terminal carboxylate of (R) homocitrate to the amide NH of αGln-191

and then through the amide oxygen of αGln-191 to the backbone NH of the αGly-61, which is adjacent to the P cluster-ligating residue, αCys-62. The P cluster is known to undergo a redox-dependent structural rearrangement that could be coupled to proton transfer to the FeMo cofactor (Peters *et al*., 1997; Lannzilotta *et al*., 1998). This arrangement could provide tight correlation between both the reduction and the protonation of bound substrate through the movement of homocitrate. Therefore, the αGln-191 may critically impact the binding, protonation, and/or reduction of all nitrogense substrates (Fisher *et al*., 2000b).

We sought insight for the effect in C_2H_2 reduction and CO inhibition of six individual substitutions of the αGln-191 residue (Pro, Ser, Thr, His, Glu, and Arg). The altered MoFe proteins have been purified and characterized (Chapter 3). When these altered MoFe proteins are complemented with saturating levels of wild type Fe protein, they express a variety of phenotypes for H^+, C_2H_2, and N_2 reduction. All six altered MoFe proteins exhibit H_2 evolution that is inhibited by CO. Electron distribution to C_2H_4 production during C_2H_2 reduction with these altered proteins varies from 21% to 80% but all are less than wild type at 89%. A decrease in apparent binding affinity for C_2H_2 with the αLys-191 altered MoFe protein could be a reasonable explanation for the observed decrease in C_2H_2-reducing ability of this protein (Scott *et al*., 1992; Fisher *et al*., 2000a). However, recent kinetic data from substitution of amino acid residues close to the FeMo cofactor has lead to the proposal of at least two C_2H_2-binding sites (Shen *et al*., 1997; Christiansen *et al*., 2000a) and also an C_2H_2-binding site that inhibits electron flux on the wild type MoFe protein (Fisher *et al*., 2000a).

Three altered MoFe proteins, αHis-191, αGlu-191, and αArg-191, cannot reduce N_2 and only reduce C_2H_2 to C_2H_4 poorly. These three MoFe proteins also produce different amounts of C_2H_6 during C_2H_2 reduction. C_2H_6 is the product of reducing C_2H_2 by four electrons plus four protons. C_2H_6 could be produced because a bound intermediate stays for a longer time at the active site and becomes further reduced to produce C_2H_6 before being finally released. Figure 4.1 represents a postulated mechanism for C_2H_2 reduction to C_2H_4 plus C_2H_6, and includes an explanation for the

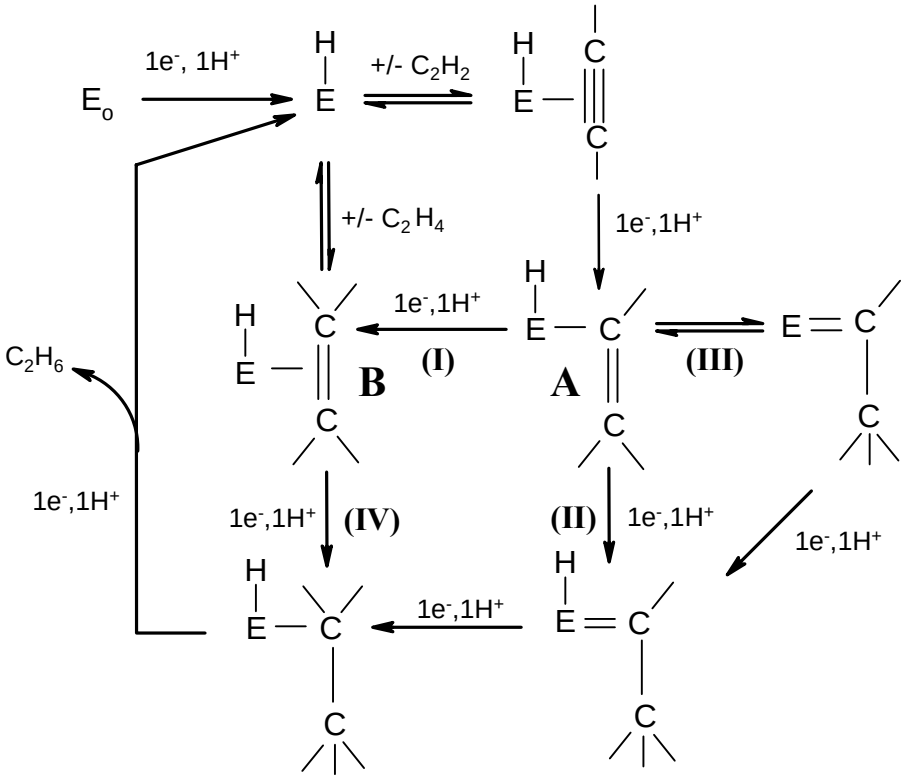

Figure 4.1 Scheme is postulated mechanism for C_2H_2 reduction to C_2H_4 plus C_2H_6 catalyzed by Mo-nitrogenase (Fisher *et al*., 2000a). (Note: All protons attached to C atoms are omitted for clarity)

observed stereospecific protonation by Mo-nitrogenase (Fisher *et al*., 2000a). The two postulated intermediates in this scheme, a σ-alkenyl intermediate (labeled A) and bound C_2H_4 intermediate (labeled B), could play a role in C_2H_6 formation. The σ-alkenyl intermediate can accept one more electron and one more proton to become either bound C_2H_4 if the proton is transferred to its α-carbon (route I) or bound $=CH–CH_3$ if the proton is transferred to its β-carbon (route II). It was hypothesized that, when the proton is transferred slower than the electron, the σ-alkenyl may languish at the site and become further reduced to produce C_2H_6 (route II). Route I is used when the rate of both proton and electron transfer are similar. A second option for C_2H_6 formation depends on the relative binding affinity of the enzyme for C_2H_2 versus C_2H_4. If the binding affinity of the altered enzyme is lower for C_2H_2 but higher for C_2H_4 than with wild type, the binding equilibria will be shifted in favor of bound C_2H_4 remaining on the site, so having time to accept more electrons and protons to produce C_2H_6 (route IV).

Here, we have used six purified MoFe proteins that have amino acid substitutions at α-191 to test the above suggestions. First, we attempted to identify the acid-base groups within the MoFe protein that are required for catalysis from the effects of changing pH on substrate reduction (H^+ and C_2H_2) and inhibitor binding (CO). Our goal was to determine whether any of these amino acid substitutions can be correlated with any change in the pK_a of the catalytically relevant residues. Second, the K_m for C_2H_4 formation from C_2H_2 has been estimated at both the normal assay pH (pH 7.0) and at higher pH (pH 8.0) by measuring the C_2H_4-production rate as a function of C_2H_2 concentration to determine whether or not there are any changes in apparent binding affinities. Third, changes in the rate of formation of C_2H_6, when either C_2H_2 concentration or pH is increased, were investigated. The results show that these altered MoFe proteins function differently from wild type and provide important insights into C_2H_2 and CO binding to the MoFe protein and into C_2H_6 formation from C_2H_2, including identifying possible acid-base groups that deliver protons for substrate reduction.

4.2 Experimental procedures

The experiment procedures in this chapter have been described in detail in an individual section in Chapter 2.

4.2.1 Cell growth and protein purification

Wild type and mutant strains were grown according to protocols described in section 2.3.4. Crude extract was prepared by the same protocol as stated in section 2.4 and the supernatant was subjected to purification using the procedure in section 2.5. Homocitrate was detected in all purified MoFe proteins by GC-MS as described in section 2.6.

4.2.2 Nitrogenase activity assay and analysis of products

All activities of wild type and altered MoFe proteins were performed at 30°C in 9.25-mL reaction vials containing 0.5 mg of total nitrogenase proteins with a 20-fold molar excess of wild type Fe protein, unless otherwise stated. Substrate reduction assays, electron flux titration assay, substrate concentration dependence assays, and pH profile determinations were performed as stated in section 2.7 and products were analyzed as described in section 2.8. The time course of C_2H_4 and C_2H_6 production from C_2H_2 with purified protein was monitored under normal assay conditions and terminated after 1, 2, 3, 4, 8, and 12 min. A total of 1.0 mg of nitrogenase proteins was used at time 1, 2, 3, and 4 min in order to overcome problems associated with measuring a low amount of products. The effect of temperature on rates of electron flux to C_2H_4 and C_2H_6 was assessed by performing the usual C_2H_2-reduction assays in the presence of saturating levels of purified, wild type Fe protein, but at temperatures of 10, 20, 30, 35 and 40°C. Linearity of the rates at the various temperatures was established by measuring activities over a time period of 5-15 min at 30, 35 and 40°C. The optimum assay times were determined to be 12, 9, and 5 min at temperature of 30, 35 and 40°C, respectively. In order to get more products, both a total of 1.0 mg of nitrogenase proteins and an extended assay time were employed (30 and 20 min for 10 and 20°C, respectively).

The effect of CO on C_2H_2-reduction (K_i) was measured using normal assay conditions. CO was added by gas-tight syringe to give the required final CO concentration after releasing the internal pressure to 1 atm during the incubation period and prior to the addition of the purified nitrogenase component proteins.

4.2.3 pH-activity assay

The pH-activity assay was performed by determining the specific activity of product formation when pH was varied from 5.00 - 9.00. The procedure was described in section 2.7.4.3. Substrates used were 100% Ar (H^+ only), 10% C_2H_2/90% Ar and 10% CO/90% Ar. All atmospheres were prepared as described in section 2.7.2. The specific activity of product formation at each pH was also normalized as a percentage of the maximum specific activity. The S-plus program (S-plus 2000 Guide to Statistics) was used to generate a local linear regression fit (LLR) from the percentage of maximum specific activity vs pH data set.

4.3 Results

4.3.1 pH-activity profile with wild type and six altered MoFe proteins

Although there is convincing biochemical and genetic evidence that the FeMo cofactor provides the substrate-binding and -reducing site(s), the nature of the proton donor(s) is unknown. A pH profile of the enzyme's activity was obtained in order to study the effect of pH on nitrogenase catalysis and to gain insight into how protons are delivered to the substrate during the reduction. A three-buffer assay system (modified from Pham and Burgess, 1993) was used in this experiment. This buffer system allows nitrogenase to be assayed in the pH range 5.00 - 9.00 and eliminates problems encountered when different buffers are used individually to cover different pH ranges.

Approximately bell-shaped pH-activity profiles were seen for all products from catalysis by all nitrogenase MoFe proteins either under Ar or in the presence of either C_2H_2 as a substrate or CO as an inhibitor, indicating the presence of at least two ionizable groups required for reducing activity. The pK_a of the deprotonated group on the acid side of the curve and that of the protonated group on the basic side were determined by the pH that gave 50% maximum specific activity. The standard deviation (SD) at 95% confidence of each pK_a was also determined from the data that was generated from the S-plus program.

The pH for maximum activity could be determined by either taking the pH for the maximum specific activity or taking the average pH of those values that give 95% maximum specific activity on both sides of the pH profile. The results from both

determinations give similar values for the pH for maximum activity. For example, the pH for maximum activity for wild type MoFe protein determined from its maximum specific activity is 7.00 ± 0.01 and by taking the average pH at 95% maximum specific activity is 6.99 ± 0.01. The pH for maximum activity has been determined by taking the pH from maximum specific activity because it is simple and convenient.

4.3.1.1 pK_a of acid-base groups in H_2 evolution under Ar alone

Table 4.1 shows the pK_a of the group(s) that must be deprotonated for activity (deprotonated group), the pK_a of the group(s) that must be protonated for activity (protonated group), and the pH for maximum activity of H_2 evolution under 100% Ar with wild type and the six altered MoFe proteins. With wild type MoFe protein, the pK_a of the protonated group(s) (the higher pK_a) is ca. 8.3 and that of the deprotonated group(s) (the lower pK_a) is ca. 6.0. With the αPro-191, αSer-191, α-Thr-191 and αHis-191 altered MoFe proteins, the pK_a of the protonated group(s) and the pK_a of the deprotonated group(s) shift toward each other, from ca. 8.3 of wild type to about ca. 8.0 and from ca. 6.0 of wild type to about ca. 6.2, respectively. Interestingly, with the αGlu-191 MoFe protein, both pK_a values shift in the acid direction compared with wild type, from 8.30 to 7.94 and 6.05 to 5.86, respectively. The αArg-191 substitution shows the biggest impact on the pK_a of the protonated group(s), shifting from 8.30 to 7.60 (ΔpH = - 0.70) with no change in the pK_a of the deprotonated group(s).

The pH for maximum activity correlates well with the changes in pK_a for the protonated/deprotonated groups. The αGlu-191 MoFe protein, which shifts both pK_a's in the acid direction, also shows a maximum pH activity shift from pH 7.00 of wild type to 6.60 (ΔpH = - 0.40). The αArg-191 MoFe protein, which is only affected at its protonated group, shows a slight shift from pH 7.00 of wild type to 6.76 (ΔpH = - 0.24) in the pH necessary for maximum activity. However, the αPro-191, αSer-191, αThr-191, and αHis-191 MoFe proteins exhibit only a small change in the pH for maximum activity because the shift in the pK_a of the protonated group is balanced by the shift in the opposite direction of the pK_a of the protonated group.

The different degree by which the protonated group pK_a shifts in the acid

Table 4.1 pK_a of deprotonated group, pK_a of protonated group, and pH for maximum activity from pH-profile curve of normalized H_2-evolution activity under 100% Ar from wild type and altered MoFe proteins

	100% Argon		
Substitutions	pK_a of deprotonated group[a]	pH for maximum activity[b]	pK_a of protonated group[c]
WT (Gln)	6.05 ± 0.04	7.00 ± 0.02	8.30 ± 0.06
αPro-191	6.30 ± 0.05	7.10 ± 0.01	8.10 ± 0.06
αSer-191	6.22 ± 0.06	7.00 ± 0.01	8.11 ± 0.08
αThr-191	6.22 ± 0.05	7.05 ± 0.02	8.05 ± 0.07
αHis-191	6.24 ± 0.06	7.08 ± 0.00	8.04 ± 0.06
αGlu-191	5.86 ± 0.03	6.60 ± 0.03	7.94 ± 0.07
Arg-191α	6.05 ± 0.06	6.76 ± 0.01	7.60 ± 0.10

Bell-shaped pH profile curve was generated from the nonparametric regression by S-plus program with 95% confidence for mean response (± SD). [a and c] Determined as pH at 50% of maximum activity of H_2-evolution on the acid side and basic side, respectively, of the pH profile curve. [b] Determined as pH at maximum activity of H_2-evolution from pH profile curve.

direction with the six altered MoFe proteins indicates that the αGln-191 residue has an impact on the pK_a of the acid-base group(s) that must be protonated for nitrogenase activity. The shift in either the acid direction of the deprotonated group(s) by the αGlu-191 MoFe protein or no shift with αArg-191 MoFe protein differs from the shift in the basic direction with the αPro-191, αSer-191, αThr-191, and αHis-191 MoFe proteins. This result suggests a different effect of a charged residue at this position on the required deprotonated group.

4.3.1.2 pK_a of acid-base groups related to H_2 evolution with and without adding CO

The effect of adding 10% CO on the pK_a of the protonated and deprotonated groups by changing the assay pH was also investigated for each MoFe proteins. The pK_a of the deprotonated group(s) required for H_2 evolution for all proteins shows no significant change compared to under Ar alone. Table 4.2 shows the pK_a of the required protonated group(s) for H_2 evolution with and without 10% CO added. Adding 10% CO to wild type MoFe protein shifts the pK_a of the protonated group(s) in the acid direction from ca. 8.3 under Ar alone to ca. 8.0. This pK_a shift by wild type with 10% CO is similar to the pK_a shift by substitutions to give the αPro-191, αSer-191, αThr-191, αHis-191, and αGlu-191 altered MoFe proteins that also shift to ca. 8.0. However, the corresponding pK_a of the αArg-191 altered MoFe protein shifts more to ca. 7.6.

When 10% CO was added to assays of each of the altered MoFe proteins, the pK_a of protonated group(s) shift even more in the acid direction from ca. 8.0 to ca. 7.5. The αArg-191 altered MoFe protein exhibits no shift in the pK_a of the protonated group(s) when 10% CO was added.

Figure 4.2 shows the impact of both the substitution and added CO on the pK_a of the acid-base groups contributing to the pH-activity profile for wild type and αHis-191 MoFe proteins. The curves on the acid side of the profile essentially overlap whereas the curves on the basic side separate into three sets. The first set is the curve of wild type in the absence of CO. This curve has a pK_a of ca. 8.3. The second set consists of two curves, those of the wild type MoFe protein with CO present and the αHIs-191 altered MoFe protein, which represents all altered MoFe proteins except αArg-191, without CO.

Table 4.2 Inhibition of H_2-evolution by CO and pK_a of protonated group from pH-profile curve of normalized H_2-evolution under 100% Ar and 10% CO/90% Ar

Substitutions	CO inhibition (%)[a]	CO inhibition of H_2-evolution[b]	pK_a of protonated group[c]		ΔpH[d]
			100% Ar	10% CO in Ar	
WT (Gln)	0	0	8.30 ± 0.06	7.98 ± 0.06	- 0.32
αPro-191	19	320	8.10 ± 0.06	7.65 ± 0.08	- 0.45
αSer-191	35	530	8.11 ± 0.08	7.52 ± 0.08	- 0.59
αThr-191	23	220	8.05 ± 0.07	7.55 ± 0.08	- 0.50
αHis-191	25	410	8.04 ± 0.06	7.61 ± 0.09	- 0.43
αGlu-191	19	190	7.94 ± 0.07	7.66 ± 0.09	- 0.28
αArg-191	45	220	7.60 ± 0.10	7.51 ± 0.09	- 0.09

[a] Expressed in percentage of specific activity of H_2 evolution under 100% Ar inhibited by 10%CO. [b] Expressed in nmole H_2 evolution per min per mg MoFe protein under 100% Ar inhibited by 10% CO. [c] Determined as pH at 50% 0f maximum activity on the basic side of pH profile curve generated by S-plus program under 100% Ar or 10% CO/90% Ar. [d] Shift in the acid direction of the pK_a of the protonated group in pH unit from assays under 10% CO/90% Ar compared to assays under 100% Ar.

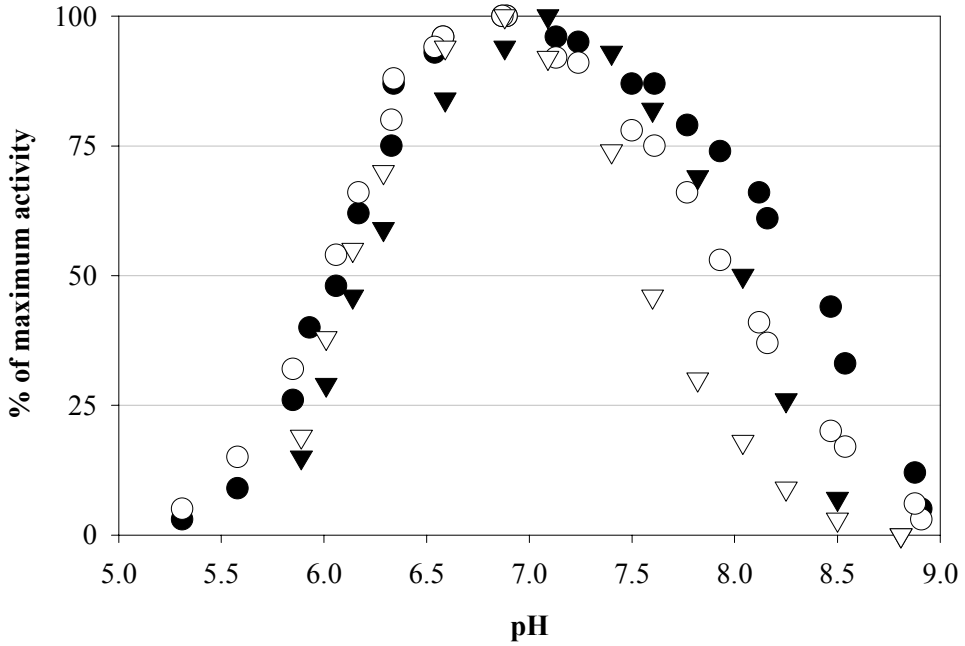

Figure 4.2 Normalized H_2-evolution in percent of maximum activity vs pH for the wild type and αHis-191 MoFe proteins either with and without 10% CO in Ar. ●, wild type; ○, wild type + CO; ▼, αHis-191; ∇, αHis-191 + CO.

They are essentially overlapping with an average pK_a of ca. 8.0. The third set is the curve representing all altered MoFe proteins with CO present. This curve has a more bell-like shape and has a pK_a of ca. 7.5.

Table 4.2 also shows the inhibition of H_2 evolution (both percentage of inhibition and decrease in nmole of H_2 evolution $(min.mg)^{-1}$) and the shift in pK_a of the protonated group(s) (ΔpH) by adding CO. When these two sets of results are compared, there is no significant correlation between them. Figures 4.3, 4.4, and 4.5 show the inhibitory impact of added CO on the H_2 evolution activity curve of wild type, αHis-191, αArg-191 MoFe proteins (panels A) and after the activities have been normalized (panels B). The difference in the effect of CO on H_2 evolution activity of the three proteins is clearly shown. For the wild type MoFe protein (Figure 4.3), although a shift in the acid direction by CO on the pK_a of the protonated group(s) has occurred (panel B), the inhibiting effect on the H_2-evolution activity only occurs above pH 7.5 (panel A). A similar shift in the pK_a of protonated group(s) in the acid direction also occurs with added CO for the αHis-191 altered MoFe protein (Figure 4.4) but the inhibiting effect on the H_2-evolution activity occurs above pH 6.0 (panel A). Thus, at the normal assay pH 7.4, the αHis-191 MoFe protein exhibits CO inhibition of H_2-evolution activity, whereas wild type MoFe protein does not. For the αArg-191 altered MoFe protein (Figure 4.5), although inhibition by CO has obviously occurred above pH 6.0 (panel A), there is only a slight impact of added CO on the pK_a of the acid-base groups contributing to the curve (panel B). The two curves, with and without CO, are essentially overlapping.

4.3.1.3 pK_a of acid-base groups in C_2H_2-reduction and related to H_2 evolution

The effect of adding 10% C_2H_2 on the pK_a of the required protonated/deprotonated groups for each of the individual MoFe proteins was investigated. The pK_a of the deprotonated group required for either H_2 evolution or C_2H_4 formation for all proteins shows no significant change compared to under 100% Ar. However, the wild type, αPro-191, αSer-191, and αThr-191 MoFe proteins, exhibit a significant shift in the pK_a of the protonated group (Table 4.3) for both H_2 evolution (ΔpH = - 0.38, - 0.41, - 0.34, and - 0.27, respectively) and C_2H_4 formation (ΔpH = - 0.24, - 0.31, - 0.42, and - 0.37, respectively). The corresponding values are only slightly

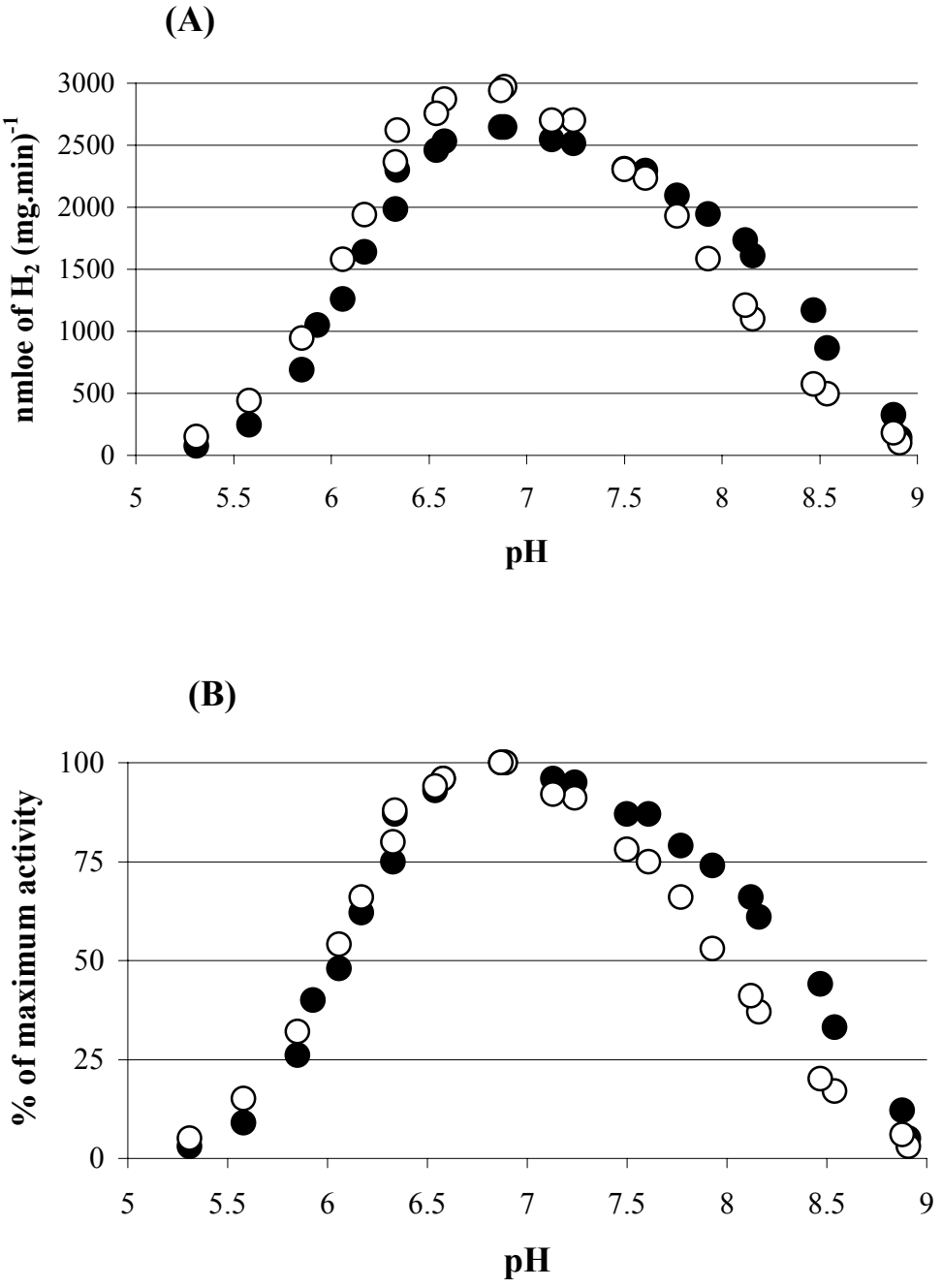

Figure 4.3 H_2-evolution activity of the wild type MoFe protein under either 100% Ar (●) or 10% CO in Ar (O) plotted as a function of pH. Panel A: measured specific activity vs. pH. Panel B: normalized in percent of maximum activity vs pH

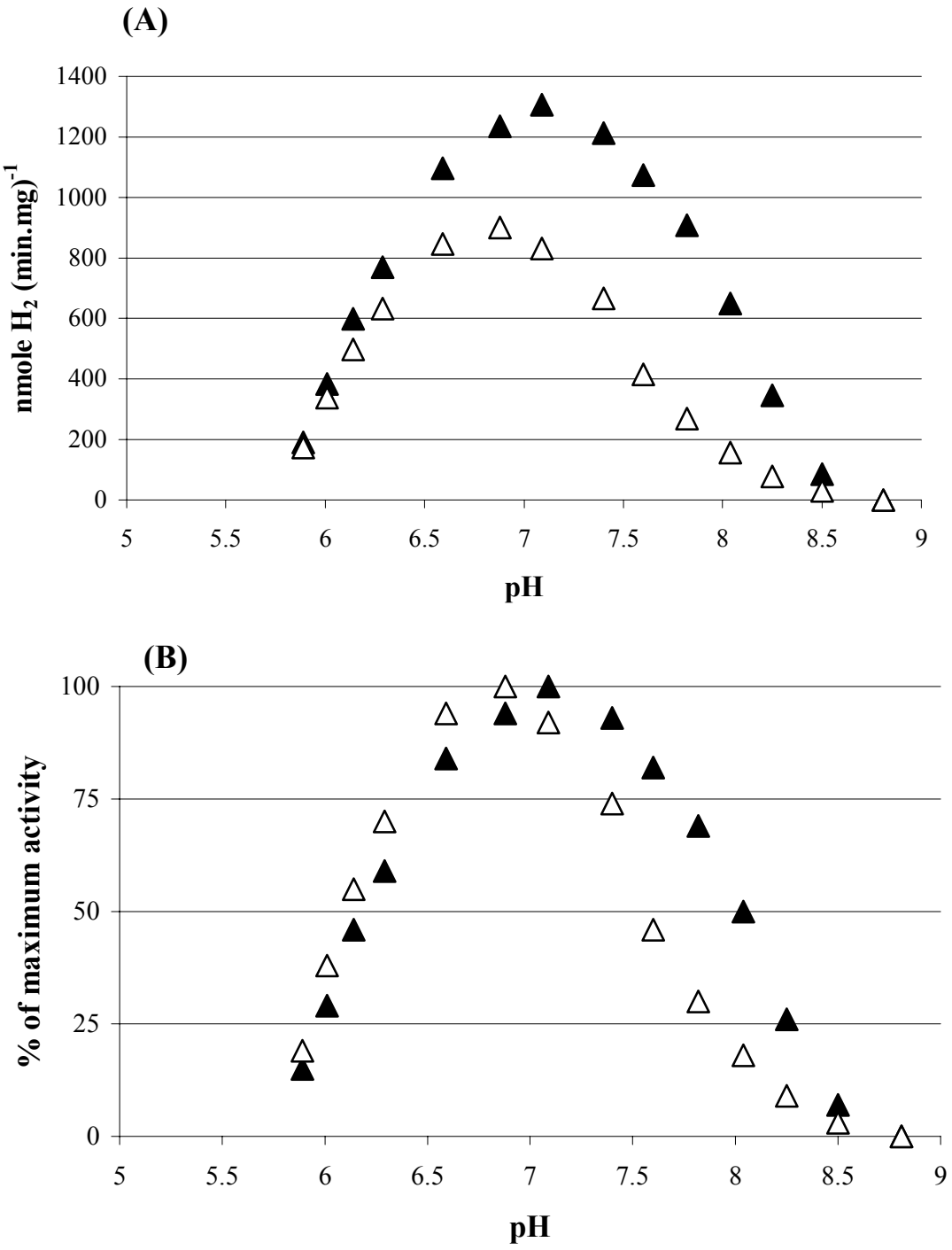

Figure 4.4 H_2-evolution activity of the αHis-191 MoFe protein under either 100% Ar (▲) or 10% CO in Ar (Δ) plotted as a function of pH. Panel A: measured specific activity vs pH. Panel B: normalized in percent of maximum activity vs pH.

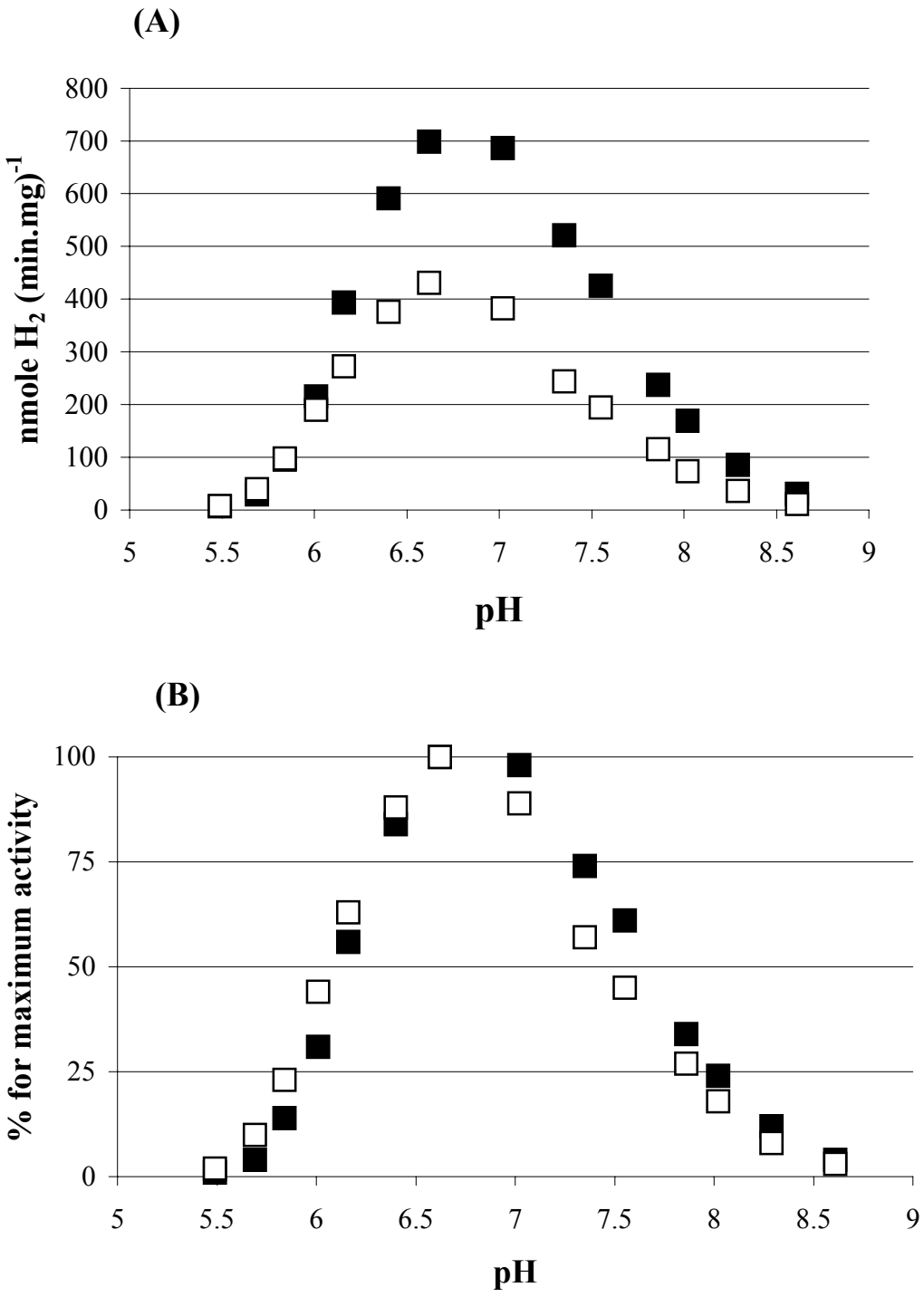

Figure 4.5 H_2-evolution activity of αArg-191 MoFe protein under either 100% Ar (■) or 10% CO in Ar (□) plotted as a function of pH. Panel A; measured specific activity vs. pH. Panel B: normalized in percent of maximum activity vs. pH.

Table 4.3 pK_a of protonated group from pH profile curve of products under 100% Ar and 10% C_2H_2/90% Ar from wild type and altered MoFe proteins

	pK_a of protonated Group [a]			
	100% Ar	10% C_2H_2/ 90% Ar		
Substitutions	H_2	H_2	C_2H_4	C_2H_6
WT (Gln)	8.30 ± 0.06	7.92 ± 0.10	8.06 ± 0.08	–
αPro-191	8.10 ± 0.06	7.69 ± 0.11	7.79 ± 0.08	ND [b]
αSer-191	8.11 ± 0.08	7.77 ± 0.09	7.69 ± 0.08	ND
αThr-191	8.05 ± 0.07	7.78 ± 0.10	7.68 ± 0.09	–
αHis-191	8.04 ± 0.06	8.16 ± 0.06	7.93 ± 0.09	ND
αGlu-191	7.94 ± 0.07	7.94 ± 0.08	7.85 ± 0.07	8.60 ± 0.10
αArg-191	7.60 ± 0.10	7.56 ± 0.11	7.68 ± 0.13	8.11 ± 0.13

[a] Determined as pH at 50% of maximum activity of electron pairs produced product on the basic side of bell-shaped pH profile curve generated by S-plus program under 100% Ar or 10% C_2H_2/90% Ar. [b] ND represents not determinable because very low rates of product formation makes it not possible to accurately determine the pK_a value.

changed with αHis-191, αGlu-191, and αArg-191 MoFe proteins. The interaction of C_2H_2 must in some way impact the protonated group's pK_a. The pH for maximum activity of both H_2 evolution and C_2H_4 formation is hardly changed with all proteins under 10% C_2H_2/90% Ar when compared with 100% Ar.

Under 10% C_2H_2, the pK_a's of both the protonated and deprotonated groups required for C_2H_6 formation by the αArg-191 MoFe protein are shifted to the basic side compared with those required for C_2H_4 production. Figure 4.6, panel A shows that the pK_a of protonated group shifts from ca. 7.7 to ca. 8.1(ΔpH = + 0.4), the pK_a of deprotonated group shifts from ca. 6.0 to ca. 6.6 (ΔpH = + 0.6), and the pH for maximum activity also shifts from ca. 6.7 to ca. 7.4 (ΔpH = + 0.7). Interestingly, the C_2H_6 formation by the αGlu-191 MoFe protein exhibits an atypical bell-shape curve on the acid side of the pH profile (Figure 4.6, panel B). The biphasic curve implies that there are at least two deprotonated groups (pK_a at ca. 6.0 and pK_a at ca. 7.4) involved in the catalysis. One of these groups (pK_a at ca. 6.0) may be the same as that involved in C_2H_4 production. The pH for maximum activity of this MoFe protein is also shift from ca 6.6 to ca. 8.0. The αHis-191 MoFe protein also produces C_2H_6, but at a very low rate, so low that it is not possible to accurately determine the pK_a values. Thus, because the pK_a of both the protonated/deprotonated groups for C_2H_6-formation are higher than the pK_a of C_2H_4-production, the formation for C_2H_6 may simply use different protonated/deprotonated groups from those for C_2H_4 production.

4.3.2 Determination of kinetic parameters for C_2H_2 reduction

C_2H_2 reduction accounts for 89% of the electron flux to products for wild type MoFe protein but decreases to 80%, 46%, 78%, 21%, 31%, and 28% for αPro-191, αSer-191, αThr-191, αHis-191, αGlu-191, and αArg-191 altered MoFe proteins, respectively. Interestingly, the proteins that are poor C_2H_2 reducers (αHis-191, αGlu-191, and αArg-191) can form C_2H_6. C_2H_6 is not produced by wild type, αPro-191, αSer-191 and αThr-191 MoFe proteins during assays at normal pH (7.0 - 7.4). The difference in the binding affinity for C_2H_2 of these proteins likely affects C_2H_6 formation. The apparent binding affinity of the enzyme for the substrate was determined *via* the Michaelis constant, K_m,

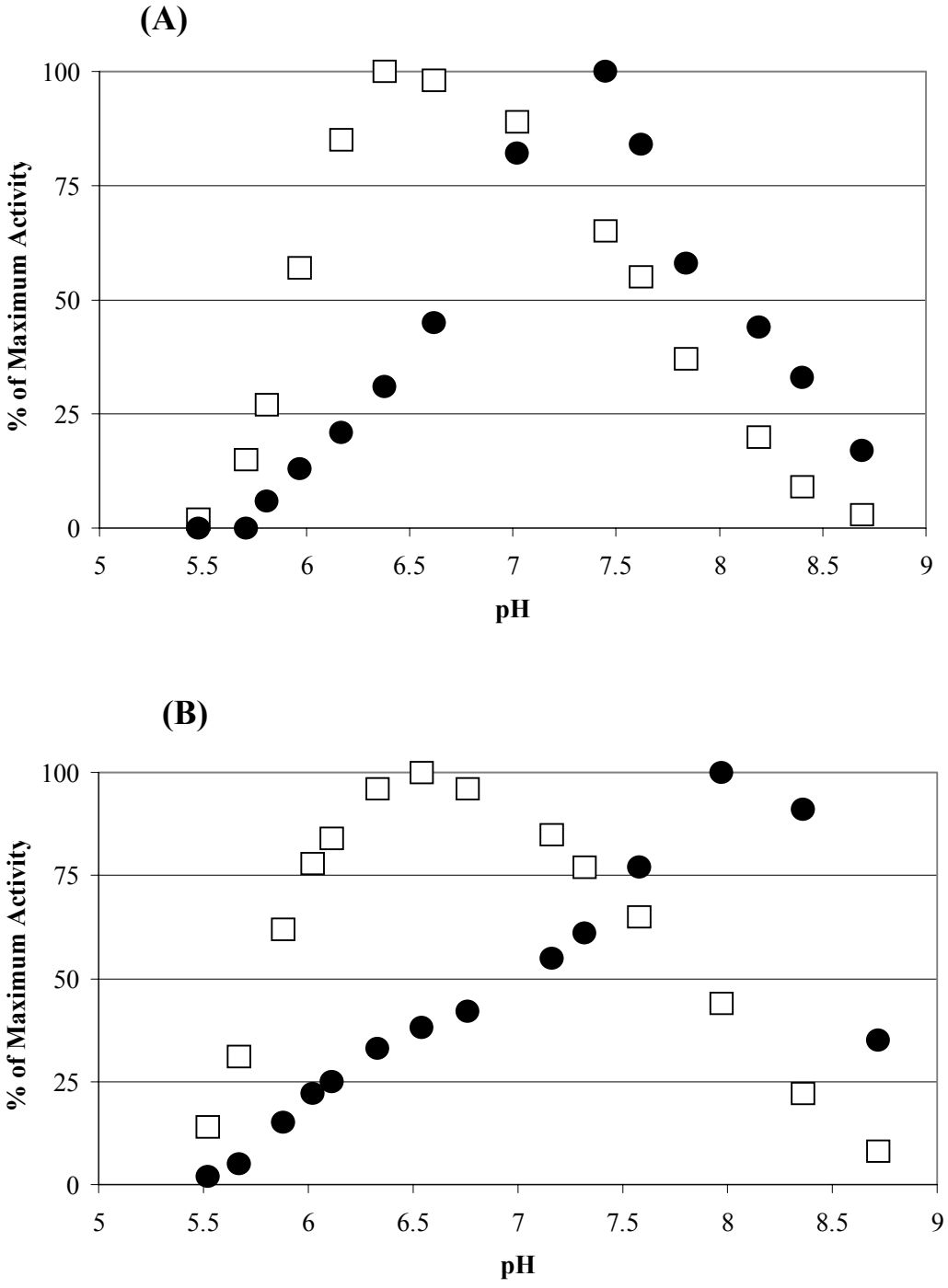

Figure 4.6 pH profile of C_2H_4 ( ) and C_2H_6 (•) formation under 10% C_2H_2/90% Ar by αArg-191 (A) and αGlu-191 (B) altered MoFe protein

which is the substrate concentration at which the specific activity of the enzyme of interest is half the value of maximum specific activity (V_{max}). The K_m for C_2H_4 production from C_2H_2 at pH 7.0 and pH 8.0 was determined by measuring the C_2H_4-product-formation rate as a function of C_2H_2 concentration. The apparent K_m values obtained from Lineweaver-Burk plots are shown in Table 4.4.

The K_m for C_2H_4 formation for wild type MoFe protein at pH 7.00 is 0.006 atm and the value does not change when pH is increased to 8.0. At pH 7.0, the K_m values, for the αSer-191, αHis-191, αGlu-191, and αArg-191 MoFe proteins are 0.021, 0.050, 0.030, and 0.057 atm, respectively, all of which are higher than the K_m for wild type MoFe protein. The K_m values for the αPro-191 and αThr-191 MoFe proteins are similar to that of wild type MoFe protein. The higher K_m than wild type MoFe protein for C_2H_4 production for αHis-191, αGlu-191, and αArg-191 altered MoFe protein suggests a lower binding affinity than for wild type and is a likely reason why these proteins can produce C_2H_6.

When the pH is increased to 8.0, the K_m for C_2H_4 production for the αPro-191, αThr-191, αHis-191, and αGlu-191 MoFe protein increases to 0.058, 0.013, 0.100, and 0.050, respectively, whereas the K_m of αArg-191 MoFe protein does not change. The higher K_m for C_2H_4 production by the αPro-191, αHis-191, and αGlu-191 MoFe protein at pH 8.0 again correlates with their ability to produce more C_2H_6. However, no C_2H_6 is produced with αThr-191 MoFe protein when pH is increased to 8.0, even though the K_m increased. The αSer-191 MoFe protein cannot produce C_2H_6 at pH 7.0 even though its K_m is higher than the K_m of wild type MoFe protein but C_2H_6 is formed at pH 8.0. Interestingly, the αSer-191 MoFe protein exhibits a biphasic response with C_2H_2 concentration at pH 8.0 (Figure 4.7) and two K_m's of 0.007 and 0.800 atm were determined. This result reflects at least two independent C_2H_4-evolving sites.

Because H_2 evolution by αSer-191 MoFe protein is sensitive to CO inhibition and its electron distribution during C_2H_2 reduction is different from wild type (46% to C_2H_4 compared to 89% with wild type), the K_i for CO-inhibition of C_2H_2 reduction was measured. The K_i for CO inhibition of C_2H_2 reduction is determined as a function of C_2H_2 concentration (varied from 0.02 - 0.1 atm) at various fixed concentrations of CO

Table 4.4 K_m for C_2H_4 production from C_2H_2 reduction by wild type and altered MoFe proteins

	K_m [C_2H_2] (atm)	
Substitutions	pH 7.00	pH 8.00
WT (Gln)	0.006	0.006
αPro-191	0.008	0.058*
αSer-191	0.021	0.007 and 0.800*
αThr-191	0.005	0.013
αHis-191	0.050*	0.100*
αGlu-191	0.030*	0.050*
αArg-191	0.057*	0.056*

K_m is expressed in atm of C_2H_2 concentration that gives half of the maximum activity of C_2H_4 production at pH 7.00 and 8.00. * C_2H_6 is produced by these MoFe proteins under 10% C_2H_2/90% Ar.

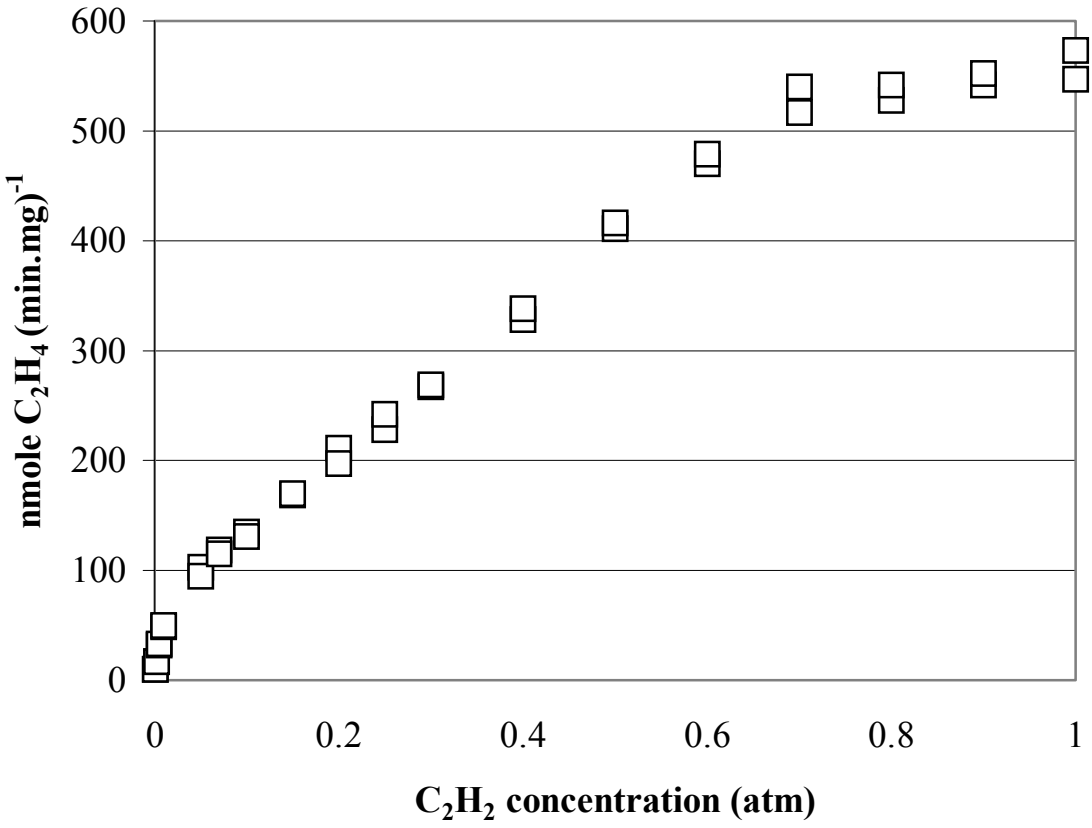

Figure 4.7 C_2H_4 production with αSer-191 at pH 8.0 presents a biphasic response with C_2H_2 binding sites and two K_m (0.007 and 0.800 atm) were determined from Lineweaver-Burk plot.

(from 0.0001 - 0.0009 atm with wild type and 0.000025 - 0.0003 atm with αSer-191). CO was found to be a non-competitive inhibitor with both wild type and αSer-191 MoFe proteins. The K_i determined from a Lineweaver-Burk plot for αSer-191 (0.00005 atm of CO) is four times lower than that of the wild type value of 0.0002 atm, showing C_2H_2 reduction by this altered protein to be more sensitive to CO inhibition than wild type. This result suggests that the αSer-191 substitution not only decreases the rate of C_2H_2-reduction (by decreasing the ability to bind the substrate) but also introduces an increased sensitivity of C_2H_2-reduction to the presence of CO when compared to wild type.

4.3.3 Effect of varying C_2H_2 concentration

The K_m values for C_2H_4 production from C_2H_2 measured for the wild type MoFe protein and six altered MoFe proteins vary from 0.006 to 0.100 atm of C_2H_2. In some proteins, when 10% C_2H_2 (0.1 atm) was used in an assay, it was not enough to saturate the system and a lower rate of C_2H_2 reduction was observed. Therefore, the distribution of electron flux to H_2 evolution, C_2H_4 production and C_2H_6 formation was determined under both 100% C_2H_2 (1 atm) and 10% C_2H_2 with the six altered MoFe proteins and compared to wild type MoFe protein. The results are shown in Table 4.5.

The αPro-191 and αThr-191 MoFe proteins have a similar K_m for C_2H_4 production to that of wild type and distribute electrons to products in almost the same percentage as wild type under both 10% C_2H_2 and 100% C_2H_2. In contrast, the αSer-191 MoFe protein, which has a higher K_m for C_2H_4 production and uses only 45% of the electron flux for C_2H_4 production under 10% C_2H_2, diverts 88% of the flux to C_2H_4 under 100% C_2H_2. Thus it appears that the C_2H_2-binding sites remain intact and operational. However, the αHis-191, αGlu-191, and αArg-191 MoFe proteins can only divert a maximum of 32%, 44%, and 45%, respectively, to C_2H_4 plus C_2H_6 production under 100% C_2H_2. When it is considered that 100% C_2H_2 is 10 times higher than the K_m for C_2H_4 production by the αHis-191, αGlu-191, and αArg-191 MoFe proteins, the possibility exists that one of the C_2H_2-binding sites may be damaged by these amino acid substitutions so that it cannot reduce C_2H_2, even at high C_2H_2 concentration.

The total electron flux to all products under either 10% C_2H_2 or 100% C_2H_2 was also determined compared to the total flux under 100% Ar for all MoFe proteins. The

Table 4.5 Rate of electron distribution to products under 100% Ar, 10% C_2H_2/90% Ar, and 100% C_2H_2 by wild type and altered MoFe proteins

Substitu-Tions	100% Ar	10% C_2H_2/90% Ar					100% C_2H_2				
			Hydrocarbon products					Hydrocarbon products			
	H_2	H_2	C_2H_4	C_2H_6	(%)[g]	Total e^- flux	H_2	C_2H_4	C_2H_6	(%)[h]	Total e^- flux
WT (Gln)	2610	360(13)[a]	2320	0	87	2680(0)[c]	180(10)[b]	1610	0	90	1790(31)[d]
αPro-191	2150	360(20)	1470	0	80	1830(15)	90(8)	970	0	92	1060(51)
αSer-191	1930	930(55)	750	0	45	1680(13)	110(12)	790	0	88	900(53)
αThr-191	770	160(21)	610	0	79	770(0)	90(20)	360	0	80	450(42)
αHis-191	1760	1400(82)	310	1(<1)[e]	18	1711(3)	690(68)	320	8(2)[f]	32	1018(42)
αGlu-191	1070	650(70)	250	23(8)	30	923(14)	300(56)	230	8(3)	44	538(50)
αArg-191	410	290(70)	120	3(2)	30	413(0)	150(55)	120	3(2)	45	273(33)

Rate of electron to each product is expressed in nmole of electron pair per min per mg MoFe protein. [a or b] Number in parenthesis is determined in percentage of electron distribution to H_2 evolution assayed under 10% C_2H_2/90% Ar or 100% C_2H_2. [c or d] Number in parenthesis is determined in percentage of total electron flux inhibition from assayed under 100% Ar when 10% C_2H_2/90% Ar or 100% C_2H_2 is added. [e or f] Number in parenthesis determined in percentage of electron distribution to C_2H_6 (if it is formed) of total hydrocarbon products assayed under 10% C_2H_2/90% Ar or 100% C_2H_2. [g or h] Percentage of electron distribution to hydrocarbon products assayed under 10% C_2H_2/90% Ar or 100% C_2H_2.

results are also shown in Table 4.5. All of these proteins exhibit, at most, only a slight change in the rate of the electron flux to all products under 10% C_2H_2 when compared with 100% Ar. Under 100% C_2H_2, the rate of electron flux was inhibited for all proteins from a minimum inhibition of 31% with the wild type MoFe protein to a maximum of 53% with the αSer-191 MoFe protein.

Table 4.6 shows both the rate of MgATP hydrolysis, which is expressed in nmole of creatine formation (min.mg MoFe protein)$^{-1}$, and the ratio of the rate of MgATP hydrolysis and product formation, which is expressed in electron pairs (ATP/2e^- ratio), for wild type and the six altered MoFe proteins. Added 10% C_2H_2 did not substantially inhibit either the rate of MgATP hydrolysis or the rate of product formation by all MoFe proteins. Therefore, the rate of MgATP hydrolysis per electron pair does not change when compared with the rate under 100% Ar. In contrast, both the rate of MgATP hydrolysis and the rate of product formation were inhibited with all MoFe proteins, when 100% C_2H_2 was present compared with either 100% Ar or 10% C_2H_2. However, 100% C_2H_2 inhibits the rate of MgATP hydrolysis less than rate of product formation and, therefore, the ATP/2e^- ratio is slightly higher than under either 10% C_2H_2 or 100% Ar.

4.3.4 C_2H_6 formation with αGlu-191 altered MoFe protein

The αHis-191, αGlu-191, and αArg-191 MoFe proteins exhibit different effects on the rate of C_2H_6 formation when C_2H_2 concentration is increased from 10% C_2H_2 to 100% C_2H_2. The rate of C_2H_6 formation is increased 8-fold with the αHis-191 MoFe protein, remains unchanged with the αArg-191 MoFe protein, and is decreased 3-fold with αGlu-191 MoFe protein.The result with the αGlu-191 MoFe protein is interesting because C_2H_6 formation decreases as C_2H_2 concentration increases. The electron distribution between C_2H_4 and C_2H_6 production with the αGlu-191 MoFe protein under C_2H_2 reduction was measured as a function of the electron flux, time, or temperature. The procedures used are modified from Scott *et al*. (1992). The time course for both C_2H_4 and C_2H_6 formation from C_2H_2 reduction was determined from 1 min to 12 min and showed no lag phase for either C_2H_4 or C_2H_6 production. The effect of the assay temperature on C_2H_4 and C_2H_6 production over the temperature range from 10 - 40ºC was performed. Over the temperature 20 - 40ºC, the ratio of rates of C_2H_4 and C_2H_6

Table 4.6 ATP hydrolysis and ATP/2e$^-$ assayed under 100% Ar, 10% C_2H_2/90% Ar, and 100% C_2H_2 atmosphere with wild type and altered MoFe proteins.

	100% Ar		10% C_2H_2/90% Ar		100% C_2H_2	
Substitutions	ATP hydrolysis[a]	ATP/2e$^-$[b]	ATP hydrolysis[a]	ATP/2e$^-$[b]	ATP hydrolysis[a]	ATP/2e$^-$[b]
WT (Gln)	11370	4.4	11200	4.1	7160	4.0
αPro-191	-	-	-	-	-	-
αSer-191	10100	5.2	9600	5.7	6070	6.7
αThr-191	4810	6.3	4630	6.0	3850	8.6
αHis-191	8840	5.0	9010	5.2	5250	5.2
αGlu-191	5910	5.5	5780	6.2	4130	7.5
αArg-191	3920	9.7	4040	9.8	3530	12.9

[a] Expressed as nmole creatine production per min per mg MoFe protein. [b] Determined as the number of ATP molecules hydrolyzed for each electron pair found in measured products.

production remains constant at 12. At 10ºC, the electron allocation to C_2H_4 and C_2H_6 is higher (20 instead of 12) but, because the protein changes conformation at this temperature, this value is less insightful. The electron flux titration, attained by varying the ratio of Fe protein to MoFe protein from a 2:1 to 40:1 molar ratio, showed that the relative rate of C_2H_6 formation increased from 5.5% (at a ratio of 2:1 Fe protein:MoFe protein) to 8.5% (at a 40:1 molar ratio).

4.4 Discussion

Various aspects of the reactivity of six altered MoFe proteins and wild type used in this present work have been studied with H^+-, C_2H_2-, and N_2- reduction and CO-inhibition in Chapter 3. Of interest here, under normal assay conditions, the substitutions that have charged and/or increased size of the amino acid side chains (αGlu-191, αArg-191, and αHis-191) exhibit poor C_2H_2 reduction activity. In these cases, the majority of electron flux appears as H_2 under 10% C_2H_2. In contrast, those substitutions, which either eliminate or weaken the putative hydrogen bonding to homocitrate (αPro-191, αSer-191, and αThr-191) have less effect. This information suggests that changing either the size or charge of the functional group of the amino-acid side chain could affect the strength of the hydrogen bond. This effect could, in turn, impact the proposed movement of the terminal carboxylate of homocitrate and, therefore, the catalytic efficiency of the resulting nitrogenase.

One consequence of these substitutions could be to disrupt proton delivery to the C_2H_2 binding/reduction site. Moreover, C_2H_6 formation is a product of catalyzed C_2H_2 reduction by the αHis-191, αGlu-191, and αArg-191 altered MoFe proteins. The lower apparent affinity of the C_2H_2-binding site(s) and/or the decreased ability for proton transfer to substrate exhibited by these altered MoFe proteins suggests that the substituted amino acid side-chain could be responsible. Furthermore, because CO is known to inhibit H_2-evolution activity with some altered MoFe proteins, we attempted to determine if CO binding either disrupts some contribution of the acid-base groups to proton transfer or interrupts electron flux to substrate to cause the decrease in H_2-evolution activity.

4.4.1 Effect of amino acid substitution, CO binding, and C_2H_2 binding on the pK_a of acid-base groups

In the absence of added reducible substrate, nitrogenase catalyzes an ATP dependent H_2 evolution reaction (Burn and Bulen, 1965). Studies of the ratios of H_2:HD:D_2 evolved from H_2O-D_2O mixtures (Jackson *et al*., 1968) demonstrate that hydronium ions are the ultimate source of this H_2 evolution. The chemical mechanism of H_2 evolution by this reaction is not known. Proton transfer pathways from solvent to the buried active sites of nitrogenase that involve protonatable groups have been proposed (Durrant, 2001). One possibility is that protons are conducted in a concerted fashion through a chain of hydrogen-bonded proton donor groups.

By assaying at various pH values, the pH-activity profile for H_2 evolution for the six altered MoFe proteins (in the absence of added reducible substrate) showed the effect of amino acid substitution at position 191 on the pK_a of both the deprotonated and the protonated groups. Because the pK_a of the amide side chain of Gln is more than pH 14, it seems unlikely that the Gln at position α-191 can have a pK_a around 8.3 or 6.0. Therefore, it is unlikely that this Gln is a responsible acid-base group. However, the pK_a values of both the deprotonated and protonated groups were shifted by substitutions at αGln-191 residue, but the apparent pK_a of both the deprotonated and protonated groups do not correlate with the pK_a of these substituting residues. Therefore, it is also unlikely that these substitutions are the responsible acid-base groups. So, substitution at this position probably affects the pK_a of another residue(s). Most likely, it modifies the αGln-191-homocitrate hydrogen-bonding system, which affects other acid-base groups that are directly involved in proton transfer. Homocitrate is a likely candidate for one of these acid-base groups and homocitrate was found in all altered MoFe proteins studied.

The pH-activity profiles of *A. vinelandii* Mo-nitrogenase under Ar and Ar plus CO have been described previously by Pham and Burgess (1993). Added CO was shown to shift only the pK_a of the protonated group(s) without affecting the deprotonated group(s). Our data are consistent with their results. We have investigated the response of the pK_a of required protonated group(s) and found that it shifts in the acid direction in an additive fashion with both CO and specific substitutions at the αGln-191 residue.

In the absence of CO, the pK_a of the protonated group(s) for the six altered MoFe proteins are shifted in the acid direction compared to wild type. Five of them are shifted similarly from that of the wild type from ca. 8.3 to ca. 8.0, but the αArg-191 substitution is shifted more to ca. 7.5. The initial - 0.3 pH unit shift suggests that elimination, weakening or strengthening of the hydrogen bond between Gln and homocitrate removes the contribution of (at least) one of the protonated group(s) involved in the pK_a at ca. 8.3 such that a new pK_a at ca. 8.0 results. The positive charge of Arg might remove not only the contribution of this first protonated group but also the contribution of a second acid-base group such that a new pK_a of ca. 7.5 results. Thus, the αGln-191-homocitrate is a likely component of the system that must be protonated for H_2 evolution.

In the presence of CO, the pK_a of the protonated group(s) shifts in the acid direction for both the wild type MoFe protein and the altered MoFe proteins. With wild type MoFe protein, CO shifts the pK_a of the protonated group(s) from ca. 8.3 to ca. 8.0, which resembles the shift resulting from the substitutions at α-191. This result suggests that the effect of disturbing the αGln-191-homocitrate hydrogen-bonding system is equivalent to that arising from CO binding. Thus, added CO "masks" the contribution of at least one of the acid-base groups contributing to the pK_a at ca. 8.3 and this "masked" group is, therefore, likely to be part of the αGln-191-homocitrate system. Moreover, all altered MoFe proteins (except αArg-191) show an additional shift in the pK_a of the protonated group(s), from ca. 8.0 to ca. 7.5, when CO is present. This exacerbating effect of CO with these altered MoFe proteins suggests that CO binding may "mask" the contribution of a second pK_a at ca. 8.0. These results also suggest that a CO-binding site is close to αGln-191-homocitrate system and that at least three acid-base groups, which have a pK_a at ca. 8.3, 8.0, and 7.5, must be contributing to the pK_a of protonated group(s) required for efficient catalysis. Furthermore, because substitutions at position α-191 of the αGln-191-homocitrate system impacts both the pK_a at ca. 8.3 and at ca. 8.0, both acid-base groups are likely to be provided by this system.

The CO-induced shift in pK_a that occurs with the wild type MoFe protein results in CO inhibition of H_2 evolution but only when the pH is above 7.5 (Figure 4.3, panel A). Because activity assays are usually run at a pH of 7.4 or less, this inhibitory effect of CO on wild type H_2 evolution is not normally observed. Added CO does not affect the pH

for maximum activity for wild type. However, CO inhibition of H_2 evolution is observed with the αHis-191 MoFe protein throughout the pH range. The CO-induced shift in the acid direction of both the pK_a of the protonated group(s) and the pH for maximum activity ensures that assays run at pH 7.4 suffer considerable inhibition (Figure 4.4). In addition, for the αHis-191 MoFe protein, added CO lowers the rate of electron transfer for H_2 evolution (Figure 4.4, panel A), an effect not observed with wild type MoFe protein (Figure 4.3, panel A). A lower rate of electron transfer under 10% CO was also found for all altered MoFe proteins (Results not shown).

In contrast, added CO has only a slight impact on both the pK_a at ca. 7.5 and on the pH for maximum activity with the αArg-191 MoFe protein. Instead, CO inhibition of H_2 evolution is observed throughout the pH range (Figure 4.5). So, CO induces at least two separate effects and, therefore, the shift in the pK_a of protonated groups induced by CO is not necessarily correlated with the inhibition of H_2 evolution by CO when assays run at pH 7.4. Unlike wild type, added CO lowers the rate of electron transfer for H_2 evolution for all the altered MoFe proteins. The above results indicate that inhibition of H_2 evolution activities by CO binding for MoFe proteins with substitutions at the αGln-191 residue occur from both a shift in the acid direction of the pK_a of the protonated group(s) and a decreased rate of electron transfer to the H^+-reduction site.

In the presence of 10% C_2H_2, the pK_a of wild type MoFe protein's protonated group responsible for H_2 evolution and C_2H_4 production shifts in the acid direction. The αPro-191, αSer-191, and αThr-191 altered MoFe proteins under 10% C_2H_2 show an additional shift of the pK_a of the protonated group to that observed under Ar. Essentially the same pK_a was found for the protonated group for both H_2 evolution and C_2H_4 production under C_2H_2 for wild type. The same situation also occurred for each of the three altered MoFe proteins. The C_2H_2 effect on the protonated group's pK_a correlates with the ability of the MoFe protein to reduce C_2H_2 well. This observation implies that, when C_2H_2 binds to wild type, αPro-191, αSer-191, or αThr-191 MoFe protein, a different protonated group(s) is utilized from that used for H_2 evolution under Ar. This suggestion makes sense because αHis-191, αGlu-191, and αArg-191 MoFe proteins reduce C_2H_2 poorly and do not show any additional shift the protonated group's pK_a when C_2H_2 is present compared to that observed under Ar alone. These results suggest

that with wild type, αPro-191, αSer-191, and αThr-191 MoFe proteins, C_2H_2 binds and uses different basic groups from those used for H^+-reduction under Ar. In contrast, the αHis-191, αGlu-191, and αArg-191 substitutions in the altered MoFe proteins probably use the same basic groups as those used for H^+-reduction under Ar. It is likely that these basic pK_a groups required for C_2H_2 reduction are either eliminated or severely damaged by the αHis-191, αGlu-191, and αArg-191 substitutions. These results suggest the C_2H_2 binding site(s) and the proton transfer pathway for C_2H_2-reduction are likely located near the αGln-191-homocitrate system.

The pK_a of the deprotonated group(s) shows no additional shift when 10% C_2H_2 was added to either wild type or the altered MoFe proteins. This result suggests that the acid-base group responsible for the acidic pK_a must be unaffected by added C_2H_2. It is likely that the same acid-base group(s) is used in both H_2 evolution under Ar and H_2 evolution and C_2H_4 production under C_2H_2.

4.4.2 Effect of amino acid substitutions on the apparent C_2H_2 binding affinity (K_m)

It has previously been reported that substituting αGln-191 by lysine (αLys-191), in normal assays, results in a lowered electron distribution to C_2H_4 (7%) and C_2H_6 (2%) formation and a K_m for C_2H_4 formation of 0.35 atm, which is 60-fold higher than for wild type (Fisher *et al*., 2000a). Because both amino acid substitution and C_2H_2 binding induce a change in the pK_a of the protonated group, the K_m for C_2H_4 production at pH 7.0 and 8.0 was determined with the wild type and six altered MoFe proteins. At an optimum H^+ concentration (pH 7.0), only MoFe proteins carrying charged and bulky amino acid side chains substituted at the αGln-191 residue exhibited a substantial decrease in apparent C_2H_2-binding affinity (higher K_m). At a lower H^+ concentration (pH 8.00), higher K_m's were determined for all altered proteins but not wild type. Thus, C_2H_2 either affects the proton-transfer pathway to C_2H_2 or a lower H^+ concentration (increased pH) decreases the affinity of C_2H_2 binding to nitrogenase.

C_2H_2 binds to nitrogenase only after the MoFe protein has accepted at least one electron (Fisher *et al*., 1990). If, as suggested in the scheme in Figure 4.1, each electron accepted is accompanied by one proton, then a decrease in the rate of proton transfer

could also explain the low apparent affinities for C_2H_2 observed with the altered MoFe proteins.

4.4.3 C_2H_6 formation from C_2H_2 reduction

Unlike wild type Mo-nitrogenase, the NifV$^-$ MoFe protein of Mo-nitrogenase from *A. vinelandii*, where the homocitrate of FeMo cofactor is replaced by citrate (Newton *et al*., 2001) can produce C_2H_6 from C_2H_2. C_2H_6 is also formed by the αLys-191 altered MoFe protein (Scott *et al*., 1992; Fisher *et al*., 2000a). How is C_2H_6 formed? One hint comes from the loss of stereospecificity of protein addition across the triple bond of bound C_2H_2 and this is reflected in the relative amounts of the *cis*- and *trans*-isomer of $C_2H_2D_2$ formed from C_2D_2. With wild type, only 4% of the C_2H_4 formed is *trans*-$C_2H_2D_2$ and no C_2H_6 is formed. With the αLys-191 MoFe proteins 21% is *trans*-$C_2H_2D_2$ and 13% of total hydrocarbon product is C_2H_6. The suggestion, then, is that some proteins allow the bound intermediate to stay for a longer time at active site so allowing either the loss of stereochemistry or further reduction to C_2H_6 (Fisher *et al*., 2000a). Two key intermediates, an σ-alkenyl (label A) and a bound C_2H_4 (label B) intermediate, were hypothesized to play a key role in C_2H_6 formation (Figure 4.1).

Applying the scheme in Figure 4.1 to our data, the fate of the bound C_2H_4 intermediate may be determined in the next step by the relative binding affinities of C_2H_2 and C_2H_4 to the active site of the protein. Three groups of MoFe proteins have been identified in this study to correlate C_2H_6 production with the K_m for C_2H_4 production when assayed at pH 7.0 or 8.0.

The first group exhibits a K_m similar to wild type and does not produce C_2H_6. This group is wild type, when assayed at pH 7.0 and pH 8.0, plus αPro-191 and Thr-191 MoFe proteins (assayed at pH 7.0). All exhibit a K_m for C_2H_4 production of around 0.006 atm of C_2H_2.

The second group exhibits a higher K_m than wild type and produces C_2H_6. This group consists of αHis-191, αGlu-191, and αArg-191 MoFe proteins (assayed at both pH 7.0 and pH 8.0) plus αSer-191 and αPro-191 MoFe protein (only when assayed at pH 8.0). The K_m values vary from 0.030 to 0.800 atm of C_2H_2.

The third group has a K_m that is higher than wild type but does not produce C_2H_6. The αSer-191 MoFe protein, when assayed at pH 7.0, and the αThr-191 MoFe protein, when assayed at pH 8.0, exhibit an apparent K_m of 0.021 and 0.013 atm of C_2H_2, respectively.

The scheme in Figure 4.1 suggests that K_m may determine whether C_2H_6 formation occurs. When we examine the first group, it has high apparent affinity for C_2H_2 (low K_m) and, when bound C_2H_4 is formed, it is not reduced to C_2H_6. The second group has the K_m for C_2H_4 production higher than 0.030 atm of C_2H_2 and apparently allows bound C_2H_4 stay long enough to get more electrons and protons to form C_2H_6. C_2H_6 is formed. However, not all the MoFe proteins with K_m's that are higher than 0.006 atm of C_2H_2 produce C_2H_6. The third group has the K_m's higher than 0.006 atm of C_2H_2 but less than 0.030 atm of C_2H_2. No C_2H_6 is formed. It is likely that the affinities for C_2H_2 are still high enough not to let bound C_2H_4 stay long enough to get two more electrons and two protons to form C_2H_6.

The response of the σ-alkenyl intermediate may depend on the rates of electron and proton transfer. When electron and proton transfer are coupled, the σ-alkenyl intermediate responds such that only C_2H_4 is produced, i.e., only route I is used. This situation holds for wild type and the αPro-191, αSer-191, and αThr-191 altered MoFe proteins. When electron transfer and proton transfer are not coupled, some of the σ-alkenyl intermediate is further reduced and both C_2H_4 and C_2H_6 are produced, i.e., both route I and II are used. The αHis-191, αGlu-191, and αArg-191 altered MoFe proteins may favor this second situation because they appear less effective in inducing proton transfer to C_2H_2 reduction.

With the αArg-191 MoFe protein, both the rate of C_2H_6 formation and K_m for C_2H_2 reduction to C_2H_4 are the same when assayed at either pH 7.0 or 8.0. Furthermore, the αHis-191 and αGlu-191 altered MoFe proteins can produce C_2H_6 when assayed at pH 7.0 and produce more C_2H_6 when assayed at pH 8.0. However, the increase in the rate of C_2H_6 formation at pH 8.0 is greater than the increase in K_m for C_2H_4 production at pH 8.0, so that they are not well correlated. Thus, both the lower apparent binding affinity for C_2H_2 and the decrease in proton-transfer ability are suggested to be affected in C_2H_6 formation.

4.4.4 C_2H_6 formation by αGlu-191 uses different mechanism from V-nitrogenase

The rate of C_2H_6 production by the αLys-191 MoFe protein increases when the C_2H_2 concentration is increased from 10% to 100% (Fisher *et al*., 2000a). A similar effect is observed with αHis-191 where the rate of C_2H_6 formation increases 8-fold. In contrast, the rate of C_2H_6 formation does not increase with αArg-191 MoFe protein and decreases 3-fold with αGlu-191 MoFe protein as C_2H_2 concentration is increased from 10% to 100%. The C_2H_6 produced by αLys-191 has been shown to use a mechanism different from that of the V-nitrogenase (Scott *et al*., 1992). We were interested in determining whether the αGlu-191 substitution shares a common mechanism of C_2H_6 production with V-nitrogenase. However, we found several differences.

The first difference is that, whereas the V-nitrogenase exhibits a 3-min lag before the catalyzed production of C_2H_6 occurs (Dilworth *et al*., 1988), no lag is observed with the αGlu-191 MoFe protein. The 3-min lag is suggested to be due to the slow accumulation of an intermediate species that is not free C_2H_4. Thus, there is no requirement for accumulation of a similar intermediate with the αGlu-191 MoFe protein.

Second, the temperature dependence of product distribution between C_2H_4 and C_2H_6 during C_2H_2 reduction by V-nitrogenase shows that the C_2H_6/C_2H_4 ratio increases 11-fold when the temperature is increased from 10 - 40^{o}C (Dilworth *et al*., 1988). No increase in the C_2H_6/C_2H_4 ratio is observed with the αGlu-191 MoFe protein when the temperature is varied from 20 - 40^{o}C. Thus, in contrast to the V-nitrogenase, the activation energy for the production of C_2H_6 by the αGlu-191 MoFe protein appears to be similar to that for C_2H_4 production.

Third, the C_2H_6/C_2H_4 ratio does increase with the αGlu-191 MoFe protein when electron flux is increased in a similar fashion to that observed with the V-nitrogenase. Taken together, these data suggest that both C_2H_6 and C_2H_4 formation from C_2H_2 catalyzed by the altered Mo-nitrogenase occur on a common mechanistic pathway (Figure 4.1) and that this mechanism differs from that operating in V-nitrogenase.

The decrease in the rate of C_2H_6 production with increasing C_2H_2 concentration by the αGlu-191 MoFe protein is unique among this group of altered MoFe proteins. However, the rate of C_2H_4 formation under 100% C_2H_2 is unchanged compared with the

rate under 10% C_2H_2 in Ar (Table 4.5). Two deprotonated groups have been shown to be involved in C_2H_6 formation under 10% C_2H_2 (Figure 4.6, panel B) and the group with the lower pK_a appears involved in C_2H_4 production. One possible explanation is that high C_2H_2 concentration somehow "masks" the contribution to C_2H_6 formation of the required deprotonated group with the higher pK_a. However, the pH-activity profile of C_2H_6 formation under 100% C_2H_2 also exhibits dependency on two deprotonated groups indicating that the group with the higher pK_a is still functional in C_2H_6 production (data not shown). So, this possibility is eliminated. How the αGlu-191 altered MoFe protein decreases the rate of C_2H_6 formation when C_2H_2 concentration is increased is unknown.

4.4.5 Support for two C_2H_2-binding sites from amino acid substitution

Kinetic and spectroscopic evidence obtained using wild type MoFe protein (Lowe *et al*., 1978; Davis *et al*., 1979) as well as from MoFe proteins altered by amino acid substitution (Shen *et al*., 1997; Christiansen *et al*., 2000a; Fisher *et al*., 2000a) indicate that there are at least two C_2H_2-binding sites located within the MoFe protein. Two pieces of evidence from the C_2H_2-reduction results obtained with the six altered MoFe proteins studied support the two C_2H_2-binding sites hypothesis.

The first point is the K_m determination at pH 8.00 with the αSer-191 MoFe protein exhibits a biphasic Michaelis-Menten plot with K_m of 0.007 and 0.800 atm (Figure 4.7). The second point is based on the fact that, although the ability to reduce C_2H_2 varied among the six altered MoFe proteins, the percentage of electron distribution to C_2H_2 reduction for some of these proteins becomes similar to wild type when the C_2H_2 concentration was increased to 100%. The αPro-191 and αThr-191 MoFe proteins distribute electrons among C_2H_4 and H_2 comparably to wild type under both 10% and 100% C_2H_2. Under 100% C_2H_2 and normal pH assay conditions, the αSer-191 MoFe protein can achieve the same percentage distribution to C_2H_4 production (88%) as wild type whereas the αHis-191, αGlu-191, and αArg-191 MoFe proteins cannot. Their bulky and charged amino-acid side chains could be affecting access to one of the C_2H_2-binding sites such that it cannot be utilized. In contrast, the αSer-191 MoFe protein can access this site but with low affinity for C_2H_2. If an C_2H_2-binding site is eliminated by the substituting amino acids, which have side chains that could block the movement of

homocitrate, homocitrate movement may be associated in facilitating a site for C_2H_2 binding.

The elimination of the high-affinity C_2H_2-binding site has been reported by the substitution of αGly-69 by serine, to give a αSer-69 altered MoFe protein (Christiansen *et al*., 2000a,b). Those authors suggest from structural information (Kim and Rees, 1992a) that the effect of this serine substitution on C_2H_2-binding is through αVal-70 to an [4Fe-4S] face of the FeMo cofactor. The αGln-191 residue, therefore, could impact the second C_2H_2-binding site (the low-affinity C_2H_2-binding site) possibly by an effect through homocitrate to the FeMo cofactor. On the other hand, it is possible that the αGln-191-homocitrate system impacts the high-affinity C_2H_2-binding site and the effect of altered αSer-69 altered MoFe protein could be transmitted to this system (more discussion in section 4.4.6).

K_m determinations for these altered MoFe proteins were used to inspect the high and the low-affinity C_2H_2 binding sites. Because the K_m for C_2H_4 production by the αPro-191 and αThr-191 MoFe proteins are both close to that of wild type MoFe protein ($K_m \sim 0.006$), the two C_2H_2 binding sites appear to be intact. The K_m values for αHis-191, αGlu-191, and αArg-191 MoFe proteins are 5-10 times higher than the K_m of wild type. It is, therefore, likely that the high-affinity C_2H_2 binding site has been lost with these substitutions and only the low-affinity C_2H_2 binding site remains accessible. Previous work reported the elimination of the high-affinity C_2H_2 binding site with the αSer-69 altered MoFe protein and stated that the remaining low-affinity C_2H_2 binding site has a K_m of ca. 0.14 atm (Christiansen *et al*., 2000a). This value is similar to the highest K_m reported here for αArg-191 altered protein (0.06 atm). Thus, there is clear evidence that at least two C_2H_2 binding sites are located within the MoFe protein.

Furthermore, C_2H_2 inhibited both total electron flux and the rate of ATP hydrolysis with all six altered MoFe proteins to the same extent as with wild type but with the ATP/$2e^-$ ratio slightly uncoupled. This result can be interpreted in terms of a C_2H_2-binding inhibition site that interrupts both electron flux to products and ATP hydrolysis, which drives the dissociation of Fe protein-MoFe protein complex. This observation indicated that the flux inhibition caused by C_2H_2 binding is not directly

affected by these substitutions. This site, therefore, is located away from the αGln-191 residue. The slightly uncoupled ATP/$2e^-$ ratio and the higher percent inhibition shown by the six altered MoFe proteins, when compared to wild type, could be induced by a small rearrangement of the polypeptide around the FeMo cofactor caused by these substitutions at the αGln-191 residue.

There is also an interesting distribution of electron flux when the rate of electron flux to both H_2 evolution and C_2H_4 production were compared in assays under either 10% C_2H_2 or 100% C_2H_2. Under 100% C_2H_2, both the H_2-evolution rate and the C_2H_4-production rate are inhibited with the wild type, αPro-191, and αThr-191 MoFe proteins, whereas only the H_2-evolution rate is inhibited with the αSer-191, αHis-191, αGlu-191, and αArg-191 (Table 4.5). The product profiles under various C_2H_2 concentrations (in Figure D-G of the Appendix) of the latter group of altered MoFe protein confirm that the C_2H_4-production rate does not decrease. In Figure A-C (Appendix), the former group of MoFe proteins show substantial inhibition of both the H_2-evolution rate and the C_2H_4-production rate under both 10% C_2H_2 and 100% C_2H_2. It is most likely that the low-affinity C_2H_2-binding site escapes from the sharing of electron flux between the H_2-evolution site and the C_2H_4-production site (high-affinity C_2H_2-binding site) (Figure 4.8). Because the αHis-191, αGlu-191, and αArg-191 MoFe proteins may have lost the high-affinity C_2H_2-binding site, C_2H_2 is reduced only at the low-affinity C_2H_2-binding site and this situation results in inhibition of electron flux only to H_2 evolution when the C_2H_2 concentration is increased. This low-affinity C_2H_2-binding site could be located elsewhere and well before both the high-affinity C_2H_2-binding site and H_2-evolving site on the electron-transfer pathway. These results support the report from Fisher *et al.* (2000a) that, with wild type MoFe protein, the low-affinity C_2H_2-binding site contributes to C_2H_2 reduction under normal assay condition but, when occupied by C_2H_2 under high-substrate-concentration conditions, may cause inhibition of total electron flux.

For the wild type MoFe protein assayed under maximal electron flux conditions, a K_m of 0.006 atm C_2H_2 for C_2H_4 production and a K_i of 0.0002 atm CO for inhibition of C_2H_2 reduction were calculated. These values fall with in the range of values reported previously (Kim *et al*., 1995; Shen *et al*., 1997). For the αSer-191 MoFe protein, the K_m

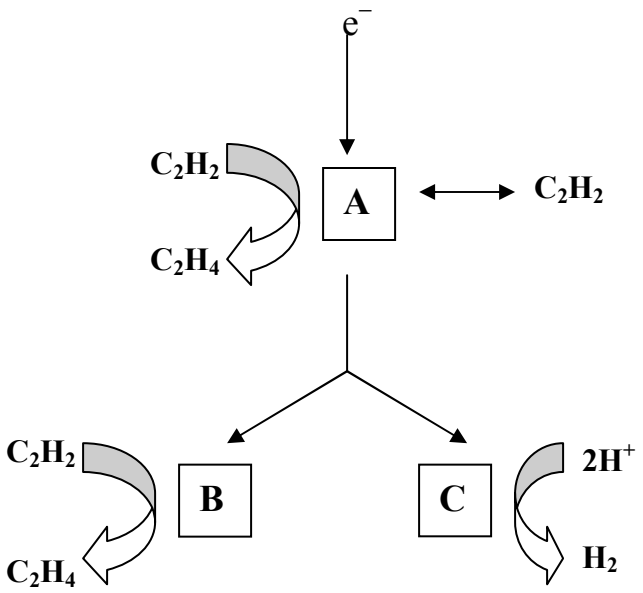

Figure 4.8 Scheme is a postulated arrangement of substrate-binding sites on the Mo-nitrogenase MoFe protein along the electron-transfer pathway (Adapted from Fisher *et al*., 2000a). Site A may represent the low-affinity C_2H_2-binding/reduction site, which at a high C_2H_2 concentration condition may cause inhibition of total electron flux. Sites B and C share the electron distribution between the H_2-evolution site and the C_2H_4-production site, respectively.

for C_2H_4 production is increased whereas the K_i of CO inhibition of C_2H_2 reduction is decreased. These differential effects suggest that the CO- and C_2H_2-binding sites are independent of each other, which is consistent with the known noncompetitive pattern of inhibition by CO of C_2H_2 reduction. However, the effect of substitutions at the αGln-191 residue on both C_2H_2- and CO-binding sites suggests that these binding sites are located close to αGln-191-homocitrate system of Mo-nitrogenase.

Furthermore, C_2H_2 reduction catalyzed by αSer-191 altered MoFe protein in the presence of nonsaturating amounts of CO exhibits hyperbolic kinetics in contrast to the MoFe protein substituted at αArg-277 by His (Shen *et al*., 1997). It is reasonable to speculate that the high-affinity C_2H_2-binding site is close to αGln-191-homocitrate system whereas the low-affinity C_2H_2-binding site is located somewhere else. Thus, CO-induced cooperativity was not observed although at least one of the C_2H_2-binding sites and a CO-binding site are probably close together.

4.4.6 Structure - Function Insights.

The X-ray crystallographic structure of the MoFe protein (Kim and Rees, 1992a) has indicated that the glutamine at position α-191 is not covalently bonded but is hydrogen-bonded to homocitrate of FeMo cofactor. The amide O of the αGln-191 residue is also hydrogen-bonded to the backbone NH of αGly-61, which is adjacent to the P cluster-ligating residue, αCys-62 (Figure 3.1). Under N_2 reduction, the homocitrate component of FeMo cofactor has been suggested to become monodentate at the Mo atom by dissociation of its 2-carboxylate, therefore, freeing up a site for substrate binding to the Mo atom (Pickett, 1996). The freed 2-carboxylate could then become protonated and, thus, a potential proton donor to bound substrate (Grönberg *et al*., 1998). Whether or not this proposal is correct, any substantial movement of homocitrate would be modulated by the residue at position α-191 because the amide NH of the αGln-191 residue is hydrogen-bonded to a terminal carboxylate O of homocitrate.

Previously, examination of the kinetic characteristics of the αSer-69 altered MoFe protein suggests that it has lost one of at least two C_2H_2-binding sites present on wild type (Christiansen *et al*., 2000a,b). These studies have led to the suggestion that both sites are close to the 4Fe-4S face of FeMo cofactor capped by αVal-70. The high-affinity C_2H_2-

binding site is lost by serine substituting for αGly-69 in the MoFe protein, whereas the low-affinity C_2H_2-binding site, where N_2 and azide may also bind, remains intact. In addition, inspection of the FeMo cofactor polypeptide environment shows that the ε-nitrogen of imidazole of the αHis-195 residue is hydrogen-bonded to a central sulfur atom (Kim and Rees, 1992a). This hydrogen bond has been suggested to be an important proton conductor to substrate bound at the FeMo cofactor center and to be specifically required for reduction of N_2 and azide (Dilworth *et al*., 1998). Thus, it may also be involved in binding/reduction/protonation at the low-affinity C_2H_2-binding site.

Where are the high-affinity C_2H_2-binding site and its proton conductor? The αGln-191 residue and its resulting interaction with homocitrate have been suggested to have an effect on C_2H_2 binding/reduction (Fisher *et al*., 2000a). In addition, the hydrogen-bonded linkage from the P cluster to the αGln-191-homocitrate combination appears to be a good candidate for proton delivery (Fisher *et al*., 2000b). When glutamine is substituted by lysine, the bond would be strengthened and any movement that required scission of the stronger ionic lysinyl-homocitrate bond would be inhibited. The αHis-191, αGlu-191, and αArg-191 altered MoFe proteins have amino acid side chains that could potentially block the movement of homocitrate and so result in poor C_2H_2 reduction activity. This inability to either make or break a bond with homocitrate could be reflected in the low activity of the αLys-191, αHis-191, αGlu-191, and αArg-191 altered MoFe proteins toward C_2H_2 binding/reduction by interfering with the suggested ability of homocitrate to deliver protons for substrate reduction. Thus, αGln-191-homocitrate system may also be involved in binding/reduction/protonation at the high-affinity C_2H_2-binding site.

The high-affinity C_2H_2-binding site that is eliminated in the αSer-69 MoFe protein may be impacted through the αVal-70 residue. The αVal-70 is located at the end of a short helix that is connected to the P cluster through the cluster-coordinating αCys-62. When the αGln-191-homocitrate hydrogen-bonding system is considered, the αGln-191 of this system also forms a hydrogen bond to αGly-61 residue, which is adjacent to αCys-62. It is likely that both connections, which span from the P cluster to the FeMo cofactor, provide communication between the two cluster types. Thus, it can be

reasonably considered that the effect of the αSer-69 altered protein could be transmitted through αCys-62 to αGln-191 residue. The substitutions at αGln-191 residue have previously been proposed to be involved in the high-affinity C_2H_2-binding site. The loss of the high-affinity C_2H_2-binding site with the αSer-69 altered protein could be through the movement of αGln-191-homocitrate system or *vice versa*.

Chapter 5

Azotobacter vinelandii Mo-Nitrogenase: Effect of Amino Acid Substitutions at the αGln-191 residue of MoFe protein on Cyanide Reduction

Summary

The six altered MoFe proteins under study exhibit differences in HCN reduction and CN^- inhibition compared to wild type MoFe protein. Both HCN reduction and CN^- inhibition of electron flux to product with these altered MoFe proteins correlate with the apparent binding affinity for HCN and the apparent binding affinity for CN^-, respectively. The exception is the αHis-191 altered MoFe protein. The αHis-191 altered MoFe protein exhibits a higher apparent affinity for HCN but a lower apparent binding affinity for CN^- than wild type. The opposite response to HCN compared to CN^- by this altered MoFe protein supports the suggestion that HCN and CN^- bind to wild type MoFe protein at independent sites (Li *et al*., 1982). The HCN and CN^- binding sites may be close together, however, and are likely located near the αGln-191 residue.

Substitutions with amino acid residues that have either large (His) or charged (Glu and Arg) side chains have a lower rate of HCN reduction and show less inhibition by CN^- than wild type. This observation suggests that either blocking or strengthening the bonding to homocitrate significantly decreases the interactions with both HCN and CN^-. The αPro-191, αSer-191, and αThr-191 altered MoFe proteins use a higher percentage of the electron flux to reduce HCN than does wild type but suffer a similar percentage inhibition by CN^- compared to wild type but also produce C_2H_4 and C_2H_6 in the presence of 5mM NaCN. No C_2H_4 and no C_2H_6 were detected in assays with wild type, αHis-191, αGlu-191, and αArg-191 MoFe proteins when 5 mM NaCN was added.

The αSer-191 altered MoFe protein, which exhibits the highest rate of C_2H_6 production, was selected to determine the likely substrate for C_2H_6 production. The results of the C_2H_6-production dependence on either HCN concentration or CN^- concentration suggests that both HCN and CN^- are involved in C_2H_6 formation.

5.1 Introduction

Cyanide reduction catalyzed by nitrogenase was first demonstrated in 1967 (Hardy and Knight). Because HCN is a relatively weak acid ($pK_a \sim 9.11$), sodium cyanide in solution produces both HCN and CN^- with the relative amounts varying with pH. In the normal assay (pH ~ 7.4), the relative amount of HCN dominates (more than 95%) and the CN^- concentration is dramatically changed by changes in pH. With wild type Mo-nitrogenase, HCN is the substrate that can be reduced by six electrons to give two easily quantifiable products, namely NH_3 and CH_4. Some CH_3NH_2 is also formed. In contrast, CN^- anion acts as a potent inhibitor of electron flux without affecting the rate of MgATP hydrolysis (Li *et al*., 1982) resulting in significant increase in the ATP/$2e^-$ ratio.

The proposed mechanism for HCN reduction is as a series of two-electron/two proton steps (Li *et al*., 1982). The scheme for its reduction pathway was shown in section 1.5.1.4. The detectable products are CH_3NH_2 from four-electron/four-proton reduction and CH_4 plus NH_3 from six-electron/six-proton reduction. "Excess NH_3" is often detected, that is, an amount of NH_3 in excess of the CH_4 produced. The "excess NH_3" has been suggested to arise from a putative two-electron/two-proton product, which is CH_2=NH. If any of the CH_2=NH intermediate escapes from the active site, it would be hydrolyzed to H_2C=O (which has never been detected) and the "excess NH_3". Besides the above products, very small amounts of C_2H_4 and C_2H_6 are formed during HCN reduction catalyzed by wild type nitrogenase (Kelly *et al*., 1967).

HCN reduction and CN^- inhibition have been studied in wild type MoFe protein (Li *et al*., 1982) and with an altered MoFe protein with the αGln-191 substituted by lysine (Fisher *et al*., 2000b). This αLys-191 altered MoFe protein exhibits poor ability to reduce HCN and is less sensitive to CN^- inhibition than wild type. This substitution would result in an ionic bond to homocitrate that would be harder to break than a hydrogen bond. The inability to break an ionic bond with homocitrate could be responsible for the low activity of the αLys-191 MoFe protein toward HCN/CN^-. Consistent with its lower activity toward HCN, the αLys-191 MoFe protein exhibits a higher K_m for CH_4 formation than wild type. Thus, HCN reduction with amino acid

substitutions at the αGln-191 residue other than lysine should give insight into nitrogrnase-catalyzed HCN/CN^- reduction.

In a preliminary study of HCN reduction, the activity of altered MoFe proteins, which were constructed with one of six amino acid substitutions at position 191 in α-subunit (αPro-191, αSer-191, αThr-191, α-His-191, αGlu-191, and α-Arg-191 altered MoFe proteins), was compared with that of wild type MoFe protein. The results indicate that the altered MoFe proteins exist as two groups based on their sensitivity to HCN reduction, CN^- inhibition, and formation of C_2H_4 and C_2H_6 as assay products. These last two products are not readily detected in normal assays with wild type Mo-nitrogenase.

The first group consists of the αPro-191, αSer-191, and αThr-191 altered MoFe proteins. They distribute electron flux when reducing HCN such that the ratio of electron pairs going to CH_4 produced compared with electron pairs going to H_2 evolution is similar to or higher than wild type. Furthermore, CN^- inhibits the total electron flux by the same percentage as for wild type. These three substitutions also produce C_2H_4 and C_2H_6 in the normal assay.

The second group consists of the αHis-191, αGlu-191, and α-Arg-191 altered MoFe proteins. They are poor reducers of HCN, CN^- is less inhibiting of electron flux than with wild type, and no C_2H_4 and C_2H_6 is produced. Interestingly, their decreased ability to interact with HCN and CN^- implies a negative effect of 'bulky' and charged residues at position 191 on the ability to reduce the HCN substrate and on the ability of CN^- to inhibit the total electron flux. This result, which corresponds with their decreased activity for C_2H_2 reduction and inability to reduce N_2, again indicates an important role for the αGln-191 residue in substrate binding, protonation and/or reduction.

Why and how do the αPro-191, αSer-191, and αThr-191 altered MoFe proteins produce C_2H_4 and C_2H_6 under normal assay conditions? Although HCN is the known substrate of wild type nitrogenase (Li *et al*., 1982), can CN^- also be a substrate of nitrogenase? The "single HCN/CN^- binding site" hypothesis (Lowe *et al*., 1989) suggests that CN^- becomes the substrate, HCN, when it is protonated after binding at its binding site. Is HCN or CN^- or both the substrate for C_2H_4 and C_2H_6 production? The αSer-191 altered MoFe protein, which produces a high amount of C_2H_6 during catalyzed

reduction, give an opportunity to gain insight into C_2H_6 production from cyanide reduction.

In this report, we have used wild type MoFe protein and the six altered MoFe proteins described above to gain insight into the interaction of these proteins with HCN/CN^-. There were two questions for this study. First, do the substituting residues at the α-191 position have an effect on the ability of the resulting nitrogenase to catalyze HCN reduction and do they also affect the interaction of these proteins with CN^-? Second, is there any change in the rate of formation of C_2H_4 and C_2H_6 when the HCN and CN^- concentrations are changed? This latter approach should indicate whether or not C_2H_4 and C_2H_6 are formed from HCN or CN^- or both. The observations described below show that these altered MoFe proteins interact with HCN/CN^- differently to wild type.

5.2 Experimental procedures

The experimental procedures in this chapter have been described in more detail in an individual section of Chapter 2.

5.2.1 Cell growth and protein purification

Cell cultures of both wild type and mutant *A. vinelandii* strains were grown in a 24-L fermentor as described in section 2.3.4. The MoFe proteins were purified according to sections 2.5.1 and 2.5.2.

5.2.2 Activity assay and product determination

All activity assays were performed at 30°C in 9.25-mL reaction vials containing either 0.5 mg or 1.0 mg of total nitrogenase protein with a 20-fold molar excess of wild type Fe protein present, unless otherwise stated. Reaction mixture and NaCN solution were prepared as in sections 2.7.1 and 2.7.2, respectively. Products were analyzed as described in section 2.8. Substrate concentration dependence assays were prepared by adding appropriate volume of anaerobic 100 mM stock NaCN solution, pH 7.4, to an assay mixture.

5.2.3 Determination of the substrate for C_2H_4 and C_2H_6 production

The amounts of HCN and CN^- in the assay vial can be adjusted by changing either the NaCN concentration or the pH. An increase in the concentration of NaCN always increases both HCN and CN^- concentration. An increase in the pH, however, increases the CN^- concentration but decreases the HCN concentration in solution. In this experiment, we used both methods to change the amount of HCN and CN^- in the assay in order to create a data set in which the HCN concentration is constant whereas the CN^-concentration is varied or *vice versa*. Different pH values from 7.00 to 8.00 of the 100 mM NaCN stock solution were obtained by adding a predetermined amount of degassed 6 M HCl to obtain the desired pH. Each of these 100 mM NaCN stock solutions was then used individually in otherwise normal activity assays. An appropriate aliquot of one pH-adjusted 100 mM NaCN stock solution was added to a set of assay vials. One vial in each pH assay set was spared for measuring the actual pH of the assay because, in all the others, 0.5 M sodium EDTA (pH 8.0) was added to terminate the reaction. The activity assay was performed as described in section 5.2.2. Because only a small amount of products were formed, 1.0 mg of total protein was used for this experiment.

5.2.4 Data analysis

The relative amounts of HCN and CN^- in a buffered solution of NaCN are determined by the pH. The concentration of both HCN and CN^- were calculated from the NaCN concentration and actual pH in each reaction by using equation (1) (Li *et al*., 1982).

$$[CN^-] = [NaCN]/[\text{antilog}\,(9.11 - pH) + 1] \quad (1)$$

This formula comes from the relationship of pK_a to pH.

$$pK_a\,^{30°C} = 9.11 = pH + \log\,([HCN]/[CN^-]) \text{ and } [NaCN] = [HCN] + [CN^-] \quad (2)$$

The rate of nitrogenase turnover (as measured by H_2 evolution in the absence of cyanide) is also dependent on pH. The dependence of H_2 evolution on pH under Ar alone has been measured for the αSer-191 altered MoFe protein (Chapter 4). Thus, the electron flux data, when pH was varied, have been "normalized" to the rate found at pH 7.0 (pH for maximum activity). In the experiment, the actual rates observed at pH 7.1, 7.2, 7.4, 7.6 and 7.8 have been multiplied by the factor 1, 1, 1, 1.1 and 1.4, respectively.

5.3 Results

5.3.1 Product formation from HCN reduction

Table 5.1 shows both the products of wild type MoFe protein and of the six altered MoFe proteins and the ATP/$2e^-$ ratio with and without 5mM NaCN added under Ar. In the absence of 5 mM NaCN, H_2 was the only product of these MoFe proteins. When 5 mM NaCN was added, CH_4 and NH_3 from catalyzed HCN reduction, plus concomitant H_2 evolution was observed for wild type MoFe protein and the six altered MoFe proteins. Because different products account for different numbers of electrons, the rates of CH_4, NH_3, and H_2 production are expressed as nmoles of electron pairs used in each product per min per mg of MoFe protein. CH_3NH_2, which is produced by wild type *A. vinelandii* Mo-nitrogenase in a constant 0.35:1 molar ratio with CH_4 (Li *et al.*, 1982), was not measured in these experiments.

Ignoring CH_3NH_2 production, total electron flux through the wild type, αPro-191, αSer-191, αThr-191, αHis-191, αGlu-191, and αArg-191 altered MoFe proteins was inhibited by 72%, 73%, 68%, 69%, 22%, 22%, and 8%, respectively, by 5 mM NaCN (Table 5.2). The decrease in total electron flux for the wild type, αPro-191, αSer-191, and αThr-191 MoFe proteins was associated with a 3 to 6-fold increase in the ATP/$2e^-$ ratio because the rate of MgATP hydrolysis was unaffected by adding 5 mM NaCN. Only a minimal effect on total electron flux for αHis-191, αGlu-191, and αArg-191 altered MoFe proteins was observed and the ATP/$2e^-$ ratio was only slightly higher when 5 mM NaCN was added. In the presence of 5 mM NaCN, both C_2H_4 and C_2H_6 were detected as assay products from the αPro-191, αSer-191, and αThr-191 altered MoFe

Table 5.1 Product Formation, Total Electron Flux and ATP/$2e^-$ Ratio for Cyanide Reduction Using Wild Type and Altered MoFe proteins.

MoFe protein	Conditions [a]	SA of electron pairs appearing in products [b]			SA of total electron pairs [c]	ATP/$2e^-$ [d]
		H_2	CH_4	NH_3		
Wild type	Ar alone	2700	-	-	2700	4.4
	+ NaCN	420	180	160	760	21
αPro-191	Ar alone	2100	-	-	2100	4.8
	+ NaCN	82	250	240	572	25
αSer-191	Ar alone	1500	-	-	1500	5.6
	+ NaCN	54	200	220	474	23
αThr-191	Ar alone	790	-	-	790	6.0
	+ NaCN	99	69	78	246	23
αHis-191	Ar alone	1700	-	-	1700	5.0
	+ NaCN	1200	64	60	1324	6.9
αGlu-191	Ar alone	650	-	-	650	5.8
	+ NaCN	450	29	28	507	8.1
αArg-191	Ar alone	660	-	-	660	7.0
	+ NaCN	550	26	23	599	8.9

[a] Normal assay conditions under 100% Ar and a 20-fold molar excess of wild type Fe protein, with and without the addition of 5mM NaCN. [b] Product formation expressed as specific activity in nmole of electron pairs·(min·mg of MoFe protein)$^{-1}$ appearing in each product. For specific activity of CH_4 and NH_3 production, the listed specific activity must be divided by 1.5 for nmole of product·(min·mg of MoFe protein)$^{-1}$. [c] Represents the sum of the individual specific activity for each product. [d] Expressed as the number of ATP molecules hydrolyzed for each electron pair found in measured products. All data are reported at most to two significant figures.

Table 5.2 Summary of the Behavior of Wild Type and Altered MoFe Proteins in Relation to HCN Reduction[a].

	Properties			
MoFe protein	Electron pairs appearing as CH_4 plus NH_3 products (%) [b]	Inhibition of total electron flux by CN^- anion (%) [c]	Apparent affinity for CH_4 production (K_m of HCN, mM) [d]	Specific activity of C_2H_6 [e]
Wild type	45	72	1.5	0
αPro-191	86	73	0.2	1.2
αSer-191	89	68	0.3	2.6
αThr-191	60	69	0.3	0.5
αHis-191	9	22	0.6	0
αGlu-191	11	22	2.0	0
αArg-191	8	9	5.2	0

[a] Assays were performed under 100% Ar with 5 mM NaCN at pH 7.4 and a 20-fold molar excess of wild type Fe protein with 0.077 mg of total protein. [b] Determined from electron pairs allocated to CH_4 plus NH_3 compared with electron pairs appearing as total products, which is a combined measure of CH_4, NH_3, and H_2 production. [c] Percentage of total electron flux inhibited when 5 mM NaCN is present under 100% Ar. [d] K_m value for CH_4 production from HCN reduction. [e] Expressed as nmole of C_2H_6 per min per mg MoFe protein. C_2H_4 is also detected by GC as an assay product for αPro-191, αSer-191, and αThr-191 altered MoFe proteins but at very low rates of product formation.

proteins. Because C_2H_4 formation was very low, its specific activity cannot be accurately determined. However, the specific activity of C_2H_6 production, which is expressed as nmoles of C_2H_6 per min per mg of MoFe protein, could be determined. The specific activity of C_2H_6 formation by αPro-191, αSer-191, and αThr-191 altered MoFe proteins was 1.2, 2.6, and 0.5, respectively. No C_2H_4 and no C_2H_6 were detected in assays with wild type, αHis-191, αGlu-191, and αArg-191 MoFe proteins when 5 mM NaCN was added.

Of the four MoFe proteins that show significant inhibition of total electron flux, the αPro-191, αSer-191, and αThr-191 MoFe proteins all use a higher percentage (86%, 89%, and 60%, respectively) of electron flux to reduce HCN (measured as the combined rates of CH_4 and NH_3 production) than does wild type at only 45%. In contrast, those MoFe proteins suffering only mild inhibition of electron flux, only provide a small percentage (about 10% for each) to HCN reduction (Table 5.2).

The K_m for CH_4 production from HCN was determined for each of the wild type and six altered MoFe proteins by measuring the CH_4 produced in assays over the range 0.05 - 50 mM NaCN at pH 7.4. The concentration of HCN present was calculated from the NaCN concentration at pH 7.4 by using equation 1 in section 5.2.4. The K_m values for wild type, αPro-191, αSer-191, αThr-191, αHis-191, αGlu-191, and αArg-191 MoFe proteins are listed in Table 5.2. K_m for wild type MoFe protein is in an agreement with the previously reported value of 1.6 mM NaCN (Fisher *at al*., 2000b). Compared with the wild type MoFe protein, the apparent binding affinity for HCN for the αPro-191, αSer-191, αThr-191, and αHis-191 altered MoFe proteins are higher but for αGlu-191 and αArg-191 altered MoFe proteins are lower. The αHis-191 altered MoFe protein exhibits an interesting interaction with HCN. Although the apparent binding affinity for HCN for the αHis-191 altered MoFe protein is higher than that for wild type, its ability to reduce HCN is poorer. Moreover, this altered MoFe protein is less sensitive to inhibition by CN^- than is wild type MoFe protein.

5.3.2 Is HCN or CN^- the substrate for C_2H_6 production?

The αSer-191 altered MoFe protein was selected to determine the substrate for C_2H_6 formation because it exhibits a high rate of C_2H_6 formation. C_2H_6 produced by this altered protein was a true product of the reaction because it could not be detected as an impurity in the substrate and because the variation in its production from either different MoFe protein concentrations or different experimental conditions was inconsistent with it being formed from impurities.

In order to differentiate among the possible roles of HCN and CN^- in cyanide reduction to C_2H_6 production, a series of NaCN-concentration dependence experiments at three different pH values was performed. In this experiment, NaCN concentrations used at pH 7.1 were 3.0 and 5.0 mM, at pH 7.6 were 2.0 and 3.0 mM, and at pH 7.8 were 1.0 and 3.0 mM. Figure 5.1 is a plot of the normalized rates of H_2, CH_4 and C_2H_6 production (see section 5.2.4) as a function of the actual HCN concentration (varied from 1.0-5.0 mM HCN) at an approximately constant CN^- concentration (~ 0.05 mM of CN^-). A significant correlation was found. The increase in C_2H_6 production was dependent on the increase in the HCN concentration. Because the K_m of CH_4 formation from HCN is 0.3 mM, at HCN concentrations from 1.0 to 5.0 mM, there is only a small increase in the rate of CH_4 production. In contrast, the increase in HCN concentration causes a decrease in the rate of H_2 evolution.

Figure 5.2 is a plot of the same data but versus the CN^- concentration at approximately constant HCN concentration (~ 3.0 mM of HCN). The rate of C_2H_6 formation was only slightly increased when the CN^- concentration increased from 0.04 to 0.16 mM. In contrast, both the rate of H_2 evolution and CH_4 formation decreased when the CN^- concentration increased.

Another set of experiments has been done by using a single NaCN concentration 1.0 mM but at the different pH values of 7.0, 7.2 and 7.4. In this way, the CN^- concentration could be decreased below 0.04 mM. Figure 5.3 is a plot of these data with the HCN concentration staying constant around 1.0 mM and with the CN^- concentration varying from 0.008 to 0.02 mM. A significant correlation was found between C_2H_6

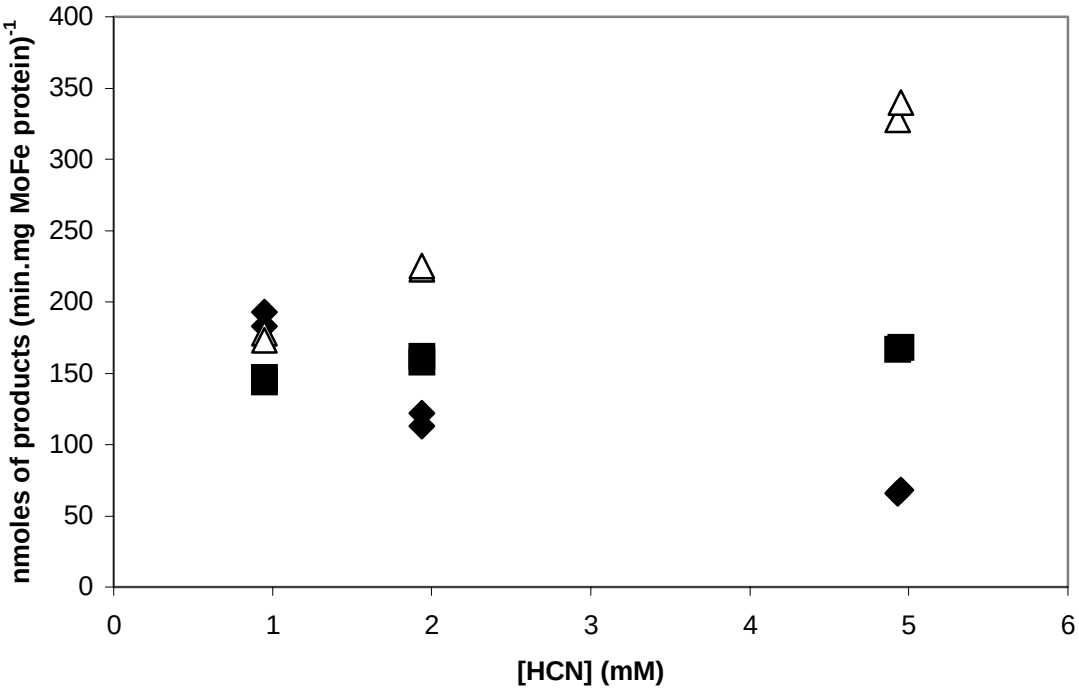

Figure 5.1 Plot of normalized nmoles of H_2 evolution (♦), CH_4 production (■), and C_2H_6 production $\times 10^{-2}$ (Δ) per minute per milligram of αSer-191 altered MoFe protein vs the calculated HCN concentration (mM) when the CN^- concentration is constant around 0.05 mM. Assay conditions and calculations are as described under experimental procedures.

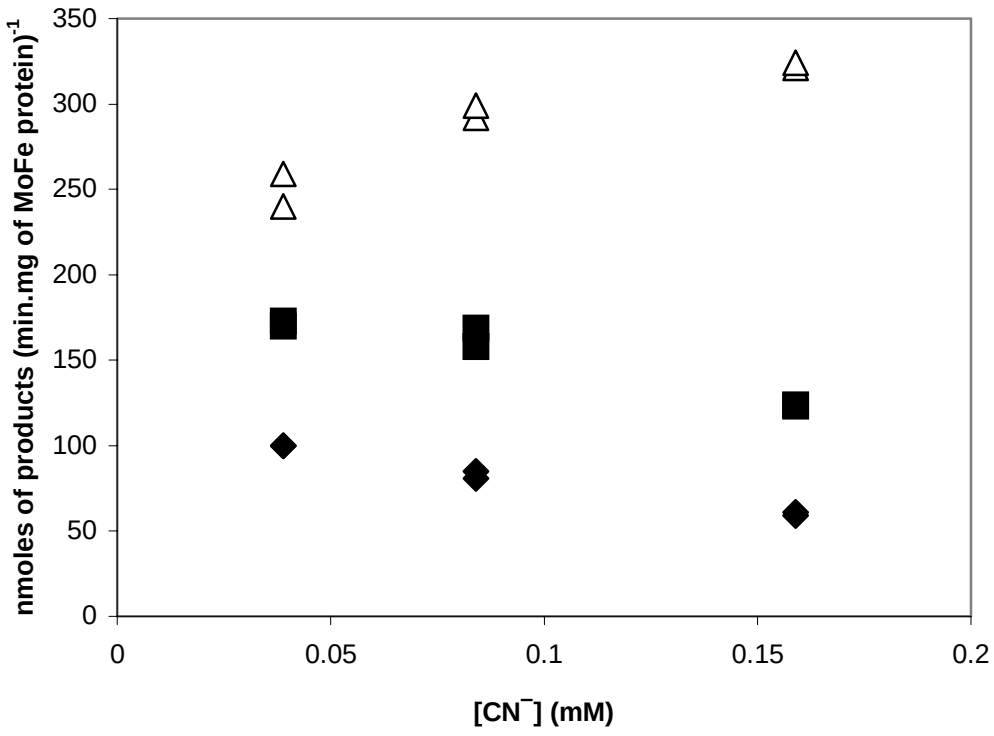

Figure 5.2 Plot of normalized nmoles of H_2 evolution (♦), CH_4 production (■), and C_2H_6 production $\times 10^{-2}$ (Δ) per minute per milligram of αSer-191 altered MoFe protein vs the calculated CN^- concentration (mM) when the HCN concentration is constant around 3.0 mM. Assay conditions and calculations are as described under experimental procedures.

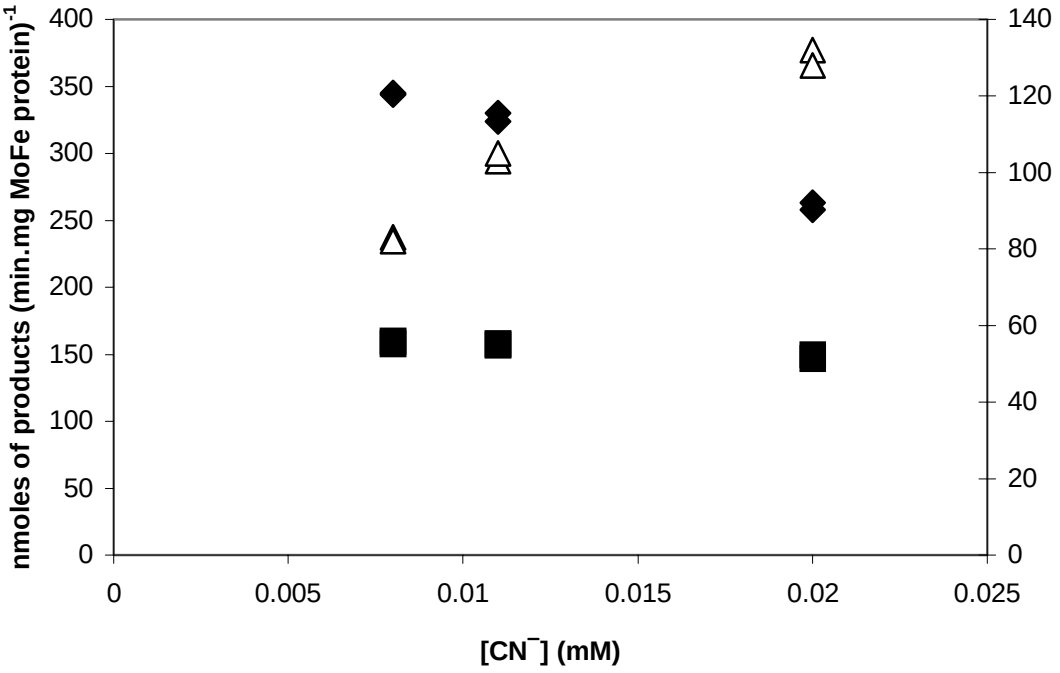

Figure 5.3 Plot of normalized nmoles of H_2 evolution (♦), CH_4 production (■), and C_2H_6 production $\times 10^{-2}$ (Δ) per minute per milligram of αSer-191 altered MoFe protein vs the calculated CN^- concentration (mM) when the HCN concentration is constant around 1.0 mM. Assay conditions and calculations are as described under experimental procedures. H_2 evolution and CH_4 production use the scale on the left, whereas C_2H_6 formation uses the scale on the right.

production and CN^- concentration. However, varying the CN^- concentration from 0.08 to 0.02 mM only decreases the rate of H_2 evolution but not of CH_4 formation.

These results are consistent with both HCN and CN^- being substrates for C_2H_6 formation because, whenever either the HCN or the CN^- concentration increases, C_2H_6 production also increases. The previous suggestion that HCN acts as the substrate and CN^- inhibits electron flux to products (Li *et al*., 1982) is in accord with our result of decreased rates of H_2 evolution by increases in either HCN or CN^- concentration.

5.4 Discussion

5.4.1 Effect of the amino acid substitutions on the interactions with HCN and CN^-

The reduction of cyanide by wild type *A. vinelandii* Mo-nitrogenase has been examined by Li *et al* (1982). They proposed that CN^-, one of two species present in NaCN solution, was a potent reversible inhibitor of total electron flow but not of MgATP hydrolysis so an uncoupling of MgATP hydrolysis from electron transfer was found. Another species, HCN, was shown to be the substrate. This proposal was applied to explain our data. In the presence of 5 mM NaCN, wild type MoFe protein provides 45% of total electron flow for HCN reduction and 72% of total electron flow is inhibited by the CN^- present. The ATP/$2e^-$ ratio is increased to 21 compared with 4.4 under Ar alone. The αPro-191, αSer-191, αThr-191 altered MoFe proteins use a higher percentage of the electron flux to reduce HCN than does wild type but suffer a similar inhibition by CN^- as does wild type. These last observations could be interpreted to indicate that the hydrogen bonding from the α-191 position to homocitrate is not absolutely required for HCN reduction. Even so, in the absence of hydrogen bonding, the homocitrate could still move during catalysis. However, the αHis-191, αGlu-191, and αArg-191 altered MoFe proteins, which have 'bulky' and charged amino acid side chains, exhibit a more detrimental effect on catalyzed HCN reduction, resulting in a decrease in both HCN reduction and CN^- inhibition. These observations suggest that hindering the movement of homocitrate by either blocking or strengthening the bonding to the carboxylate of homocitrate significantly impacts the ability of these altered MoFe proteins to reduce HCN and interact with CN^-.

The K_m determined for CH_4 production from HCN for most of the altered MoFe proteins exhibits a good correlation with the percentage of electron flux used to reduce HCN. The exception is the αHis-191 altered MoFe protein. Although the αHis-191 MoFe protein has an apparent HCN binding affinity higher than wild type, the protein is a poorer HCN reducer. This result clearly indicates an altered interaction with the terminal carboxylate of homocitrate by the residue at position α-191. The altered character of the hydrogen bond, together with either a retarding or blocking of the movement of homocitrate by the imidazole ring of the αHis-191 residue, likely impacts proton- and/or electron-transfer to HCN reduction.

The αHis-191 altered MoFe protein also exhibits a higher apparent affinity for HCN but a lower apparent affinity for CN^- when compared with wild type MoFe protein. These opposite responses to HCN and CN^- illustrate that this αHis-191 altered MoFe protein can differentiate between HCN and CN^- binding. So, this result is consistent with the suggestion that HCN and CN^- bind to wild type MoFe protein at independent sites (Li *et al.,* 1982). In addition, all six altered MoFe proteins with an amino acid substitution at residue α-191 alter the ability to interact with both HCN and CN^-. These results imply that HCN and CN^- binding sites are close together and both located nearby the αGln-191 and homocitrate.

5.4.2 C_2H_6 formation from both HCN and CN^-.

Our results show that C_2H_6 formation is dependent on both CN^- and HCN concentration. Thus, CN^- and HCN could both be the substrate for C_2H_6 formation. The evidence for CN^- as a substrate for C_2H_4 and C_2H_6 production (C_2 products) comes from the comparative experiments of CN^- and methyl isocyanide (CH_3NC) reduction with nitrogenase (Kelly *et al*., 1969). CH_3NC is reduced to CH_4, CH_3NH_2, and dimethylamine plus small amount of C_2H_4 and C_2H_6. The CH_3NC is not only a substrate of wild type nitrogenase but also a potent reversible inhibitor of total electron flow (Rubinson *et al*., 1983). Both CH_3NC and CN^- inhibit the total electron flux to substrate reduction but they do not inhibit MgATP hydrolysis (Rubinson *et al*., 1983; Li *et al*., 1982). CH_3NC reduction in D_2O yields the CH_4 product as CD_4, which must arise from the isocyanide

carbon (Kelly *et al*., 1967). They, therefore, suggested that CH_3NC bound end-on to nitrogenase through the terminal carbon atom (Rubinson *et al*., 1983). Then, CN^- could be both substrate and inhibitor, just like CH_3NC, by binding through the carbon atom. Binding through the nitrogen atom is unlikely because methyl cyanide (acetonitrile; CH_3CN), is not a substrate of nitrogenase (Kelly *et al*., 1967). Further, using D_2O demonstrated that both carbon atoms in the C_2 products also arose from isocyanide carbon. C_2 products were consistently produced in small amounts, suggesting that C_1 radicals were formed during the reduction and interacted to a limited extent to give C_2 by-products (Kelly *et al*., 1967).

In principle, this process could occur by two mechanisms: either bonding between the two bound C_1 radicals on adjacent binding sites or insertion of a second molecule of substrate on a C_1 radical could form C_2 products. Hardy (1979) proposed a reduction followed by an insertion mechanism whereby C_2 products are formed by interaction of a single bound C_1 radical with a free molecule of CH_3NC. The insertion mechanism predicts that the active site has to be large enough to accommodate a bound C_1 radical and an incoming CH_3NC to give the insertion product (Rubinson *et al*., 1983).

If this proposed mechanism for C_2 product formation is true for cyanide reduction also, the relative ease with which C_2H_6 is formed by the αSer-191 altered MoFe protein may be explained. C_2H_6 cannot be detected from cyanide reduction by wild type MoFe protein in a normal assay even through the protein concentration was doubled (data not shown) but αSer-191 altered MoFe protein can produce easily detectable amounts of C_2H_6. The shorter and smaller side chain of serine in the αSer-191 altered MoFe protein compared to the larger side chain of glutamine in wild type might provide sufficient space to accommodate both a bound C_1 radical (whenever it forms from HCN or CN^-) and an incoming CN^- to give the insertion product. Support for this suggestion comes from: 1) both αThr-191 and αPro-191 altered MoFe proteins, with side chains small enough to accommodate CN^- insertion, can produce C_2H_6; and 2) the αHis-191 and αArg-191 altered MoFe proteins that have either bigger and longer, respectively, side chains than glutamine or even the same size as wild type in the αGlu-191 altered MoFe

protein, cannot produce C_2H_6. Whether this suggestion is true or not, HCN may be the source of C_1 radical whereas CN^- is the insertion source to produce C_2 products.

Finally, it is also seems unlikely that the hydrogen-bond between homocitrate and glutamine at position α-191 directly affects HCN and CN^- binding and proton delivery to the HCN and CN^--reducing sites. The observed effects of amino-acid substitutions at αGln-191 residue could be disseminated through the movement of homocitrate and/or the FeMo cofactor framework to modify the response of these altered MoFe proteins to interaction with HCN and CN^- and to cyanide reduction.

CHAPTER 6

Summary and Outlook

Accumulated evidence strongly supports the FeMo cofactor of the MoFe protein as providing the substrate binding and reduction site(s). However, both the structural details of substrate binding to the FeMo cofactor and the sequence of electron and proton transfer to the bound substrates are yet to be revealed. Binding interactions between substrates and one or more of the Fe, Mo, and/or S sites are all reasonable. However, the contribution of the polypeptide environment around the FeMo cofactor also affects substrate binding and reduction. This dissertation has been mainly on the determination of potential roles of the αGln-191 residue in nitrogenase catalysis. Because this key residue occupies an intermediate position between the P cluster and the FeMo cofactor and also forms a putative hydrogen bond to homocitrate of the FeMo cofactor, it could play an important role through its association with homocitrate in directing intra-MoFe-protein electron and/or proton transfer as well as substrate reduction and inhibitor binding. By using a site-directed mutagenesis approach, individual substitutions at this position have been constructed and the biochemical and spectroscopic properties of purified wild type MoFe proteins (with αGln-191) and six altered MoFe proteins (with αPro-191, αSer-191, αThr-191, αHis-191, αGlu-191, or αArg-191) isolated from these strains have been determined.

First, all six altered MoFe proteins exhibit rates of proton reduction under Ar lower than wild type in HEPES buffer at pH 7.4. Unlike wild type, H_2 evolution by these altered MoFe proteins is inhibited by CO resulting in an increase in the MgATP/$2e^-$ ratio. This increase indicates that CO only affects the rate of electron transfer but does not affect the Fe protein-MoFe protein interaction (no change in the rate of MgATP hydrolysis).

Second, because there are no significant differences in the EPR spectra of the wild type and the six altered MoFe proteins in terms of either the line shape or the *g*-value of the characteristic FeMo cofactor EPR signal, these altered MoFe proteins suffer most likely only a minor perturbation within the local FeMo cofactor environment. However,

both the αSer-191 and αGlu-191 altered MoFe proteins exhibit lower EPR signal intensity than wild type. This result correlates with both their low specific activity of H_2 evolution under Ar and their lower Mo content compared to wild type. Therefore, both the low EPR signal intensity for the resting state and the low activity of substrate reduction for the turnover state indicate that these altered MoFe proteins are most likely affected at or near the substrate-reduction site.

Third, both the inability to reduce N_2 and the substantially decreased ability to reduce both C_2H_2 and HCN with the αHis-191, αGlu-191, and αArg-191 altered MoFe proteins is likely due to the effect of changing the nature of the bonding between this residue and the terminal carboxylate of homocitrate and thus interfering with its suggested movement during nitrogenase turnover. However, the small effect of the substitutions, which either eliminate or weaken the putative hydrogen bonding to homocitrate, i.e., with the αPro-191, αSer-191, and αThr-191 altered MoFe proteins, suggests that the hydrogen-bonding link to homocitrate by the αGln-191 residue is not absolutely required for reducing these substrates.

Fourth, the pH-activity profile study of H_2 evolution illustrates the effect of the substitutions at the α-191 position on the pK_a of both the required deprotonated and protonated group(s). The shifts in pK_a of the protonated group(s) in the acid direction with these six altered MoFe proteins from that of the wild type suggest that eliminating or replacing a partner in the αGln-191-homocitrate hydrogen-bonding system removes the contribution of some of the acid-base groups involved in the pK_a of protonated group. Thus, the αGln-191-homocitrate is a likely component of the system that must be protonated for catalyzed H_2 evolution.

Fifth, CO inhibits H_2 evolution in the normal pH assay due to both a CO-induced shift of the pK_a of the protonated group in the acid direction and a lower rate of electron transfer to the proton reduction site. Furthermore, the substitutions that produce the αPro-191, αSer-191, αThr-191, αHis-191, or αGlu-191 altered MoFe proteins induce the pK_a of the protonated group to shift close to the pK_a value for "wild type plus CO". This resemblance suggests that the effect of disturbing the αGln-191-homocitrate system is equivalent to that arising from CO binding. This result suggests that a CO-binding site is close to the αGln-191-homocitrate system.

Sixth, C_2H_4 production from C_2H_2 with the αSer-191 altered MoFe protein, when assayed at pH 8.0, exhibits a biphasic Michaelis-Menten plot and two K_m values were separately detected. This result suggests that at least two C_2H_2 binding sites may be present on wild type MoFe protein but they are indistinguishable from one another under normal assay conditions. In addition, some of the altered MoFe proteins allocate a higher percentage of electron flux to H_2 evolution under 10% C_2H_2 than does wild type. However, when the C_2H_2 concentration is increased to 100%, the αSer-191 altered MoFe protein can achieve the same percentage distribution to H_2 evolution as wild type whereas αHis-191, αGlu-191, and αArg-191 altered MoFe proteins cannot do so. The interpretation of these data is that the high-affinity C_2H_2-binding site is affected in the αSer-191 altered MoFe protein but is eliminated in the αHis-191, αGlu-191, and αArg-191 altered MoFe proteins. In all MoFe proteins, the low-affinity C_2H_2-binding site is still intact. The loss of the high-affinity C_2H_2-binding site suggests that this site is located close to the αGln-191-homocitrate system of Mo-nitrogenase whereas the low-affinity C_2H_2-binding site is located elsewhere.

Seventh, C_2H_6 formation by some substitutions at the α-191 position may be explained based on K_m determinations and on rates of electron and proton transfer. Unlike wild type, a low apparent binding affinity for C_2H_2 was found for the αHis-191, αGlu-191, and αArg-191 altered MoFe proteins compared to that of wild type. The low apparent binding affinity for C_2H_2 suggests that C_2H_4 bound as an intermediate stays longer at the active site and so then has time to get two more electrons and two more protons to form C_2H_6. The greater C_2H_6 production when assayed at pH 8.0 compared to the assay at pH 7.0 suggests that C_2H_6 production uses acid-base group(s) with a higher pK_a (for the deprotonated group) than for C_2H_4 production. However, both C_2H_4 and C_2H_6 formation from C_2H_2, as catalyzed by these altered MoFe proteins, occur on a common mechanistic pathway and this mechanism differs from that operating in V-nitrogenase.

Eighth, the amino acid substitutions at αGln-191 MoFe protein impact on HCN catalysis and the apparent binding affinity of both HCN and CN^-. Moreover the low rate of HCN reduction by substitutions with amino acid residues that have large and charged

side chains, is suggested to results from hindering the movement of homocitrate. The results from the αHis-191 altered MoFe protein, which shows an increase in apparent affinity for HCN and a decreased apparent affinity for CN^- suggests that HCN and CN^- bind to wild type MoFe protein at independent sites.

Ninth, the dependence of C_2H_6 production on both HCN and CN^- concentrations with αSer-191 altered MoFe protein suggests that both HCN and CN^- are involved in C_2H_6 formation with CN^- possibly inserting into a partially reduced HCN substrate bound at the active site.

Finally, all of our kinetic results from amino-acid substitutions at the αGln-191 residue, using a variety of different substrates and inhibitors, can be viewed in the context of the hydrogen bonding connection through the αGln-191 residue from the P cluster to the homocitrate bound to the FeMo cofactor. Homocitrate is coordinated to the Mo, is surrounded by a number of buried water molecules, and is on the side of the FeMo cofactor nearest to the P cluster. The results from the substitutions at αGln-191 residue support the proposed movement of homocitrate as being necessary for substrate binding and reduction during nitrogenase catalysis. It seems likely that this movement is responsible for either opening the site for substrate binding or in proton delivery to substrate.

Until now, there is no agreement on where substrates bind on the FeMo cofactor or how they are reduced. Recent work suggests that different substrates likely bind to different areas of the FeMo cofactor and that each may have multiple binding sites (Shen *et al*., 1997, Dilworth *et al*., 1998, Fisher *et al*., 2000a,b; Christiansen *et al*., 2000a,b). N_2 could bind to either Fe or Mo, end-on, side-on or in bridging modes (reviewed by Howard and Rees, 1996 and see section 1.5.3). One report has proposed that N_2 might bind to Mo by displacement of the αHis-442 ligand in a reaction stabilized by homocitrate (Grönberg *et al*., 1998 and see section 1.5.3.3). The potential proton-transfer routes have been proposed as a water-filled channel running from the protein exterior to the homocitrate ligand of FeMo cofactor and two hydrogen-bonded chains of residues that bond to specific FeMo cofactor sulfur atoms (Durrant, 2001). Although progress has been made, the critical mechanistic questions of how and where substrates bind and by what mechanism they receive their electrons and protons remain open for future research.

REFERENCES

Arnold, W., Rump, A., Klipp, W., Priefer, U.B. and Puhler, A. (1988) Nucleotide sequence of a 24,206-base-pair DNA fragment carrying the entire nitrogen fixation gene cluster of *Klebsiella pneumoniae*. *J. Mol. Biol.* **203**: 715-738.

Ashby, G.A., Dilworth, M.J. and Thorneley, R.N.F. (1987) *Klebsiella pneumoniae* nitrogenase. Inhibition of hydrogen evolution by ethylene and the reduction of ethylene to ethane. *Biochem. J.* **247**: 547-554.

Bishop, P.E., Jarlenski, D.M. and Hetherington, D.R. (1980) Evidence for an alternative nitrogen fixation system in *Azotobacter vinelandii*. *Proc. Natl. Acad. Sci. U.S.A.* **77**: 7342-7346.

Bishop, P.E. and Premakumar, R. (1992) Alternative nitrogen fixation systems. In *Biological nitrogen fixation*. Stacey, G., Roberts, G.P., and Evans, D.J. (eds.) New York: Chapman & Hill, pp. 736-762.

Bolin, J.T., Ronco, A.E., Morgan, T.V., Mortenson, L.E. and Xuong, N.H. (1993) The unusual metal clusters of nitrogenase: structural features revealed by x-ray anomalous diffraction studies of the MoFe protein from *Clostridium pasteurianum*. *Proc. Natl. Acad. Sci. U.S.A.* **90**: 1078-1082.

Brigle, K.E., Newton, W.E. and Dean, D.R. (1985) Complete nucleotide sequence of the *Azotobacter vinelandii* nitrogenase structural gene cluster. *Gene*. **37**: 37-44.

Brigle, K.E., Weiss, M.C., Newton, W.E. and Dean, D.R. (1987) Products of the iron-molybdenum cofactor-specific biosynthetic genes, *nifE* and *nifN*, are structurally homologous to the products of the nitrogenase molybdenum-iron protein genes, *nifD* and *nifK*. *J. Bacteriol.* **169**: 1547-1553.

Bulen, W.A., Burns, R. and LeComte, J.R. (1965) Nitrogenase fixation: hydrosulfide as electron donor with cell-free preparations of *Azotobacter vinelandii* and *Rhodospirillum rubrum*. *Proc. Natl. Acad. Sci. U.S.A.* **53**: 532-539.

Bulen, W.A. and LeComte, J.R. (1966) The nitrogenase system from *Azotobacter*: two-enzyme requirement for N_2 reduction, ATP-dependent H_2 evolution, and ATP hydrolysis. *Proc. Natl. Acad. Sci. U.S.A.* **56**: 979-986.

Bulen, W.A. (1976) Nitrogenase from *Azotobacter vinelandii* and reactions affecting mechanistic interpretations. In *Proc. 1st symp. nitrogenfixation*. Newton, W.E., and Nyman, C.J. (eds.): Washington state university press, pp. 177-186.

Burgess, B.K., Stiefel, E.I. and Newton, W.E. (1980) Oxidation-reduction properties and complexation reactions of the iron-molybdenum cofactor of nitrogenase. *J. Biol. Chem.* **255**: 353-356.

Burgess, B.K., Wherland, S., Newton, W.E. and Stiefel, E.I. (1981) Nitrogenase reactivity: insight into the nitrogen-fixing process through hydrogen-inhibition and HD-forming reactions. *Biochemistry*. **20**: 5140-5146.

Burgess, B.K. and Lowe, D.J. (1996) Mechanism of molybdenum nitrogenase. *Chem. Rev.* **96**: 2983-3011.

Burns, R.C. and Bulen, W.A. (1965) ATP-dependent hydrogen evolution by cell-free preparations of *Azotobacter vinelandii*. *Biochem. Biophys. Acta*. **105**: 437-445.

Chan, M.K., Kim, J. and Rees, D.C. (1993) The nitrogenase FeMo-cofactor and P-cluster pair: 2.2 Å resolution structures. *Science*. **260**: 792-794.

Chisnell, J.R., Premakumar, R. and Bishop, P.E. (1988) Purification of a second alternative nitrogenase from a *nifHDK* deletion strain of *Azotobacter vinelandii*. *J. Bacteriol.* **170**: 27-33.

Christiansen, J., Cash, V.L., Seefeldt, L.C. and Dean, D.R. (2000a) Isolation and characterization of an acetylene-resistant nitrogenase. *J. Biol. Chem.* **275**: 11459-11464.

Christiansen, J., Seefeldt, L.C. and Dean, D.R. (2000b) Competitive substrate and inhibitor interactions at the physiologically relevant active site of nitrogenase. *J. Biol. Chem.* **275**: 36104-36107.

Christiansen, J. and Dean, D.R. (2001) Mechanistic features of the Mo-containing nitrogenase. *Annu. Rev. Plant Physiol. Plant Mol. Biol.* **52**: 269-295.

Christie, P.D., Lee, H.I., Cameron, L.M., Hales, B.J. and Orme-Johnson, W.H. (1996) Identification of the CO-binding cluster in nitrogenase MoFe protein by ENDOR of ^{57}Fe isotopomer. *J. Am. Chem. Soc.* **118**: 8707-8709.

Conradson, S.D., Burgess, B.K. and Holm, R.H. (1988) Fluorine-19 chemical shifts as probes of the structure and reactivity of the iron-molybdenum cofactor of nitrogenase. *J. Biol. Chem.* **263**: 13743-13749.

Conradson, S.D., Burgess, B.K., Vaughn, S.A., Roe, A.L., Hedman, B., Hodgson, K.O. and Holm, R.H. (1989) Cyanide and methylisocyanide binding to the isolated iron-molybdenum cofactor of nitrogenase. *J. Biol. Chem.* **264**: 15967-15974.

Corbin, J.L. (1978) A simple, automated apparatus for the rapid multiple flush of reaction (assay) vessels with gases. *Anal. Biochem.* **84**: 340-342.

Dance, I.G. (1994) The binding and reduction of dinitrogen at the Fe_4 face of the FeMo cluster of nitrogenase. *Aust. J. Chem.* **47**: 970-990.

Dance, I.G. (1996) Theoretical investigations of the mechanism of biological nitrogen fixation at the FeMo cluster site. *J. Bioinorg. Chem.* **1**: 581-586.

Dance, I.G. (1997) Calculated details of a mechanism for conversion of N_2 to NH_3 at the FeMo cluster of nitrogenase. *Chem. Commun.*: 165-166.

Davis, L.C., Henzl, M.T., Burris, R.H. and Orme-Johnson, W.H. (1979) Iron-sulfur clusters in the molybdenum-iron protein component of nitrogenase. Electron paramagnetic resonance of the carbon monoxide inhibited state. *Biochemistry*. **18**: 4860-4869.

Dean, D.R., Scott, D.J. and Newton, W.E. (1990) Identification of FeMoco domains within the nitrogenase MoFe protein. In *Nitrogen fixation: achievements and objectives*. Gresshoff, P.M., Roth, R.L., Stacey, G., and Newton, W.E. (eds.) New York: Chapmam & Hall, pp. 95-102.

Dean, D.R. and Jacobson, M.R. (1992) Biochemical genetics of nitrogenase. In *Biological nitrogen fixation*. Stacey, G., Burris, R.H., and Evans, H.R. (eds.) New York: Chapman & Hall, pp. 763-834.

Deng, H. and Hoffman, R. (1993) How N_2 might be activated by the FeMo-cofactor in nitrogenase. *Angew. Chem. Int. Ed. Engl.* **32**: 1062-1065.

Dilworth, M.J. (1966) Acetylene reduction by nitrogen-fixing preparations from *Clostridium pasteurianum*. *Biochim. Biophys. Acta*. **127**: 285-294.

Dilworth, M.J., Eady, R.R., Robson, R.L. and Miller, R.W. (1987) Ethane formation from acetylene as a potential test for vanadium nitrogenase in vivo. *Nature*. **27**: 167-168.

Dilworth, M.J., Eady, R.R. and Eldridge, M.E. (1988) The vanadium nitrogenase of *Azotobacter chroococcum*. Reduction of acetylene and ethylene to ethane. *Biochem. J.* **249**: 745-751.

Dilworth, M.J., Eldridge, M.E. and Eady, R.R. (1992) Correction for creatine interference with the direct indophenol measurement of NH_3 in steady-state nitrogenase assays. *Anal. Biochem.* **207**: 6-10.

Dilworth, M.J., Eldridge, M.E. and Eady, R.R. (1993) The molybdenum and vanadium nitrogenases of *Azotobacter chroococcum*: effect of elevated temperature on N_2 reduction. *Biochem. J.* **289**: 395-400.

Dilworth, M.J., Fisher, K., Kim, C.H. and Newton, W.E. (1998) Effects on substrate reduction of substitution of histidine-195 by glutamine in the alpha-subunit of the MoFe protein of *Azotobacter vinelandii* nitrogenase. *Biochemistry*. **37**: 17495-17505.

Dilworth, M.J. and Fisher, K. (1998) Elimination of creatine interference with the indophenol measurement of NH_3 produced during nitrogenase assays. *Anal. Biochem.* **256**: 242-244.

Dixon, R. (1998) The oxygen-responsive NIFL-NIFA complex: a novel two-component regulatory system controlling nitrogenase synthesis in gamma-proteobacteria. *Arch. Microbiol.* **169**: 371-380.

Durrant, M.C. (2001) Controlled protonation of iron-molyndenum cofactor by nitrogenase: a structural and theoretical analysis. *Biochem. J.* **355**: 569-576.

Duyvis, M.G., Wassink, H. and Haaker, H. (1996) Pre-steady-state kinetics of nitrogenase from *Azotobacter vinelandii*. Evidence for an ATP-induced conformational change of the nitrogenase complex as part of the reaction mechanism. *J. Biol. Chem.* **271**: 29632-29636.

Duyvis, M.G., Mensink, R.E., Wassink, H. and Haaker, H. (1997) Evidence for multiple steps in the pre-steady-state electron transfer reaction of nitrogenase from *Azotobacter vinelandii*. *Biochim. Biophys. Acta*. **1320**: 34-44.

Eady, R.R., Robson, R.L., Richardson, T.H., Miller, R.W. and Hawkins, M. (1987) The vanadium nitrogenase of *Azotobacter chroococcum*. Purification and properties of the VFe protein. *Biochem. J.* **244**: 197-207.

Eady, R.R. (1992) The dinitrogen-fixing bacteria. In *The procaryotes*. Balows, A., Truper, H.G., Dworkin, M., Harder, W., and Schleifer, K.H. (eds.): Springer-Verlag, pp. 534-553.

Eady, R.R. (1996) Structure-function relationships of alternative nitrogenase. *Chem. Rev.* **96**: 3013-3030.

Ennor, A.H. (1957) Determination and preparation of N-phosphates of biological origin. *Methods Enzymol.* **3**: 850-856.

Evans, D.J., Henderson, R.A. and Smith, B.E. (1993) Catalysis by nitrogenase and synthesis analogs. In *Bioinorganic catalysis*. Reedijk, J. (ed.) New York: Marcel Dekker, Inc., pp. 89-130.

Evans, D.J., Henderson, R.A. and Smith, B.E. (1999) Catalysis by nitrogenases and synthetic analogs. In *Bioinorganic catalysis*. Reedijk, J., and Bouwman, E. (eds.) New York: Marcel Dekker, Inc., pp. 153-208.

Filler, W.A., Kemp, R.M., Ng, J.C., Hawkes, T.R., Dixon, R.A. and Smith, B.E. (1986) The *nifH* gene product is required for the synthesis or stability of the iron-molybdenum cofactor of nitrogenase from *Klebsiella pneumoniae*. *Eur. J. Biochem.* **160**: 371-377.

Fisher, K., Thorneley, R.N.F. and Lowe, D.J. (1990) Nitrogenase of *Klebsiella pneumoniae*: mechanism of acetylene reduction. *Biochem. J.* **272**: 621-625.

Fisher, K., Lowe, D.J. and Thorneley, R.N.F. (1991) *Klebsiella pneumoniae* nitrogenase. The pre-steady-state kinetics of MoFe-protein reduction and hydrogen evolution under conditions of limiting electron flux show that the rates of association with the Fe-protein and electron transfer are independent of the oxidation level of the MoFe-protein. *Biochem. J.* **279**: 81-85.

Fisher, K., Dilworth, M.J., Kim, C.H. and Newton, W.E. (2000a) *Azotobacter vinelandii* nitrogenases containing altered MoFe proteins with substitutions in the FeMo-cofactor environment: effects on the catalyzed reduction of acetylene and ethylene. *Biochemistry*. **39**: 2970-2979.

Fisher, K., Dilworth, M.J., Kim, C.H. and Newton, W.E. (2000b) *Azotobacter vinelandii* nitrogenases with substitutions in the FeMo-cofactor environment of the MoFe protein: effects of acetylene or ethylene on interactions with H^+, HCN, and CN^-. *Biochemistry*. **39**: 10855-10865.

Fisher, K., Dilworth, M.J. and Newton, W.E. (2000c) Differential effects on N_2 binding and reduction, HD formation, and azide reduction with alpha-195^{His}- and alpha-191^{Gln}-substituted MoFe proteins of *Azotobacter vinelandii* nitrogenase. *Biochemistry*. **39**: 15570-15577.

Flint, D.H. (1996) *Escherichia coli* contains a protein that is homologous in function and N-terminal sequence to the protein encoded by the *nifS* gene of *Azotobacter vinelandii* and that can participate in the synthesis of the Fe-S cluster of dihydroxy-acid dehydratase. *J. Biol. Chem.* **271**: 16068-16074.

Fu, W., Jack, R.F., Morgan, T.V., Dean, D.R. and Johnson, M.K. (1994) *nifU* gene product from *Azotobacter vinelandii* is a homodimer that contains two identical [2Fe-2S] clusters. *Biochemistry*. **33**: 13455-13463.

Gavini, N. and Burgess, B.K. (1992) FeMo cofactor synthesis by a *nifH* mutant with altered MgATP reactivity. *J. Biol. Chem.* **267**: 21179-21186.

George, S.J., Ashby, G.A., Wharton, C.W. and Thorneley, R.N.F. (1997) Time-resolved binding of carbon monoxide to nitrogenase monitored by stopped-flow infrared spectroscopy. *J. Am. Chem. Soc.* **119**: 6450-6451.

Georgiadis, M.M., Komiya, H., Chakrabarti, P., Woo, D., Kornuc, J.J. and Rees, D.C. (1992) Crystallographic structure of the nitrogenase iron protein from *Azotobacter vinelandii*. *Science*. **257**: 1653-1659.

Grönberg, K.L.C., Gormal, C.A., Smith, B.E. and Henderson, R.A. (1997) A new approach to identifying substrate binding sites on isolated FeMo-cofactor of nitrogenase. *Chem. Commun.*: 713-714.

Grönberg, K.L.C., Gormal, C.A., Durrant, M.C., Smith, B.E. and Henderson, R.A. (1998) Why R-homocitrate is essential to the reactivity of FeMo-cofactor of nitrogenase: studies on NifV$^-$-extracted FeMo-cofactor. *J. Am. Chem. Soc.* **120-21**: 10613-10621.

Guth, J.H. and Burris, R.H. (1983) Inhibition of nitrogenase-catalyzed NH_3 formation by H_2. *Biochemistry*. **22**: 5111-5122.

Hadfield, K.L. and Bulen, W.A. (1969) Adenosine triphosphate requirement of nitrogenase from *Azotobacter vinelandii*. *Biochemistry*. **8**: 5103-5108.

Hageman, R.V. and Burris, R.H. (1978) Kinetic studies on electron transfer and interaction between nitrogenase components from *Azotobacter vinelandii*. *Biochemistry*. **17**: 4117-4124.

Hageman, R.V. and Burris, R.H. (1980) Electron allocation to alternative substrates of *Azotobacter* nitrogenase is controlled by the electron flux through dinitrogenase. *Biochim. Biophys. Acta*. **591**: 63-75.

Hales, B.J., Case, E.E., Morningstar, J.E., Dzeda, M.F. and Mauterer, L.A. (1986) Isolation of a new vanadium-containing nitrogenase from *Azotobacter vinelandii*. *Biochemistry*. **25**: 7251-7255.

Hardy, R.W.F., Knight, E., Jr. and D'Eustachio, A.J. (1965) An energy-dependent hydrogen-evolution from dithionite in nitrogen-fixing extracts of *Clostridium pasteurianum*. *Biochem. Biophys. Res. Commun.* **20**: 539-544.

Hardy, R.W.F. and Knight, E., Jr. (1967) ATP-dependent reduction of azide and HCN by N_2-fixing enzymes of *Azotobacter vinelandii* and *Clostridium pasteurianum*. *Biochim. Biophys. Acta*. **139**: 69-90.

Hardy, R.W.F., Burns, R.C. and Holsten, R.D. (1973) Applications of the acetylene-ethylene assay for measurements of nitrogen fixation. *Soil Biol. Biochem.* **5**: 47-81.

Hardy, R.W.F. (1979) In *A treatise on dinitrogen fixation*. Hardy, R.W., and Burns, R.C. (eds.) New York: Wiley, pp. 407-489.

Hawkes, T.R., McLean, P.A. and Smith, B.E. (1984) Nitrogenase from *nifV* mutants of *Klebsiella pneumoniae* contains an altered form of the iron-molybdenum cofactor. *Biochem. J.* **217**: 317-321.

Henderson, R.A. (1996) Protonation of unsaturated hydrocarbon ligands: regioselectivity, stereoselectivity, and product specificity. *Angew. Chem. Int. Ed. Engl.* **35**: 946-967.

Homer, M.J., Paustian, T.D., Shah, V.K. and Roberts, G.P. (1993) The *nifY* product of *Klebsiella pneumoniae* is associated with apodinitrogenase and dissociates upon activation with the iron-molybdenum cofactor. *J. Bacteriol.* **175**: 4907-4910.

Homer, M.J., Dean, D.R. and Roberts, G.P. (1995) Characterization of the gamma protein and its involvement in the metallocluster assembly and maturation of dinitrogenase from *Azotobacter vinelandii*. *J. Biol. Chem.* **270**: 24745-24752.

Hoover, T.R., Shah, V.K., Roberts, G.P. and Ludden, P.W. (1986) *nifV*-dependent, low-molecular-weight factor required for in vitro synthesis of iron-molybdenum cofactor of nitrogenase. *J Bacteriol*. **167**: 999-1003.

Hoover, T.R., Robertson, A.D., Cerny, R.L., Hayes, R.N., Imperial, J., Shah, V.K. and Ludden, P.W. (1987) Identification of the V factor needed for synthesis of the iron-molybdenum cofactor of nitrogenase as homocitrate. *Nature*. **329**: 855-857.

Hoover, T.R., Imperial, J., Liang, J.H., Ludden, P.W. and Shah, V.K. (1988) Dinitrogenase with altered substrate specificity results from the use of homocitrate analogues for in vitro synthesis of the iron-molybdenum cofactor. *Biochemistry*. **27**: 3647-3652.

Hoover, T.R., Imperial, J., Ludden, P.W. and Shah, V.K. (1989) Homocitrate is a component of the iron-molybdenum cofactor of nitrogenase. *Biochemistry*. **28**: 2768-2771.

Howard, J.B. (1993) Protein component complex formation and adenosine triphosphate hydrolysis in nitrogenase. In *Molybdenum enzymes, cofactors, and model systems*. Stiefel, E.I., Coucouvanis, D., and Newton, W.E. (eds.) Washington, DC: American Chemical Society, pp. 271-289.

Howard, J.B. and Rees, D.C. (1994) Nitrogenase: a nucleotide-dependent molecular switch. *Annu. Rev. Biochem.* **63**: 235-264.

Howard, J.B. and Rees, D.C. (1996) Structural basis of biological nitrogen fixation. *Chem. Rev.* **96**: 2965-2982.

Howard, K.S., McLean, P.A., Hansen, F.B., Lemley, P.V., Koblan, K.S. and Orme-Johnson, W.H. (1986) *Klebsiella pneumoniae nifM* gene product is required for

stabilization and activation of nitrogenase iron protein in *Escherichia coli*. *J. Biol. Chem.* **261**: 772-778.

Hughes, D.L., Ibrahim, S.K., Pickett, C.J., Querne, G., Laouenan, A., Talarmin, J., *et al* (1994) On carboxylate as a leaving group at the active site of Mo-nitrogenase: electrochemical reactions of some Mo and W carboxylates, formation of mono-, di-, and tri-hydrides and the detection of an $MoH_2(N_2)$ intermediate. *Polyhedron*. **13**: 3341-3348.

Hwang, J.C., Chen, C.H. and Burris, R.H. (1973) Inhibition of nitrogenase-catalyzed reductions. *Biochim. Biophys. Acta*. **292**: 256-270.

Hyman, M.R., Seefeldt, L.C., Morgan, T.V., Arp, D.J. and Mortenson, L.E. (1992) Kinetic and spectroscopic analysis of the inactivating effects of nitric oxide on the individual components of *Azotobacter vinelandii* nitrogenase. *Biochemistry*. **31**: 2947-2955.

Imperial, J., Hoover, T.R., Madden, M.S., Ludden, P.W. and Shah, V.K. (1989) Substrate reduction properties of dinitrogenase activated in vitro are dependent upon the presence of homocitrate or its analogues during iron-molybdenum cofactor synthesis. *Biochemistry*. **28**: 7796-7799.

Jackson, E.K., Parshall, G.W. and Hardy, R.W. (1968) Hydrogen reactions of nitrogenase. Formation of the molecule HD by nitrogenase and by an inorganic model. *J. Biol. Chem.* **243**: 4952-4958.

Jacobson, M.R., Brigle, K.E., Bennett, L.T., Setterquist, R.A., Wilson, M.S., Cash, V.L., *et al* (1989) Physical and genetic map of the major *nif* gene cluster from *Azotobacter vinelandii*. *J. Bacteriol.* **171**: 1017-1027.

Jang, S.B., Seefeldt, L.C. and Peters, J.W. (2000) Insights into nucleotide signal transduction in nitrogenase: structure of an iron protein with MgADP bound. *Biochemistry*. **39**: 14745-14752.

Kelly, M., Postgate, J.R. and Richards, R.L. (1967) Reduction of cyanide and isocyanide by nitrogenase of *Azotobacter chroococcum*. *Biochem. J.* **102**: 1C-3C.

Kelly, M. (1969) Comparisons and cross reactions of nitrogenase from *Klebsiella pneumoniae*, *Azotobacter chroococcum* and *Bacillus polymyxa*. *Biochim. Biophys. Acta*. **191**: 527-540.

Kennedy, I.R., Morris, J.A. and Mortenson, L.E. (1968) N_2 fixation by purified components of the N_2-fixing system of *Clostridium pasteurianum*. *Biochim. Biophys. Acta*. **153**: 777-786.

Kent, H.M., Ioannidis, I., Gormal, C., Smith, B.E. and Buck, M. (1989) Site-directed mutagenesis of the *Klebsiella pneumoniae* nitrogenase. Effects of modifying conserved cysteine residues in the alpha- and beta- subunits. *Biochem. J.* **264**: 257-264.

Kent, H.M., Baines, M., Gormal, C., Smith, B.E. and Buck, M. (1990) Analysis of site-directed mutations in the alpha- and beta-subunits of *Klebsiella pneumoniae* nitrogenase. *Mol. Microbiol.* **4**: 1497-1504.

Kim, C.H., Newton, W.E. and Dean, D.R. (1995) Role of the MoFe protein alpha-subunit histidine-195 residue in FeMo-cofactor binding and nitrogenase catalysis. *Biochemistry*. **34**: 2798-2808.

Kim, J. and Rees, D.C. (1992a) Crystallographic structure and functional implications of the nitrogenase molybdenum-iron protein from *Azotobacter vinelandii*. *Nature*. **360**: 553-560.

Kim, J. and Rees, D.C. (1992b) Structural models for the metal centers in the nitrogenase molybdenum-iron protein. *Science*. **257**: 1677-1682.

Kim, J., Woo, D. and Rees, D.C. (1993) X-ray crystal structure of the nitrogenase molybdenum-iron protein from *Clostridium pasteurianum* at 3.0-Å resolution. *Biochemistry*. **32**: 7104-7115.

Kim, J. and Rees, D.C. (1994) Nitrogenase and biological nitrogen fixation. *Biochemistry*. **33**: 389-397.

Laemmli, U.K. (1970) Cleavage of structural proteins during assembly of the head of bacteriophage T_4. *Nature*. **227**: 680-685.

Lanzilotta, W.N., Holz, R.C. and Seefeldt, L.C. (1995a) Proton NMR investigation of the $[4Fe\text{-}4S]^{1+}$ cluster environment of nitrogenase iron protein from *Azotobacter vinelandii*: defining nucleotide-induced conformational changes. *Biochemistry*. **34**: 15646-15653.

Lanzilotta, W.N., Ryle, M.J. and Seefeldt, L.C. (1995b) Nucleotide hydrolysis and protein conformational changes in *Azotobacter vinelandii* nitrogenase iron protein: defining the function of aspartate 129. *Biochemistry*. **34**: 10713-10723.

Lanzilotta, W.N. and Seefeldt, L.C. (1996) Electron transfer from the nitrogenase iron protein to the [8Fe-(7/8)S] clusters of the molybdenum-iron protein. *Biochemistry*. **35**: 16770-16776.

Lanzilotta, W.N., Fisher, K. and Seefeldt, L.C. (1996) Evidence for electron transfer from the nitrogenase iron protein to the molybdenum-iron protein without MgATP hydrolysis: characterization of a tight protein-protein complex. *Biochemistry*. **35**: 7188-7196.

Lanzilotta, W.N. and Seefeldt, L.C. (1997) Changes in the midpoint potentials of the nitrogenase metal centers as a result of iron protein-molybdenum-iron protein complex formation. *Biochemistry*. **36**: 12976-12983.

Lanzilotta, W.N., Fisher, K. and Seefeldt, L.C. (1997) Evidence for electron transfer-dependent formation of a nitrogenase iron protein-molybdenum-iron protein tight complex. The role of aspartate 39. *J. Biol. Chem.* **272**: 4157-4165.

Lanzilotta, W.N., Christiansen, J., Dean, D.R. and Seefeldt, L.C. (1998) Evidence for coupled electron and proton transfer in the [8Fe-7S] cluster of nitrogenase. *Biochemistry*. **37**: 11376-11384.

Lee, H.I., Cameron, L.M., Hales, B.J. and Hoffman, B.M. (1997) CO binding to the FeMo cofactor of CO-inhibited nitrogenase: ^{13}CO and ^{1}H Q-band ENDOR investigation. *J. Am. Chem. Soc.* **119**: 10121-10126.

Lee, H.I., Thrasher, K.S., Dean, D.R., Newton, W.E. and Hoffman, B.M. (1998) ^{14}N electron spin-echo envelope modulation of the S = 3/2 spin system of the *Azotobacter vinelandii* nitrogenase iron-molybdenum cofactor. *Biochemistry*. **37**: 13370-13378.

Li, J., Burgess, B.K. and Corbin, J.L. (1982) Nitrogenase reactivity: cyanide as substrate and inhibitor. *Biochemistry*. **21**: 4393-4402.

Liang, J. and Burris, R.H. (1988a) Hydrogen burst associated with nitrogenase-catalyzed reactions. *Proc. Natl. Acad. Sci. U.S.A.* **85**: 9446-9450.

Liang, J. and Burris, R.H. (1988b) Interaction among N_2, N_2O, and C_2H_2 as substrates and inhibitors of nitrogenase from *Azotobacter vinelandii*. *Biochemistry.* **27**: 6726-6732.

Liang, J. and Burris, R.H. (1988c) Inhibition of nitrogenase by NO. *Indian J. Biochem. Biophys.* **25**: 636-641.

Liang, J., Madden, M., Shah, V.K. and Burris, R.H. (1990) Citrate substitutes for homocitrate in nitrogenase of a *nifV* mutant of *Klebsiella pneumoniae*. *Biochemistry*. **29**: 8577-8581.

Lindahl, P.A., Day, E.P., Kent, T.A., Orme-Johnson, W.H. and Münck, E. (1985) Mössbauer, EPR, and magnetization studies of the *Azotobacter vinelandii* Fe protein. Evidence for a $[4Fe\text{-}4S]^{1+}$ cluster with spin S = 3/2. *J. Biol. Chem.* **260**: 11160-11173.

Lin-Vien, D., Fateley, W.G. and Davis, L.C. (1989) Estimation of nitrogenase activity in the presence of ethylene biosynthesis by use of deuterated acetylene as a substrate. *Appl. Environ. Microbiol.* **55**: 354-359.

Lockshin, A. and Burris, R.H. (1965) Inhibitors of nitrogen fixation in extracts from *Clostridium pasteurianum*. *Biochim. Biophys. Acta*. **111**: 1-10.

Lowe, D.J., Eady, R.R. and Thorneley, R.N.F. (1978) Electron-paramagnetic-resonance studies on nitrogenase of *Klebsiella pneumoniae*. Evidence for acetylene- and ethylene-nitrogenase transient complexes. *Biochem. J.* **173**: 277-290.

Lowe, D.J. and Thorneley, R.N.F. (1984a) The mechanism of *Klebsiella pneumoniae* nitrogenase action. The determination of rate constants required for the simulation of the kinetics of N_2 reduction and H_2 evolution. *Biochem. J.* **224**: 895-901.

Lowe, D.J. and Thorneley, R.N.F. (1984b) The mechanism of *Klebsiella pneumoniae* nitrogenase action. Pre-steady-state kinetics of H_2 formation. *Biochem. J.* **224**: 877-886.

Lowe, D.J., Fisher, K., Thorneley, R.N.F., Vaughn, S.A. and Burgess, B.K. (1989) Kinetics and mechanism of the reaction of cyanide with molybdenum nitrogenase from *Azotobacter vinelandii*. *Biochemistry*. **28**: 8460-8466.

Lowe, D.J., Fisher, K. and Thorneley, R.N.F. (1993) *Klebsiella pneumoniae* nitrogenase: pre-steady-state absorbance changes show that redox changes occur in the MoFe protein that depend on substrate and component protein ratio; a role for P-centres in reducing dinitrogen? *Biochem. J.* **292**: 93-98.

Lowe, D.J., Ashby, G.A., Brune, M., Knights, H., Webb, M.R. and Thorneley, R.N.F. (1995) ATP hydrolysis and energy transduction by nitrogenase. In *Nitrogen fixation: fundamental and application*. Tikhonovich, N.A., Provorov, N.A., Romanov, V.I., and Newton, W.E. (eds.) Dordrecht: Kluwer Acadamic Publicsher, pp. 103-108.

Lowry, O.H., Rosebrough, N.J., Farr, A.L. and Randall, R.H. (1951) Protein measurement with the folin phenol reagent. *J. Biol. Chem.* **193**: 265-275.

Ludden, P.W., Shah, V.K., Roberts, G.P., Homer, M., Allen, R., Paustian, T.*, et al* (1993) Biosynthesis of the iron-molybdenum cofactor of nitrogenase. In *Molybdenum enzymes, cofactors, and model systems*. Stiefel, E.I., Coucouvanis, D., and Newton, W.E. (eds.) Washington DC: Amercan Chemical Society, pp. 196-215.

Luque, F. and Pau, R.N. (1991) Transcriptional regulation by metals of structural genes for *Azotobacter vinelandii* nitrogenases. *Mol. Gen. Genet.* **227**: 481-487.

Madden, M.S., Kindon, N.D., Ludden, P.W. and Shah, V.K. (1990) Diastereomer-dependent substrate reduction properties of a dinitrogenase containing 1-fluorohomocitrate in the iron-molybdenum cofactor. *Proc. Natl. Acad. Sci. U.S.A.* **87**: 6517-6521.

Madden, M.S., Paustian, T.D., Ludden, P.W. and Shah, V.K. (1991) Effects of homocitrate, homocitrate lactone, and fluorohomocitrate on nitrogenase in $NifV^-$ mutants of *Azotobacter vinelandii*. *J. Bacteriol.* **173**: 5403-5405.

Madden, M.S., Krezel, A.M., Allen, R.M., Ludden, P.W. and Shah, V.K. (1992) Plausible structure of the iron-molybdenum cofactor of nitrogenase. *Proc. Natl. Acad. Sci. U.S.A.* **89**: 6487-6491.

Martin, A.E., Burgess, B.K., Iismaa, S.E., Smartt, C.T., Jacobson, M.R. and Dean, D.R. (1989) Construction and characterization of an *Azotobacter vinelandii* strain with mutations in the genes encoding flavodoxin and ferredoxin. *J. Bacteriol.* **171**: 3162-3167.

Mascharak, P.K., Smith, M.C., Armstrong, W.H., Burgess, B.K. and Holm, R.H. (1982) Fluorine-19 chemical shifts as structural probes of metal-sulfur clusters and the cofactor of nitrogenase. *Proc. Natl. Acad. Sci. U.S.A.* **79**: 7056-7060.

Masepohl, B., Angermuller, S., Hennecke, S., Hubner, P., Moreno-Vivian, C. and Klipp, W. (1993) Nucleotide sequence and genetic analysis of the *Rhodobacter capsulatus ORF6-nifUI SVW* gene region: possible role of NifW in homocitrate processing. *Mol. Gen. Genet.* **238**: 369-382.

May, H.D., Dean, D.R. and Newton, W.E. (1991) Altered nitrogenase MoFe proteins from *Azotobacter vinelandii*. Analysis of MoFe proteins having amino acid substitutions for the conserved cysteine residues within the beta-subunit. *Biochem. J.* **277**: 457-464.

Mayer, S.M., Lawson, D.M., Gormal, C.A., Roe, S.M. and Smith, B.E. (1999) New insights into structure-function relationships in nitrogenase: a 1.6 Å resolution X-ray crystallographic study of *Klebsiella pneumoniae* MoFe-protein. *J. Mol. Biol.* **292**: 871-891.

McLean, P.A. and Dixon, R.A. (1981) Requirement of *nifV* gene for production of wild-type nitrogenase enzyme in *Klebsiella pneumoniae*. *Nature*. **292**: 655-656.

McLean, P.A., Smith, B.E. and Dixon, R.A. (1983) Nitrogenase of *Klebsiella pneumoniae nifV* mutants. *Biochem. J.* **211**: 589-597.

Meyer, J. (1981) Comparison of carbon monoxide, nitric oxide, and nitrite as inhibitors of the nitrogenase from *Clostridium pasteurianum*. *Arch. Biochem. Biophys.* **210**: 246-256.

Newton, W.E., Gheller, S.F., Hedman, B., Hodgson, K.O., Lough, S.M. and McDonald, J.W. (1985) Redox and compositional insights into the iron-molybdenum cofactor of *Azotobacter vinelandii* nitrogenase as a guide to synthesis of new Mo-Fe-S clusters. In *Nitrogen fixation research progress*. Evans, D.J., Bottomley, P.J., and Newton, W.E. (eds.) Dordrecht: Martinus Nijhoff, pp. 605-610.

Newton, W.E., Corbin, J.L. and McDonald, J.W. (1976) In *Proceeding of the First International Symposium on Nitrogen Fixation*. Newton, W.E., and Nyman, C.J. (eds.) Pullman, WA: Washington State University Press.

Newton, W.E. and Dean, D.R. (1993) Role of the iron-molybdenum cofactor polypeptide environment in *Azotobacter vinelandii* molybdenum-nitrogenase catalysis. In *Molybdenum enzymes, cofactors, and model systems*. Stiefel, E.I., Coucouvanis, D., and Newton, W.E. (eds.) Washington, DC: American Chemical Society, pp. 216-230.

Newton, W.E. (1996) Nitrogen fixation. In *Kirk-othmer Encyclopedia of Chemical Technology*: John Wiley & Sons, pp. 172-204.

Newton, W.E., Vichitphan, K. and Fisher, K. (2001) Comparison of α-191^{Gln} and *Δnifv* altered *Azotobacter vinelandii* nitrogenase MoFe protein. 13th International Congress on Nitrogen Fixation, Hamilton, Ontario, Canada.

Orme-Johnson, W.H., Hamilton, W.D., Jones, T.L., Tso, M.Y., Burris, R.H., Shah, V.K. and Brill, W.J. (1972) Electron paramagnetic resonance of nitrogenase and nitrogenase components from *Clostridium pasteurianum W5* and *Azotobacter vinelandii OP*. *Proc. Natl. Acad. Sci. U.S.A.* **69**: 3142-3145.

Orme-Johnson, W.H. (1992) Nitrogenase structure: where to now? *Science*. **257**: 1639-1640.

Pau, R.N., Mitchenall, L.A. and Robson, R.L. (1989) Genetic evidence for an *Azotobacter vinelandii* nitrogenase lacking molybdenum and vanadium. *J. Bacteriol.* **171**: 124-129.

Paustian, T.D., Shah, V.K. and Roberts, G.P. (1989) Purification and characterization of the *nifN* and *nifE* gene products from *Azotobacter vinelandii* mutant UW45. *Proc. Natl. Acad. Sci. U.S.A.* **86**: 6082-6086.

Paustian, T.D., Shah, V.K. and Roberts, G.P. (1990) Apodinitrogenase: purification, association with a 20-kilodalton protein, and activation by the iron-molybdenum cofactor in the absence of dinitrogenase reductase. *Biochemistry*. **29**: 3515-3522.

Peters, J.W., Fisher, K. and Dean, D.R. (1994) Identification of a nitrogenase protein-protein interaction site defined by residues 59 through 67 within the *Azotobacter vinelandii* Fe protein. *J. Biol. Chem.* **269**: 28076-28083.

Peters, J.W., Fisher, K., Newton, W.E. and Dean, D.R. (1995a) Involvement of the P cluster in intramolecular electron transfer within the nitrogenase MoFe protein. *J. Biol. Chem.* **270**: 27007-27013.

Peters, J.W., Fisher, K. and Dean, D.R. (1995b) Nitrogenase structure and function: a biochemical-genetic perspective. *Annu. Rev. Microbiol.* **49**: 335-366.

Peters, J.W., Stowell, M.H., Soltis, S.M., Finnegan, M.G., Johnson, M.K. and Rees, D.C. (1997) Redox-dependent structural changes in the nitrogenase P-cluster. *Biochemistry*. **36**: 1181-1187.

Pham, D.N. and Burgess, B.K. (1993) Nitrogenase reactivity: effects of pH on substrate reduction and CO inhibition. *Biochemistry*. **32**: 13725-13731.

Pickett, C.J. (1996) The Chatt cycle and the mechanism of enzymic reduction of molecular nitrogen. *J. Bioinorg. Chem.* **1**: 601-606.

Pierik, A.J., Wassink, H., Haaker, H. and Hagen, W.R. (1993) Redox properties and EPR spectroscopy of the P clusters of *Azotobacter vinelandii* MoFe protein. *Eur. J. Biochem.* **212**: 51-61.

Pollock, R.C., Lee, H.I., Cameron, L.M., De Rose, V.J., Hales, B.J. and Orme-Johnson, W.H. (1995) Investigation of CO bound to inhibited forms of nitrogenase MoFe protein by ^{13}C ENDOR. *J. Am. Chem. Soc.* **117**: 8686-8687.

Rasche, M.E. and Seefeldt, L.C. (1997) Reduction of thiocyanate, cyanate, and carbon disulfide by nitrogenase: kinetic characterization and EPR spectroscopic analysis. *Biochemistry*. **36**: 8574-8585.

Rawlings, J., Shah, V.K., Chisnell, J.R., Brill, W.J., Zimmermann, R., Munch, E. and Orme-Johnson, W.H. (1978) Novel metal cluster in the iron-molybdenum cofactor of nitrogenase. *J. Biol. Chem.* **253**: 1001-1004.

Ribbe, M., Gadkari, D. and Meyer, O. (1997) N_2 fixation by *Streptomyces thermoautotrophicus* involves a molybdenum-dinitrogenase and a manganese-superoxide oxidoreductase that couple N_2 reduction to the oxidation of superoxide produced from O_2 by a molybdenum-CO dehydrogenase. *J. Biol. Chem.* **272**: 26627-26633.

Richards, A.J., Lowe, D.J., Richards, R.L., Thomson, A.J. and Smith, B.E. (1994) Electron-paramagnetic-resonance and magnetic-circular-dichroism studies of the binding of cyanide and thiols to the thiols to the iron-molybdenum cofactor from *Klebsiella pneumoniae* nitrogenase. *Biochem. J.* **297**: 373-378.

Rivera-Ortiz, J.M. and Burris, R.H. (1975) Interactions among substrates and inhibitors of nitrogenase. *J. Bacteriol.* **123**: 537-545.

Robinson, A.C., Dean, D.R. and Burgess, B.K. (1987) Iron-molybdenum cofactor biosynthesis in *Azotobacter vinelandii* requires the iron protein of nitrogenase. *J. Biol. Chem.* **262**: 14327-14332.

Robson, R.L. (1984) Identification of possible adenine nucleotide-binding sites in nitrogenase Fe- and MoFe-proteins by amino acid sequence comparison. *FEBS Lett.* **173**: 394-398.

Robson, R.L., Eady, R.R., Richardson, T.H., Miller, R.W., Hawkins, M. and Postgate, J.R. (1986) The alternative nitrogenase of *Azotobacter chroococcum* is a vanadium enzyme. *Nature*. **322**: 388-390.

Roll, J.T., Shah, V.K., Dean, D.R. and Roberts, G.P. (1995) Characteristics of NIFNE in *Azotobacter vinelandii* strains. Implications for the synthesis of the iron-molybdenum cofactor of dinitrogenase. *J. Biol. Chem.* **270**: 4432-4437.

Rubinson, J.F., Corbin, J.L. and Burgess, B.K. (1983) Nitrogenase reactivity: methyl isocyanide as substrate and inhibitor. *Biochemistry*. **22**: 6260-6268.

Rudd, K.E., Sofia, H.J., Koonin, E.V., Plunkett, G., Lazar, S. and Rouviere, P.E. (1995) A new family of peptide-prolyl isomerase. *Trends Biochem. Sci.* **20**: 12-14.

Ryle, M.J., Lanzilotta, W.N., Mortenson, L.E., Watt, G.D. and Seefeldt, L.C. (1995) Evidence for a central role of lysine 15 of *Azotobacter vinelandii* nitrogenase iron protein in nucleotide binding and protein conformational changes. *J. Biol. Chem.* **270**: 13112-13117.

Ryle, M.J. and Seefeldt, L.C. (1996) Elucidation of a MgATP signal transduction pathway in the nitrogenase iron protein: formation of a conformation resembling the MgATP-bound state by protein engineering. *Biochemistry*. **35**: 4766-4775.

Ryle, M.J., Lanzilotta, W.N., Seefeldt, L.C., Scarrow, R.C. and Jensen, G.M. (1996) Circular dichroism and x-ray spectroscopies of *Azotobacter vinelandii* nitrogenase iron protein. MgATP and MgADP induced protein conformational changes affecting the [4Fe-4S] cluster and characterization of a [2Fe-2S] form. *J. Biol. Chem.* **271**: 1551-1557.

Schindelin, H., Kisker, C., Schlessman, J.L., Howard, J.B. and Rees, D.C. (1997) Structure of ADP:AlF_4^--stabilized nitrogenase complex and its implications for signal transduction. *Nature*. **387**: 370-376.

Schultz, F.A., Gheller, S.F., Burgess, B.K., Lough, S. and Newton, W.E. (1985) Electrochemical characterization of the iron-molybdenum cofactor from *Azotobacter vinelandii* nitrogenase. *J. Am. Chem. Soc.* **107**: 5364-5368.

Scott, D.J., May, H.D., Newton, W.E., Brigle, K.E. and Dean, D.R. (1990) Role for the nitrogenase MoFe protein alpha-subunit in FeMo-cofactor binding and catalysis. *Nature*. **343**: 188-190.

Scott, D.J., Dean, D.R. and Newton, W.E. (1992) Nitrogenase-catalyzed ethane production and CO-sensitive hydrogen evolution from MoFe proteins having amino acid substitutions in an alpha-subunit FeMo cofactor-binding domain. *J. Biol. Chem.* **267**: 20002-20010.

Seefeldt, L.C., Morgan, T.V., Dean, D.R. and Mortenson, L.E. (1992) Mapping the site(s) of MgATP and MgADP interaction with the nitrogenase of *Azotobacter vinelandii*. Lysine 15 of the iron protein plays a major role in MgATP interaction. *J. Biol. Chem.* **267**: 6680-6688.

Seefeldt, L.C., Rasche, M.E. and Ensign, S.A. (1995) Carbonyl sulfide and carbon dioxide as new substrates, and carbon disulfide as a new inhibitor, of nitrogenase. *Biochemistry*. **34**: 5382-5389.

Shah, V.K. and Brill, W.J. (1977) Isolation of an iron-molybdenum cofactor from nitrogenase. *Proc. Natl. Acad. Sci. U.S.A.* **74**: 3249-3253.

Shah, V.K., Allen, J.R., Spangler, N.J. and Ludden, P.W. (1994) In vitro synthesis of the iron-molybdenum cofactor of nitrogenase. Purification and characterization of NifB cofactor, the product of NIFB protein. *J. Biol. Chem.* **269**: 1154-1158.

Shah, V.K., Rangaraj, P., Chatterjee, R., Allen, R.M., Roll, J.T., Roberts, G.P. and Ludden, P.W. (1998) Requirement of NIFX for the in vitro biosynthesis of the iron-molybdenum cofactor of nitrogenase. In *Biological nitrogen fixation for the 21st century*. Elmerich, C., Kondorosi, A., and Newton, W.E. (eds.) Dordrecht: The Netherlands: Kluwer Academic, pp. 51-52.

Shen, J. (1994) Role of MoFe protein α-274-histidine, α-276-tyrosine and α-277-arginine residues in *Azotobacter vinelandii* nitrogenase catalysis [dissertation] Virginia (VA): Virginia Polytechnic Institutute and State University.

Shen, J., Dean, D.R. and Newton, W.E. (1997) Evidence for multiple substrate-reduction sites and distinct inhibitor-binding sites from an altered *Azotobacter vinelandii* nitrogenase MoFe protein. *Biochemistry*. **36**: 4884-4894.

Simpson, F.B. and Burris, R.H. (1984) A nitrogen pressure of 50 atmospheres does not prevent evolution of hydrogen by nitrogenase. *Science*. **224**: 1095-1097.

Smith, B.E., Lowe, D.J. and Bray, R.C. (1973) Studies by electron paramagnetic resonance on the catalytic mechanism of nitrogenase of *Klebsiella pneumoniae*. *Biochem. J.* **135**: 331-341.

Smith, B.E. (1999) Structure, function, and biosynthesis of the metallosulfur clusters in nitrogenase. In *Advances in inorganic chemistry*. Sykes, A.G., and Cammack, R. (eds.) London: Acadamic Press, pp. 159-218.

Sørlie, M., Christiansen, J., Lemon, B.J., Peters, J.W., Dean, D.R. and Hales, B.J. (2001) Mechanistic features and structure of the nitrogenase α-Gln^{195} MoFe protein. *Biochemistry*. **40**: 1540-1549.

Stiefel, E.I. (1973) Proposed molecular mechanism for the action of molybedenum in enzymes: coupled proton and electron transfer. *Proc. Natl. Acad. Sci. U.S.A.* **70**: 988-992.

Strandberg, G.W. and Wilson, P.W. (1968) Formation of the nitrogen-fixing enzyme system in *Azotobacter vinelandii*. *Can. J. Microbiol.* **14**: 25-31.

Surerus, K.R., Hendrich, M.P., Christie, P.D., Rottgardt, D., Orme-Johnson, W.H. and Münch, E. (1992) Mössbauer and integer-spin EPR of oxidized P-cluster of nitrogenase: P^{OX} is a non-Kramers system with a nearly degenerate ground doublet. *J. Am. Chem. Soc.* **114**: 8580-8590.

Thomann, H., Morgan, T.V., Jin, H., Burgmayer, S.N.J., Bare, R.E. and Stiefel, E.I. (1987) Protein nitrogen coordination to the FeMo center of nitrogenase fron *Clostridium pasteurianum*. *J. Am. Chem. Soc.* **109**: 7913-7914.

Thomann, H., Bernardo, M., Newton, W.E. and Dean, D.R. (1991) N coordination of FeMo-cofactor requires His-195 of the MoFe proteins alpha subunit and is essential for biological nitrogen fixation. *Proc. Natl. Acad. Sci. U.S.A.* **88**: 6620-6623.

Thorneley, R.N.F., Eady, R.R. and Lowe, D.J. (1978) Biological nitrogen fixation by way of an enzyme-bound dinitrogen-hydride intermediate. *Nature*. **272**: 557-558.

Thorneley, R.N.F. and Lowe, D.J. (1983) Nitrogenase of *Klebsiella pneumoniae*. Kinetics of the dissociation of oxidized iron protein from molybdenum-iron protein: identification of the rate-limiting step for substrate reduction. *Biochem. J.* **215**: 393-403.

Thorneley, R.N.F. and Lowe, D.J. (1984a) The mechanism of *Klebsiella pneumoniae* nitrogenase action. Simulation of the dependences of H_2-evolution rate on component-protein concentration and ratio and sodium dithionite concentration. *Biochem. J.* **224**: 903-909.

Thorneley, R.N.F. and Lowe, D.J. (1984b) The mechanism of *Klebsiella pneumoniae* nitrogenase action. Pre-steady-state kinetics of an enzyme-bound intermediate in N_2 reduction and of NH_3 formation. *Biochem. J.* **224**: 887-894.

Thorneley, R.N.F. and Lowe, D.J. (1985) Kinetic and mechanism of the nitrogenase enzyme system. In *Molybdenum enzymes*. Spiro, T.G. (ed.): Wiley & Sons, pp. 221-284.

Thorneley, R.N.F., Ashby, G., Howarth, J.V., Millar, N.C. and Gutfreund, H. (1989) A transient-kinetic study of the nitrogenase of *Klebsiella pneumoniae* by stopped-flow calorimetry. Comparison with the myosin ATPase. *Biochem. J.* **264**: 657-661.

Tittsworth, R.C. and Hales, B.J. (1993) Detection of EPR signals assigned to the 1-equiv-oxidized P-cluster of the nitrogenase MoFe-protein from *Azotobacter vinelandii*. *J. Am. Chem. Soc.* **115**: 9763-9767.

Trinchant, J.C. and Rigaud, J. (1982) Nitrite and nitric oxide as inhibitors of nitrogenase from soybean bacteroids. *Applied Environ. Microbiol.* **44**: 1385-1388.

Ugalde, R.A., Imperial, J., Shah, V.K. and Brill, W.J. (1984) Biosynthesis of iron-molybdenum cofactor in the absence of nitrogenase. *J. Bacteriol.* **159**: 888-893.

Yuvaniyama, P., Agar, J.N., Cash, V.L., Johnson, M.K., and Dean, D.R. (2000) NifS-directed assembly of a transient [2Fe-2S] cluster within the NifU protein. *Proc. Natl. Acad. Sci. U.S.A.* **97**: 599-604.

Walker, J.E., Saraste, M., Runswick, M.J. and Gay, N.J. (1982) Distantly related sequences in the alpha- and beta-subunits of ATP synthase, myosin, kinases and other ATP-requiring enzymes and a common nucleotide binding fold. *Embo. J.* **1**: 945-951.

Walters, M.A., Chapman, S.K. and Orme-Johnson, W.H. (1986) The nature of amide ligation to the metal sites of FeMoco. *Polyhedron*. **5**: 561-565.

Watt, G.D. and MacDonald, J.W. (1985) Electron paramagnetic resonance spectrum of the iron protein of nitrogenase: existence of a $g = 4$ spectral component and its effect on spin quantization. *Biochemistry*. **24**: 7226-7231.

Watt, G.D., Wang, Z.-C. and Knotts, R.R. (1986) Redox reaction of and nucleotide binding to the iron protein of *Azotobarter vinelandii*. *Biochemistry*. **25**: 8156-8162.

Watt, G.D. and Reddy, K.R.N. (1994) Formation of an all ferrous Fe_4S_4 cluster in the iron protein component of *Azotobacter vinelandii* nitrogenase. *J. inorg. biochem.* **53**: 281-294.

Wherland, S., Burgess, B.K., Stiefel, E.I. and Newton, W.E. (1981) Nitrogenase reactivity: effects of component ratio on electron flow and distribution during nitrogen fixation. *Biochemistry*. **20**: 5132-5140.

White, T.C., Harris, G.S. and Orme-Johnson, W.H. (1992) Electrophoretic studies on the assembly of the nitrogenase molybdenum-iron protein from the *Klebsiella pneumoniae nifD* and *nifK* gene products. *J. Biol. Chem.* **267**: 24007-24016.

Wolle, D., Dean, D.R. and Howard, J.B. (1992) Nucleotide-iron-sulfur cluster signal transduction in the nitrogenase iron-protein: the role of Asp125. *Science*. **258**: 992-995.

Yates, M.G. and Lowe, D.J. (1976) Nitrogenase of *Azotobacter chroococcum*: a new electron-paramagnetic-resonance signal associated with a transient species of the Mo-Fe protein during catalysis. *FEBS Lett.* **72**: 121-126.

Yates, M.G. (1992) The enzymology of molybdenum-dependent nitrogen fixation. In *Biological nitrogen fixation*. Stacey, G., Burris, R.H., and Evans, D.J. (eds.) New York: Chapman & Hall, pp. 685-735.

Zheng, L., White, R.H., Cash, V.L., Jack, R.F. and Dean, D.R. (1993) Cysteine desulfurase activity indicates a role for NIFS in metallocluster biosynthesis. *Proc. Natl. Acad. Sci. U.S.A.* **90**: 2754-2758.

Zheng, L., White, R.H., Cash, V.L. and Dean, D.R. (1994) Mechanism for the desulfurization of L-cysteine catalyzed by the *nifS* gene product. *Biochemistry*. **33**: 4714-4720.

Zheng, L. and Dean, D.R. (1994) Catalytic formation of a nitrogenase iron-sulfur cluster. *J. Biol. Chem.* **269**: 18723-18726.

Zheng, L., White, R.H. and Dean, D.R. (1997) Purification of the *Azotobacter vinelandii nifV*-encoded homocitrate synthase. *J. Bacteriol.* **179**: 5963-5966.

Zimmermann, R., Münck, E., Brill, W.J., Shah, V.K., Henzl, M.T., Rawlings, J. and Orme-Johnson, W.H. (1978) Nitrogenase X: Mössbauer and EPR studies on reversibly oxidized MoFe protein from *Azotobacter vinelandii OP*. *Biochem. Biophys. Acta*. **537**: 185-207.

Zumft, W.G., Cretney, W.C., Huang, T.C., Mortenson, L.E. and Palmer, G. (1972) On the structure and function of nitrogenase from *Clostridium pasteurianum W5*. *Biochem. Biophys. Res. Commun.* **48**: 1525-1532.

APPENDIX

Figures A-G show the specific activity of H_2 evolution (▲), C_2H_4 production (□), and H_2 evolution plus C_2H_4 production (●) in terms of nmole of electron pair per min per mg of MoFe protein when the C_2H_2 concentration is varied from 0 to 1 atm. Both H_2 evolution and C_2H_4 production were inhibited when the C_2H_2 concentration is increased with wild type (A), αPro-191 (B), αThr-191 (C) MoFe proteins. Only H_2 evolution is inhibited when the C_2H_2 concentration is increased with αSer-191 (D), αHis-191 (E), αGlu-191 (F), and αArg-191 (G) altered MoFe proteins.

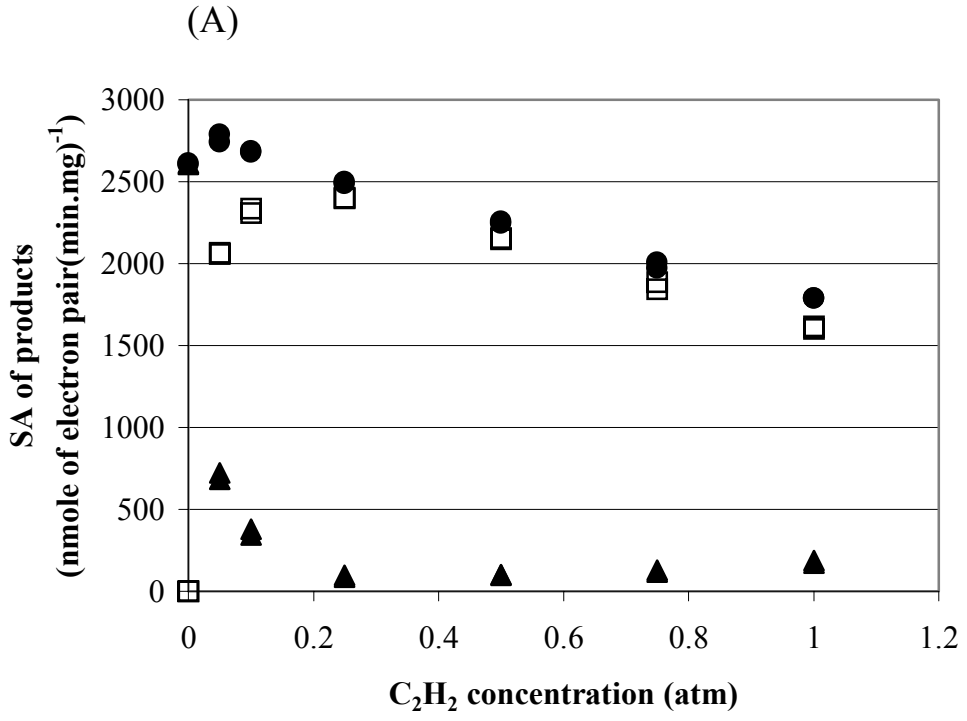

(B)

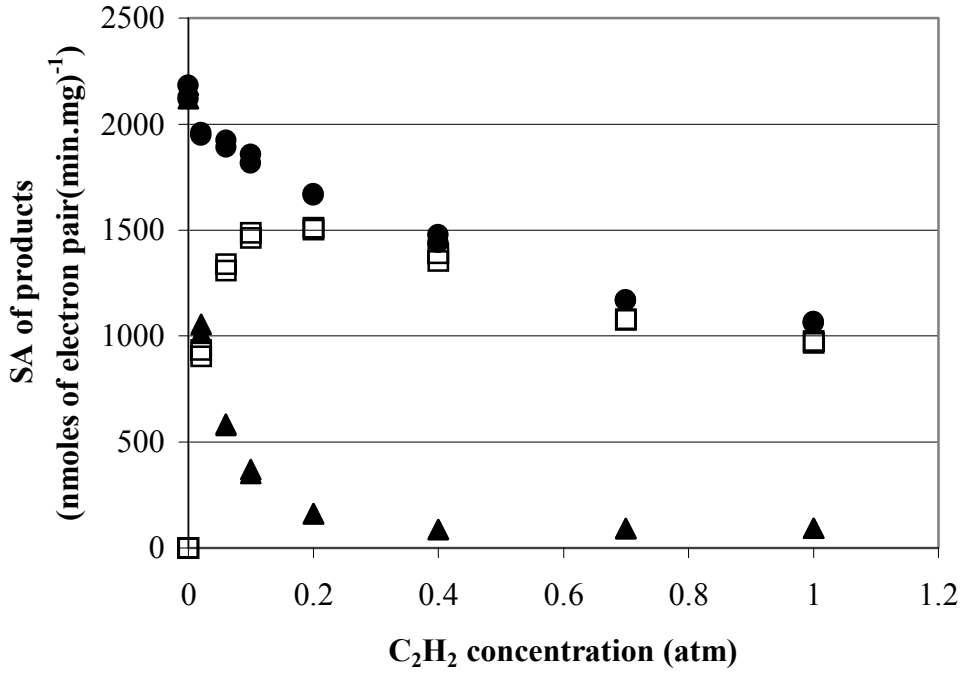
2500
2000
1500
1000
500
0
SA of products
(nmoles of electron pair(min.mg)-1)
0
0.2
0.4
0.6
0.8
1
1.2
C2H2 concentration (atm)

(C)

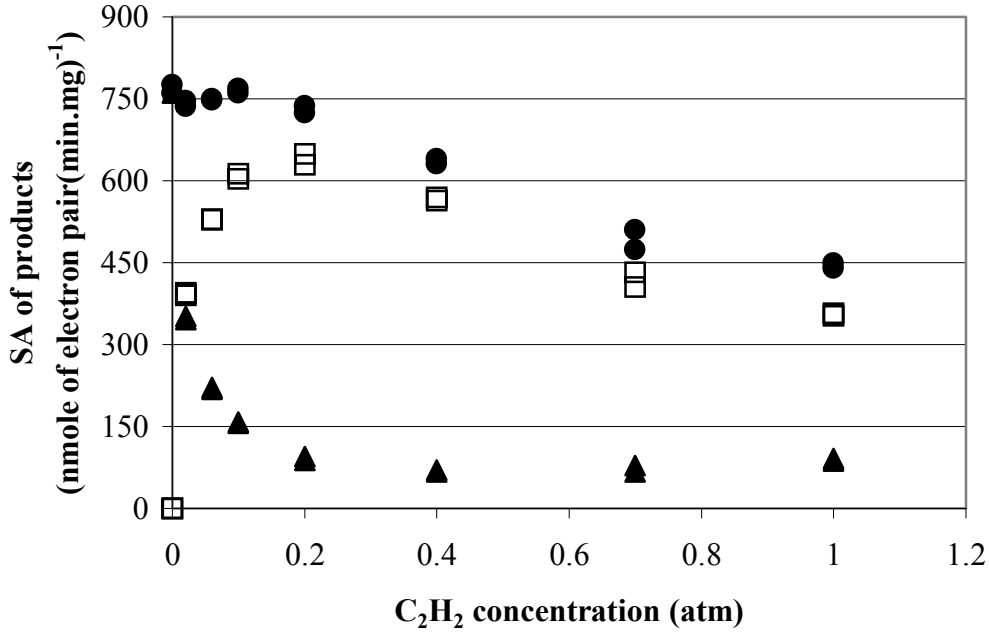
900
750
600
450
300
150
0
SA of products
(nmole of electron pair(min.mg)-1)
0
0.2
0.4
0.6
0.8
1
1.2
C2H2 concentration (atm)

(D)

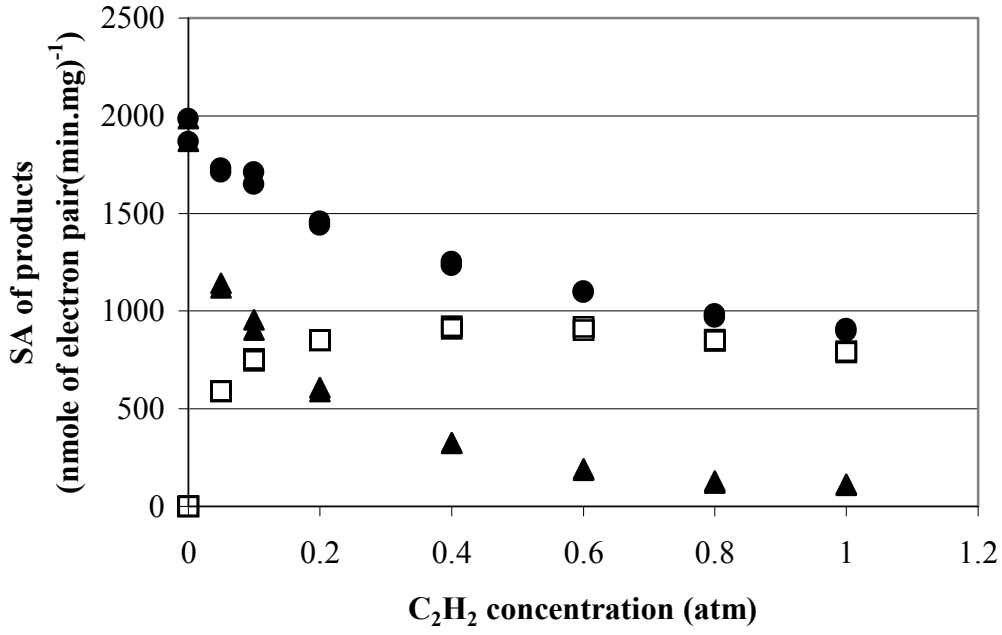
SA of products
(nmole of electron pair(min.mg)-1)
2500
2000
1500
1000
500
0
0
0.2
0.4
0.6
0.8
1
1.2
C2H2 concentration (atm)

(E)

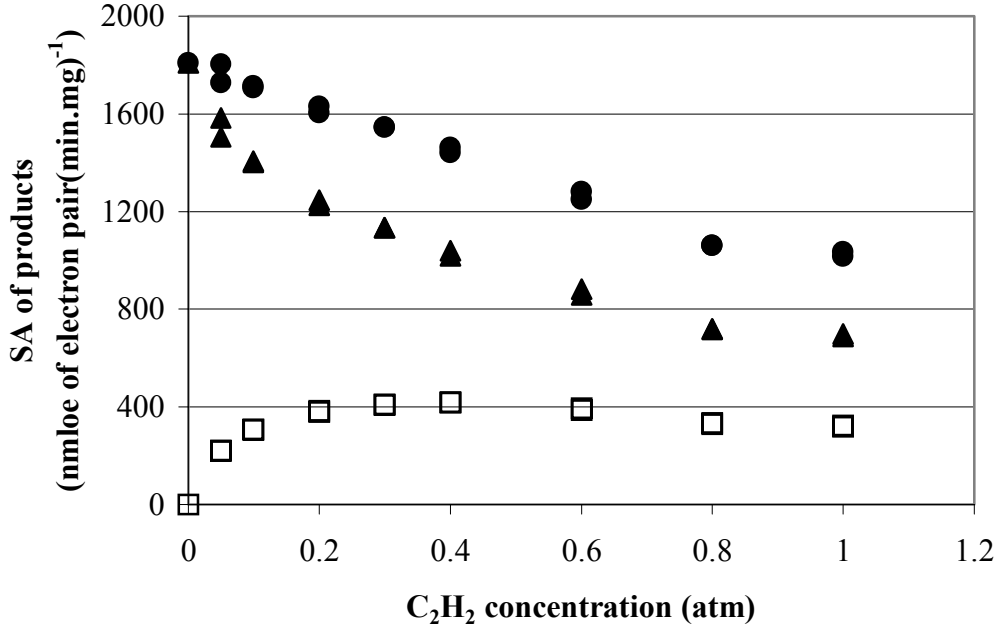
SA of products
(nmloe of electron pair(min.mg)-1)
2000
1600
1200
800
400
0
0
0.2
0.4
0.6
0.8
1
1.2
C2H2 concentration (atm)

(F)

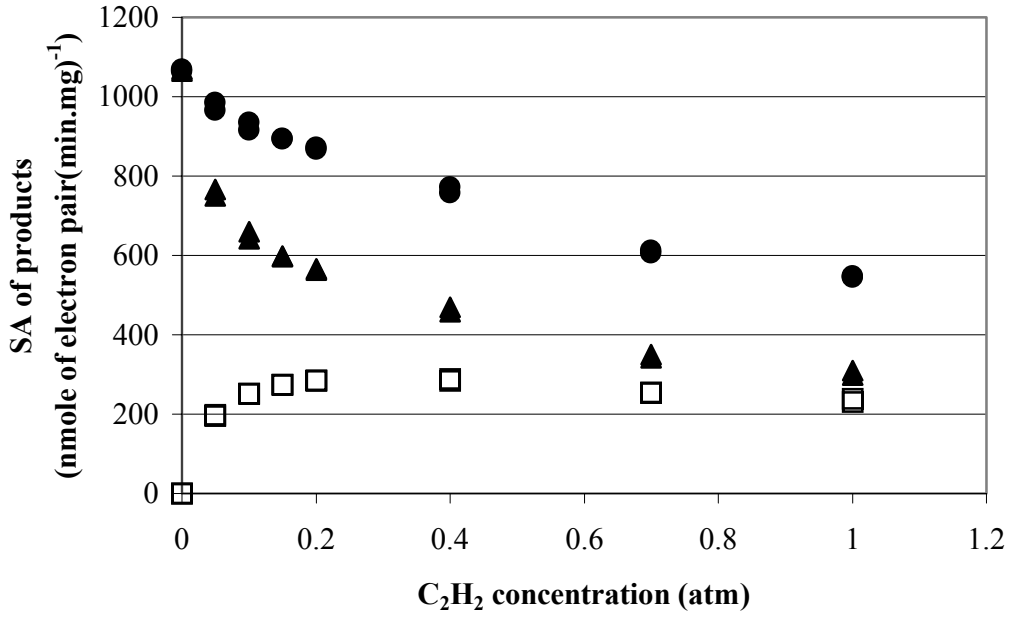
SA of products
(nmole of electron pair(min.mg)-1)
1200
1000
800
600
400
200
0
0
0.2
0.4
0.6
0.8
1
1.2
C2H2 concentration (atm)

(G)

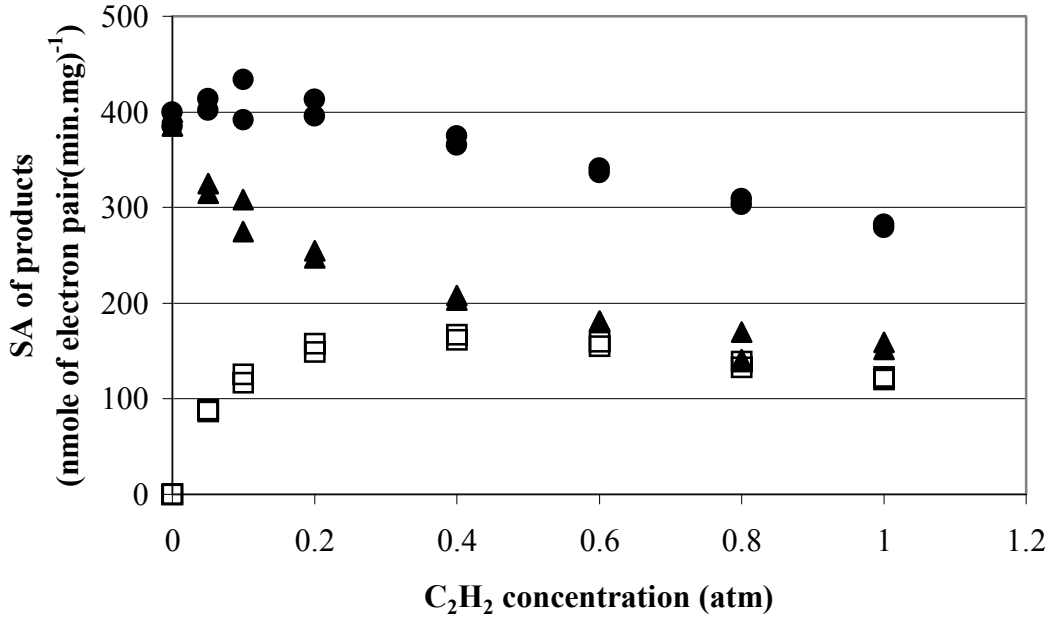
SA of products
(nmole of electron pair(min.mg)-1)
500
400
300
200
100
0
0
0.2
0.4
0.6
0.8
1
1.2
C2H2 concentration (atm)

VITA

Kanit Vichitphan was born on November 27, 1959, in Uttaradit province, Thailand. He graduated from Chiengmai University in Chiengmai with a Bachelor of Science degree in Chemistry in 1982. After graduation he took a job as staff scientist in the Department of Pathology, Ramathibodi Hospital, Mahidol University. During his work, he further studied Master degree in Biochemistry, Mahidol University. In 1993, he was selected by the Faculty's committee to be an instructor in the Department of Biotechnology, Khon Kaen University. In 1996, he got the scholarship from Royal Thai Government to study aboard. At the same year, he came to Virginia Polytechnic Institute and State University and started a doctoral program in the Department of Biochemistry. After completing his Ph. D. at Virginia Tech, he will go back to his country and continue his work at Khon Kaen University, Khon Kaen in Department of Biotechnology.